

H24/3052

**MONASH UNIVERSITY**  
**THESIS ACCEPTED IN SATISFACTION OF THE**  
**REQUIREMENTS FOR THE DEGREE OF**  
**DOCTOR OF PHILOSOPHY**

ON..... 5 October 2001 .....

.....  
Prof. Sec. Research Graduate School Committee

Under the copyright Act 1968, this thesis must be used only under the normal conditions of scholarly fair dealing for the purposes of research, criticism or review. In particular no results or conclusions should be extracted from it, nor should it be copied or closely paraphrased in whole or in part without the written consent of the author. Proper written acknowledgement should be made for any assistance obtained from this thesis.

## AMENDMENTS TO THESIS

Table of Contents: 11<sup>th</sup> line from the bottom: "estimayion" should be corrected as "estimation".

Page 60: 1<sup>st</sup> paragraph, last sentence should be modified as follows: "This is because the second threshold intensity is intentionally set so high (by using an unrealistically high value of 100 for F2) to ensure that no additional storms can be selected."

Page 120: 1<sup>st</sup> paragraph, 1<sup>st</sup> line: Add at the end of "threshold value of 0.01mm/h was exceeded": "Although this threshold seems low, Hill et al (1996a) found this value to produce the best results from the 3 values tested. They also noted that the design peak flow is relatively insensitive to the choice of surface runoff threshold."

Page 155: 9<sup>th</sup> line from the top: "Therefore, it is difficult assess how..." should be corrected as "Therefore, it is difficult to assess how..."

Department of Civil Engineering  
Monash University  
Clayton, Victoria, Australia

as  
the  
igh  
was  
e to  
eak  
be

**A JOINT PROBABILITY MODEL FOR  
RAINFALL-BASED DESIGN FLOOD ESTIMATION**

**Tam Minh Thi Hoang**  
**Bachelor of Civil Engineering (First Class Honours)**

A thesis submitted for the Degree of Doctor of Philosophy  
May, 2001

# TABLE OF CONTENTS

STATEMENT.....	I
ACKNOWLEDGMENTS.....	II
SUMMARY.....	IV
LIST OF FIGURES.....	VI
LIST OF TABLES.....	VIII
LIST OF NOTATIONS.....	X
LIST OF ABBREVIATIONS.....	XIV
<b>CHAPTER 1: INTRODUCTION.....</b>	<b>1</b>
1.1 RESEARCH BACKGROUND.....	1
1.2 RESEARCH RATIONALE.....	4
1.3 RESEARCH OBJECTIVES.....	6
1.4 THESIS OUTLINE.....	6
<b>CHAPTER 2: REVIEW OF RAINFALL-BASED DESIGN FLOOD ESTIMATION METHODS</b> .....	<b>9</b>
2.1 INTRODUCTION.....	9
2.2 THE DESIGN EVENT APPROACH.....	10
2.2.1 Procedure.....	10
2.2.2 Features.....	11
2.2.3 Limitations.....	14
2.3 ALTERNATIVES TO THE DESIGN EVENT APPROACH.....	15
2.3.1 Empirical Methods.....	16
2.3.2 Continuous Simulation.....	16
2.3.3 The Runoff Files Approach.....	18
2.3.4 The 'Improved' Design Event Approach.....	18
2.3.5 The Joint Probability Approach.....	19
2.3.6 Best alternatives to the Design Event Approach.....	20
2.4 THE JOINT PROBABILITY APPROACH.....	21
2.4.1 Derived distribution theory.....	21
2.4.1.1 Analytical methods.....	22
2.4.1.2 Approximate numerical methods.....	22
2.4.1.3 Simulation techniques.....	23
2.4.2 Review of previous studies of the Joint Probability Approach.....	23
2.4.2.1 Studies based on analytical methods.....	24
2.4.2.2 Studies based on approximate numerical methods.....	26
2.4.2.3 Studies based on Monte Carlo simulation.....	28
2.4.2.4 Concluding remarks.....	30
2.5 SUMMARY.....	31
<b>CHAPTER 3: DEVELOPMENT OF A JOINT PROBABILITY MODEL FOR DESIGN FLOOD</b> <b>ESTIMAYION.....</b>	<b>33</b>
3.1 INTRODUCTION.....	33
3.2 DETERMINISTIC ELEMENTS.....	34
3.2.1 Loss model.....	34
3.2.2 Runoff routing model.....	36
3.3 STOCHASTIC ELEMENTS.....	37
3.3.1 Determination of key inputs to be treated as random variables.....	38
3.3.2 Selection of a Joint Probability Method.....	41
3.3.3 Correlations of random variables.....	42
3.4 RESEARCH PROCEDURE.....	44
3.5 SUMMARY.....	47

<b>CHAPTER 4: DETERMINATION OF MODELLING ELEMENTS.....</b>	<b>48</b>
4.1 INTRODUCTION .....	48
4.2 DATA COLLECTION AND VERIFICATION .....	49
4.2.1 Selection of test catchments.....	49
4.2.2 Rainfall data.....	51
4.2.3 Streamflow data.....	54
4.2.4 Summary.....	54
4.3 STORM EVENT DEFINITION .....	55
4.3.1 Overview.....	55
4.3.2 Development of storm definition.....	56
4.3.2.1 Start and end of storm events.....	56
4.3.2.2 Storm threshold intensities.....	57
4.3.2.3 Visual check of the extracted events.....	60
4.3.2.4 Refinement of storm definition.....	62
4.3.3 Extraction of storm events.....	64
4.3.4 Checking of extracted events for consistency of hourly rainfalls.....	65
4.3.5 Summary.....	66
4.4 FREQUENCY DISTRIBUTION OF STORM DURATION .....	67
4.4.1 Background .....	67
4.4.2 The Hosking and Wallis method of regional frequency analysis.....	68
4.4.3 Application and results.....	70
4.4.4 Summary.....	76
4.5 CONDITIONAL FREQUENCY DISTRIBUTION OF RAINFALL INTENSITY .....	77
4.5.1 Background .....	77
4.5.2 Correlation between rainfall intensity and duration .....	78
4.5.3 Development of the IFD curves.....	79
4.5.4 Preliminary results.....	84
4.5.5 Adjustment of the derived IFD curves .....	86
4.5.6 Discussion .....	90
4.5.7 Summary.....	91
4.6 STOCHASTIC REPRESENTATION OF TEMPORAL PATTERNS.....	92
4.6.1 Background .....	92
4.6.2 Data.....	93
4.6.3 Representation of temporal patterns .....	94
4.6.4 Dependence of temporal patterns on season, storm duration and depth.....	97
4.6.4.1 Correlation analysis .....	98
4.6.4.2 The chi-square test of independence.....	100
4.6.4.3 Discussion.....	110
4.6.5 Development of a stochastic model to reproduce observed storm mass curves .....	111
4.6.6 Summary.....	118
4.7 PROBABILITY DISTRIBUTION OF INITIAL LOSS .....	119
4.7.1 Background .....	119
4.7.2 Correlations of initial loss with rainfall duration and average rainfall intensity .....	120
4.7.3 Development of the probability distribution of initial loss .....	121
4.7.3.1 Selection of a distributional type .....	121
4.7.3.2 Estimation of distributional parameters .....	122
4.7.3.3 Checking of the adequacy of the fitted distribution .....	124
4.7.4 Summary.....	125
4.8 PARAMETERS OF THE LUMPED RUNOFF ROUTING MODEL.....	126
4.8.1 Background .....	126
4.8.2 Determination of the lumped model parameters .....	126
4.8.2.1 Event selection.....	127
4.8.2.2 Baseflow separation.....	127
4.8.2.3 Model calibration.....	129
4.8.2.4 Model testing.....	131
4.8.2.5 Discussion.....	132
4.8.3 Comparison of lumped and distributed runoff routing models.....	134
4.8.4 Summary.....	137
4.9 OTHER FIXED DESIGN INPUTS.....	138
4.10 SUMMARY .....	139

<b>CHAPTER 5: MODEL APPLICATION</b> .....	<b>142</b>
5.1 INTRODUCTION .....	142
5.2 GENERATION OF RANDOM NUMBERS FROM THE INPUT DISTRIBUTIONS .....	143
5.2.1 <i>Background</i> .....	143
5.2.2 <i>Number of generated data</i> .....	144
5.2.3 <i>Storm duration</i> .....	145
5.2.4 <i>Rainfall intensity</i> .....	146
5.2.5 <i>Temporal patterns</i> .....	147
5.2.5.1 <i>Generation of design temporal patterns</i> .....	147
5.2.5.2 <i>Model verification</i> .....	148
5.2.6 <i>Initial loss</i> .....	154
5.3 ESTIMATION OF FLOOD EVENTS BY MONTE CARLO SIMULATION .....	155
5.3.1 <i>Correlations of flood causing factors</i> .....	156
5.3.2 <i>Simulation procedure</i> .....	157
5.4 DETERMINATION OF DESIGN FLOOD FREQUENCY CURVES .....	158
5.5 SUMMARY .....	160
<b>CHAPTER 6: MODEL EVALUATION</b> .....	<b>162</b>
6.1 INTRODUCTION .....	162
6.2 ESTIMATION OF DESIGN FLOODS BY DIRECT FLOOD FREQUENCY ANALYSIS .....	163
6.2.1 <i>Theoretical basis</i> .....	164
6.2.2 <i>Application to the La Trobe River catchment at Noojee</i> .....	165
6.2.3 <i>Discussion</i> .....	167
6.3 ESTIMATION OF DESIGN FLOODS BY THE DESIGN EVENT APPROACH .....	169
6.3.1 <i>Estimation of the design rainfall</i> .....	170
6.3.2 <i>Estimation of initial loss</i> .....	172
6.3.3 <i>Estimation of design floods</i> .....	173
6.3.4 <i>Discussion</i> .....	174
6.4 COMPARISON WITH THE JOINT PROBABILITY MODEL .....	174
6.5 SENSITIVITY ANALYSES .....	179
6.5.1 <i>Effects of design rainfall intensity</i> .....	180
6.5.2 <i>Effects of initial loss</i> .....	181
6.5.3 <i>Effects of temporal pattern groups</i> .....	182
6.5.4 <i>Effects of number of time increments used to describe temporal patterns</i> .....	184
6.5.5 <i>Effects of fixed design inputs</i> .....	185
6.5.6 <i>Effects of sample size</i> .....	188
6.5.7 <i>Discussion</i> .....	189
6.6 ADDITIONAL METHOD TESTING .....	191
6.6.1 <i>Estimation of model elements</i> .....	191
6.6.2 <i>Estimation of the derived flood frequency curve</i> .....	193
6.6.3 <i>Evaluation of the proposed model</i> .....	194
6.7 OVERALL ASSESSMENT OF THE JOINT PROBABILITY MODEL .....	197
6.8 SUMMARY .....	199
<b>CHAPTER 7: CONCLUSION</b> .....	<b>202</b>
7.1 SUMMARY OF WORK DONE .....	202
7.2 CONCLUSIONS .....	207
7.3 RECOMMENDATIONS FOR FUTURE STUDIES .....	209
<b>REFERENCES</b> .....	<b>213</b>
<b>APPENDICES</b> .....	
APPENDIX A: JOINT PROBABILITY APPROACH: STATISTICAL BASIS .....	225
APPENDIX B: PREVIOUS STUDIES OF THE JOINT PROBABILITY APPROACH TO DESIGN FLOOD ESTIMATION .....	230
APPENDIX C: LOSS MODELS .....	238
APPENDIX D: DATA VERIFICATION .....	250

---

APPENDIX E: THE HOSKING AND WALLIS REGIONAL FREQUENCY ANALYSIS STATISTICS.....	258
APPENDIX F: STATISTICAL DISTRIBUTIONS.....	264
APPENDIX G: THE CHI-SQUARE TEST OF INDEPENDENCE.....	268
APPENDIX H: METHODS FOR DEVELOPING DESIGN TEMPORAL PATTERNS .....	271
APPENDIX I: AT-SITE FREQUENCY ANALYSIS METHODS .....	278
APPENDIX J: SELECTION OF A DISTRIBUTED RUNOFF ROUTING MODEL FOR THE LA TROBE CATCHMENT .....	286
APPENDIX K: DATA GENERATION.....	294
APPENDIX L: CONFERENCE PAPERS .....	297

---

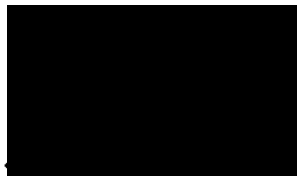
## STATEMENT

This thesis contains no material that has been accepted for the award of any other degree in any university or institution. To the best of my knowledge, the thesis contains no material previously published or written by any other person, except where due reference is made in the text.



Tam Minh Thi Hoang

This thesis is a part of project FL1 "Holistic Approach to Rainfall-Based Design Flood Estimation" undertaken by the Cooperative Research Centre for Catchment Hydrology. Two separate approaches were investigated, one dealing with 'complete storms' (summarized in this thesis), and the other dealing with 'storm cores' (undertaken by A. Rahman). For the work reported in Sections 4.5 and 4.7 and parts of 5.2 and 5.4, there was considerable overlap between these two investigations, as acknowledged in the relevant sections of the thesis. The remainder of the thesis reports on my original work.



Tam Minh Thi Hoang

---

## ACKNOWLEDGMENTS

This thesis marks the end of my doctoral research. It also terminates that part of my life when it was crucial for me to go back to university to acquire appropriate knowledge and skills in order to commence my working life in Australia.

On the completion of this research, I would like to send my sincere thanks to a number of people who have contributed to my achievement today. First of all, I wish to express my deep gratitude to my main supervisor, Mr. P. E. Weinmann, for his invaluable help, guidance and suggestions during the course of my research. The technical and problem solving skills that I learnt from Erwin have made a significant contribution, not only to this thesis, but also in my working life. I am also indebted to Erwin for those parts of his precious time that were given to me whenever I needed them.

I would also like to express my sincere appreciation to my associate supervisor, Emeritus Professor E. M. Laurenson, for his wise counsel and assistance. I greatly value his continuing help in reading the drafts of my thesis during his retirement.

I am also sincerely thankful to:

- Dr. A. Rahman and Dr. J. R. M. Hosking for permission to use some of their FORTRAN programs;
- Ms. E. Romey, Mrs. R. Clerehan, and especially Mrs. J. Moodie at the Language and Learning Services (Monash University) for their advice and assistance in English writing;
- The Reference Panel of Project FL1 'Holistic Approach to Rainfall-Based Design Flood Estimation', including Professor R. G. Mein, Professor T. A. McMahon, Dr. R. Srikanthan, Dr. R. Nathan, and Dr. Q. J. Wang, for their inputs to the project (of which the work for this thesis was a part);
- Staff of the Department of Civil Engineering and the Cooperative Research Centre for Catchment Hydrology at Monash University, especially Mrs. J. Manson, Mrs.

---

Sgouras, I., Mrs. V. Verrelli, Mr. A. Haines, Mr. D. McCarthy, and Mr. A. Taylor for their administrative help and computing support;

- The Training and Research Branch and the Cooperative Research Centre for Catchment Hydrology at Monash University for their financial support of this research;
- Dr. R. Srikanthan and Mr. L. Siriwardena for sharing their experience; and
- Ms. B. Dworakovski (Thiess Environmental Services) for providing some of the flow data used in the research.

My former lecturers at Royal Melbourne Institute of Technology (RMIT), including Dr. M. J. Moore and Mr. G. A. Hodge, provided me with encouragement and support during my first years of study in Australia, and for this I am always grateful. I would also like to acknowledge Dr. N. Jayasuriya at RMIT for her lectures in hydrology, which provoked my very first interests in the subject. I especially thank Professor R. G. Mein of the Cooperative Research Centre for Catchment Hydrology for giving me my first job in Australia, the Vacation Studentship in 1995, which opened the door to my profession as a hydrologist.

I would also like to express my sincere and deep gratitude to Associate Professor R. J. Keller for his very kind support and encouragement throughout my course of study at Monash University. I treasure his friendship.

Finally, the fulfilment of my doctoral degree is not only an achievement of my own but also of my husband who had brought future into my life, and who has been supporting me during my past nine years in Australia. My achievement is also dedicated to my parents, brothers, sisters, and other family members, without whom the time and effort that I have been spending to achieve this degree would have become meaningless. My final thanks are sent to my second fatherland, Australia, for giving me the freedom and opportunities to develop my capability and to live the life I wish.

---

## SUMMARY

The objective of this research was to develop a Joint Probability Model for estimating design floods (with average recurrence intervals of 1 to 100 years) from design rainfalls. The proposed model treats the key design inputs (rainfall intensity, duration, temporal pattern, and initial loss) and the flood output as random variables, and takes account of the correlations between these variables in the flood generation process. In the current study, the model was applied to determine the frequency curve of the design flood peak for unregulated rural catchments of medium size. However, scope of its application can be broadened to estimate more extreme floods or the frequency curve of other hydrograph characteristics (flood volume or time to flood peak).

In developing the proposed model, the initial loss – continuing loss model was adopted for computing rainfall excess, and a single, concentrated non-linear runoff routing model for computing design flood hydrographs. The adopted runoff routing model assumes that both rainfall and routing effects are spatially lumped. To compute the probability distribution of design floods, Monte Carlo simulation was adopted. The interaction of random variables involved in the design was taken into account by using conditional probability distributions.

The proposed model was tested on two Victorian catchments. A storm definition was first developed to extract significant stochastic storm events from rainfall records. The correlations between the stochastic inputs were then examined, with an emphasis on the dependence of the temporal pattern on season, storm duration, and depth. The conditional probability distributions of the stochastic inputs were next derived, and other fixed design inputs determined. Monte Carlo simulation was then used to generate synthetic flood events. The derived flood frequency curves were finally determined using a frequency analysis method.

To evaluate the proposed model, design floods estimated by the model were compared with those obtained by direct flood frequency analysis and the Design Event Approach.

---

It was shown that the proposed Joint Probability Model provided more reliable flood estimates than those obtained from the Design Event Approach for one test catchment, but, like the Design Event Approach, slightly underestimated the peak flood magnitude for the other catchment. As these results are limited by the small number of test catchments and the short flow records available at these sites, further testing of the model on a larger number of catchments is required before firm conclusions about its performance can be drawn.

Sensitivity analyses indicated that the design flood estimates were very sensitive to variations in the design rainfall intensity, initial loss, and routing model parameter. Errors in the design continuing loss rate or baseflow had more influence on frequent floods than rare floods. The modelling of the dependence of the temporal pattern on season, duration, and depth was found to be of limited practical importance in the present application.

Overall, the proposed model was found to be fundamentally sound and practically workable. The results are promising, however, further work is still required to turn it into a practical design tool.

## LIST OF FIGURES

Figure 2-1: General classification of design flood estimation methods .....	9
Figure 2-2: Procedure of the Design Event Approach.....	12
Figure 2-3: Attributes of the Design Event Approach (modified from Beran, 1973).....	13
Figure 3-1: Initial loss-continuing loss model (from Hill et al., 1996a).....	36
Figure 3-2: Determination of model elements.....	45
Figure 3-3: Model application .....	46
Figure 4-1: Location map of two test catchments and all pluviometers used in this study .....	50
Figure 4-2: Formation of sub-storms of 2 hours within a storm of 4 hours.....	59
Figure 4-3: Example of a 'normal' storm (station 85237, H=6 hours, F1=0.4, F2=0.5).....	61
Figure 4-4: Examples of 'abnormal' storms (station 85237, H=6 hours, F1=0.4, F2=0.5).....	61
Figure 4-5: Proposed storm definition.....	63
Figure 4-6: Examples of storms obtained using the adopted storm definition .....	63
Figure 4-7: An example of a storm with repeated rainfall values (station 85237) .....	65
Figure 4-8: Plot of L-CV versus L-skewness for storm duration at 19 pluviometers.....	71
Figure 4-9: Plot of L-kurtosis versus L-skewness for storm duration at 19 pluviometers.....	72
Figure 4-10: Plot of average storm duration against gauge elevation at 19 pluviometers.....	73
Figure 4-11: Plot of L-CV against L-skewness for storm duration data for stations in Group 3 and some theoretical probability distributions .....	74
Figure 4-12: Plot of L-kurtosis against L-skewness for storm duration data for stations in Group 3 and some theoretical probability distributions .....	75
Figure 4-13: Observed and fitted frequency curves of storm duration for station 85237.....	76
Figure 4-14: Relationship between average rainfall intensity and duration (station 85237). ....	78
Figure 4-15: Plot of rainfall intensity versus duration for the interval of (6h, 11h) .....	80
Figure 4-16: Plot of rainfall intensity series of the 8-hour representative duration and the fitted exponential distribution .....	83
Figure 4-17: Plot of the polynomial curve fitted to the estimated intensities of representative durations (ARI = 20 years) .....	84
Figure 4-18: Derived IFD curves for station 85237 .....	85
Figure 4-19: Derived IFD curve and the IFD-HYDSYS curve for ARI=20 years (station 85237) .....	88
Figure 4-20: Plot of the polynomial rainfall intensity-duration curve (ARI = 20 years).....	89
Figure 4-21: Plot of the IFD curves at station 85237 (ARI=20 years) .....	89
Figure 4-22: The estimated IFD curves at Noojee (pluviometer 85237).....	90
Figure 4-23: Dimensionless rainfall hyetograph and its statistical characteristics .....	96
Figure 4-24: 9-ordinate representation of temporal patterns .....	97
Figure 4-25: Plot of the mean (centre of gravity) of observed dimensionless hyetographs versus rainfall depth .....	100
Figure 4-26: Plot of standard deviation (degree of dispersion) of observed dimensionless hyetographs versus rainfall duration .....	100
Figure 4-27: Independent groups of temporal patterns (by the results of the chi-square test of independence) .....	107
Figure 4-28: 4-ordinate representation of temporal patterns .....	108
Figure 4-29: Principles of the multiplicative cascade model.....	113
Figure 4-30: Dimensionless mass curve at the third level of disaggregation .....	116
Figure 4-31: Relationship between initial loss and storm duration .....	121
Figure 4-32: Relationship between initial loss and average rainfall intensity .....	121
Figure 4-33: Histogram of initial losses for the La Trobe River catchment.....	122
Figure 4-34: Plot of the cumulative distribution function of observed initial losses and the fitted beta distribution .....	123

Figure 4-35: Plot of total streamflow and the extracted baseflow (the 1963 flood).....	129
Figure 4-36: Observed and estimated hydrographs (the 1969 flood, model calibration).....	130
Figure 4-37: Observed and estimated hydrographs (the 1963 flood, model testing).....	131
Figure 4-38: Plot of observed flood and the corresponding rainfall event (the 1963 flood).....	133
Figure 4-39: Equivalent RORB model for the La Trobe River catchment at Noojee (Baker, 1997).....	135
Figure 4-40: Observed and estimated flood hydrographs (the 1969 flood).....	136
Figure 5-1: An example of a generated temporal pattern.....	148
Figure 5-2: Distributions of the maximum dimensionless intensity for observed and generated temporal patterns of Group 4.....	150
Figure 5-3: Distributions of the maximum dimensionless intensity for observed and generated temporal patterns of Group 2.....	150
Figure 5-4: Huff frequency curves of the observed and generated temporal patterns of Group 2.....	154
Figure 5-5: The generated flood frequency curve for the La Trobe River catchment.....	159
Figure 6-1: Seasonal distribution of annual floods - La Trobe River catchment.....	166
Figure 6-2: Observed peak discharges and the fitted LPIII distribution - La Trobe River catchment at Noojee.....	167
Figure 6-3: Plot of design flood peak against storm burst duration (ARI=20 years).....	174
Figure 6-4: Plot of design flood estimates for the La Trobe River catchment.....	176
Figure 6-5: Observed floods and the generated flood frequency curve - Tarwin River catchment at Dumbalk North.....	194
Figure 6-6: Observed floods and the fitted LPIII distribution - Tarwin River catchment.....	195
Figure 6-7: Flood frequency curves, Tarwin River catchment.....	196
Figure A-1: Venn diagram for the Theorem of Total Probability.....	227
Figure C-1: Components of rainfall and runoff.....	239
Figure D-1: Time-series plot of annual series of maximum daily rainfall (station 85237).....	254
Figure D-2: Time-series plot of annual series of maximum daily rainfall (station 85103).....	255
Figure D-3: Time-series plot of annual series of peak discharge (station 226205C).....	257
Figure F-1: Shapes of the beta distribution (Benjamin and Cornell, 1970).....	267
Figure H-1: Time distributions of first quartile storms (Huff, 1967).....	274
Figure J-1: Smith's RORB model for the La Trobe River catchment at Noojee (Smith, 1998).....	288
Figure J-2: Flood hydrographs estimated by Smith's and Baker's models (testing run, $m=0.8$ , the 1963 flood).....	291
Figure J-3: Observed and calculated hydrographs (Baker's model, $k_c=30$ , $m=0.8$ , the 1971 flood).....	292
Figure K-1: The inverse cumulative distribution function method (Press et al., 1989).....	295
Figure K-2: The rejection method (Press et al., 1989).....	296

## LIST OF TABLES

Table 4-1: List of flow gauging sites and 19 recording rainfall stations used and data availability .....	52
Table 4-2: Sample size of extracted storms using the proposed storm definition .....	64
Table 4-3: L-moments and the discordancy statistics of storm duration for 19 pluviometers used .....	71
Table 4-4: Heterogeneity statistics computed for various regions of storm duration .....	72
Table 4-5: The goodness-of-fit measures computed for storm duration data of Group 3 .....	74
Table 4-6: Quantile estimates of the regional growth curve (for Group 3) and of the probability distribution of storm duration for pluviometer 85237 .....	75
Table 4-7: Representative durations used to develop the IFD curves .....	80
Table 4-8: Statistical properties of the adjusted rainfall intensity series and parameters of the fitted exponential distributions (station 85237) .....	81
Table 4-9: Estimates of design rainfall intensities for ARI = 20 years .....	83
Table 4-10: Derived IFD estimates for station 85237 (rainfall intensity in mm/h) .....	85
Table 4-11: Data used to determine the intensity-duration curve (ARI = 20 years) .....	88
Table 4-12: Correlation coefficients between 3 statistical characteristics of observed dimensionless hyetographs and storm duration or depth .....	99
Table 4-13: Results of the chi-square test of independence to examine the dependence of storm temporal patterns on season .....	102
Table 4-14: Results of the chi-square test of independence to examine the dependence of temporal patterns on storm duration .....	104
Table 4-15: Results of the chi-square test of independence to investigate the dependence of temporal patterns on season, storm duration, and storm depth .....	105
Table 4-16: Effects of number of ordinates used to define temporal patterns on results of the chi-square test of independence .....	109
Table 4-17: Parameters of the beta distribution representing the disaggregation parameters of storm mass curves .....	117
Table 4-18: Results of the chi-square goodness-of-fit test on initial loss data .....	125
Table 4-19: List of observed floods used for model calibration and testing .....	127
Table 4-20: Results of model calibration (lumped runoff routing model, La Trobe River catchment) ( $m=0.8$ ) .....	130
Table 4-21: Results of model testing ( $k=53$ , $m=0.8$ ) - Lumped runoff routing model .....	132
Table 4-22: Performance of runoff routing models .....	136
Table 4-23: % difference between estimated and observed hydrographs .....	136
Table 5-1: Statistical properties of observed and simulated storm durations .....	146
Table 5-2: IFD table for observed storms at pluviometer 85237 (unit mm/h) .....	147
Table 5-3: Cumulative relative frequencies of the maximum dimensionless intensity of observed and generated temporal patterns .....	149
Table 5-4: Mean and standard deviation of lag one auto-correlation coefficients of observed and simulated storm temporal patterns .....	152
Table 5-5: 95% confidence intervals of the lag one auto-correlation coefficient .....	152
Table 5-6: Characteristics of observed and generated initial loss data .....	155
Table 5-7: Seasonal probabilities of storm occurrence .....	157
Table 5-8: Design flood estimates for the La Trobe River catchment by Monte Carlo simulation (unit: $m^3/s$ ) .....	159
Table 6-1: Annual flood series - La Trobe River catchment at Noojee .....	165
Table 6-2: Statistical properties of the annual flood series - La Trobe River catchment .....	166
Table 6-3: Flood estimates by direct flood frequency analysis (LPIII distribution) .....	167
Table 6-4: IFD estimates at station 85237 ( $37.88^\circ$ latitude, $146^\circ$ longitude) (unit: mm/h) .....	171

Table 6-5: Design initial loss - La Trobe River catchment.....	172
Table 6-6: Design flood estimates by the Design Event Approach (unit: $m^3/s$ ).....	173
Table 6-7: Summary of design flood estimates obtained from different methods .....	176
Table 6-8: Design flood estimates ( $m^3/s$ ) from variation of design rainfall intensities .....	181
Table 6-9: Design flood estimates ( $m^3/s$ ) from different representations of initial loss .....	182
Table 6-10: Design flood estimates ( $m^3/s$ ) from different numbers of temporal pattern groups .....	183
Table 6-11: Design flood estimates ( $m^3/s$ ) from different values of continuing loss rate .....	186
Table 6-12: Design flood estimates ( $m^3/s$ ) from varying values of the runoff routing model parameter k.....	187
Table 6-13: Design flood estimates ( $m^3/s$ ) from varying values of the design baseflow .....	188
Table 6-14: Design flood estimates from varying sample sizes .....	189
Table 6-15: Tarwin River catchment at Dumbalk North - Summary of design elements used in the proposed Joint Probability Model .....	192
Table 6-16: Design flood estimates for the Tarwin River catchment by different methods.....	194
Table B-1: Studies based on analytical methods .....	231
Table B-2: Studies based on approximate numerical methods.....	234
Table B-3: Studies based on Monte Carlo simulation .....	236
Table D-1: Results of homogeneity tests for 19 recording rainfall stations .....	254
Table D-2: Results of homogeneity tests (station 85103, data from 1956 onwards).....	256
Table D-3: Results of homogeneity tests on observed annual peak flows .....	257
Table G-1: Contingency table for the chi-square test of independence.....	268
Table I-1: Parameter estimation methods .....	281
Table J-1: Summary of distributed models of the La Trobe River catchment at Noojee ( $m=0.8$ ) .....	289
Table J-2: Comparison of URBS and RORB models (test run, the 1963 flood, $m=0.8$ ).....	291
Table J-3: Baker's model - Summary of model testing ( $k_c=30$ , $m=0.8$ ).....	292

## LIST OF NOTATIONS

${}^2I_D$	2-year ARI average intensity of a storm of duration D
A	Catchment area
$A^*$	Constant representing the saturated hydraulic conductivity
$\alpha$	Scale parameter of a frequency distribution (Section 4.4)
$\alpha$	URBS runoff routing parameter (Appendix J)
$a^*, b^*, c^*, e^*$	Dimensionless coefficients
a, b	Lower and upper limits of a data set of initial loss values
$B_4$	Bias correction factor in Hosking and Wallis' method of regional frequency analysis
$\alpha, \beta$	Parameters of the beta distribution
$a_0, c_0, m_0$	Integer parameter values in linear congruential method of data generation
$b_r$	$r^{\text{th}}$ probability weighted moment of a data sample
$\beta_r$	$r^{\text{th}}$ probability weighted moment of a frequency distribution
c	Number of columns in a contingency table
C1	Minimum hourly rainfall defining the start of a gross storm
C2	Minimum hourly rainfall defining the start and end of a net storm
$\chi^2$	Test statistic of the chi-square test
$C_k$	Coefficient of kurtosis
CL	Continuing loss rate
$CL_{5,95}$	5% and 95% confidence limits
$C_s$	Coefficient of skewness
CV	Critical value
$C_v$	Coefficient of variation
d	Duration of a sub-storm
$\delta$	Parameter for determining the standard error of the Pearson III distribution
D	Storm duration
D(F)	Quantile function of storm duration
$d_{av}$	Average flow distance in channel network of sub-area inflows

$D_i$	Discordancy measure for site $i$ in a region
$D_r$	Representative duration
$E(X)$	Expectation of random variable $X$
$E_i$	Expected number of observations in the $i^{\text{th}}$ class interval
$F$	Empirical factor depending on $g$ and $S_d$ (Section 6.4)
$F$	Non-exceedance probability
$f(x)$	Comparison function in rejection method of data generation
$F1$	Overall storm intensity reduction factor
$F2$	Sub-storm intensity reduction factor
$F_X(x)$	Cumulative distribution function
$F_{X,Y}(x,y)$	Joint cumulative distribution function of $X$ and $Y$
$g$	Coefficient of skewness of logarithms of annual flood peaks
$\Gamma(.)$	Gamma function
$H$	Separation time between successive storms
$h$	Dimensionless rainfall depth in a time interval
$H(t)$	Dimensionless cumulative rainfall depth at dimensionless time $t$
$H_i$	Heterogeneity measures for regional data
$I$	Average rainfall intensity
$I_0$	Minimum rainfall intensity of a data series
$I_a$	Initial abstraction in SCS Curve Number method
$IL$	Storm initial loss
$IL_b$	Initial loss of a storm burst
$j$	Rank of a data point in a series (in decreasing order of magnitude)
$k$	Storage delay parameter
$\kappa$	Shape parameter of a frequency distribution
$k^*$	Number of class intervals
$k_c$	RORB runoff routing parameter for a catchment
$k_m$	Median of a data set used in CUSUM test
$k_r$	Coefficient representing relative storage delay time
$K_Y$	Frequency factor (for use with the LPIII distribution)
$l_r$	$r^{\text{th}}$ L-moment of a data sample
$\lambda_r$	$r^{\text{th}}$ L-moment of a frequency distribution
$m$	Parameter representing catchment's non-linearity

$m$	Level of disaggregation in multiplicative cascade (Section 4.6)
$\mu$	Mean of a frequency distribution
$M$	Mean of logarithms of annual flood peaks
$M^*$	Number of data points in a series
$m_1$	Mean of a data sample
MAR	Mean annual rainfall
$\max  V_i $	CUSUM test statistic
$N$	Total number of sites in a region
$n$	Number of observations or time increments
$N^*$	Total record length
$n_j$	Sum of observed cell frequencies of a column in a contingency table
$n_i$	Record length of site $i$ in a region
$n_i$	Sum of observed cell frequencies of a row in a contingency table
$N_{ij}$	Expected frequency of cell $ij$
$n_{ij}$	Observed frequency of cell $ij$
NR	Length of a sequence of random numbers
$N_Y$	Number of years of data to be generated
$O_i$	Number of observations in the $i^{\text{th}}$ class interval
$p$	Number of parameters estimated from observed data
$P$	Rainfall depth
$p(x), p_X(x)$	Probability density function of $X$
$P5$	5-day antecedent rainfall
$p_{X,Y}(x,y)$	Joint probability density function of $X$ and $Y$
$p_{X Y}(x y)$	Conditional density function of $X$ when $Y$ is given
$Q$	Outflow discharge
$q(F)$	Regional growth factor of non-exceedance probability $F$ (dimensionless)
$q(t)$	Infiltration rate at time $t$
$Q_i(F)$	Quantile for non-exceedance probability $F$ at site $i$ in a region
$Q_Y$	Design flood peak of $Y$ -year ARI
$r$	Number of rows in a contingency table
$r_1$	Lag one auto-correlation
$R^2$	Coefficient of determination
$r_a$	Storm advancement coefficient in triangular hyetograph method
$RFI_D$	Average intensity of a storm of duration $D$

$\rho_{X,Y}$	Population correlation coefficient between X and Y
$r_{X,Y}$	Sample correlation coefficient between X and Y
$\sigma$	Standard deviation of a frequency distribution
$s$	Standard deviation of a sample
$S$	Catchment storage
$S^*$	Maximum retention after runoff begins
$S_d$	Standard deviation of logarithms of annual flood peaks
$S_o$	Sorptivity
$\sigma_{X,Y}$	Population covariance of X and Y
$s_{X,Y}$	Sample covariance of X and Y
$t$	L-CV of a data sample
$\tau$	L-CV of a frequency distribution
$T$	Mann-Kendall rank correlation statistic
$\tau$	Superscript denoting transposition of a vector or matrix
$t_c$	Time of concentration
$t_i$	Mid point of a time interval
$t_r$	$r^{\text{th}}$ L-moment ratio of a data sample
$\tau_r$	$r^{\text{th}}$ L-moment ratio of a frequency distribution
$\text{Var}(X)$	Variance of random variable X
$\omega_1$	Average number of events per year
$\omega_2$	Parameter of the exponential distribution
$w_i$	Disaggregation parameters
$\xi$	Location parameter of a frequency distribution
$X_o$	Starting value (the seed) of a sequence of random numbers
$Z^{\text{DIST}}$	Goodness-of-fit measure for regional data

---

## LIST OF ABBREVIATIONS

AEP	Annual Exceedance Probability
API	Antecedent Precipitation Index
ARBM	Australian Representative Basins Model
ARI	Average Recurrence Interval
CRCCHFFA	Cooperative Research Centre for Catchment Hydrology - Flood Frequency Analysis
GcUH	Geomorphoclimatic Unit Hydrograph
GEV	Generalised Extreme Value (distribution)
GLO	Generalised Logistic (distribution)
GP	Generalised Pareto (distribution)
GUH	Geomorphologic Unit Hydrograph
IFD	Intensity-Frequency-Duration
LN	Lognormal (distribution)
LOS	Level of significance
LPIII	Log Pearson III (distribution)
MSIMSL	Microsoft International Mathematical Statistical Library
PIII	Pearson type III (distribution)
SDLM	Stochastic Deterministic Loss Model

## Chapter 1

# INTRODUCTION

This research investigates the overall feasibility of a Joint Probability Model for rainfall-based design flood estimation. The model aims to estimate the frequency distribution of design floods from the joint distributions of rainfall and loss characteristics, taking account of their interactions. The key issue is how to represent adequately the flood production process and the variability and interaction of design inputs so that the model can still be easily applied in practice.

This research addresses this issue by using practical loss and runoff routing models to characterise catchment flood response, representing key flood producing factors by probability distributions (rather than fixed design values), and adopting a simple method to compute the design flood distribution. In particular, it introduces a storm definition that can reflect the great variability of real rainfall characteristics, and examines the dependence of rainfall temporal pattern on season, rainfall duration, and depth. The objective is to realistically represent the characteristics of real rainfall events and real catchment conditions in the flood production process.

## 1.1 RESEARCH BACKGROUND

Design floods are statistical estimates of flood characteristics. These characteristics may include peak discharge, flood volume or time to flood peak. Design flood estimates always correspond to an annual probability of exceedance, which is a measure of the likelihood of a flood characteristic reaching or exceeding a particular magnitude in any given year.

In hydrology, flood estimation can be either estimation of design floods or estimation of

floods resulting from actual rains. To estimate design floods directly from design rainfalls, a hypothetical storm of a specified annual exceedance probability is required. This hypothetical storm is used as input to the design, along with a typical value assumed to represent the catchment condition at the time of the rain. By contrast, to estimate floods at the time of actual rains, real (not hypothetical) rainfalls are used, and actual (not assumed) conditions of the catchment when the rain occurs must be considered in the estimate. Thus, design flood estimation and real-time flood estimation are different in nature, which may result in differences in the choice of flood estimation methods, or in the manner in which parameter values are derived. This research focuses on the estimation of design floods.

Design flood estimation can be undertaken using streamflow-based or rainfall-based methods. The streamflow-based methods are preferred at sites where long observed flow data are available. However, due to the relatively longer period of records, the greater number of locations at which rainfall amounts are observed, and the capability to estimate design flood hydrographs, rainfall-based methods are adopted in the majority of designs. Among these rainfall-based design flood estimation methods, the Design Event Approach is widely used in Australia, as well as in many other countries in the world.

The Design Event Approach aims to estimate a design flood of a specified annual exceedance probability from a design storm event of the same probability. To achieve this objective, several steps are undertaken, as described by Beran (1973), the Institution of Engineers, Australia (1987) and Viessman et al. (1989). In general, the design rainfall intensity of the specified annual exceedance probability for a selected storm duration is firstly determined. This probabilistic rainfall intensity is then combined with representative values of other design inputs and parameters to produce a design flood hydrograph, and the peak flood discharge is extracted. These steps are then repeated for a range of storm durations. The estimated flood peaks are next plotted against the corresponding storm durations, and a smooth curve is drawn through the plotted points. The maximum peak discharge on this curve, corresponding to the critical storm duration, is finally taken as the design flood for the given probability.

The Design Event Approach has long been criticised for its three basic limitations.

Firstly, it underestimates the variability of design rainfall inputs (namely design rainfall duration and temporal pattern) and actual catchment moisture conditions. Secondly, it adopts the critical storm duration concept that has no scientific basis and introduces bias in the probability of the design flood. Finally, in practical applications, it is difficult to select representative values of design inputs in order to correct this probability bias. These limitations result in errors in the magnitude and probability of design floods (Wood, 1976; Bloeschl and Sivapalan, 1997), which bring about significant economic consequences in design and planning.

To overcome the limitations of the Design Event Approach, a number of rainfall-based design flood estimation methods have been proposed. Among these, the Joint Probability Approach is considered to have great potential (Beran, 1973; Ahern and Weinmann, 1982; Institution of Engineers, Australia, 1987; Consuegra et al., 1993). This approach uses the same rainfall-runoff modelling elements as the Design Event Approach, but treats several design inputs and the flood output as random variables, and considers the joint probability of these inputs. Therefore, it can model the variability of design inputs, eliminate the need of determining the critical storm duration, and allow the probability of the design flood to be rigorously determined. Furthermore, the approach can provide significant improvements in rainfall-based design flood estimation in the near future because it can make use of existing data and expertise available in the Design Event Approach.

A review of previous studies of the Joint Probability Approach shows that a great deal of development is still needed before the approach can be applied in practice. This is attributed to many factors, such as their mathematical complexity and limited flexibility, along with the inappropriate selection of the models representing the flood generation process. More importantly, the variability of important flood causing factors and their interactions have still been inadequately considered.

The present research<sup>1</sup> aims to develop and test a Joint Probability Model, based on the

---

<sup>1</sup>This study is a part of project FL1 'Holistic Approach to Rainfall-Based Design Flood Estimation' undertaken by the Cooperative Research Centre for Catchment Hydrology. The overall objective of the project is to explore the potential of some holistic procedures as alternatives to the currently applied Design Event Approach. The project also investigates possible links between the proposed procedures and existing design data by using different definitions of storm events causing floods.

general Joint Probability Approach, for estimating design floods (with average recurrence intervals of 1 to 100 years) from design rainfalls. The proposed model is intended for small to medium sized rural catchments with no significant artificial storage. At this early stage of development, the model aims to determine the flood frequency curve of flood peak magnitude, even though it could also be applied to other flood hydrograph characteristics and to more extreme flood events.

Unlike past studies of the Joint Probability Approach, the proposed Joint Probability Model introduces a storm definition<sup>2</sup> that can account for the great variability of rainfall duration, average intensity, and temporal pattern. The model also considers the stochastic nature of losses from rainfall, as well as the correlations of stochastic design variables. In addition, it adopts a loss model that can not only realistically characterise the runoff production process, but also be easily applied in practice. Even though the ultimate goal is to adopt a distributed runoff routing model to represent the hydrograph formation process, in the current application, the proposed model uses a lumped conceptual model in which the spatial variation of rainfall, loss, and routing effects is neglected.

## 1.2 RESEARCH RATIONALE

Design flood estimates are necessary for two main areas of hydrologic applications: design of hydraulic structures and floodplain management.

For design purposes, estimates of design floods of some specified annual exceedance probability are vital for determining the size of hydraulic structures such as crossroad culverts, drainage ditches, urban storm drainage systems, or spillways of dams. All these hydraulic works are designed on a risk basis with the expectation that the intended structure will only fail due to a flood larger than the one used for the design (Institution of Engineers, Australia, 1987). Consequently, there are two main considerations in the design process.

---

<sup>2</sup> A variant of this storm definition, referred to as storm cores, is also investigated in another sub-project of FLI (Rahman et al., 2001).

The first consideration is the selection of an appropriate probability of the design flood for the intended structure. This essentially involves finding the optimum level of risk for the given design. The optimum risk level can be found by selecting the optimum structure size as that which minimises the total expected cost. This is the sum of structural costs and risk costs. The risk costs include the direct costs of flood and structural damages, and other indirect costs such as traffic interruptions due to floods exceeding the design value. If there were a complete knowledge of floods, it would then be possible to find the optimum design correctly.

The second consideration is the effect of errors in design flood estimates for the selected probability. Uncertainties in the probability of design floods result in errors in the optimum design, either in the form of under-design or over-design of the intended structure. In either case, there are significant economic consequences. For example, in Australia, every year, about \$800-1,000 million is spent on small hydraulic structures sized by design flood estimates, and \$30-40 million is spent on spillway upgrades (Mein, 1995). Thus, if the above structures were over-designed, it would clearly cost the nation millions of dollars. As a result, an improved approach to design flood estimation would certainly lead to significant savings on a national scale. The savings could be in the form of reducing flood damages or costs of structures.

In terms of floodplain management, planners require flood estimates in probabilistic form in order to define the areas that will be flooded at different levels of probability. As a result, the development of industrial or housing projects in high-risk areas can be avoided. However, due to errors in design flood estimates, there are always developments on some flood-prone land. Therefore, flooding continues to cause severe damage to life, property, and the environment, despite considerable efforts and expenditure in the identification of floodplain and flood-prone areas. It is estimated that, in Australia, there is an average annual cost of \$300-400 million due to flood damage (Mein, 1995). Again, better estimates of floods would help to reduce this cost, and thus have remarkable economic benefits.

### 1.3 RESEARCH OBJECTIVES

As briefly discussed in Section 1.1, the main objective of this research is to develop and test a Joint Probability Model for estimating design floods from design rainfalls. To achieve this goal, the present research has the following specific objectives:

- i) To justify the potential of the Joint Probability Approach by critically reviewing the currently used Design Event Approach and other rainfall-based methods for design flood estimation.
- ii) To review and critically assess various derived distribution methods for estimating the design flood probability distribution using the Joint Probability Approach, and select an appropriate method for this present study.
- iii) To develop the elements of a practical, conceptual Joint Probability Model for estimating design floods from design rainfalls.
- iv) To develop a storm definition that can reflect the variability of actual storm events, and examine the correlations of random variables involved in the design, with special emphasis on the dependence of temporal patterns on season of storm occurrence, storm duration and depth.
- v) To apply the proposed Joint Probability Model to estimate the design flood frequency curve for a Victorian catchment, and test it on another catchment.
- vi) To evaluate the performance of the proposed model by comparing its flood estimates with those obtained from other flood estimation methods.
- vii) To investigate the sensitivity of design flood estimates to changes in some design inputs.
- viii) To assess the advantages and limitations of the proposed model and outline future research.

### 1.4 THESIS OUTLINE

The research undertaken to achieve the above objectives is presented in this thesis. An outline of each chapter of the thesis is presented below.

Chapter 2 provides a review of methods for estimating design floods from design rainfalls. In this chapter, the commonly used Design Event Approach is examined and its limitations are discussed. Alternative methods to the Design Event Approach are then investigated. From these alternatives, methods that have the potential to overcome the limitations of the Design Event Approach are identified. The Joint Probability Approach is then examined in detail and various joint probability studies using derived distribution techniques for determining the design flood probability distribution are critically reviewed.

In Chapter 3, a Joint Probability Model for rainfall-based design flood estimation is developed. In this chapter, the deterministic model component (the loss and runoff routing models) is first examined. The development of the stochastic model component is then described. This includes the selection of key design inputs to be considered as random variables, an assessment of the correlations of random design inputs, and the selection of a derived distribution technique for design flood estimation. A research procedure is also presented.

After developing the conceptual Joint Probability Model for rainfall-based design flood estimation, elements of this model are determined in Chapter 4. This chapter firstly describes the collection and verification of data for applying the proposed model. The storm definition used to identify storm events from continuous rainfall records is then introduced. The investigation of the correlations of variables involved in the design, and the development of the frequency distribution of rainfall intensity, the probability distributions of rainfall duration and initial loss, and a stochastic model of temporal pattern are next presented. The determination of parameters of the runoff routing model is then detailed. This chapter concludes with the determination of other fixed design inputs used in the Joint Probability Model. Observed rainfall-runoff data for the La Trobe River catchment at Noojee are used for the above initial analyses.

In Chapter 5, the proposed Joint Probability Model is applied to estimating design floods for one catchment in South Eastern Australia, the La Trobe River catchment. This chapter describes the generation of random numbers from the probability distributions of flood-causing factors determined in Chapter 4. The generation of flood

events using Monte Carlo simulation is then presented. Finally, the determination of the derived flood frequency curve for the specified catchment is documented.

The proposed Joint Probability Model is evaluated in Chapter 6. In this chapter, design flood peaks for the La Trobe River catchment are also estimated by two other methods, namely direct flood frequency analysis and the Design Event Approach. A comparison of these estimates with those obtained from the proposed Joint Probability Model is then presented. Details of the sensitivity analyses carried out to determine the effects on the design flood of changes in some stochastic and fixed design inputs are next described. The chapter concludes with an additional method testing in which the proposed Joint Probability Model is applied to another Victorian catchment, the Tarwin River catchment at Dumbalk North, and the results are discussed.

A summary of the research conducted and the main conclusions that can be drawn from it are finally presented in Chapter 7. This chapter also provides some recommendations for further studies.

## Chapter 2

## REVIEW OF RAINFALL-BASED DESIGN FLOOD ESTIMATION METHODS

### 2.1 INTRODUCTION

A design flood of a specified annual exceedance probability can be estimated by different methods. The type of method selected will depend on the availability of data and the purpose of flood estimates (that is, whether it is for urban or rural catchments, or for the design of major hydraulic structures). Broadly speaking, these methods can be classified as streamflow-based or rainfall-based methods (Figure 2-1). Streamflow-based methods give estimates of floods by analysing observed streamflow data. By contrast, rainfall-based methods estimate design floods from analyses of rainfall inputs, often in conjunction with a rainfall-runoff model that represents a catchment's response to rainfall. Flow data, if available, are also used for estimating or testing parameters of the catchment response model. This project focuses on developing an improved approach for estimating design floods from design rainfalls.

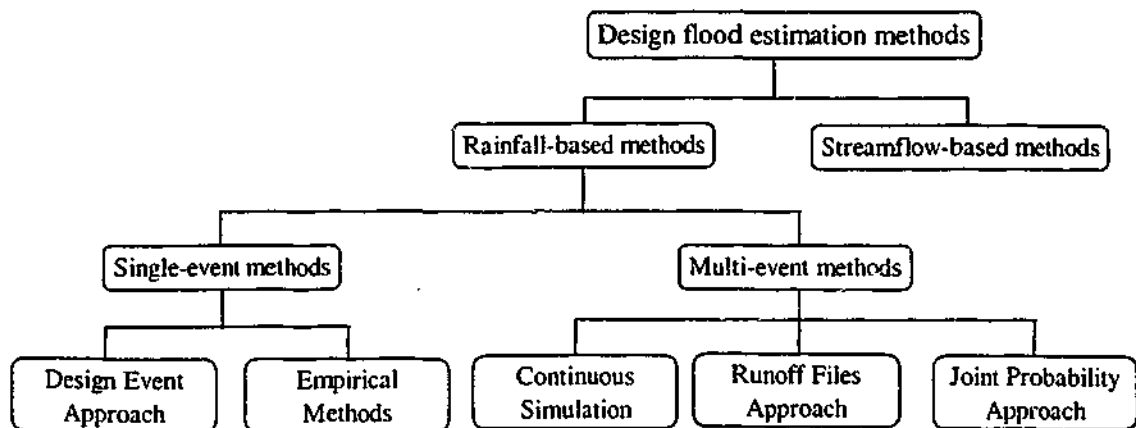


Figure 2-1: General classification of design flood estimation methods

Rainfall-based flood estimation methods can be subdivided into single-event and multi-event methods (Figure 2-1). The former uses a single design rainfall event as input, whereas the latter uses a series of historical or synthetic storms in the calculation. Single-event methods include the Design Event Approach and Empirical Methods, while multi-event methods can be divided into the Runoff Files Approach, Continuous Simulation, and the Joint Probability Approach.

The objective of this chapter is to review the various rainfall-based design flood estimation methods in order to identify their strengths and weaknesses. In this chapter, the widely used Design Event Approach is firstly reviewed. Alternative methods to the Design Event Approach are then examined and the Joint Probability Approach is identified as the most promising option for an improvement in design flood estimation in the near future. The statistical basis of the Joint Probability Approach is next introduced, together with a review of previous studies of the Joint Probability Approach to design flood estimation. This chapter concludes with a discussion of the necessary features of an improved method, based on the Joint Probability Approach, for the estimation of design floods from design rainfalls.

## **2.2 THE DESIGN EVENT APPROACH**

The Design Event Approach is a method currently used to estimate a design flood hydrograph from a design storm. To assess the need for improvements in rainfall-based design flood estimation methods, it is necessary to critically review the Design Event Approach. The procedure, features, and limitations of this approach are examined below.

### **2.2.1 Procedure**

The procedure adopted by the Design Event Approach for estimating a design flood event from a design rainfall event basically involves, firstly, the estimation of the design rainfall input and the rainfall loss due to interception, infiltration, or depression storage,

and subsequently, the routing of rainfall excess through the catchment to produce the flood hydrograph. This procedure, summarised in Figure 2-2, includes the following steps:

- (a) Select the annual exceedance probability (AEP) of the design rainfall. This AEP is assumed to be also that of the design flood.
- (b) Select an arbitrary rainfall duration  $D_i$ .
- (c) For the specified AEP and  $D_i$ , determine the average point rainfall intensity for the location of interest.
- (d) Compute the point rainfall depth for the design event.
- (e) Obtain an areal reduction factor to convert the point rainfall depth into the average rainfall depth over the catchment.
- (f) For the given  $D_i$  and AEP, specify a temporal pattern and a spatial pattern for the design rainfall.
- (g) Select a loss model and its parameters, and compute the rainfall excess hyetograph.
- (h) Select a runoff routing model, determine its parameters and compute the surface runoff hydrograph.
- (i) Select a design baseflow.
- (j) Compute the total flood hydrograph and record the peak discharge.

To determine the critical storm duration and the critical design flood, peak discharges are computed for different storm durations. For the specified AEP, these discharges are then plotted against the corresponding storm durations. A smooth curve is next drawn through the plotted points. The storm duration that gives the maximum discharge of this smooth curve is finally taken as the critical storm duration, and the corresponding peak discharge taken as the design flood for the specified AEP.

### 2.2.2 Features

In the procedure described above, various methods are available for determining the inputs and parameters of a design flood estimation problem (Institution of Engineers, Australia, 1987, Chapters 2, 6-9; Linsley et al., 1988; Viessman et al., 1989). However, there are no definite guidelines on how to select an appropriate value or method for a particular problem. It is common for a designer to have to select an input or parameter

value from a wide range. For example, in the case of Eastern Queensland (Australia), the recommended range of initial loss is 0 to 140mm (Institution of Engineers, Australia, 1987, Chapter 6). This can result in a large variation in flood estimates from the recommended design values of losses. Similarly, other inputs to the design such as the critical rainfall duration, the spatial and temporal distributions of the design storm, or the baseflow can also be determined by many methods or formulas, the choice of which is totally dependent on the various assumptions and preferences of the individual designer.

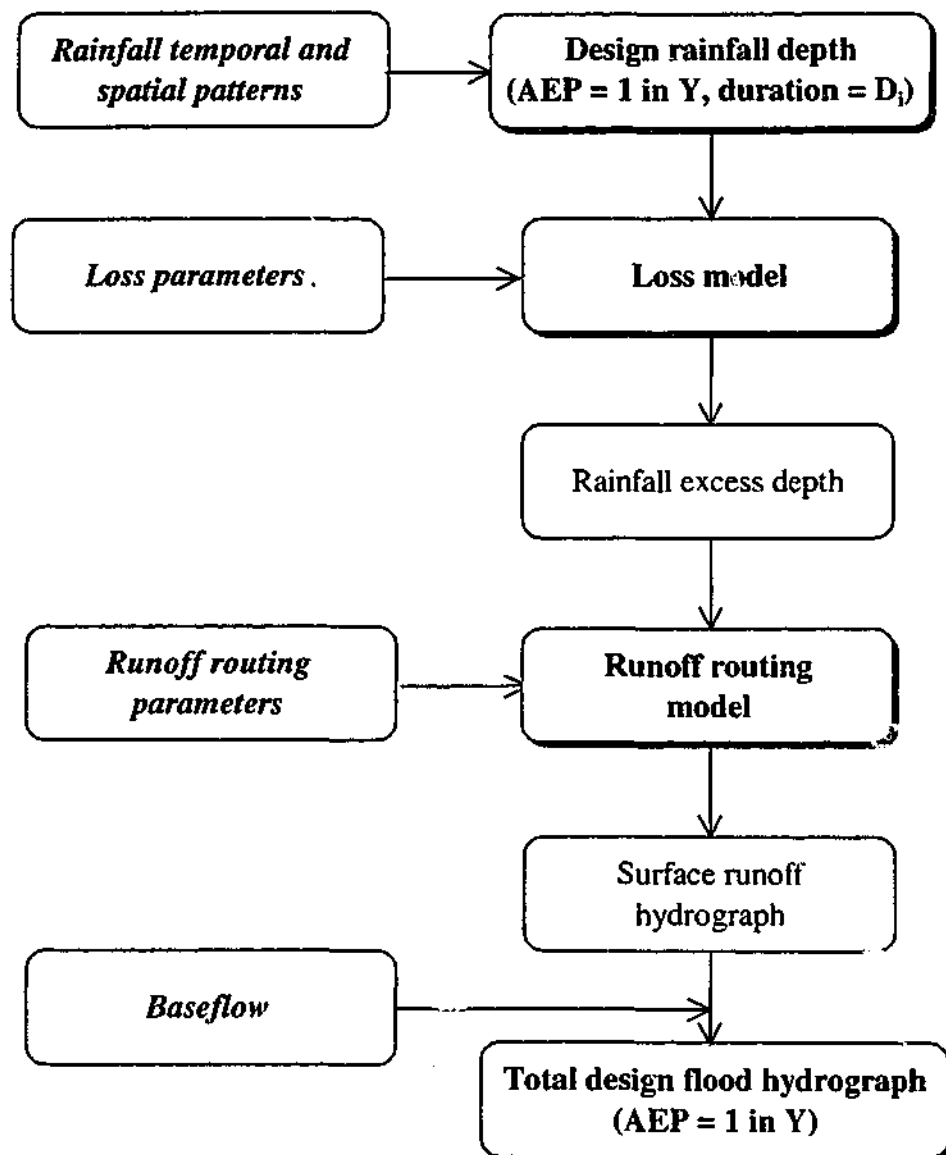


Figure 2-2: Procedure of the Design Event Approach

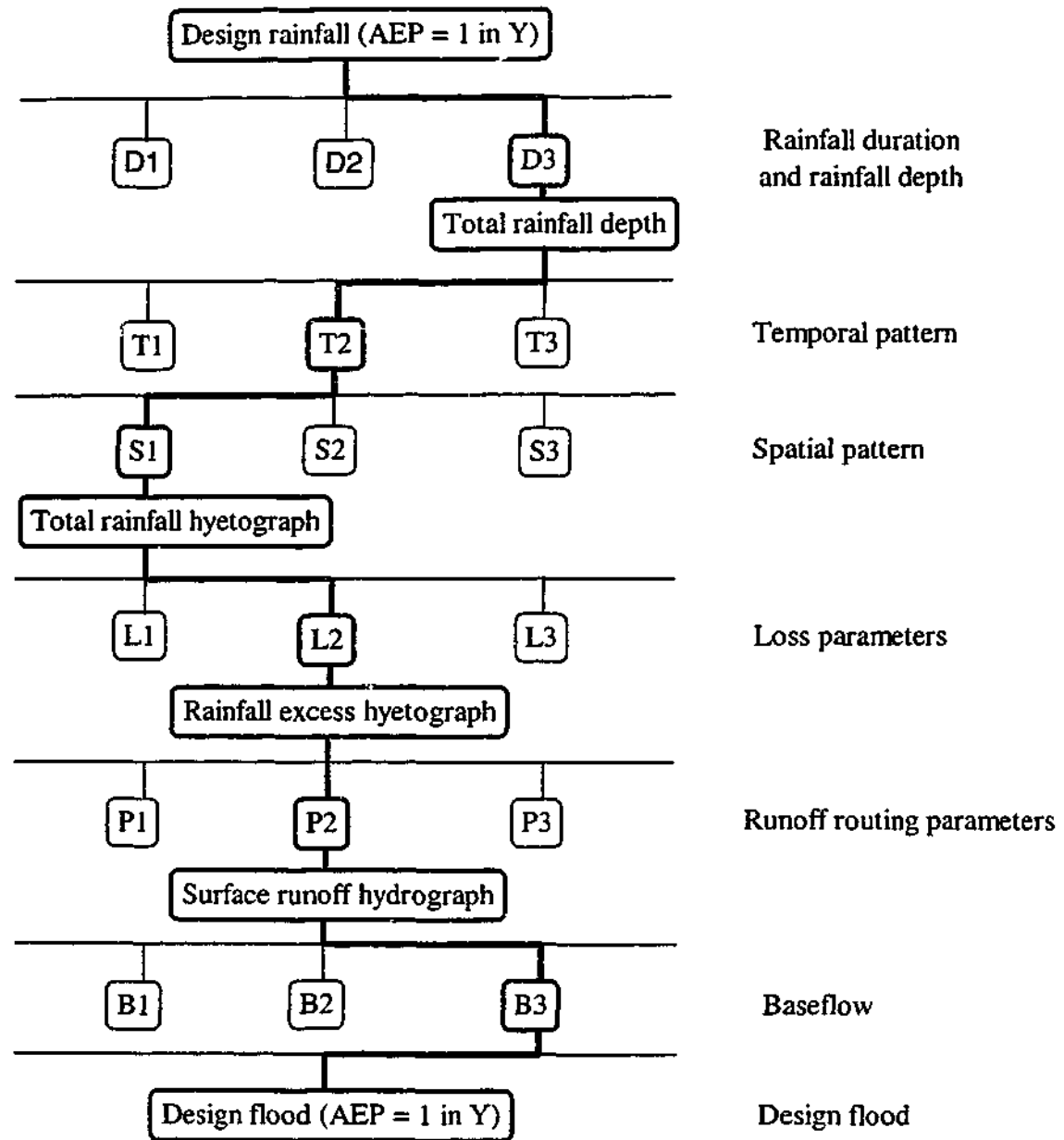


Figure 2-3: Attributes of the Design Event Approach (modified from Beran, 1973)

The uncertainty in input values to design can be illustrated by a tree diagram, as shown in Figure 2-3. This figure represents a practical design situation where the unknown inputs are shown by ranges of values. For example, the storm duration may be D1, D2 or D3, or the storm losses may take on a range of values such as L1, L2 or L3. Thus, there are various ways in which a design rainfall and other inputs can be combined to produce a design flood. However, due to the uncertainty about the correct value of each input in a design situation, designers tend to adopt the median as the representative value for each input, except for the rainfall depth, which is described by a probability

distribution. They assume that adopting these median values will lead to a flood estimate of the same probability as that of the design rainfall. Therefore, the highlighted path in Figure 2-3 illustrates designers' single choice of input values in which the storm temporal pattern is represented by a pattern of average variability, the storm loss is characterised by a median value, and so on.

The discussion above highlights the following two features of the Design Event Approach. Firstly, of the various design inputs, only the design rainfall depth is assumed to have a probability distribution. Other inputs such as the rainfall temporal pattern, duration, losses, or catchment response parameters are represented by constant values. Secondly, the probability of the design flood is assumed to equal the probability of the design rainfall.

### 2.2.3 Limitations

The procedure and features of the Design Event Approach, as discussed above, lead to three basic limitations. The first limitation is the underestimation of the variability of design inputs. It is clear that rainfall event characteristics such as rainfall duration, depth, temporal and spatial distributions are highly variable. The antecedent soil moisture of the catchment at the time of the rain also varies from event to event, not to mention its spatial variation. Therefore, the use of fixed design values for all inputs of the design except the design rainfall depth does not adequately reflect the high degree of variability of actual rainfall events and real catchment conditions, and may lead to serious errors. For example, Wood (1976) proved that a single loss rate used in design does not accurately represent a distribution of catchment antecedent conditions for design flood estimates. He showed that the use of a point estimate for the water loss underestimated the peak discharge for a given annual exceedance probability.

The second limitation is the non-scientific basis of the critical storm duration concept and the probability bias associated with its application in design flood estimation. As explained in Section 2.2.1, the critical duration is the storm duration that gives the *maximum* peak flood magnitude of a specified annual exceedance probability. It varies from catchment to catchment and is influenced by the design inputs that represent

rainfall, loss, and catchment characteristics. The application of the critical storm duration concept in design flood estimation has no sound basis and obviously does not result in an AEP-neutral transformation of design rainfalls into design floods. Instead of preserving the probability of the design rainfall input, the adopted 'worst case scenario' leads to systematic probability bias of design flood estimates. For a given flood magnitude, Bloeschl and Sivapalan (1997) proved that the design flood probability, determined by the Design Event Approach, is overestimated by a factor of at least 2, but this factor may be as large as 10.

The third limitation is the difficulties involved in selecting representative values of design inputs in order to correct this probability bias in practical design problems. As mentioned in Section 2.2.2, in order to satisfy the assumption that the probabilities of the design rainfall input and the design flood output are equal, median values of inputs and parameters (except for the design rainfall depth) are used in design. However, this would be correct only if the rainfall-runoff transformation and the frequency curves of the various transformed inputs were linear. In reality, the linear rainfall-runoff transformation is not observed due to the complex interaction of rainfall, losses, and other catchment attributes such as catchment size, shape, or drainage characteristics. Similarly, the probability distributions of various design inputs are generally represented by complex functions (curves) rather than linear relationships (straight lines). Therefore, the choice of a fixed value for each design input (or parameter) is unlikely to be representative of the particular input in a statistical sense. As a result, the probability bias in the design flood is generally not corrected for, and the true probability of the flood output becomes questionable (Hughes, 1977; Ahern and Weinmann, 1982; Huber et al., 1986).

### 2.3 ALTERNATIVES TO THE DESIGN EVENT APPROACH

To overcome the limitations of the Design Event Approach, several rainfall-based methods for flood estimation can be employed. These methods include Empirical Methods, Continuous Simulation, the Runoff Files Approach, the 'Improved' Design Event Approach, and the Joint Probability Approach. In the following sections, a

general description of each of these methods is given, followed by a discussion of how a particular method can overcome the limitations of the Design Event Approach. General characteristics of each method are also examined, and the best option in lieu of the Design Event Approach is selected.

### **2.3.1 Empirical Methods**

Broadly speaking, Empirical Methods are of a 'black-box' type because they transform rainfall into runoff using techniques that have little or no physical basis. These methods usually use an equation to represent the rainfall-runoff transformation. The coefficients of this equation are determined from rainfall and flood events of the same probability. These events are obtained from frequency analyses of observed rainfall and runoff data. One example of these methods is the Probabilistic Rational Method (Institution of Engineers, Australia, 1987, Chapter 5).

With the Empirical Methods, the uncertainty in the true probability of design floods can be avoided. This is attributable to the fact that design coefficients are determined such that a flood of a selected probability is directly linked with a rainfall of the same probability (James and Robinson, 1986; Institution of Engineers, Australia, 1987). In doing so, effects of other variables affecting floods are said to be automatically considered.

Nevertheless, for practical design problems, Empirical Methods have very limited scope because they give only peakflow estimates and can not eliminate model errors. Furthermore, they can only be applied to catchments which are representative of those used in the original research to derive the original equations (James and Robinson, 1986), making extrapolation of the results very limited.

### **2.3.2 Continuous Simulation**

Continuous Simulation uses deterministic catchment models or rainfall-runoff process models for estimating runoff sequences from rainfalls. More detailed descriptions of

this approach are given by James and Robinson (1986), the Institution of Engineers, Australia (1987), and more recently by Boughton et al. (1999). Generally speaking, Continuous Simulation generates streamflow hydrographs over lengthy periods of time from continuous rainfall and evaporation inputs and continuous modelling of losses. It usually has two essential components: a continuous simulation water balance model (for simulating losses and rainfall excesses during both dry and wet periods) and a runoff routing model (for computing flood hydrographs). A data generation model may also be needed for generating long sequences of rainfall and evaporation data. Time steps used in the simulation usually vary from one hour to one day, sometimes maybe as short as 5 or 15 minutes, and the simulation period is often many years.

Continuous Simulation is regarded as having the potential to solve the limitations of the current Design Event Approach for many reasons. It eliminates the subjectivity in selecting antecedent conditions for the land surface by using a water balance model to compute the soil moisture antecedent to each rainfall event, as described above. It also overcomes the trial and error method for determining the critical storm duration because it simulates the resultant flows for all storms during the year and selects the largest flows as the critical events (Lumb and James, 1976). In addition, it avoids the assumption of equal probability of the causative rainfalls and the resulting floods by undertaking a frequency analysis of the time series of model output to determine the frequency of the parameter of interest (such as peak flowrate or flow volume) (Huber et al., 1986). Finally, it can eliminate the underestimation of the variability of rainfall characteristics by using actual storm events.

Despite these advantages, there are still problems of Continuous Simulation to be dealt with. For example, simulation outcomes are sensitive to many factors, such as the choice of the water balance model, the appropriateness of calibration methods, and the reliability of observed rainfall-runoff data for model calibration (Lumb and James, 1976; Ahern and Weinmann, 1982; Institution of Engineers, Australia, 1987; Boughton et al., 1999). Furthermore, it may be difficult to preserve the serial-correlations of rainfalls and streamflows at short time steps. Finally, continuous simulation models have not yet been developed for applications to ungauged catchments.

### 2.3.3 The Runoff Files Approach

The Runoff Files Approach, described in detail by Lumb and James (1976), is a modified version of Continuous Simulation. It aims to convert a time series of precipitation into a time series of unrouted runoff stored in runoff files for repeated subsequent use. To apply this approach, the study area is first divided into smaller units according to surface characteristics such as land use, vegetal cover, soil types, or landslopes. A continuous water balance model is then calibrated for these units. Precipitation and other climatological data are next input to the calibrated model to simulate runoff. The resulting flood volumes for major storms are then stored on a computer file. A set of runoff files is thus obtained for the study area. These runoff files are then combined according to the distribution of the characteristics of the study area. The combined runoff is finally routed through a runoff routing model to produce the required flood estimates. This approach has been applied in some previous studies, for example, Lumb and James (1976) or Russell et al. (1979).

Compared with Continuous Simulation, the major advantage of the Runoff Files Approach is the exclusion of the cost of repeated model calibration for individual watersheds. Nevertheless, this approach is mainly useful for urban catchments where recurring hydrologic evaluation of land-use control, development of detention storage, or channel modifications, is required.

### 2.3.4 The 'Improved' Design Event Approach

Recognising the fact that one limitation of the current Design Event Approach stems from the uncertainties involved in selecting input values in design, the objective of the 'Improved' Design Event Approach is to compute design floods with better estimates of some of these design inputs or parameters. The approach also converts a design rainfall of a specified annual exceedance probability to a design flood of the same probability, but takes into account the probability distributions of some key design factors (for example the loss parameter) in determining the design flood. In other words, it derives

a distribution of the design flood peak of a specified annual exceedance probability, from which a 'best estimate' and confidence limits can be determined.

A number of research projects were carried out along this line. For example, Haan and Schulze (1987) used a probability distribution to characterise the uncertain behaviour of maximum water abstraction ( $S$ ).  $S$  is the parameter involved in the simple SCS Curve Number equation (Soil Conservation Service, 1972) for peak flow estimates ( $Q$ ). For a given rainfall event of a specified return period, different values of  $S$  were used for estimating  $Q$  and for placing confidence intervals on that estimate. In a much more complicated fashion, the Bayesian theorem was used to analyse the uncertainty of the parameters  $S$  and  $T_p$  (time to peak of the unit hydrograph) (Edwards and Haan, 1989). A few thousand values of peak flows were then computed using the SCS Unit Hydrograph (Soil Conservation Service, 1972) with stochastic inputs of  $S$  and  $T_p$  generated from their corresponding probability density functions.

Although the above methods do offer different ways of improving estimates of individual parameters in the design process, they all still have the fundamental limitation of the current Design Event Approach. That is a design rainfall input of a specified annual exceedance probability is directly converted into a corresponding design flood event of equal probability.

### **2.3.5 The Joint Probability Approach**

The Joint Probability Approach can be broadly defined as the approach to computing the probability distribution of an output from the joint occurrence of random design inputs. It employs a derived distribution method to transfer the joint probability distribution of the inputs to the probability distribution of the output via a transformation function. For design flood estimation, this approach aims to estimate design floods from design rainfalls by considering the stochastic nature of design rainfall characteristics and possible other design inputs, the flood output, their joint probabilities and interactions. It also requires design rainfalls, runoff production and runoff routing models as the Design Event Approach, but allows for the variability of design inputs, avoids the artificial concept of the critical storm duration, and treats

probability effects rigorously. Its rationale is based on the realistic fact that any flood hydrograph characteristics could result from many combinations of circumstances, rather than from a single representative combination as in the Design Event Approach. For example, the same peak flood could result from a moderate storm on a saturated basin or a large storm on a dry basin. Applications of the Joint Probability Approach to hydrology have been described by many authors, for example Laurenson (1974), Ahern and Weinmann (1982), Heideman et al. (1989), or Durrans (1995).

The Joint Probability Approach is considered to be theoretically superior to the Design Event Approach (Institution of Engineers, Australia, 1987; Consuegra et al., 1993) for three main reasons. Firstly, it uses the full range of likely values of key inputs of design and therefore solves the problem of underestimating the variability of design inputs in the Design Event Approach. Secondly, it considers explicitly all possible combinations of storm durations and other inputs to design, and thus does not need to determine the critical storm duration. Finally, it describes the design flood characteristic by a probability distribution, thereby allowing the flood probability to be rigorously estimated.

Regardless of its conceptual superiority, previous studies of the Joint Probability Approach to design flood estimation have not yet been successful in getting the approach adopted for routine applications. This is generally attributable to the mathematical complexity of the proposed approach, the lack of flexibility, the use of inappropriate models to represent the flood formation process, and the inadequate consideration of the variability of important flood causing factors and their interactions.

### **2.3.6 Best alternatives to the Design Event Approach**

It is clear that, of the methods discussed above, only Continuous Simulation and the Joint Probability Approach can fully overcome all the limitations of the current design procedure. That is, both methods can eliminate the subjective selection of antecedent moisture, the estimation of the critical storm duration, and the assignment of equal probability to rainfall and runoff. However, for significant improvements in rainfall-based flood estimation in the near future, the Joint Probability Approach is considered

to be a better alternative because it is more closely related to the current Design Event Approach, therefore, in using this approach, it is possible to make use of a large body of existing experience and data. This research is focused on the Joint Probability Approach.

## **2.4 THE JOINT PROBABILITY APPROACH**

The theoretical basis of the Joint Probability Approach is the derived distribution theory. Applying this theory to design flood estimation, the flood probability distribution can be computed from the joint probability distributions of flood causing factors. In order to provide the necessary theoretical background of the Joint Probability Approach, the derived distribution theory is introduced below. A review of previous studies of the Joint Probability Approach to design flood estimations is also presented. Some other basic statistical concepts relevant to the Joint Probability Approach and the joint probability distribution of random variables are summarised in Appendix A.

### **2.4.1 Derived distribution theory**

The aim of derived distribution theory is to determine the probability distribution of an output random variable  $D$  which is functionally dependent upon one or more input random variables  $A, B, C$  according to the functional relationship:  $D = f(A, B, C)$ . This functional relationship may be in an analytical form or in the form of a conceptual model. The probability distributions of the input random variables  $A, B, C$  and the functional relationship must be specified. For the special case in which at least two input random variables are involved in the estimation of the output distribution, it is also necessary to define the joint probability distributions of the inputs.

In applying the derived distribution theory to design flood estimation, the input random variables  $A, B, C$  may be the design rainfall parameters, loss rates, or baseflow; the output random variable  $D$  being a characteristic of the resulting flood (for example,

peakflow or flood volume); and the functional relationship being a rainfall-runoff-flood hydrograph transformation.

There are three groups of methods for determining the derived distribution of the functionally dependent random variable  $D$ . They are analytical methods, approximate numerical methods, and simulation techniques. In these groups, the model formulation is the same, but the methods used to obtain results are different. Descriptions of these methods can be found in some statistical textbooks such as Benjamin and Cornell (1970) or Haan (1977). A summary of these methods is also given by Weinmann (1994). An outline of each of these groups of methods is presented below.

#### **2.4.1.1 Analytical methods**

Using analytical methods, the probability distribution of the output random variable  $D$  is found by directly applying the principles of probability. In general, its cumulative density function should be determined. This can be done by enumeration if the probability distributions of the input random variables are discrete, or by analytical or numerical integration if the probability distributions of the input random variables are continuous. The density function of the output random variable can then be determined by differentiating the cumulative density function.

#### **2.4.1.2 Approximate numerical methods**

Numerical methods are applied when an analytical approach to determining the statistical distribution of the random variable  $D$  as a function of some random variables  $A, B, C$  becomes difficult or impossible. To simplify the calculation procedure, these methods approximate continuous distributions by discrete ones by dividing the possible range of values of each random variable into class intervals. The discrete distribution characterising each variable is thus represented by discrete points, each of which is the probability that the variable is within a certain class interval. The approximate derived distribution of the output  $D$  is finally found by numerical computation or complete

enumeration of possible input values. The degree of approximation depends on the degree of discretisation adopted, which is the size of the class intervals.

### 2.4.1.3 Simulation techniques

Simulation, often viewed as a "method of last resort" to be employed when everything else has failed (Rubinstein, 1981), may be broadly defined as a technique that involves setting up a model of a real situation and then performing experiments on the model. It is commonly used to describe the operation of a complex system or to identify important variables and how variables interact.

A special variant of simulation is stochastic simulation, also called Monte Carlo analysis (Hammersley and Handscomb, 1964). This is the branch of experimental mathematics concerned with experiments on random numbers. Monte Carlo analysis involves the performance of a sufficient number of repeated experiments to generate a large number of output values. A histogram of results can then be plotted, which approximates the desired probability distribution of the dependent variable. Even though the shape of the plotted histogram remains similar, its details will vary as the number of experiments varies.

The successful application of simulation depends on the appropriateness of the model, the interpretation of the results, as well as on the sophistication of the simulation techniques used (Benjamin and Cornell, 1970).

### 2.4.2 Review of previous studies of the Joint Probability Approach

In hydrology, the Joint Probability Approach has been extensively explored in order to apply it to different problems. For example, this approach was examined to enable the computation of drag loads on offshore structures from the joint occurrence of current profiles and waves (Heideman et al., 1989). It was also applied to compute the joint probability of flows in two tributaries of a stream (Laurenson, 1974), of flood water levels and variations in ocean water levels (Lambert et al., 1994). In addition, it was

used to derive the flood frequency curves for regulated catchments from the statistical distributions of initial reservoir-depths and peak inflows (Laurenson, 1973; Ahern and Weinmann, 1982; Durrans, 1995). For the purpose of this research, however, only previous studies of the Joint Probability Approach which aimed to compute the flood probability distributions from probabilistic characteristics of the causative rainfalls and other flood-causing factors in unregulated catchments are investigated. The derived distribution method adopted in these studies must also involve the transformation of at least two input distributions into the flood output distribution so that the joint probability of the inputs is taken into account.

Depending on the specific derived distribution method used, previous studies on the Joint Probability Approach can be assigned to three groups. These consist of studies based on analytical methods, approximate numerical methods, and Monte Carlo simulation. Recent summaries of these studies have been presented by Sivapalan et al. (1996), Loukas et al. (1996), and Rahman et al. (1998). A review of these studies is given below.

#### **2.4.2.1 Studies based on analytical methods**

The analytical methods have been studied quite extensively to enable the probability distribution of design floods to be computed from the joint probability distributions of rainfall, loss, or catchment response model parameters. Detailed descriptions of these studies, their main characteristics and results are tabulated in Appendix B. In examining these studies, the following conclusions can be made.

In terms of the design rainfall, Eagleson's rainfall model (Eagleson, 1972) has commonly been used to statistically represent point rainfall. This is a simple model that describes rainfall intensity and duration as independent exponential distributions. It ignores both the strong correlation known to be present between rainfall intensity and storm duration, and the temporal variation of rainfall intensity during the storm duration. This model was applied by Eagleson (1972), Wood (1976), Hebson and Wood (1982), Diaz-Granados et al. (1984), Shen et al. (1990), Cadavid et al. (1991), and Raines and Valdes (1993).

With respect to the generation of rainfall excess, a number of loss models have been proposed. These models vary from the very simple constant loss rate (Eagleson, 1972; Hebson and Wood, 1982), and the commonly used SCS Curve Number method (Haan and Edwards, 1988; Raines and Valdes, 1993), to the complicated Philip's infiltration equation (Diaz-Granados et al., 1984; Shen et al., 1990; Cadavid et al., 1991). The runoff coefficient has also been employed (Sivapalan et al., 1996).

To convert the rainfall excess into the flood hydrograph, the kinematic wave model has generally been adopted in some early studies (Eagleson, 1972; Wood, 1976; Cadavid et al., 1991). The unit hydrograph theory seems to have been more commonly used in more recent studies (for example, Wood and Hebson, 1986; Sivapalan et al., 1990; Raines and Valdes, 1993; Sivapalan et al., 1996).

In terms of random variables used in design and the relationship between them, in most of the above mentioned studies, only rainfall intensity and duration have been treated as random variables. The random nature of the infiltration rate or the maximum abstraction from rainfall has only been considered by Wood (1976) and Haan and Edwards (1988). The assumption of statistical independence of rainfall intensity and duration, or of rainfall and loss model parameters has very commonly been adopted (for example, Eagleson, 1972; Wood, 1976; Hebson and Wood, 1982; Diaz-Granados et al., 1984; Wood and Hebson, 1986). The dependence of rainfall intensity on duration has only been considered by Sivapalan et al. (1996).

With regard to the derivation of the flood frequency distribution, it is clear that, in previous joint probability studies based on analytical methods, mathematical expressions for computing design floods have been derived for very specific situations. For example, Eagleson (1972) developed rainfall-runoff equations for V-shape catchments, or Cadavid et al. (1991) used basins conceptualised as two symmetrical planes discharging into first order streams. In addition, the set of equations characterising the flood frequency distribution has been defined, in some cases, by very complicated functions (Hebson and Wood, 1982; Diaz-Granados et al., 1984; Wood and Hebson, 1986). Furthermore, attempts have been made to include in flood frequency behaviour physical properties of catchment and drainage networks (Hebson and Wood, 1982; Diaz-Granados et al., 1984; Raines and Valdes, 1993) or different runoff

generation processes (for example, Eagleson, 1972; Wood and Hebson, 1986; Sivapalan et al., 1990). Despite these efforts, when the derived flood frequency curves were compared with observed flood records, in general, the proposed methods did not perform well. This is mainly attributed to the simplicity of the rainfall model used, and the inaccuracies in estimating parameters of the adopted rainfall and loss models (Eagleson, 1972; Moughamian et al., 1987; Cadavid et al., 1991; Raines and Valdes, 1993). It has been suggested that removal of the assumption of independence of some stochastic inputs (rainfall intensity and duration) may lead to significant improvements in design flood estimates (Eagleson, 1972).

In summary, previous studies of the Joint Probability Approach based on the analytical methods for design flood estimation have not led to successful applications in design practice. While it is clear that the results of these studies enhance understanding of the flood frequency behaviour, and that the flood probability functions for some specific situations can be mathematically formulated, there are many drawbacks in these studies. For example, the solution of the integration of the joint distribution of inputs may be computationally demanding if the input distributions are defined by different functions over different regions. Moreover, in order to allow analytical derivation of the equations representing the design flood distribution, the design rainfall and antecedent catchment conditions are generally modelled in a very simple fashion. The interactions of inputs involved in the design are also ignored. These factors, together with the complicated mathematical equations derived for the resulting floods, make the analytical methods intractable in design situations.

#### **2.4.2.2 Studies based on approximate numerical methods**

Besides analytical methods, there have been many joint probability studies that adopt the approximate numerical derived distribution methods for estimating design floods. General features and results of these studies are summarised in Appendix B. In examining these studies, the following conclusions can be made.

With respect to rainfall models, design IFD curves have been adopted in the majority of these studies. Using the IFD curves, the dependence of rainfall intensity on duration is

taken into account. In some research, the temporal variation of rainfall intensity during storm duration has been considered (Beran, 1973; Goyen, 1983) and its stochastic nature accounted for (Beran, 1973).

In terms of loss models, the SCS Curve Number model has been commonly adopted (Hughes, 1977; Fontaine and Potter, 1993; Consuegra et al., 1993). The infiltration rate has also been employed to compute the rainfall excess (Goyen, 1983).

With regard to runoff routing models, the unit hydrograph is the model most popularly adopted (Beran, 1973; Consuegra et al., 1993). More general rainfall-runoff models such as HEC-1 (Fontaine and Potter, 1993), RAFTS (Goyen, 1983) have also been considered. One advantage of these two models is that they take into consideration spatial variations of rainfall and catchment characteristics.

In relation to random variables involved in design and the relationships between them, rainfall intensity and parameters of the adopted loss models have always been considered as random variables (for example, Goyen, 1983; Fontaine and Potter, 1993; Consuegra et al., 1993). The random nature of rainfall duration or temporal patterns has only been modelled by Beran (1973). The assumption of statistical independence of these random variables has been adopted in the majority of these studies (Beran, 1973; Hughes, 1977; Goyen, 1983; Consuegra et al., 1993).

With regard to the determination of the flood frequency distribution, the Theorem of Total Probability (see Appendix A) has been a popular means for determining the flood frequency curves (Beran, 1973; Laurenson, 1974; Hughes, 1977; Fontaine and Potter, 1993). Application of this theorem to design flood estimation is very easy for cases where random variables involved in the flood generation process are assumed to be independent of one another. A practical implementation of the theorem has been proposed by Laurenson (1974). With this method, any design problem can be solved by dividing the problem into a sequence of consecutive steps. Each step transforms an input probability distribution into an output probability distribution, which becomes the input to the next step. The probability of the output at each step can be calculated using the input probability distribution and a transition probability, which reflects the deterministic components of the system. This method has been applied by Laurenson

and Pearse (1991). In general, application of the approximate derived distribution methods to one or two catchments produced satisfactory results, but a complete verification of these methods by applying them to a variety of catchments is still required. The design rainfall depth and parameters of the loss model have been identified as the most important factors affecting the design flood (Beran, 1973).

In summary, despite the advantages of the joint probability studies based on the approximate numerical methods, these studies need to be further developed and tested before they can be applied to practice. In these studies, many design inputs involved in the flood generation process are realistically represented by probability distributions instead of fixed design values. Design floods and the corresponding probabilities are generally computed using the Theorem of Total Probability or Laurenson's method (Laurenson, 1974). Nevertheless, in applying the approximate numerical methods, it is necessary to discretize continuous random variables, and to conveniently assume that these design random variables are independent of each other. In addition, the variability of design inputs is still inadequately modelled because, in most studies, the stochastic nature of only two random variables (namely the design rainfall depth and loss model parameters) is accounted for. Moreover, the loss and runoff routing models adopted in most of these studies are not commonly used in Australia. Therefore, for an improvement in Australian design flood estimation, the random nature of design inputs other than the rainfall intensity and loss, the correlations of these stochastic inputs, and the application of loss and runoff routing models more appropriate to the Australian environment should be addressed.

#### **2.4.2.3 Studies based on Monte Carlo simulation**

Together with the analytical and approximate numerical methods, Monte Carlo simulation has also been applied to some studies that are based on the Joint Probability Approach for rainfall-based design flood estimation. Detailed descriptions of these studies, their main characteristics and results are tabulated in Appendix B. In examining these studies, the following conclusions can be made.

In terms of the design rainfall, Eagleson's model (Eagleson, 1972) has been adopted by Beven (1987), whereas IFD curves have been employed by Bloeschl and Sivapalan (1997). Alternatively, the Gumbel distribution (also called the Extreme Value type I distribution) has been used to characterise the design rainfall intensity (Muzik, 1993; Loukas et al., 1996). The variation of design rainfall intensity during storm duration has been considered by Beven (1987), and Loukas et al. (1996).

To compute the rainfall excess, the SCS Curve Number method or the infiltration rate has been adopted in a few studies such as Muzik (1993) or Loukas et al. (1996). Complicated models such as the TOPMODEL or the ARNO model have also been recommended (Beven, 1987; Franchini et al., 1996).

To compute flood hydrographs, the unit hydrograph or linear routing method has still been adopted by some authors, for example, Muzik (1993) and Loukas et al. (1996). Nevertheless, more complicated flood routing models such as those included in the TOPMODEL (Beven, 1987) or ARNO model (Franchini et al., 1996) have also been employed.

With regard to random variables involved in design and their correlations, the design rainfall intensity and soil moisture antecedent to rainfall events have always been considered as random variables. The stochastic nature of other rainfall characteristics (either rainfall duration or temporal pattern) has only been taken into account in some studies, for example, Beven (1987), Bloeschl and Sivapalan (1997), or Loukas et al. (1996). Runoff routing model parameters have been treated in a probabilistic fashion only by Loukas et al. (1996). The correlations of some of these random variables have also been taken into consideration. For example, Beven (1987) considered the relationship between discharge and initial soil moisture deficit, Muzik (1993) accounted for the dependence of potential maximum soil moisture storage and antecedent rainfall, and Bloeschl and Sivapalan (1997) adopted IFD curves in which rainfall intensity is a function of storm duration and return period.

In terms of the derivation of the flood frequency distribution, Monte Carlo simulation has been used to compute design floods from various combinations of fixed and variable inputs randomly generated from the corresponding continuous distributions.

For the limited number of test catchments used in these studies, in general, the proposed procedures gave satisfactory results. Nevertheless, there are some cases in which the estimated flood volumes were significantly different from the observed floods, as reported by Loukas et al. (1996), and Muzik (1993).

In summary, like joint probability studies based on the analytical and approximate numerical methods, previous flood studies adopted Monte Carlo simulation still need further developments so that they can be applied in design practice. In these studies, design rainfall characteristics (including intensity, duration, and temporal patterns) and parameters of the loss and catchment response models are characterised by continuous probability distributions, and their correlations are accounted for. Nevertheless, in each individual study, the variability of design inputs is still inadequately modelled, because generally only two or three inputs are considered as random variables. In addition, a linear response of catchments to rainfall is generally assumed. These factors, together with further testing required to verify results in a broader range of situations, are the main reasons that make these studies not readily applicable to flood design practice.

#### 2.4.2.4 Concluding remarks

From the review above, it is clear that for an improved method for rainfall-based design flood estimation based on the Joint Probability Approach, the following factors should be taken into account:

- (a) the incorporation in a single study of all those random inputs that have significant influence on design floods. These inputs may include design rainfall characteristics (intensity, duration, temporal and spatial patterns), loss model parameters and possibly runoff routing model parameters;
- (b) the consideration of the correlations of these design inputs and parameters;
- (c) the selection of a loss model and a runoff routing model that are not only able to realistically characterise the flood generation process but also are simple enough for practical applications;
- (d) the selection of an appropriate derived distribution method (either the approximate numerical methods or Monte Carlo simulation) for design flood estimation; and
- (e) the verification of the proposed procedure in a variety of test catchments.

It would also be desirable to examine the sensitivity of the derived flood frequency curve to the model representation of the above factors, and to estimate the uncertainty in design flood estimates.

## 2.5 SUMMARY

The Design Event Approach is a procedure commonly used to estimate design floods from design rainfalls. The design floods are estimated by assuming equal probability of the flood output and the rainfall input, using representative values for all inputs and parameters to the design (except for the rainfall depth), and adopting a critical storm duration. This design procedure leads to three limitations of the Design Event Approach. The first is the underestimation of the variability of design inputs, in particular design rainfall characteristics and antecedent soil moisture conditions. The second is the non-scientific basis of the critical storm duration concept and the probability bias associated with its application in design flood estimation. The third is the difficulties in selecting suitably representative values of design inputs in order to correct the probability bias in practical applications.

To overcome the limitations of the Design Event Approach, Empirical Methods, Continuous Simulation, the Runoff Files Approach, the 'Improved' Design Event Approach and the Joint Probability Approach can be employed. Of these alternatives, only Continuous Simulation and the Joint Probability Approach have the potential to fully overcome the limitations of the current design procedure. Continuous Simulation generates flood runoff sequences from time series of rainfall and other climatic inputs using a continuous simulation water balance model and a flood routing model. The Joint Probability Approach estimates design floods by adopting the same rainfall-runoff modelling elements as the Design Event Approach but treating key inputs of the design and the flood output as random variables and accounting for their correlations. It is concluded that the Joint Probability Approach has the potential to provide significant improvements in rainfall-based design flood estimation in the near future because, being more closely related to the Design Event Approach, it can make the best use of existing data and experience.

The theoretical basis of the Joint Probability Approach is the derived distribution theory. In design flood estimation, this theory can be applied to compute the flood probability distribution from the joint probability distributions of the flood causing factors using a rainfall-runoff transformation. Three groups of methods can be used to carry out this computation. They are analytical methods, approximate numerical methods, and simulation techniques.

A review of previous studies of the Joint Probability Approach to rainfall-based design flood estimation indicates that the analytical methods are unlikely to be successful in design practice. This is attributable to the fact that the flood probability distributions are developed from simple assumptions about the design rainfall, catchment model, and their interactions, and despite of this, the derived flood distributions are usually very mathematically complicated. The approximate numerical methods and Monte Carlo simulation are more effective means of estimating the probability distribution of design floods. Using these methods, the stochastic nature of rainfall characteristics (duration, intensity, temporal patterns), of catchment wetness antecedent to a rainfall event, or of rainfall losses can be considered and converted into a flood frequency distribution with relatively little difficulty. The correlations of random variables involved in the flood producing process can also be considered. In this way, variables representing both the design rainfall and the catchment response are modelled in a much more realistic way.

For an improvement of rainfall-based design flood estimation using the Joint Probability Approach, it is desirable to consider all the following factors in one single study. These are the incorporation of all the random inputs that have significant influence on the design floods, the consideration of their correlations, the selection of models of rainfall loss and runoff routing that can both realistically characterise the flood generation process and can be readily applied in practice, the selection of an appropriate derived distribution method for practical design flood estimation, and the verification of the proposed procedure in a variety of test catchments. The examination of the sensitivity of design floods to the model representation of the above factors, and the investigation of the uncertainty in design flood estimates would also be desirable.

## Chapter 3

# DEVELOPMENT OF A JOINT PROBABILITY MODEL FOR DESIGN FLOOD ESTIMATION

### 3.1 INTRODUCTION

The estimation of design floods from design rainfalls generally consists of two stages, namely runoff production and hydrograph formation. The objective of the runoff production stage is to compute the depth of rainfall excess (or runoff) from the design rainfall. This is undertaken by subtracting all losses due to interception, infiltration, and depression storage from the total rainfall depth. The objective of the hydrograph formation stage is to convert the rainfall excess hyetograph over the catchment into the flood hydrograph at the catchment outlet. This is carried out by selecting a runoff routing model, routing the rainfall excess hyetograph through the selected routing model, then adding the design base flow.

In the Joint Probability Approach to rainfall-based design flood estimation, each of the above two stages may have both deterministic and stochastic components. For example, the loss model applied in determining the rainfall excess from a specific rainfall input and the runoff routing model to determine the resulting flood hydrograph are the deterministic components. They represent the processes that can be modelled mathematically or graphically without probabilistic statements. By contrast, the characterisation of design inputs such as rainfall intensity, duration, or routing model parameters by probability distributions instead of representative design values, and the determination of the design flood distribution from the joint probability distributions of design inputs, are the stochastic components. It is noted that in the conventional Design Event Approach, the only stochastic component in design flood estimation is the probability distribution determining the design rainfall intensity.

To develop a Joint Probability Model that can improve estimates of design floods, both the deterministic and stochastic components need to be realistically represented. To do this, two stages can be carried out. The first stage is the selection of the deterministic components that can realistically represent the runoff production and hydrograph formation processes. The second stage is the selection of the stochastic components that can reflect the high degree of variability of design inputs, outputs, and their interactions. This stage also includes the selection of an appropriate method for computing the flood probability distribution. The success of this model will depend on its performance and practicability, that is whether or not it can give reliable flood estimates, and can be applied to routine problems.

The stages undertaken to develop a Joint Probability Model for rainfall-based design flood estimation are reported in this chapter. A research procedure for applying and evaluating the proposed model is also described.

## **3.2 DETERMINISTIC ELEMENTS**

Like the currently used Design Event Approach, the deterministic elements of the proposed Joint Probability Model consist of a loss model and a runoff routing model. The selection of these elements is discussed below.

### **3.2.1 Loss model**

In the runoff production process, a loss model is used to compute rainfall losses. The rainfall loss is the part of rainfall that does not appear as direct runoff after a storm. It is caused by interception by vegetation, infiltration into the soil, retention on the surface of the soil (called depression storage), or losses through stream beds and banks (called transmission loss) (Hill et al., 1996a).

Loss models can be broadly classified as infiltration models and practical loss models. A brief review of these models is given in Appendix C. The objective of the infiltration

models is to compute the time varying rate of storm losses at a point through infiltration. Some of the well-known infiltration models include the Horton model (Horton, 1935), the Philip model for computing vertical infiltration into non-layered homogeneous soils with a constant initial moisture content (Philip, 1969), and the modified Green-Ampt model for computing infiltration capacity for different rainfall and surface conditions (Mein and Larson, 1971). In previous joint probability studies, the infiltration rate was used by Wood (1976), Hebson and Wood (1982), and Loukas et al. (1996), whereas the Philip infiltration model was used by Diaz-Granados et al. (1984), Shen et al. (1990), and Sivapalan et al. (1990). Even though infiltration models provide an insight into the infiltration process, they may not be directly applicable to determining the loss of rainfall in flood estimation applications for two reasons. Firstly, they ignore the transmission loss and the rainfall losses caused by interception and depression storage. These forms of storm losses follow different laws from infiltration theory and may be significant under certain circumstances. For example, the interception loss may be a considerable portion of storm losses in regions with dense vegetation, or the depression loss may be significant for deep storage (Linsley et al., 1988). Secondly, it is difficult to accurately estimate a representative value of the infiltration loss on the catchment scale due to the spatial variability of catchment characteristics (such as soil types or vegetation) and limited information.

In routine applications, practical loss models are preferred to infiltration models due to their conceptual simplicity and their ability to approximate catchment runoff behaviour. These are lumped models because they ignore the spatial variation of storm losses during storm duration. The practical loss models include the loss rate model, the proportional loss model, the initial loss – continuing loss (IL-CL) model, and the SCS Curve Number model. Some of these models have been applied in previous joint probability studies for design flood estimation. For example, the constant loss rate was used by Eagleson (1972), and the SCS Curve Number method adopted by Haan and Edward (1988), or Raines and Valdes (1993).

In Australia, the IL-CL model is most commonly used (Institution of Engineers, Australia, 1987; Hill et al., 1996a), and is adopted in this project. The model has two parameters, namely the initial loss and the continuing loss. The initial loss is the rainfall loss that occurs before the commencement of surface runoff, and the continuing loss is

the average rate of rainfall loss during the remaining storm duration (see Figure 3-1). The model can be applied to compute the average loss of rainfall at the catchment or sub-catchment scale.

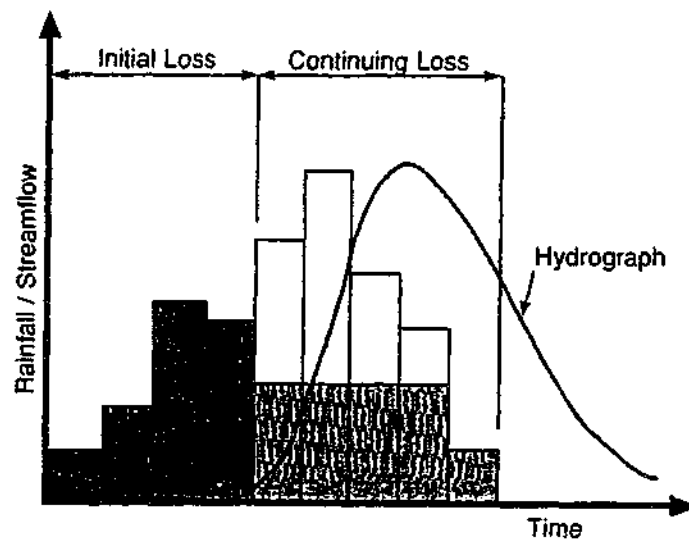


Figure 3-1: Initial loss-continuing loss model (from Hill et al., 1996a)

### 3.2.2 Runoff routing model

In the hydrograph formation process, a runoff routing model is required through which the rainfall excess hyetograph is routed to become the flood hydrograph at any location of interest or at the catchment outlet. Also, baseflow contributions need to be accounted for.

As mentioned in Chapter 2, commonly used runoff routing models in previous derived flood frequency studies are the kinematic wave, unit hydrograph, and geomorphologic unit hydrograph models. Whereas the kinematic wave models ignore attenuation of flood peaks, the unit hydrograph models assume that the rainfall-runoff relationship is linear and (for lumped models) that the rainfall excess is uniform over the entire catchment (Institution of Engineers, Australia, 1987, Chapters 8 and 9). For these reasons, the kinematic wave models and the lumped unit hydrograph models are unlikely to be successful in design practice where simplicity in application is required but the spatial and temporal variations of hydrologic variables and the non-linearity of catchment response should be accounted for to some extent.

In Australia, many runoff routing models are available for computing the flood hydrograph from the hyetograph of rainfall excess. These include RAFTS, RORB, URBS, and WBNM (Institution of Engineers, Australia, 1987, Chapter 9). All of these are distributed and non-linear models because they take into consideration the non-linear response of the catchment, the areal variability of rainfalls and losses, and the distributed nature of the catchment storage. Even though all these models are capable of reproducing realistically the flood transformation process, RORB and URBS are most widely used in design practice. However, neither of these two models could be readily incorporated in the Joint Probability Model for use in this research where Monte Carlo simulation is selected for estimating design floods (see Section 3.3.2). This is attributable to the fact that the current versions of these models are not designed to provide thousands of simulations of design floods in one computer run. Therefore a simple runoff routing model that can be readily incorporated in the present Monte Carlo simulation model is adopted in this study.

The adopted runoff routing model consists of a single, concentrated, non-linear storage at the catchment outlet. The rainfall excess over the catchment is routed through this storage using a non-linear storage routing procedure. The relationship between the storage  $S$  (unit:  $m^3$ ) and the discharge  $Q$  (unit:  $m^3/s$ ) is assumed to be as follows:

$$S = kQ^m \quad (3-1)$$

where  $k$  is a coefficient that determines the storage delay time of the model, but which also depends on the value of  $m$ , and  $m$  is a dimensionless constant, being a measure of the catchment's non-linearity. In this study,  $m$  is assumed to be 0.8, which is the value generally recommended as a first trial value (Laurenson and Mein, 1995).

For simplicity, the adopted model neglects the spatial variations of rainfall and losses over the catchment.

### 3.3 STOCHASTIC ELEMENTS

As explained in Chapter 2, the major difference between the Joint Probability Approach and the current Design Event Approach is the probabilistic treatment of inputs to and

outputs from a model. In this section, key inputs to be treated in a probabilistic fashion are first determined. A method for computing the derived distribution of floods from the distributions of input variables is then selected. Finally, issues related to the correlations of design random variables are highlighted.

### 3.3.1 Determination of key inputs to be treated as random variables

In order to improve estimates of design floods, as discussed in Section 2.4.2.4, it is important to take into account the stochastic nature of design inputs and outputs, and their interactions. Ideally, all design inputs should be treated as random variables. However, it is preferable to consider a smaller number of key stochastic inputs as this reduces the data requirements and makes practical applications easier, without sacrificing much accuracy. The selection of stochastic input variables for this study is described below.

#### Rainfall variables

Real rainfall events vary considerably with respect to rainfall intensity, rainfall duration, the temporal distribution within the event duration, and the spatial distribution of rainfall at the catchment scale. Of these factors, *average rainfall intensity*, the direct input to the rainfall-runoff process, is clearly the most important rainfall characteristic. Its stochastic behaviour has already been characterised by a probability distribution in the current Design Event Approach. Since rainfall events that have the potential to produce floods vary considerably in their duration, the inclusion of *rainfall duration* as a random variable in this study is considered essential.

Besides rainfall intensity and duration, the *temporal pattern* of rainfall is another input that is worth considering as a stochastic input. For a given rainfall depth over a specified duration, the time distribution of rainfall intensity may vary considerably for different storms. In almost all cases, rainfall intensity is distributed non-uniformly during storm duration. Moreover, the pattern adopted can have a major effect on the computed flood (Institution of Engineers, Australia, 1987). There is evidence that flood peaks may differ by up to 50% due to the use of different design temporal patterns (Askew, 1975; Brown, 1982; Wood and Alvarez, 1982; Cordery et al., 1984; Hoang,

1997). In addition, adopted extreme patterns may cause computed flood peaks to vary by up to 2.5 times for heavy rainfalls (Institution of Engineers, Australia, 1987). Viessman et al. (1989) also stated that the shape and peak magnitude of flood hydrographs are affected by temporal patterns of storms. Hence, the rainfall temporal pattern is another important input to be treated as a random variable, especially for small catchments. However, due to the multi-dimensional nature of the temporal pattern, several parameters may be required for its description.

Compared with rainfall intensity, duration and temporal patterns, the modelling of the *areal pattern* of rainfall as a random variable is considered less important in most rural catchments. Moreover, it would generally be difficult to determine the probability distribution of areal rainfall pattern due to limited observed rainfall data at a catchment scale. For these reasons, the rainfall spatial pattern is not modelled in a probabilistic fashion in this project. It might be noted that the deterministic application of temporal and areal rainfall patterns each increases the dimensionality of rainfall intensity by one. For example, in applying a temporal pattern to a constant average rainfall intensity for a given location, average recurrence interval and duration, the rainfall intensity becomes a function of time. The patterns are what Laurenson (1974) called "distributive" parameters as distinct from "concentrative" parameters like initial loss, which would convert the above constant into a different constant. The increased dimensionality adds an order of magnitude to the complexity of the computations.

The *areal reduction factor* applied to rainfall, as mentioned in Chapter 2, converts average point rainfall intensity into average catchment rainfall intensity. It takes account of the random variability of rainfall depth over the catchment. For this study, the use of a single value of the areal reduction factor for a particular rainfall duration, catchment size and average recurrence interval is considered adequate.

### **Runoff production process**

The runoff production process has been recognised as a crucial process in design flood estimation (Cordova and Rodriguez-Iturbe, 1983; Beven, 1987). It is represented by a loss model with one or more parameters. As early as the seventies, the strong impact of the loss parameters on design floods has been highlighted. For example, Beran (1973), in examining the sensitivity of the design flood to alterations to the assumed values of

design input variables, concluded that correct choice of loss rate is the most important. Wood (1976) provided evidence that the use of a constant loss rate instead of a probability distribution underestimates the exceedance probability for a given peak discharge, which may lead to serious design problems. Hoang (1997) also conducted an investigation into the effect of changes in design loss values on design floods for a small catchment in Australia. Results showed that for the test catchment, the peak discharge might increase by up to 120% when an initial loss lower than the median value but within the range of recommended design values was assumed. The strong influence of loss values on design flood estimates is based on the fact that catchment conditions (and therefore rainfall losses) can vary widely, and that a given rainfall occurring on a dry watershed produces considerably less runoff than the same rainfall occurring on a wet watershed. It is thus concluded that the rainfall loss is an important input and should be treated as a random variable in estimating design floods.

As discussed in Section 3.2.1, the initial loss – continuing loss model is adopted in this study for computing the rainfall excess. Of these two parameters, the initial loss reflects the catchment condition at the time of rainfall, and is therefore more variable than the continuing loss rate. Thus, it is considered sufficient to treat only the initial loss as a stochastic variable, whereas the continuing loss rate is represented by a fixed design value.

#### **Hydrograph formation process**

As discussed previously, the hydrograph formation process deals with routing the rainfall excess hyetograph to produce the design flood hydrograph. Factors affecting the hydrograph formation process are runoff routing characteristics (represented by model type, model structure, and model parameters) and baseflow contributions.

It is well known that, in design flood estimation, the problem is more what to route than how to route (Cordova and Rodriguez-Iturbe, 1983). This implies that the variability of runoff routing model parameters and baseflow on flood estimates is of secondary importance compared with that of the runoff production process. There are a number of reasons for this. Firstly, the event to event variability of model parameters may be the result of data errors, or model inadequacy in characterising the non-linearity of the rainfall-runoff process or the true variability in catchment response to rainfall.

Secondly, the selection of an appropriate runoff routing model and procedure can allow a single set of model parameters to be determined for a given catchment with reasonable confidence. Thirdly, except for very small floods, design baseflow generally accounts for only a very small portion of total flood flow. Even though any streamflow hydrograph has a random baseflow component, in reality, the variability in baseflow magnitude is mainly seasonal, and regarded as having a small effect on design flood estimates. Therefore, the stochastic modelling of the parameters representing the hydrograph formation process and base flow is considered as a refinement to the current method that may be examined at a later stage.

### 3.3.2 Selection of a Joint Probability Method

As discussed in Section 3.2, application of the analytical methods to derive the flood frequency distribution is unlikely to be successful in practice. This is attributed to the simplifying assumptions about rainfall, loss, and runoff routing models, the complexity in mathematical equations of the derived flood distribution, and the simplified treatment of the correlations of random variables involved in the design.

The approximate numerical methods and Monte Carlo simulation are considered as much more effective means than the analytical methods to compute the derived flood frequency distribution. With these methods, the design rainfall can be more realistically modelled (that is, the dependence of rainfall depth on duration, or the time variation of rainfall intensity during storm duration can be readily accounted for). In addition, catchment characteristics or catchment conditions at the time of the storm can be examined in a more realistic way. For example, by using distributed runoff routing models, the spatial variation of rainfall and losses over the catchment, or catchment physical characteristics can be modelled; the effects of varying catchment wetness on the computed flood can be accounted for by using an appropriate model to describe it. Moreover, using these methods, if input variables are dependent on one another, their correlations can then be taken into account without much difficulty.

Of the approximate numerical methods and Monte Carlo simulation, the Theorem of Total Probability for computing the flood distribution is the simplest for routine

applications if the assumption of statistical independence of random variables can be justified. If flood causing factors are correlated, Laurenson's general modelling scheme (Laurenson, 1974), or Monte Carlo simulation are the most promising methods. Using Laurenson's method in which a modelling problem can be divided into several modelling steps, each with only two stochastic variables, the complexity in determining the joint probability of three or more correlated random variables can be avoided. With Monte Carlo simulation, probability distributions of input variables are determined first. For each model run, a design flood is then simulated from input values generated randomly from their corresponding distributions. Any significant correlation between inputs can be allowed for through the use of conditional distributions. By running the model several thousand times, a large sample of design floods, and therefore the flood frequency distribution, can be obtained, and the reliability of the results assessed.

For this project, Monte Carlo simulation is selected because it is a general approach that can be applied to both independent and correlated random variables. In addition, a computer program for computing the probability distribution of floods from statistical distributions of flood causing factors is readily available from a parallel study (Rahman, 1999).

### 3.3.3 Correlations of random variables

As discussed in Section 2.4.2, one of the critical elements of the proposed Joint Probability Model is the representation of the variability of key flood causing factors and their correlations. In doing so, characteristics of real observed rainfall events and catchment conditions are preserved in the flood simulation process. By contrast, in the majority of previous studies of the Joint Probability Approach, only two or three design inputs are considered as random variables and their correlations are generally neglected.

With regard to the relationship between rainfall intensity and duration, it was commonly assumed in early joint probability studies that rainfall intensity is statistically independent of storm duration. However, Bloeschl and Sivapalan (1997) argued that this assumption may lead to steep flood frequency curves as a result of unrealistic combinations of high rainfall intensities and long durations. As it is generally accepted

that average rainfall intensity decreases with increasing storm duration, the consideration of this relationship in this present study seems to be indispensable. Eagleson (1972) has also recommended the removal of the assumption of statistical independence between rainfall intensity and duration in order to obtain better design flood estimates.

In the published research of temporal patterns of rainfall, there are conflicting conclusions about the relationship between temporal patterns and season of storm occurrence, storm duration, and storm depth. For example, in the currently used model of design storms in Australia, temporal patterns are developed for different climatic zones, rainfall durations, and average recurrence intervals. This implies that the temporal pattern is dependent not only on location, but also on storm duration, and storm severity. In overseas studies, Huff (1967) showed that dimensionless mass curves of observed temporal patterns in Illinois can be divided into four distinct groups, depending on whether the heaviest rainfall occurs in the first, second, third or fourth quarter of the storm duration. However, in each group, the storm duration and areal mean rainfall account for only a small portion of the variance in the time distribution of rainfall. Moreover, Yen and Chow (1980) and Bonta and Rao (1989) stated that dimensionless hyetographs of storms in summer, dominated by short duration, high intensity convective storms, are markedly different from those of other seasons, particularly long duration, low intensity cyclonic winter storms. By contrast, Garcia-Guzman and Aranda-Oliver (1993) found that the time distribution of rainfall at three stations in Southern Spain is independent of season and amount of rain. Similarly, Robinson and Sivapalan (1997), from an analysis of hourly rainfalls at a catchment in Western Australia, suggested that the rainfall temporal pattern is not correlated with storm duration.

To date, it is thus unclear whether or not the rainfall temporal pattern is dependent on factors such as season of storm occurrence, storm duration or depth. While some authors suggest that the time distribution of rainfall is independent of any of those three factors, most evidence in the literature supports the hypothesis that there is a dependence on at least some of them. Therefore, as a part of the examination of the correlations of random variables involved in design, one of the objectives of the present

research is to investigate the dependence of the rainfall temporal pattern on season of storm occurrence, storm duration or depth.

With regard to the relationship between design storm losses and other input variables, it has been found that the rainfall initial loss increases with rainfall burst duration (Hill et al., 1996a,b). This relationship is examined for the data used in this study, along with the investigation of the correlation between the initial loss and average rainfall intensity. At this development stage, the seasonal variation of the initial loss is not considered.

### 3.4 RESEARCH PROCEDURE

In order to apply and evaluate the proposed Joint Probability Model for design flood estimation, the procedure adopted in this research consists of three major steps, namely determination of model elements, model application, and model evaluation. Each of these steps is outlined below.

The determination of model elements (see Figure 3-2), documented in detail in Chapter 4, starts with the collection and verification of rainfall and streamflow data used in this study. The definition of storm events is next introduced and then applied to derive a database of storm events. A storm definition is required in this research to ensure that storm duration becomes a random variable. The correlations between the random variables involved in design are next investigated. The outcome of this investigation is necessary to assess to what extent it is necessary to develop the conditional probability distributions of design inputs. The probability distributions of rainfall duration and initial loss, the rainfall intensity-frequency-duration (IFD) curves, and a model to generate storm temporal patterns are then determined. Lastly, other fixed inputs of the design (runoff routing model parameters, design continuing loss rate and baseflow) are estimated.

After determining the deterministic and stochastic elements of the proposed Joint Probability Model, Monte Carlo simulation is applied to generate flood events for an example catchment. At this stage, a random value of *storm duration* is generated from

the probability distribution of storm duration. A random *average recurrence interval (ARI)* is then selected and assigned to the design storm with the specified duration. Given the storm duration and ARI, the *average design rainfall intensity* for the design storm is then determined from the IFD curves developed for the design location. Next, a random *temporal pattern* is generated for the design storm of the specified duration and depth. This design rainfall event is then combined with a random value of *initial loss* generated from the probability distribution of the storm initial loss to produce a rainfall excess hyetograph. The design rainfall excess hyetograph is then passed through a runoff routing model, from which a flood hydrograph is determined, and the *peak flood* recorded. By repeating the above procedure thousands of times, thousands of values of floodpeaks are generated. A frequency analysis of the generated floodpeaks is finally carried out to determine the *derived flood frequency curve*. The procedure described above is illustrated in Figure 3-3 and documented in Chapter 5.

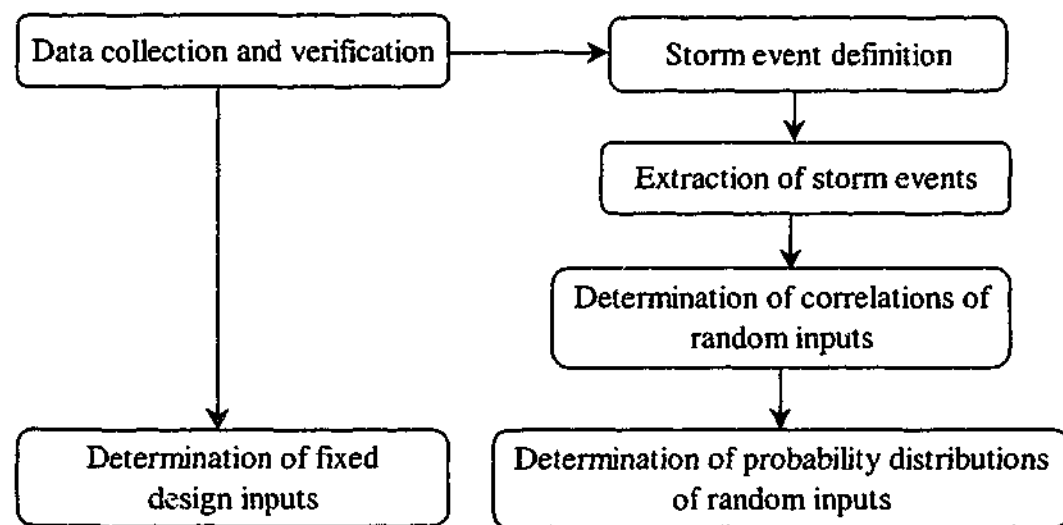


Figure 3-2: Determination of model elements

To evaluate the proposed model for design flood estimation, the generated flood frequency curve obtained by Monte Carlo Simulation is then compared with that obtained from flood frequency analysis and the Design Event Approach (see Chapter 6). The sensitivity of design flood estimates to variations in some stochastic and deterministic design inputs is next examined and some conclusions are drawn on the

reliability of the derived flood estimates. The model is finally tested on another catchment and the results are discussed.

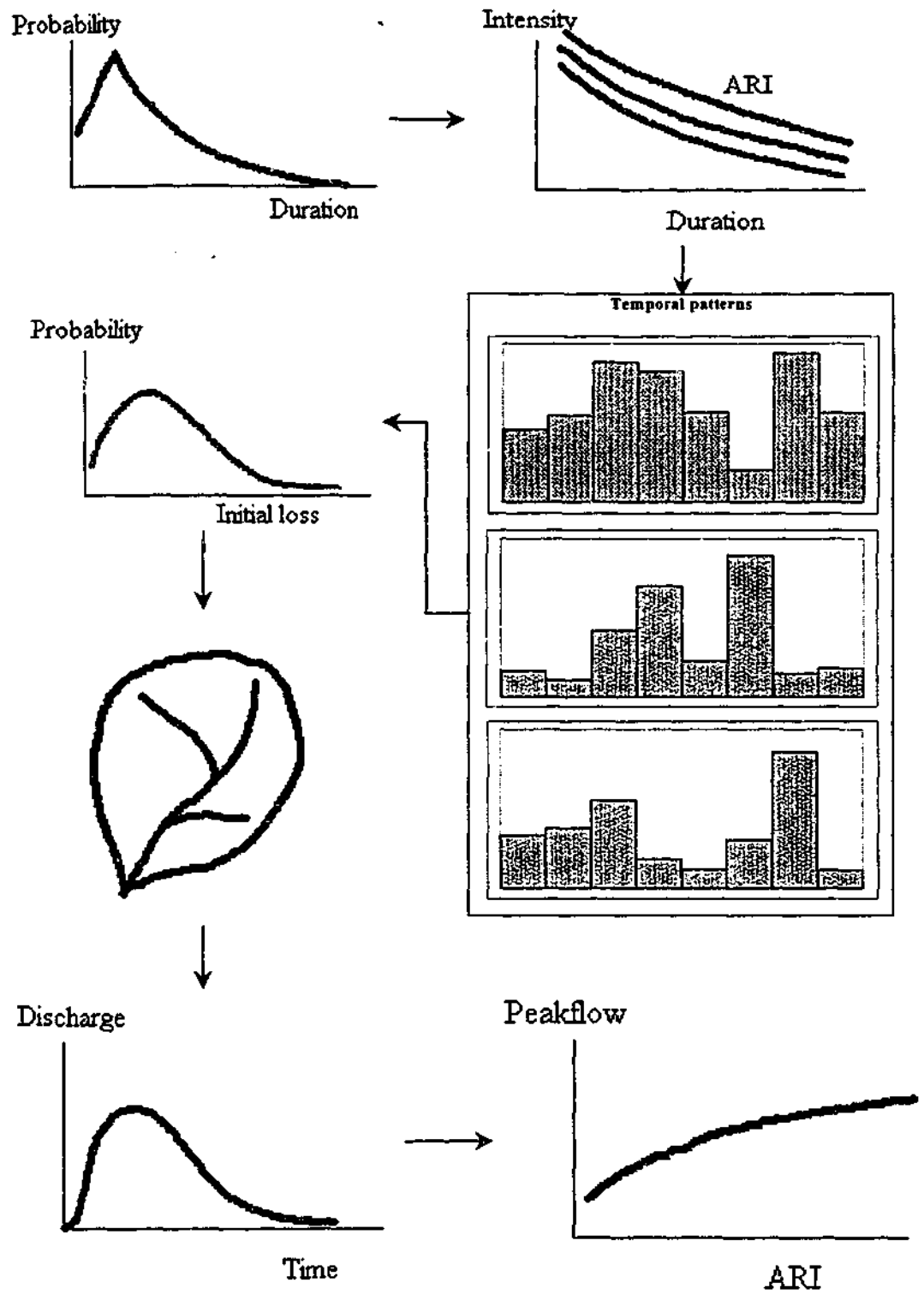


Figure 3-3: Model application

### 3.5 SUMMARY

In this chapter, a Joint Probability Model for rainfall-based design flood estimation is proposed. This model consists of a deterministic component and a stochastic component. The deterministic component uses the initial loss – continuing loss (IL-CL) model for computing a rainfall excess hyetograph from given design rainfall inputs, and a lumped non-linear runoff routing model to convert this rainfall excess hyetograph into a corresponding flood hydrograph. The stochastic component defines the design rainfall intensity, duration, temporal pattern, and initial loss as random inputs, and employs Monte Carlo simulation method to estimate design floods.

A research procedure is recommended for applying and evaluating the proposed Joint Probability Model. This includes the determination of the deterministic and stochastic elements of the proposed model, the application of Monte Carlo simulation for generating design floods for two example catchments, and the evaluation of the proposed model by comparing results with those obtained from flood frequency analysis and the Design Event Approach. In the next chapter, the first step of the procedure, the determination of model elements, is presented.

## Chapter 4

# DETERMINATION OF MODELLING ELEMENTS

### 4.1 INTRODUCTION

The proposed Joint Probability Model for rainfall-based design flood estimation has two components: a deterministic and a stochastic component. The deterministic component includes a loss model for computing rainfall excess, and a lumped runoff routing model for estimating design flood hydrographs. The stochastic component models the statistical behaviour of four important design inputs to the flood generation process (namely the average rainfall intensity, duration, temporal pattern, and initial loss), the flood output, and the interactions of the stochastic inputs.

The objective of this chapter is to document the development of the above stochastic and deterministic components of the proposed Joint Probability Model. In particular, this chapter first describes the selection of test catchments, and the collection and verification of rainfall and streamflow data used in this study. It then introduces the storm definition developed to extract storm events from the rainfall database. The determination of the stochastic elements of the proposed model is presented next. This includes the development of the probability distribution of rainfall duration, the frequency curves of rainfall intensity, the stochastic representation of design temporal patterns and the statistical distribution of storm initial loss. Finally, the derivation of the deterministic modelling elements, including the estimation of the parameters of the lumped runoff routing model and other fixed design inputs, is discussed. For illustration, observed rainfall-runoff data at one Victorian catchment, the La Trobe River catchment at Noojee, were used in this development. Testing of the Joint Probability Model on another catchment is dealt with in Chapter 6.

## 4.2 DATA COLLECTION AND VERIFICATION

For this project, two types of data were needed: rainfall and streamflow data. Observed rainfall data were used to extract storm events from records, from which the probability distributions of rainfall characteristics (duration, intensity, and temporal patterns) were developed. Streamflow data (annual maximum series) were used in the development of the flood frequency curve for evaluating the proposed Joint Probability Model. The derivation of the statistical distribution of the initial loss and the calibration of runoff routing model parameters required concurrent rainfall and streamflow events.

The collection and verification of data necessary for this study include the selection of test catchments, along with the extraction and checking of rainfall and streamflow data. These steps are described below.

### 4.2.1 Selection of test catchments

In order to select test catchments for applying the proposed Joint Probability Model, catchment type, size, and data availability were important considerations. The selected catchments should be rural and have no significant artificial storage. Furthermore, they should be small to medium-sized (up to 500km<sup>2</sup> in mountainous regions, or 1000km<sup>2</sup> in flat areas). In addition, they should have readily obtainable rainfall and streamflow data of good quality and quantity. It is also desirable that the selected catchments cover a wide range of locations, rainfall regimes, or catchment characteristics.

It would have been preferable to select several catchments to apply the proposed model. However, due to the limited project time, only two catchments, the La Trobe River catchment at Noojee (station number 226205C), and the Tarwin River catchment at Dumbalk North (station number 227226) were finally used in this study. These catchments were selected from a database compiled by Hill (1994) because they satisfied the above considerations. In particular, they have relatively long records of streamflow (at least 27 years of data) necessary for flood frequency analysis. Furthermore, observed rainfalls from some recording rain gauges in or near the

catchments were also available for periods concurrent with recorded streamflow. This is an important condition that enables the comparison of rainfall-based flood estimates with those from flood frequency analysis. Due to the small number of catchments selected, the test catchments cover only a limited range of catchment conditions.

The La Trobe River catchment at Noojee (see Figure 4-1), with centroid located at  $37.83^{\circ}$  latitude and  $145.96^{\circ}$  longitude in south-eastern Victoria, is a rural and unregulated basin. It covers an area of  $290\text{km}^2$ , and the length of the mainstream channel, the La Trobe River, is 27.8km. There are a few pluviometers inside this catchment, among which pluviometer 85237 has the longest length of rainfall record (22 years). This catchment is characterised by dense forest (93% of catchment area), relatively high mean annual rainfall (1360mm), and high baseflow (Smith, 1998).

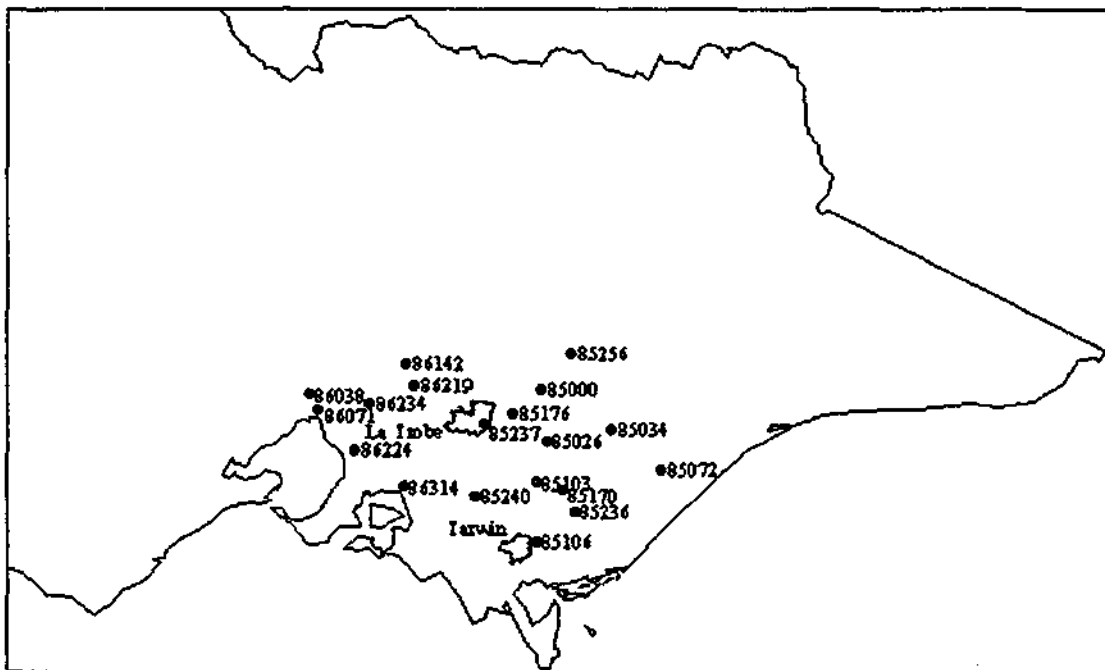


Figure 4-1: Location map of two test catchments and all pluviometers used in this study

The Tarwin River catchment at Dumbalk North (see Figure 4-1) is also a rural and unregulated basin in south-eastern Victoria. Its centroid is located at  $38.51^{\circ}$  latitude and  $146.20^{\circ}$  longitude. The catchment area is  $127\text{km}^2$ , and the mean annual rainfall is 1020mm. There are a few pluviometers in and around the catchment, of which pluviometer 85106 just outside the catchment boundary has the longest record length (22 years).

## 4.2.2 Rainfall data

Observed rainfall data used in this study were extracted not only at pluviometer 85237 (for the La Trobe River catchment) and at pluviometer 85106 (for the Tarwin River catchment), but also at surrounding pluviometers. While the recorded rainfalls at the specified pluviometers may have been sufficient for the derivation of the probability distributions of rainfall intensity and duration, the development of a stochastic model for the rainfall temporal pattern clearly requires a larger database of rainfalls. Therefore, rainfall records at 19 pluviometers in and around the selected catchments were used, not only to facilitate the derivation of temporal pattern distribution, but also to gain an understanding of the variability of other rainfall characteristics. A location map of the 19 pluviometers used in this study is also presented in Figure 4-1.

Recorded rainfalls at six-minute intervals at the 19 pluviometers are stored on a HYDSYS database maintained by the Cooperative Research Centre for Catchment Hydrology (CRCCH). These data can be extracted from the database and cumulated over any time step using the HYDSYS program (HYDSYS, 1994). In this study, a one-hour time step was considered to be a reasonable compromise for rainfall extraction, as longer accumulation periods lead to the loss of information on the temporal variation of rainfall and flood events. On the other hand, the use of finer time steps requires more time for rainfall event extraction and produces very large data files, as rainfall data were recorded over many years at the stations used in this study.

The availability of data stored on the HYDSYS database for the selected 19 recording rainfall stations is summarised in Table 4-1. Station identification numbers (station ID), station names, start and end dates of each record, record lengths and periods of missing data or gaps are summarised in this table. These periods were determined by extracting annual totals of rainfall at a site together with the corresponding data quality codes. Data quality codes are those used by the HYDSYS program to indicate the quality of data stored (for example, codes 1, 80, 151, and 255 denote good continuous data, accumulated data, missing data, and gaps in records, respectively). At some rainfall stations, it is also noted that, there are some years in the record during which annual rainfall totals were zero but flagged with code 1, possibly due to errors in data transcription. For example, at station 85034, the whole year of 1992 was recorded as

having good continuous records, but the annual rainfall total for the year was given as zero. In Table 4-1 this situation is described as "zero rainfall in 1992".

Table 4-1: List of flow gauging sites and 19 recording rainfall stations used and data availability

No.	Station ID	Station name	Start of record	End of record	Record length (years)	Remarks
1	226205C	La Trobe River at Noojee	1961	1995	35	This is a flow gauging station
2	227226	Tarwin River at Dumbalk	1971	1997	27	This is a flow gauging station
1	85000	Aberfeldy	10/1969	08/1984	14	Gaps in 1981-1982 (inclusive)
2	85026	Erica State Forest	04/1959	09/1975	16	Zero rainfall in 1966
3	85034	Glenmaggie Weir	12/1957	11/1993	36	Zero rainfall in 1992
4	85072	East Sale AMO	05/1953	12/1991	39	
5	85103	Yallourn SEC	11/1949	01/1972	24	
6	85106	Oisens Bridge	01/1957	12/1978	22	
7	85170	Traralgon L.V.W	08/1961	12/1975	15	
8	85176	Tanjil Bren PO	06/1957	12/1979	22	Gap in 1960
9	85236	Callignee North	08/1961	12/1975	14	Zero rainfall in 1973
10	85237	Noojee Eng. HMSD	03/1959	12/1980	22	
11	85240	Ellinbank	08/1961	12/1993	32	Gap in 1969
12	85256	Barkley River	04/1974	11/1993	19	Gap in 1992
13	86038	Essendon Airport	02/1951	11/1986	36	
14	86071	Melb. Regional Office	04/1873	07/1997	109	Gaps in 1996-97; zero rainfall in 1874-1876, 1995, and 1915-1924.
15	86142	Mt. St Leonard	01/1954	01/1983	30	
16	86219	Coranderrk	12/1955	12/1977	23	
17	86224	Dandenong Composite	01/1965	10/1991	27	
18	86234	Croydon South	04/1965	10/1991	24	Gap in 1976-1978
19	86314	Koo-Wee-Rup	01/1957	12/1991	35	
				Min	14	
				Max	109	
				Average	29.4	

In the present study, in order to ensure the quality of outputs, only periods with good continuous records were included in the analysis, whereas periods with missing or accumulated data, gaps, or errors in data transcription were not taken into consideration. The accumulated data were discarded because they were considered of very little use, especially in the analysis of rainfall temporal patterns. For the 19 recording rain gauges, it is evident from Table 4-1 that the record lengths of these good data vary from a minimum of 14 years to a maximum of 109 years, with an average of 29 years. It can also be seen in Table 4-1 that most of the pluviometers used only have concurrent data of 15 years from 1961 to 1975. However, possible effects on the regional analysis of part of the pooled data coming from non-concurrent rainfall periods are considered small and therefore neglected in this study.

Before deriving the statistical distributions of rainfall characteristics, it was considered essential to check the homogeneity<sup>1</sup> and consistency<sup>2</sup> of these observed rainfall data. The importance of data verification has long been emphasised in the literature. For instance, the WMO (1966) stated that "homogeneity can not be taken for granted; indeed, it can be safely assumed that any series longer than 10 or 20 years has some kind of inhomogeneity in it, and possibly several kinds". Linsley et al. (1988) and Hosking and Wallis (1997) confirmed that before beginning any statistical hydrologic analysis, it is important to be sure that the data are homogeneous. Further support is given by Stedinger et al. (1993) who warned users of precipitation data about possible errors in data collection caused by wind effects, changes in station environments and observers, and stated that precipitation data should be checked for outliers and consistency. Searcy and Hardison (1960) also confirmed that a consistency check is one of the first steps in the analysis of a long record.

In order to check the homogeneity of rainfall at each individual station, a combined procedure using both graphical and statistical methods was employed in this research. The graphical technique, in the form of time-series plots, enabled a quick visual detection of any apparent trend or change in the mean value in the plotted series. The CUSUM test for discontinuity (McGilchrist and Woodyer, 1975) and the Mann-Kendall rank correlation test for trend (WHO, 1966) were then used to verify the conclusions obtained from the time-series plots, as well as to compute the statistical significance of any departure from homogeneity. These tests were applied to annual series of maximum daily rainfalls at each of the 19 rainfall stations. Details of the tests, the procedure used to check the homogeneity of rainfalls, together with test results are presented and discussed in Appendix D. Results of the homogeneity tests showed that the observed rainfall data at station 85103 from 1956 onwards, and at other 18 pluviometers during their periods of record satisfy the requirement of homogeneity. It was then assumed that the conclusions from the homogeneity tests on daily rainfall data also apply to the hourly data observed at the same sites.

---

<sup>1</sup>The requirement of homogeneity is that data should be drawn from the same statistical distribution.

<sup>2</sup>The requirement of consistency is that types and techniques of measurement or the manner of data processing should be consistent.

Checking of the consistency of rainfall data was carried out for rainfall events extracted from the rainfall database. As the event definition used in this study is introduced in Section 4.3, the consistency check of the extracted events is also described in the same section.

### **4.2.3 Streamflow data**

Streamflow data used in this study are those recorded at station 226205C (at the outlet of the La Trobe River catchment at Noojee) and station 227226 (at the outlet of the Tarwin River catchment at Dumbalk North). Like observed rainfall, observed streamflow data are stored on the HYDSYS database.

The availability of streamflow data stored on the HYDSYS database for the specified flow gauging sites is also summarised in Table 4-1. It can be seen from this table that recorded flow data are available for 35 years (from 1961 to 1995) for the La Trobe River catchment, and 27 years (from 1971 to 1997) for the Tarwin River catchment.

Like rainfall data, observed streamflow data at the two catchments under study were also checked for homogeneity. The CUSUM and Mann-Kendall tests were applied to annual maximum instantaneous flows at each of the two sites. Test results, tabulated in Appendix D, indicated that there is no evidence to reject the assumption of homogeneity of the recorded flow data at these two sites.

### **4.2.4 Summary**

To apply and evaluate the proposed Joint Probability Model for design flood estimation, two catchments and 19 recording rain gauges were selected. The selected test catchments were the La Trobe River catchment at Noojee (station number 226205C) and the Tarwin River catchment at Dumbalk North (station number 227226). The 19 selected pluviometers were in and around these test catchments. The La Trobe and Tarwin catchments have 35 years of flow data (from 1961 to 1995), and 27 years (from 1971 to 1997), respectively, whereas record lengths at the 19 pluviometers range from

14 years to 109 years, with an average of 29 years of data. These observed rainfall and streamflow data are stored on the HYDSYS database.

In this study, the verification of observed rainfall and flow data for homogeneity and consistency was considered essential to make sure that the data were drawn from the same probability distribution at any given site. To achieve this, annual series of maximum daily rainfalls at each of the 19 rainfall stations and annual maximum instantaneous flows obtained at the flow gauging stations were checked for homogeneity over time. Test results indicated that the observed rainfall and flow data at the selected stations satisfy the requirement of homogeneity. Checking of the consistency of rainfall data was carried out for storm events extracted from the rainfall database and is described in Section 4.3.

### **4.3 STORM EVENT DEFINITION**

#### **4.3.1 Overview**

Application of the proposed Joint Probability Model involves the generation of rainfall and flood events that will simulate observed events. Before the statistical distributions of these event characteristics can be determined, it is necessary to develop a clear concept of what is meant by an 'event', that is, to come up with an event definition. For the case of rainfall, once a storm event is clearly defined, these events can be extracted from the rainfall database and their characteristics (intensity, duration, and temporal patterns) analysed. Additional checking of the extracted events is then necessary to ensure the requirement of consistency for statistical analyses is satisfied.

There are various ways to define a storm event. For example, Huff (1967) described a storm as a rain period separated from preceding and succeeding rainfall by 6 hours or more. He used all storms in which the network average rainfall exceeded 0.5 inch, and/or one or more gauges recorded over one inch. In another study, Beran (1973) defined the beginning of a storm as the onset of rain, and the end to be when there was less than X mm of rain in the preceding Y hours. X and Y were chosen to represent the

conditions under which a flood hydrograph would return to near baseflow and to allow short spells of zero rainfall to occur within a storm event. Other researchers such as Yen and Chow (1980), Istok and Boersma (1986), and Sivapalan et al. (1996) simply defined storms as periods of rain separated from each other by at least one, six, and two hours of zero rainfall, respectively. Thus, it can be seen that, in order to define a storm event, the start and end of the event must be specified. Additionally, a threshold average rainfall intensity (or depth) may also be required to exclude small events that are insignificant in producing flood runoff.

This section first details the development of a storm definition used in this research. It then describes an application of the adopted storm definition to extract storm events from the time series of observed hourly rainfalls at the 19 selected rainfall stations. Finally, it outlines the verification of the extracted storm events for consistency.

### **4.3.2 Development of storm definition**

For the purpose of this study, three criteria were used to define storm events. Firstly, they are mutually exclusive stochastic events so that storm duration becomes a random variable. That is, any wet spell contributes only a single data point to the frequency distribution of each rainfall characteristic. Secondly, the events must have the potential to produce significant runoff. In other words, the average rainfall intensity during the duration of an event should exceed some threshold value. Lastly, the events should exclude periods of insignificant rain at the start or end of the rainfall period. A storm definition to satisfy these three criteria was developed in the four steps outlined below.

#### **4.3.2.1 Start and end of storm events**

In the literature, the start of a storm event is usually the onset of rain after a minimum separation time from the previous event. This separation time represents a rainless or 'dry' period when no significant rainfall occurs. The end of the event is also defined by the separation time.

There are different methods for determining the separation time between storms. Some examples are the combined rainfall-streamflow analysis (Beran, 1973), the 'critical duration' method (Bonta and Rao, 1988), and the subjective method (Huff, 1967; Yen and Chow, 1980; Nguyen and Rousselle, 1981; Sivapalan et al., 1996). With the subjective method, the break between individual events can be subjectively chosen, say at least one hour (Yen and Chow, 1980; Nguyen and Rousselle, 1981), two hours (Sivapalan et al., 1996), or six hours (Huff, 1967; Istok and Boersma, 1986). This method is the simplest for practical applications, and therefore was adopted for determining the separation time between storms used in this study.

Using the subjective method for determining the event separation time ( $H$ ), first of all, a storm was preliminarily defined as beginning with a non-zero hourly rainfall and being separated from the previous and the next events by at least  $H$  hours of no rain. In order to determine an appropriate value of  $H$ , an exploratory analysis was then carried out for observed hourly rainfalls at pluviometer 85237. Three values of  $H$  (1, 3, and 6 hours, minimum) were tried. Results of the exploratory analysis indicated that, *as  $H$  increases, the size of the resulting storm sample decreases but the mean and the maximum storm durations increase*. In examining the extracted events, it can be seen that some periods of no rain can occur within storm events separated by 3 hours or 6 hours. However, the use of the separation time  $H$  of one hour tends to produce many very short events (with duration of 1 or 2 hours) that are very likely to belong to the same weather mechanism.

From the results of the exploratory analysis, the minimum separation time of six hours of *no rain* between successive storms was preliminarily selected as the most suitable for the catchment sizes used in this study (290km<sup>2</sup> and 127km<sup>2</sup>). This separation time tends to produce long duration storms (with average duration of at least 15 hours) which are generally more responsible for producing runoff for the given catchment sizes. In addition, it avoids breaking up storms of the same weather system into separate, very short and small events.

#### 4.3.2.2 Storm threshold intensities

To eliminate small storms that are not able to produce floods, a threshold average

rainfall intensity was required. This threshold intensity could be selected as a constant, or as a function of storm duration. However, it is reasonable to vary the average threshold rainfall intensity with storm duration, as high average intensities are often associated with short duration storms and vice versa. In this research, for convenience, the 2-year ARI average rainfall intensities of various durations at the design location, as provided by the Institution of Engineers, Australia (1987, Chapter 2), were used as the basis for computing two threshold intensities for storms obtained from the record at that location.

The first threshold intensity was defined to be the product of the overall intensity reduction factor ( $F_1$ ) and the 2-year ARI average intensity ( ${}^2I_D$ ) for a storm of duration  $D$  at the design location. Using this threshold value, a storm event, separated from the previous and the subsequent events by at least six hours of no rain, was included in the storm sample if its average intensity ( $RFI_D$ ) during the whole storm duration ( $D$ ) satisfied the following condition:

$$RFI_D \geq F_1 \times ({}^2I_D)$$

where  $0 < F_1 < 1$ .

However, in the storms that were discarded from the above selection process on the basis of average rainfall intensity over the whole storm duration, there could have been storms that had some internal periods of intense rain. Such storms may have caused a rise of flood hydrographs if the catchment surface was already wet, and therefore were worth included in the rainfall analysis. To include such storms, the concept of sub-storms was required.

A sub-storm of duration  $d$  was defined as  $d$  successive hourly periods during a given storm of duration  $D$ , on the condition that  $d < D$ . For example, in a storm of four-hour duration ( $D = 4$  hours), there are four sub-storms of one hour, three sub-storms of two hours, and two sub-storms of three hours. In other words, a complete sample of sub-storms having a duration  $d$  within a storm of duration  $D$  is an overlapping series of all sub-storms lasting  $d$  hours. Figure 4-2 illustrates how sub-storms of two hours can be formed within a rain period of four hours.

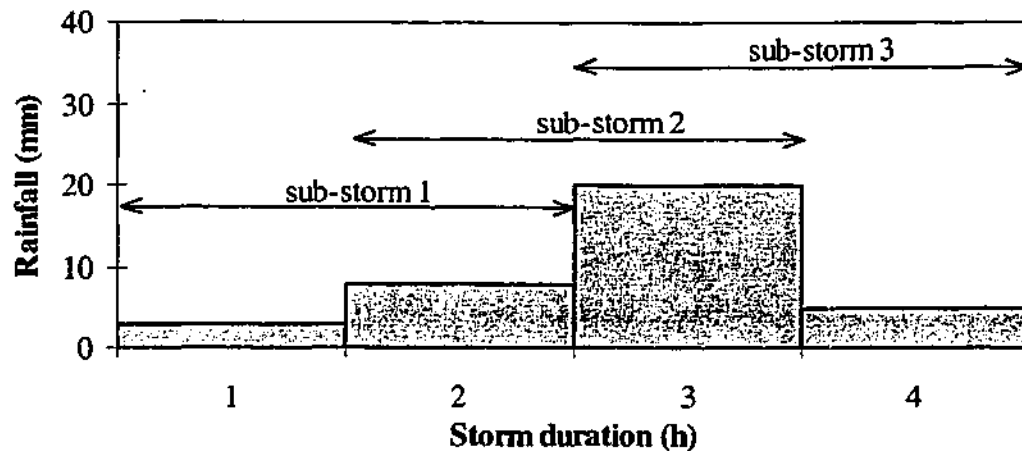


Figure 4-2: Formation of sub-storms of 2 hours within a storm of 4 hours

To select extra storms that have relatively low average intensity but include periods of intense rain, a second threshold average rainfall intensity was used. This threshold intensity was defined to be the product of the internal sub-storm intensity reduction factor ( $F2$ ) and the 2-year ARI average intensity for a sub-storm of duration  $d$  at the design location ( ${}^2I_d$ ). Thus, a storm was also selected if the maximum average intensity from all sub-storms of duration  $d$  ( $RFI_d^{\max}$ ) satisfied the following requirement:

$$RFI_d^{\max} \geq F2 \times ({}^2I_d)$$

where  $F2 > 0$ .

This requirement was checked for all values of sub-storm duration  $d$  ( $d < D$ ).

In order to determine numerical values for  $F1$  and  $F2$ , an exploratory analysis was again carried out using hourly rainfall records at pluviometer 85237 inside the La Trobe River catchment. In this analysis, to extract storm events from the record, the minimum event separation time of six hours of no rain was used with various combinations of  $F1$  and  $F2$ . The values of  $F1$  used ranged from 0.3 to 0.7 at 0.1 increments, and the values of  $F2$  were 0.3 to 0.6 at 0.1 increments. For some cases,  $F2$  of 100 was also used (for reasons explained below).

From the results of the exploratory analysis, two important conclusions were drawn. Firstly, the values of the intensity reduction factors  $F1$  and  $F2$  directly affect the number of storms in the storm sample, and therefore the 'quality' of the extracted storms. *The*

*lower the intensity reduction factors are, the bigger the storm sample becomes, but this sample may also include storms that have relatively low average intensities.* In other words, the use of low threshold rainfall intensities produces more storms that may be insignificant in producing runoff, and vice versa. Secondly, in order to include additional storms that may have some potential in producing runoff, it is necessary to set F2 not too high. For example, the number of storms obtained using F1 of 0.5 and F2 of 100 is equal to the number of storms obtained using only F1 of 0.5. This is because the second threshold intensity is so high that no additional storms can be selected.

Results of the exploratory analysis for station 85237 indicated that any of the following four combinations of F1 and F2 would be appropriate. They are F1=0.4 and F2=0.5, F1=0.4 and F2=0.6, F1=F2=0.5, and F1=0.5 and F2=0.6. On average, each of these combinations gives about 4 to 7 storms per year.

In order to determine the best combination of F1 and F2 for the 19 rainfall stations in the test region, a sensitivity analysis was also carried out. In this analysis, the above four combinations of F1 and F2 determined for station 85237 were applied to extract storm events for the other 18 sites. Results of this analysis showed that these combinations gave an average of about 5 to 7 events per year per station. For this study, the combination of F1=0.4 and F2=0.5, giving an average of 7 events per year per station, was adopted.

#### **4.3.2.3 Visual check of the extracted events**

After determining the separation time and the intensity reduction factors for defining storm events, the next step was to visually check the extracted events. This was carried out by plotting all storms in the sample obtained at pluviometer 85237 and visually examining them. Results indicated that, whereas there were mostly 'normal' storms in the sample (see an example in Figure 4-3), a number of storms could be considered as 'abnormal' (see examples in Figure 4-4). These are the storms that have lengthy periods of insignificant rain at the start or at the end of the storm, or even during the storm duration. For flood analysis, these periods could be considered as unimportant in producing runoff. Therefore, the storm definition had to be refined.

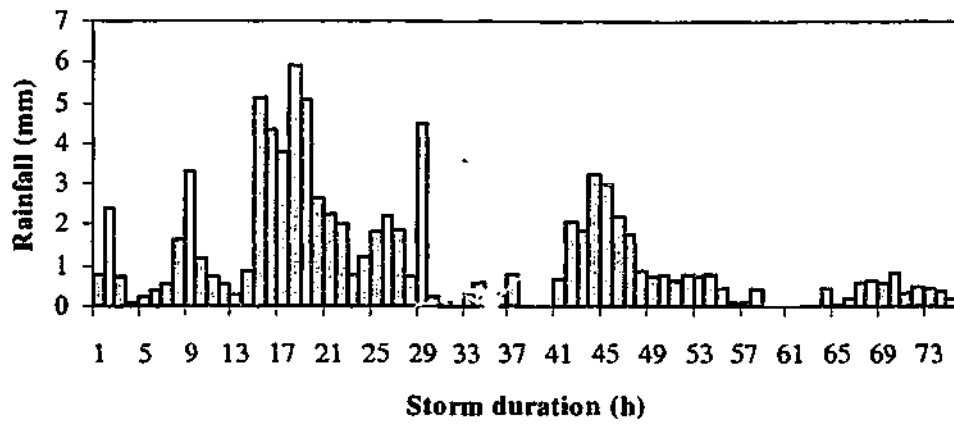


Figure 4-3: Example of a 'normal' storm (station 85237, H=6 hours, F1=0.4, F2=0.5)

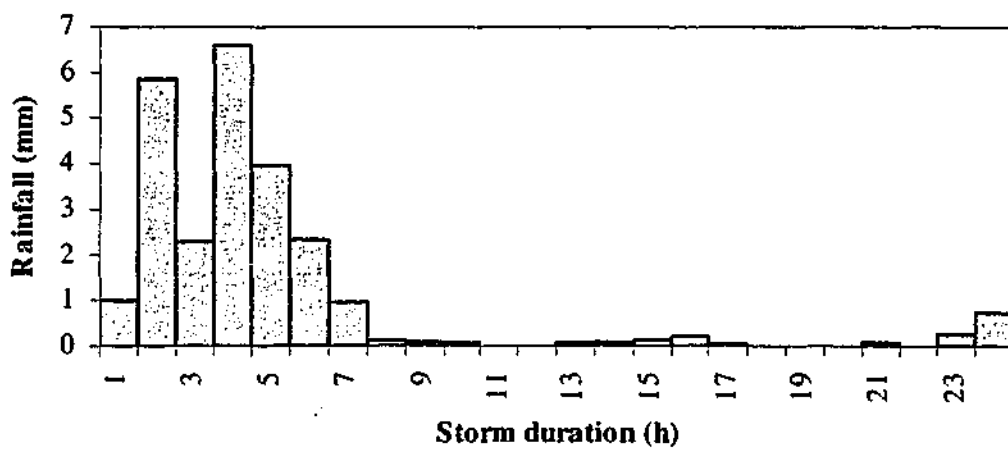
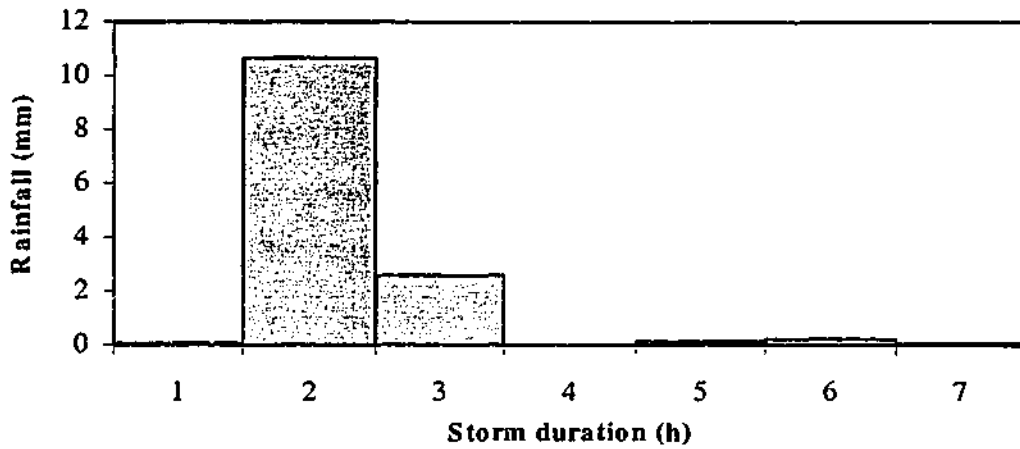


Figure 4-4: Examples of 'abnormal' storms (station 85237, H=6 hours, F1=0.4, F2=0.5)

#### 4.3.2.4 Refinement of storm definition

In order to reduce possible biases in storm duration due to periods of very little rain at the start or end of storm events, and to produce storm events that are more appropriate for flood analysis and simple to analyse, periods of very little rain at the beginning or end of the events were eliminated. Storms with internal periods of very little rain were also separated into two or more events. To do this, the following two additional criteria were introduced.

- *The 'dry hour' criterion:* An hour was considered as dry if its rainfall amount was less than or equal to C1 mm of rain.
- *The 'insignificant period' criterion:* A rainfall period was considered to be insignificant if all hourly rainfalls in the period were less than or equal to C2 mm of rain, and the average rainfall intensity during the period was less than or equal C1 (mm/h).

Incorporating these two criteria in the previous storm definition that made use of the separation time between storms and the two threshold intensities, a storm (see Figure 4-5) was defined in three steps:

- Step 1: A 'gross' storm was a period of rain starting and ending with a 'non-dry hour', preceded and followed by at least H 'dry hours'.
- Step 2: Any 'insignificant' period of rainfall at the beginning or end of a gross storm was then cut off from the gross storm to produce the 'net' storm of duration D.
- Step 3: The net storm was then assessed with regard to its severity and only kept as a 'significant' storm if it had the potential to produce a flood. This assessment was performed by firstly comparing the average rainfall intensity of the net storm ( $RFI_D$ ) with a threshold average intensity for that storm duration:  $RFI_D \geq F1 \times (I_D^2)$ . A second criterion was then applied to allow for the possibility of a storm-internal period of heavy rainfall (duration d and average intensity  $RFI_d$ ) producing a flood:  $RFI_d^{max} \geq F2 \times (I_d^2)$ , where  $I_D$  and  $I_d$  were respectively the estimated 2-year ARI intensities for the durations D and d.

In this analysis, the following values were adopted: H=6 (hours), F1=0.4, F2=0.5, C1=0.25 (mm/h), and C2=1.2 (mm/h).

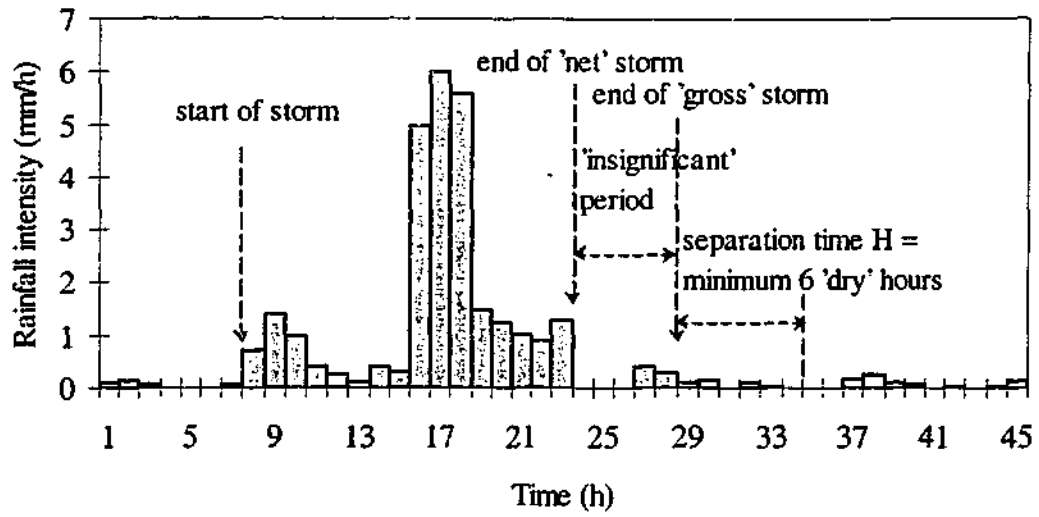


Figure 4-5: Proposed storm definition

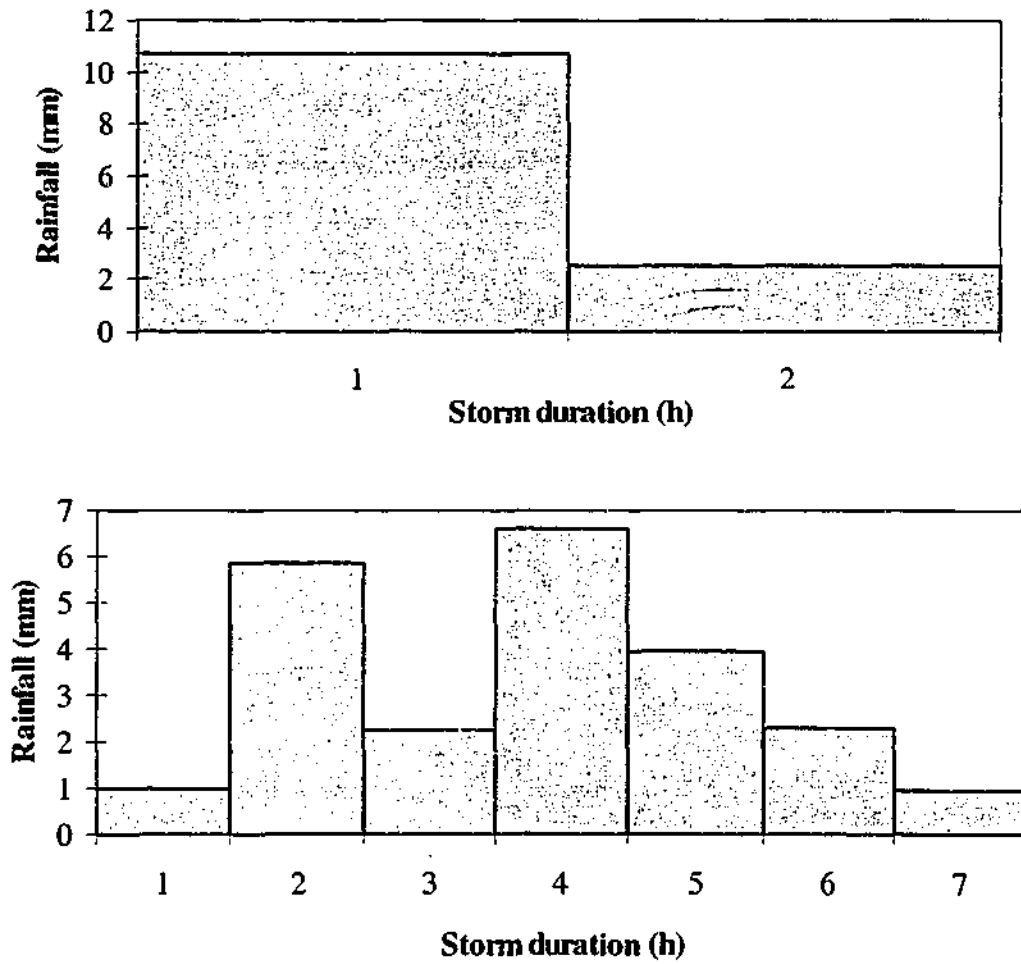


Figure 4-6: Examples of storms obtained using the adopted storm definition

Using the extracted storm data at station 85237 for illustration, it was concluded that the inclusion of two additional parameters C1 and C2 in the storm definition results in events that better satisfy the criteria described in Section 4.3.2. Figure 4-6 shows how 'abnormal' storms in Figure 4-4 change using the refined storm definition with the adopted parameter values.

### 4.3.3 Extraction of storm events

The storm definition with the specified five parameters was applied to extract storm events from hourly rainfall records at each of the 19 rainfall stations used in this research. The resulting number of events obtained at each site is summarised in column 3 of Table 4-2. This table shows that the number of events per station ranges from 51 to 797 with an average of 210 events.

Table 4-2: Sample size of extracted storms using the proposed storm definition  
[H=6 hours, F1=0.4, F2=0.5, C1=0.25 (mm/h), C2=1.2 (mm/h)]

Station ID	Record length (years)	Number of storms		Average number of events per year
		before discarding events with repeated values	after discarding events with repeated values	
85000	14	51	50	3.6
85026	16	129	129	8.1
85034	36	178	178	4.9
85072	39	231	231	5.9
85103	24	143	143	6.0
85106	22	208	206	9.4
85170	15	113	113	7.5
85176	22	185	179	8.1
85236	14	74	74	5.3
85237	22	168	167	7.6
85240	32	335	331	10.3
85256	19	94	92	4.8
86038	36	210	209	5.8
86071	109	797	797	7.3
86142	30	230	229	7.6
86219	23	196	195	8.5
86224	27	176	176	6.5
86234	24	209	207	8.6
86314	35	269	269	7.7
Average	29	210	209	7

#### 4.3.4 Checking of extracted events for consistency of hourly rainfalls

As discussed in Section 4.2.2, only recorded hourly rainfalls of good quality were used to extract individual events, but this criterion was insufficient to guarantee the resulting events are free of errors. These errors may occur in the form of repeated or outlying hourly values, which may arise from errors in recording or transcribing the data. A consistency analysis was therefore needed as a final check of the event data before further analyses were undertaken.

A preliminary investigation of the storm events at station 85237 indicated that there were a few observed storms that contained periods of repeated hourly data during the storm duration. An example of such a storm is given in Figure 4-7.

For this analysis, a storm was excluded from the storm sample if it has a period with repeated data whose length is greater than a quarter of the storm duration. Using this criterion, the extracted storms at the 19 pluviometers were inspected, and 21 events at 10 stations were discarded from the original storm samples. The number of the remaining storms at each of the 19 stations is given in column 4 of Table 4-2. The average number of storms per year at each rain gauge is shown in Table 4-2 (column 5). On average, over the 19 selected rainfall stations used in this study, the proposed storm definition gives 7 storms per year per station.

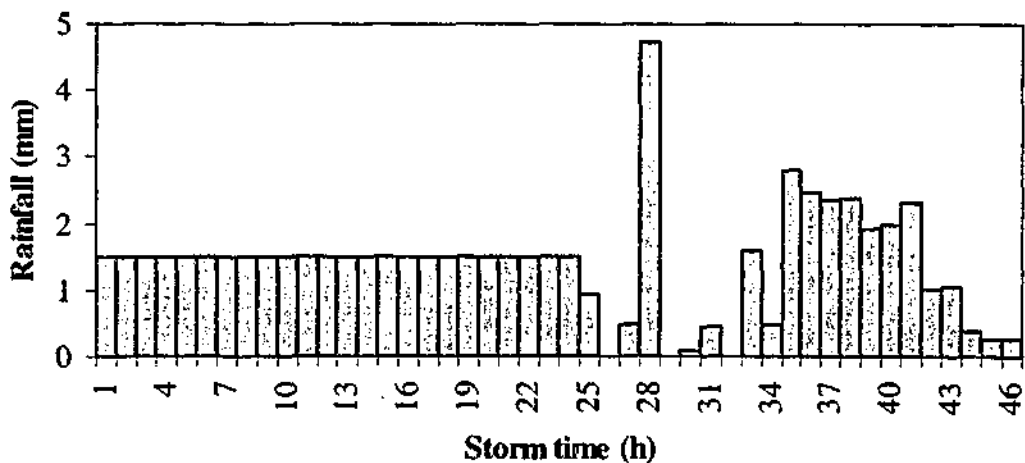


Figure 4-7: An example of a storm with repeated rainfall values (station 85237)

### 4.3.5 Summary

In this research, a storm definition was developed in order to extract storm events from continuous rainfall records for developing the probability distributions of event characteristics. These probability distributions are to be used as inputs to the proposed Joint Probability Model for design flood estimation.

Storm events were defined such that they are stochastic events, have no periods of insignificant rain at the start and end of the events, and have the potential to produce floods. Five parameters were used to extract those events, namely the minimum hourly rainfall when a gross storm starts (C1), the minimum hourly rainfall to define the start and end of the corresponding net storm (C2), the minimum separation time between successive events (H), and the intensity reduction factors (F1 and F2) to compute the threshold average rainfall intensities during the entire storm duration or during internal periods of intense rain. Values of these parameters were determined by exploratory and sensitivity analyses.

Using the proposed storm definition, samples of rainfall events were extracted from continuous rainfall records at the 19 pluviometers used in this study. The extracted events were then visually examined for possible errors in recording or transcribing hourly rainfall in each individual event. In some samples, there were a number of events that had long periods of repeated hourly rainfalls, so these storms were discarded from the corresponding samples. With the remaining storms, the adopted storm definition gave an average of 7 storms per year per station.

With respect to rainfall analysis, it can now be concluded that the samples of significant storm events were extracted from homogeneous observed data (with respect to time), and that they were free of detectable errors in data transcription or recording. Such storm samples can now be statistically analysed for characteristics such as storm duration, average intensity, and temporal patterns. In the next section, the development of the frequency distribution of storm duration is presented.

## 4.4 FREQUENCY DISTRIBUTION OF STORM DURATION

### 4.4.1 Background

Frequency analysis refers to methods for determining how frequently possible values of a random variable occur. The analysis is carried out on a sample in order to make inferences about the probability distribution of the population from which the sample is drawn. In hydrology, the selected random variable may be the flowrate of a stream, the average rainfall intensity of a storm, or the duration of a storm event. Frequency analyses can be conducted using at-site or regional methods. Broadly speaking, at-site frequency analysis uses observed data at a particular site to produce probability estimates of the particular variable. In contrast, regional frequency analysis uses multiple samples of the same variable at different measuring sites and is often employed for frequency estimates at ungauged sites where there is no or insufficient observed data.

In order to develop the frequency distribution for storm duration at pluviometer 85237 in the La Trobe River catchment at Noojee, either at-site or regional frequency analysis could be used. There is a sufficient number of the extracted storm events at the specified site (167 events) for at-site frequency analysis, but samples of storm duration data are also available at other gauges around this site that can be used for regional frequency analysis. However, regional frequency analysis was adopted because, when used at gauged sites, it can yield more accurate estimates of the frequency of storm duration (due to the availability of more data). In addition, extrapolation can be made to ungauged sites in the region of interest, if necessary.

Many regional frequency analysis methods are available. A description of these is given by Cunnane (1988). Among the available methods, the procedure developed by Hosking and Wallis (1997) has been widely applied in regional flood frequency analyses, low flow analyses, as well as in rainfall regionalization (Fill and Stedinger, 1995). The popularity of this procedure stems from its many advantages. For example, it can yield reasonably accurate quantile estimates even when there are plausible departures from the assumptions used in the procedure. In addition, it employs L-moments that can provide simple and reasonably efficient estimates of distributional

parameters. Furthermore, a complete computer program for applying the procedure is readily available (Hosking, 1997). For these reasons, this procedure was adopted in this study for determining the frequency distribution of storm duration.

This section first describes the Hosking and Wallis method of regional frequency analysis. The application of this method to derive the frequency distribution of storm duration at pluviometer 85237 is then presented in detail, and the results are discussed.

#### 4.4.2 The Hosking and Wallis method of regional frequency analysis

The Hosking and Wallis regional frequency analysis method (Hosking and Wallis, 1997) is developed from the assumption that the frequency distributions of a random variable at  $N$  sites in a homogeneous region are identical apart from a site-specific scaling factor. The objective of this method is to compute the regional growth curve  $q(F)$  for a group of sites, from which the frequency curve at each individual site  $Q_i(F)$  can be computed from the following relationship:

$$Q_i(F) = \mu_i q(F) \quad i = 1, 2, \dots, N \quad (4-1)$$

in which  $Q_i(F)$  is the quantile of non-exceedance probability  $F$  ( $0 < F < 1$ ) at site  $i$ ;  $\mu_i$  is the scale factor at site  $i$ , usually taken as the mean of the observed data;  $q(F)$  is the dimensionless regional frequency distribution common to all sites (called the regional growth curve); and  $N$  is the number of sites.

To estimate the regional growth curve, four stages are required, namely the screening of data, the identification of homogeneous regions, the choice of a regional frequency distribution, and the estimation of the parameters of the regional frequency distribution. These stages are discussed below.

The aim of data screening is to ensure that the data at each site are homogeneous and consistent over time. At this stage, sites that seem to have erroneous data are flagged as discordant sites. Data at these discordant sites then need to be closely examined to eliminate gross errors and inconsistencies. In practice, to screen the data, the *discordancy measure*  $D_i$  (see Appendix E) is computed for each individual site. A site

is discordant with others in the group if its discordancy measure exceeds a critical value suggested by Hosking and Wallis (1997).

After inspecting the data, the next step is to define the homogeneous region<sup>3</sup> for the group of sites. This region can be tentatively defined by geographical contiguity, site characteristics, or statistics computed from at-site measurements of the variable of interest. The homogeneity of the proposed region can then be tested by comparing the between-site variability of site statistics with what would be expected of a homogeneous region. In practice, this is undertaken by computing the *heterogeneity measures*  $H_1$ ,  $H_2$  or  $H_3$  (see Appendix E). The region is declared to be heterogeneous if any of the heterogeneity measures is sufficiently large (that is,  $H_1$ ,  $H_2$  or  $H_3 \geq 2$ ).

In the choice of an appropriate regional frequency distribution for the homogeneous region, a goodness-of-fit test is applied, which involves computing summary statistics of the data and testing whether their values are consistent with what would be expected if the data were a random sample from some hypothesised distribution. In the estimation of the parameters of the regional frequency distribution, the distributional parameters are first estimated separately at each site. These at-site estimates are then combined to give a regional average. In practice, the above two steps are carried out by computing the *goodness-of-fit measure*  $Z^{\text{DIST}}$  (see Appendix E) for each of five general distributions. These distributions are the Generalised Logistic (GLO), Generalised Extreme Value (GEV), Generalised Pareto (GP), Lognormal (LN), and Pearson type III (PIII). A given distribution is considered to give an acceptable fit to the observed data if  $Z$  is sufficiently close to zero (that is,  $|Z^{\text{DIST}}| \leq 1.64$ ).

A FORTRAN subroutine to compute the above three statistics for regional frequency analysis has been written and provided by Hosking (1997). The theoretical background of L-moments, on which the Hosking and Wallis regional frequency analysis method is based, is also summarised in Appendix E.

---

<sup>3</sup> A homogeneous region is a group of sites whose frequency distributions of a random variable are considered to be the same, after appropriate scaling.

### 4.4.3 Application and results

In order to derive the frequency curve of the storm duration at pluviometer 85237 using the Hosking and Wallis method of regional frequency analysis, the following procedure was adopted. First of all, unbiased estimates of sample L-moments of storm durations at all 19 pluviometers were calculated using the formulas documented in Appendix E. The computed L-moments include the sample mean ( $l_1$ ), sample L-CV ( $t_2$ ), sample L-skewness ( $t_3$ ), and sample L-kurtosis ( $t_4$ ). The discordancy measures were next estimated for each of the 19 rainfall sites. The computed value of each site was then compared with the critical value of 3 suggested by Hosking and Wallis (1997). If there were any discordant sites, data at these sites would then be examined to eliminate possible errors. Next, the homogeneous region of the storm duration was tentatively defined. The heterogeneity statistics were then computed to decide whether or not the defined region was acceptably homogeneous. Finally, for the accepted homogeneous region, the goodness-of-fit measures were determined for each of the five candidate distributions and the distribution that best fitted the observed duration data at the specified sites was selected.

The L-moment statistics computed for the observed storm durations at the 19 selected pluviometers, and the corresponding discordancy statistics ( $D_i$ ) are presented in Table 4-3. Plots of these L-moment statistics are shown in Figure 4-8 and Figure 4-9. From Table 4-3, it is clear that none of the  $D_i$  values exceeds the critical value of 3. This implies that there is no evidence of gross errors or inconsistencies in the storm duration data at any of the 19 rainfall stations used. This result is not surprising because the rainfall data at all these pluviometers had already been checked for consistency and homogeneity in time, as described in Sections 4.2 and 4.3. Of all the computed  $D_i$ , the largest value is 2.71 at pluviometer 86314. This indicates that the variability of sample L-moments at this site is quite large compared with other sites in the group. This large variability is associated with the largest L-skewness ( $t_3=0.362$ ) and L-kurtosis ( $t_4=0.21$ ) of this site. However, as shown in Figure 4-8 and Figure 4-9, the large deviation of the L-moment ratios at this site from the group average is in a direction concordant with the corresponding deviations of other sites in the group. As there is no evidence of errors in data at this site, there are no physical grounds to move this site to another region, or to eliminate it from the group.

Table 4-3: L-moments and the discordancy statistics of storm duration for 19 pluviometers used

Site ID	Number of storms	$l_1$ (h)	$t$	$t_3$	$t_4$	$D_i$
85000	50	18.66	0.472	0.270	0.079	2.440
85026	129	20.38	0.457	0.280	0.132	1.400
85034	178	16.51	0.441	0.290	0.139	0.260
85072	231	14.16	0.421	0.238	0.097	0.340
85103	143	18.99	0.394	0.195	0.118	1.630
85106	206	24.58	0.422	0.245	0.125	0.210
85170	113	15.58	0.382	0.184	0.089	1.650
85176	179	29.07	0.410	0.187	0.094	1.280
85236	74	16.14	0.424	0.230	0.086	0.510
85237	167	23.49	0.420	0.209	0.089	0.420
85240	331	15.58	0.445	0.311	0.156	0.560
85256	92	18.50	0.423	0.276	0.159	0.740
86038	209	13.18	0.401	0.224	0.087	1.820
86071	797	12.62	0.415	0.287	0.140	0.830
86142	229	20.23	0.411	0.291	0.177	1.080
86219	195	22.31	0.435	0.244	0.092	0.430
86224	176	10.95	0.445	0.312	0.143	0.600
86234	207	15.17	0.432	0.255	0.118	0.090
86314	269	15.10	0.421	0.362	0.210	2.710
Regional weighted mean		16.96	0.423	0.268	0.131	

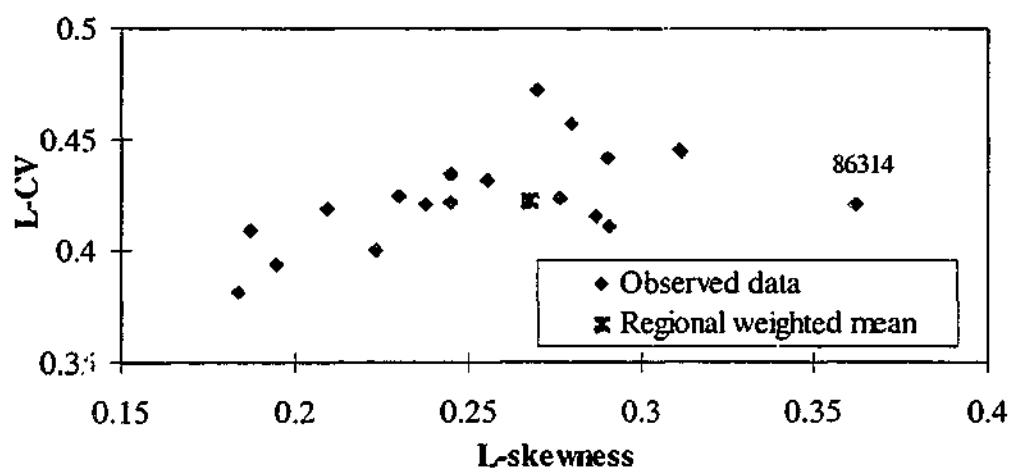


Figure 4-8: Plot of L-CV versus L-skewness for storm duration at 19 pluviometers

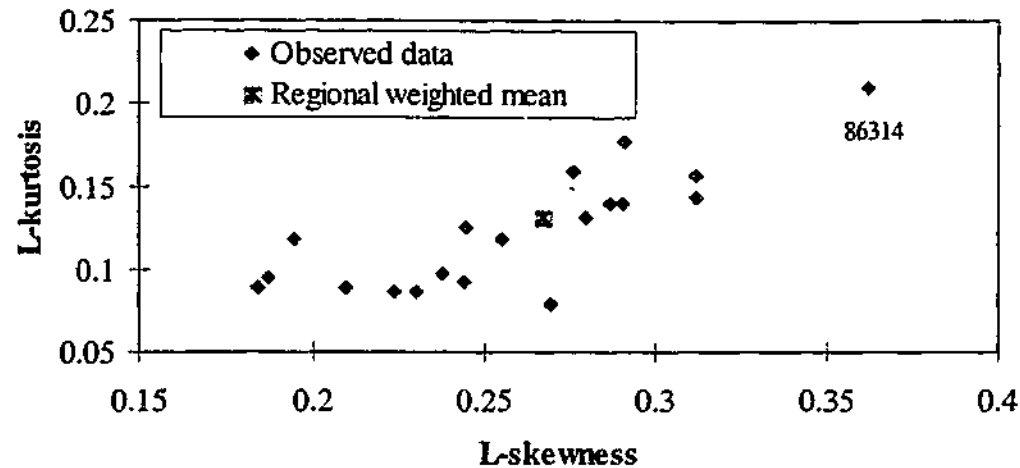


Figure 4-9: Plot of L-kurtosis versus L-skewness for storm duration at 19 pluviometers

To define the homogeneous region for storm duration, three attempts were made. In the first attempt (Trial 1), all 19 sites were included a single group. However, the heterogeneity measures  $H_2$  and  $H_3$  computed for this group were greater than 3 (see Table 4-4), indicating that the intended region was definitely heterogeneous as far as the L-skewness and L-kurtosis were concerned. Therefore, the region of 19 pluviometers could not be regarded as homogeneous in terms of storm duration and had to be redefined.

Table 4-4: Heterogeneity statistics computed for various regions of storm duration

Trial	Number of sites	Region name	Heterogeneity measures		
			$H_1$	$H_2$	$H_3$
1	19	All 19 sites	0.20	3.08	3.29
2	11	Group 1	0.03	1.66	2.06
	8	Group 2	0.46	2.39	2.42
3	6	Group 3	0.06	1.42	1.30

In the second attempt (Trial 2), site elevation was used as a criterion to define the region, because when plotting gauge elevation against the average storm duration at each site (see Figure 4-10), there seemed to be a trend for the average duration of storms to increase as gauge elevation increases. In this trial, the 19 sites were divided into two groups (Group 1 and Group 2) using an arbitrary threshold elevation of 150m. Nevertheless, the heterogeneity measures  $H_2$  and  $H_3$  computed for the sites in these two

groups still exceeded 2 (see Table 4-4), suggesting that the groups so formed were heterogeneous. As a result, another criterion was needed to define the homogeneous region of storm duration.

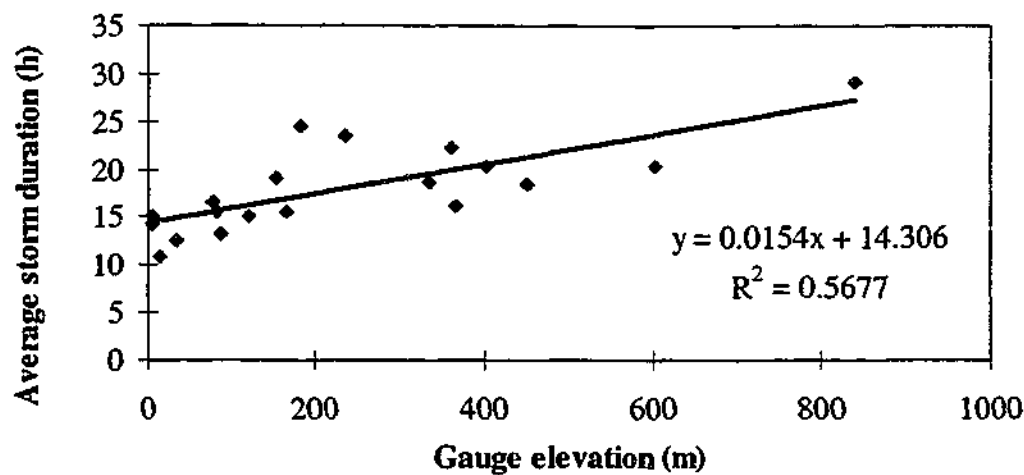


Figure 4-10: Plot of average storm duration against gauge elevation at 19 pluviometers

In the last attempt (Trial 3), sites contiguous to the pluviometer under consideration (station 85237) were grouped together. This group (called Group 3) consisted of 6 sites as follows: 85000, 85026, 85034, 85176, 85237, and 85256. The heterogeneity measures computed for the group of 6 sites in Trial 3, tabulated in Table 4-4, are:  $H_1=0.06$ ,  $H_2=1.42$ , and  $H_3=1.30$ . As  $H_1$  is very close to zero, it can be concluded that the proposed region of six sites is acceptably homogeneous with respect to L-CV. Nevertheless, the values between 1 and 2 of  $H_2$  and  $H_3$  suggest that the population distributions of storm duration for the six pluviometers in Group 3 are possibly different. The possible heterogeneity of the storm duration is in the form of sites having equal L-CV but slightly different L-skewness and L-kurtosis. As discussed by Hosking and Wallis (1997), this form of heterogeneity has little effect on the accuracy of quantile estimates except very far into the extreme tails of the distribution. For the current application in which frequency estimates of very long storm duration are of little interest, this form of heterogeneity is not important. Therefore, at this stage, it is reasonable to consider Group 3 as acceptably homogeneous.

The goodness-of-fit measures computed for the five distributions fitted to the storm duration data of six pluviometers in Group 3 are presented in Table 4-5. Plots of the L-

CV and L-kurtosis of these sites against the corresponding L-skewness, along with those of some theoretical distributions are given in Figure 4-11 and Figure 4-12. These plots, called L-moment ratio diagrams, are graphical tools used to select a theoretical distribution that gives the best fit to an observed set of data. Mathematical expressions used to plot the theoretical distributions shown in these plots are documented by Hosking (1991), and Vogel and Wilson (1996).

Table 4-5: The goodness-of-fit measures computed for storm duration data of Group 3

Number of sites	Region	Goodness-of-fit measure ( $Z^{\text{DIST}}$ )				
		GLO	GEV	LN	PIII	GP
6	Group 3	7.86	5.33	4.02	2.17	-0.90

From Table 4-5, it can be seen that, of the five candidate distributions, only the  $Z^{\text{DIST}}$  statistic computed for the Generalised Pareto distribution (GP) is less than 1.64. Therefore, this distribution was selected as the parent distribution of storm duration because it gave an adequate fit to the storm duration data for all six sites in the proposed group. This selection is supported by evidence shown in the L-moment diagrams (Figure 4-11 and Figure 4-12). For example, in Figure 4-11, the GP and Weibull distributions give the best fit to the observed storm duration data, as observed sample L-moments cluster more closely around these distributions. Similarly, in Figure 4-12, the GP distribution gives the best fit to the observed storm durations for the six selected sites.

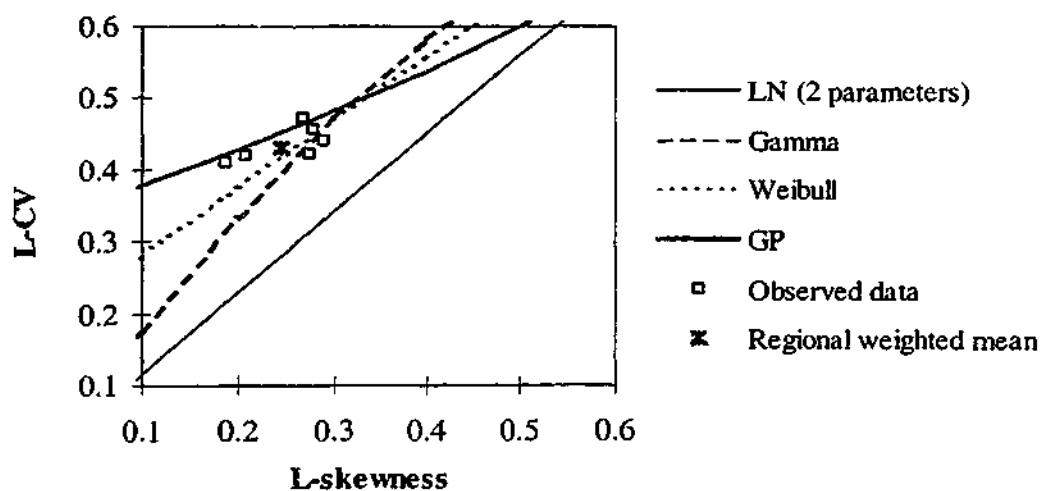


Figure 4-11: Plot of L-CV against L-skewness for storm duration data for stations in Group 3 and some theoretical probability distributions

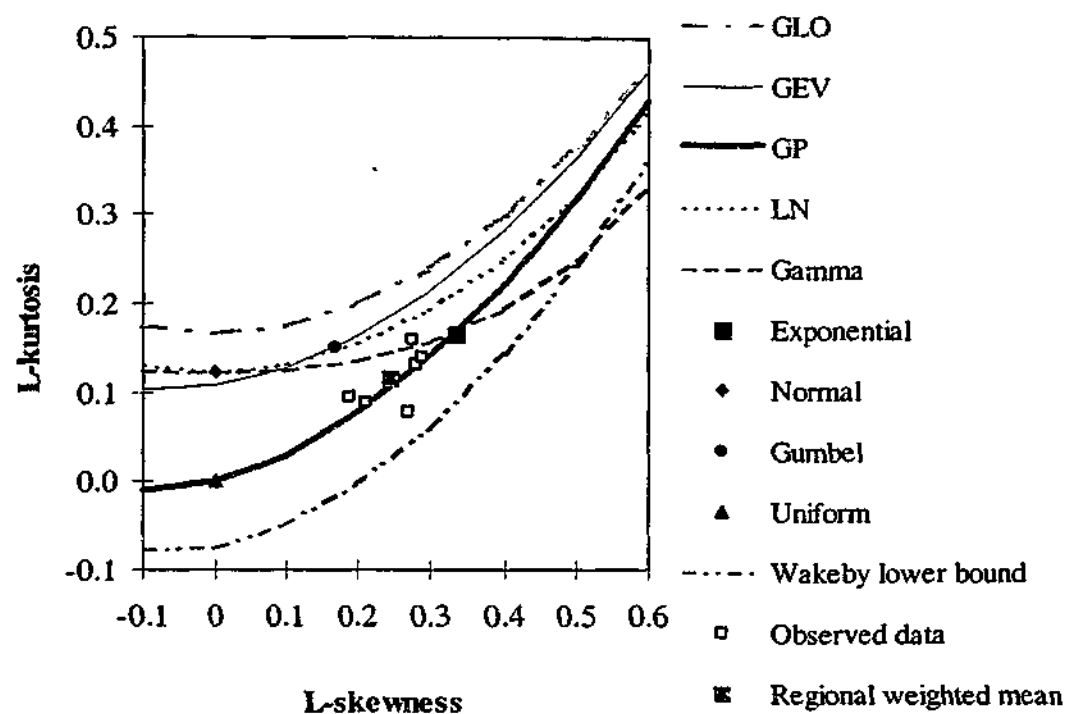


Figure 4-12: Plot of L-kurtosis against L-skewness for storm duration data for stations in Group 3 and some theoretical probability distributions

The GP distribution is a three-parameter distribution with the following parameters:  $\xi$  (location),  $\alpha$  (scale),  $\kappa$  (shape). More details of this distribution are given in Appendix F. For the region of the six selected pluviometers, the parameters of the fitted regional GP distribution are:  $\xi=0.045$ ,  $\alpha=1.158$ ,  $\kappa=0.212$ . Quantile estimates [D(F)] of the regional growth curve fitted to the observed storm duration data for six stations in Group 3 are given in the second row of Table 4-6.

Table 4-6: Quantile estimates of the regional growth curve (for Group 3) and of the probability distribution of storm duration for pluviometer 85237

F	0.01	0.05	0.1	0.2	0.5	0.8	0.9	0.95	0.98	0.99
D(F)	0.06	0.10	0.17	0.30	0.79	1.62	2.15	2.61	3.12	3.45
$I_1 \cdot D(F)$ (hours)	1.3	2.4	3.9	7.0	18.6	38.1	50.6	61.4	73.4	81.1

To determine the frequency distribution of the storm duration for pluviometer 85237, quantile estimates of the regional growth curve were multiplied by the at-site average storm duration ( $I_1=23.49$  hours, in this case). Results of this calculation are given in the

third row of Table 4-6. This table shows that 10%, 50% and 95% of storms at station 85237 have estimated duration less than or equal to 3.9 hours, 18.6 hours, and 61.4 hours, respectively.

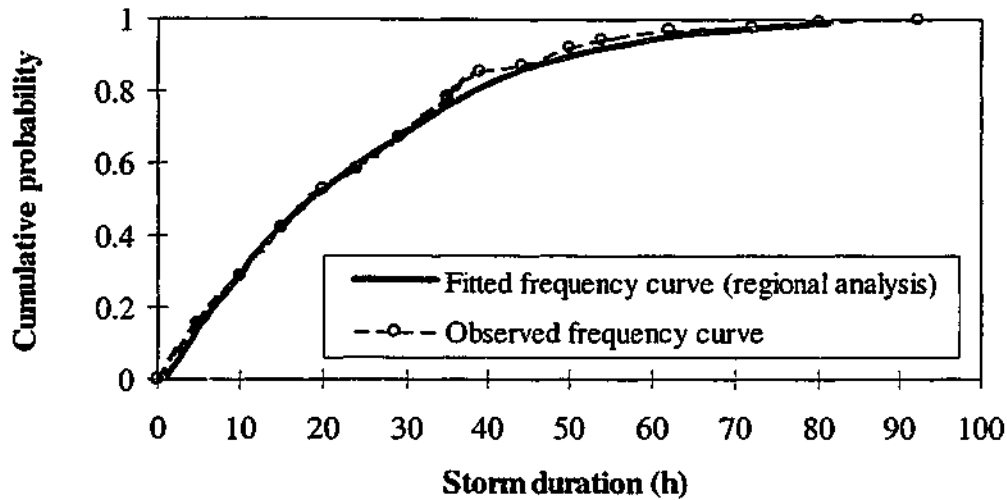


Figure 4-13: Observed and fitted frequency curves of storm duration for station 85237

A plot of the observed and fitted cumulative distributions of the storm duration for station 85237 is given in Figure 4-13. As these two frequency curves are almost identical, it can be concluded that the adopted GP distribution is a suitable representative of the duration of the observed storm events.

#### 4.4.4 Summary

In this section, the probability distribution of storm duration for station 85237 was determined using the regional frequency analysis procedure developed by Hosking and Wallis (1997). Analysis results indicated that there was no evidence of gross errors or inconsistencies in the storm duration data, and that the duration of the observed rainfall events for the rainfall sites used in this study had very similar L-CV but quite variable L-skewness and L-kurtosis. In order to determine the homogeneous region of storm duration, sites contiguous to the site of interest were grouped together. The group of sites so-formed was homogeneous in terms of L-CV, but possibly heterogeneous in

terms of L-skewness and L-kurtosis. However, this form of heterogeneity was assumed not to have an effect on the quantiles of duration of interest.

The three-parameter Generalised Pareto distribution was used to characterise storm duration. The fitted and observed probability distributions at the specified site were almost identical, confirming the suitability of the adopted GP distribution.

## **4.5 CONDITIONAL FREQUENCY DISTRIBUTION OF RAINFALL INTENSITY**

### **4.5.1 Background**

In rainfall-based design flood estimation, rainfall intensity is considered to be one of the inputs that have significant influence on flood estimates. Therefore, in the proposed Joint Probability Model as well as in the current Design Event Approach, rainfall intensity is used as a stochastic input to the flood estimation process.

With the current Design Event Approach, at any location in Australia, estimates of the average intensity of a rainfall event of a specified average recurrence interval (ARI) for a given duration can be determined from a set of intensity-frequency-duration (IFD) curves readily available for any design location (Institution of Engineers, Australia, 1987, Chapter 2). These design IFD curves, developed for intense rainfall bursts within storms, represent the frequency distributions of point rainfall intensity as functions of rainfall duration. The current design IFD curves are accurate and consistent because these curves have been obtained from a regional analysis of observed data collected at a large number of sites.

In this research, a rainfall event is defined very differently from the definition of bursts used by the Institution of Engineers, Australia (1987) for deriving the current design IFD curves. As a result of the discrepancy in these event definitions, the current IFD curves cannot be used directly in the present research, so new IFD curves based on the

present rainfall event definition must be derived. This section presents the work undertaken to achieve this objective for pluviometer 85237.

This section starts with the investigation of the correlation between rainfall intensity and duration for observed rainfall events at the specified pluviometer. A description of an at-site frequency analysis procedure is then given, along with the application of the procedure to the observed data at the given site. The evaluation of the derived IFD curves is then documented and the results are discussed.

#### 4.5.2 Correlation between rainfall intensity and duration

To determine the degree of correlation between rainfall intensity and rainfall duration, average intensities of the observed events at station 85237 were plotted against the corresponding storm durations (see Figure 4-14). A regression line was then fitted to the plotted data points, and the coefficient of determination ( $R^2$ ) of this line was computed.

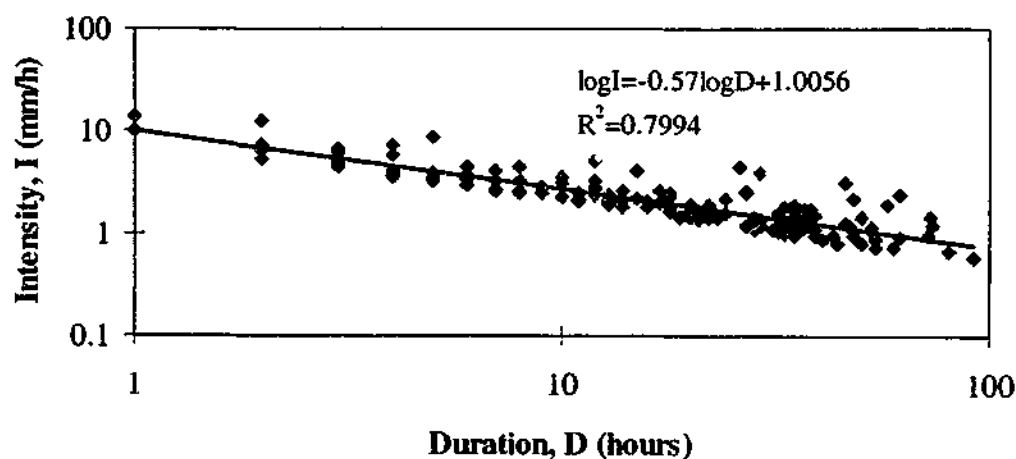


Figure 4-14: Relationship between average rainfall intensity and duration (station 85237).

The plot of rainfall intensity versus rainfall duration for station 85237 shows a strong relationship between them. There are three points to note about this. Firstly, the form of the relationship between rainfall intensity and duration is a power function,

represented by a straight line on a log-log plot. Secondly,  $R^2$  is approximately 0.80, indicating that 80% of the variation in rainfall intensity is attributable to the variation in rainfall duration. Thirdly, the slope of the regression line between intensity and duration is negative (-0.57), implying that average rainfall intensity is inversely related to storm duration. In other words, as the storm duration increases, the average rainfall intensity decreases, and vice versa. As a result of the strong correlation between rainfall intensity and duration, the frequency distribution of rainfall intensity needs to be conditioned on duration.

### 4.5.3 Development of the IFD curves

To develop the frequency curves of rainfall intensity, either an at-site or a regional frequency analysis method can be used. In this study, initially, the rainfall intensity frequency curves for station 85237 were determined using the regional frequency analysis method developed by Hosking and Wallis (1997). However, further investigation into the IFD curves was undertaken using an at-site frequency analysis procedure readily available from a parallel project (Rahman et al., 2001). For the present study, this procedure was modified slightly to include a goodness-of-fit test for the fitted distribution.

With the modified procedure, the rainfall intensities for storm events in predefined duration intervals are pooled for frequency analysis. This analysis involves the compilation of series of rainfall intensities for some representative duration, the fitting of a distribution to each intensity series, the checking of the goodness-of-fit of the fitted distributions, and the interpolation and extrapolation of the intensity-frequency curves to other durations. The modified procedure comprises four steps, as described in more detail below.

#### **Step1: Compilation of rainfall intensity series**

The objective of this step is to convert the average rainfall intensity for storms of various durations into the corresponding average intensity at some selected duration. This is achieved in the following steps:

- The range of storm durations is divided into a number of intervals. The number of intervals is selected such that there is a sufficient number of storms in each interval for distributional fitting, and that the lengths of the class intervals are similar on a logarithmic scale. Each interval is then represented by a single duration approximately at the middle of the interval (on the logarithmic scale). This duration is termed the representative duration. For pluviometer 85237, five representative durations were used to characterise five class intervals of storm durations, as shown in Table 4-7.

Table 4-7: Representative durations used to develop the IFD curves

Duration intervals (h)	Representative durations (h)
1 - 5	2
6 - 11	8
12 - 24	16
25 - 36	32
> 36	48

- Average intensities of all observed storms whose durations are within a duration interval are extracted together with the corresponding durations.
- For each duration interval, a linear regression line is fitted between the logarithm of the extracted intensities ( $\log I$ ) and the logarithm of the extracted durations ( $\log D$ ). An example is given in Figure 4-15.

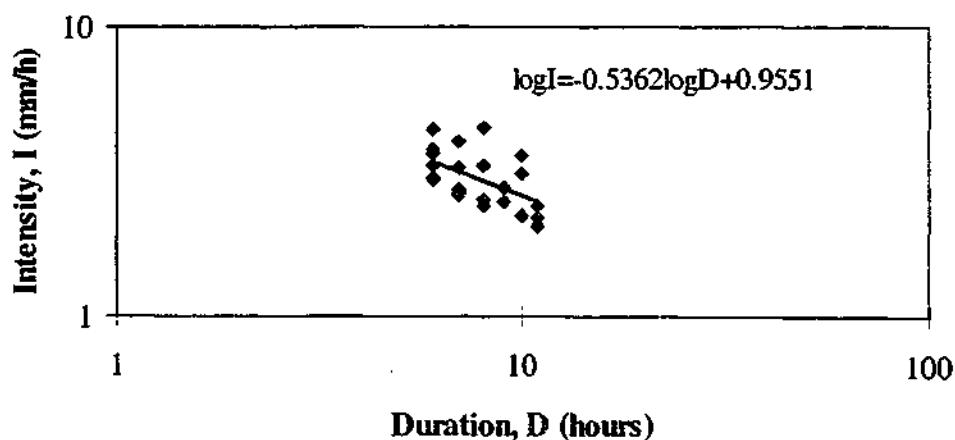


Figure 4-15: Plot of rainfall intensity versus duration for the interval of (6h, 11h)

- For each duration interval, the extracted intensities for various durations are adjusted to the corresponding representative duration using the slope of the fitted regression line and the following formula:

$$I_{\text{adjusted}} = 10^W, \text{ in which } W = \log I_D + a^*(\log D - \log D_r) \quad (4-2)$$

where  $D$  is the duration of the storm under consideration,  $I_D$  is the corresponding average rainfall intensity of the storm,  $D_r$  is the representative duration under consideration,  $I_{\text{adjusted}}$  is the average rainfall intensity of the storm event adjusted to the representative duration, and  $a^*$  is the slope of the regression line.

For station 85237, the observed rainfall intensities for various durations were transformed into five intensity series having representative durations of 2h, 8h, 16h, 32h, and 48h. A summary of the statistical properties of these series is given in Table 4-8.

Table 4-8: Statistical properties of the adjusted rainfall intensity series and parameters of the fitted exponential distributions (station 85237)

	Representative durations				
	2h	8h	16h	32h	48h
Maximum intensity (mm/h)	15.86	4.50	4.07	3.30	3.03
Minimum intensity (mm/h)	5.39	2.42	1.59	0.92	0.76
Average intensity (mm/h)	7.58	3.01	2.13	1.42	1.27
Standard deviation (mm/h)	2.46	0.58	0.54	0.54	0.54
Coefficient of skewness	2.08	1.02	2.23	2.30	1.81
Parameter ( $\omega_1$ )	1.18	1.09	1.86	1.73	1.45
Parameter ( $\omega_2$ )	2.19	0.59	0.54	0.50	0.51

### Step2: Determination of the intensity-frequency curves for representative durations

At this stage, it is noted that the storm sample obtained from the observed record at station 85237 forms a partial duration series of rainfall intensity. This sample consists of storm events with the average intensity at least equal to some threshold value, as mentioned in Section 4.3.2.

To develop the intensity-frequency curve for each partial duration series of rainfall intensities, the procedure is as follows:

- An exponential distribution<sup>4</sup> is fitted to each series of rainfall intensities. Parameters  $\omega_1$  and  $\omega_2$  of this distribution can be computed by:

$$\begin{aligned}\omega_1 &= M^* / N^* \\ \omega_2 &= \sum_{i=1}^{M^*} I_i / M^* - I_0\end{aligned}\quad (4-3)$$

where  $\omega_1$  is the average number of events per year in each series,  $M^*$  is the number of data points in the series,  $N^*$  is the record length (years), and  $I_0$  is the minimum value of rainfall intensity in the series.

- The design average rainfall intensity (of the representative duration under consideration) for any average recurrence interval (T) is then calculated as follows:

$$I(T) = I_0 + \omega_2 \ln(\omega_1 T) \quad (4-4)$$

where  $I(T)$  is the T-year design rainfall intensity for the given duration, and T is the average recurrence interval (ARI) of the design rainfall. In this analysis, the ARIs used were: T = ARI = 1, 2, 5, 10, 20, 50, 100 years.

For station 85237, parameters of the beta distributions fitted to the five series of rainfall intensities are also summarised in Table 4-8.

### Step3: Checking of the intensity-frequency curves

In order to check whether each of the fitted exponential distributions can reproduce well the observed rainfall intensity data, the following steps can be undertaken:

- The rainfall intensity series of each representative duration is plotted on a graph using the following plotting position:

$$PP(j) = (N^* + 0.2) / (j - 0.4) \quad (4-5)$$

where  $PP(j)$  is the plotting position of a data point ranked  $j$  in the series (in decreasing order of magnitude) and  $N^*$  is the record length in years.

- The exponential distribution fitted to the intensity series is plotted on the same graph.
- The goodness-of-fit of the fitted distribution is visually checked, outliers are eliminated, and the distribution is refitted, if necessary.

<sup>4</sup> Initially, both the Log Pearson III and the exponential distributions were fitted to the observed data, however the exponential distribution was adopted because it gave a better fit.

An example of the plot of the exponential distribution fitted to the rainfall intensities series for the representative duration of 8h (for station 85237) is given in Figure 4-16.

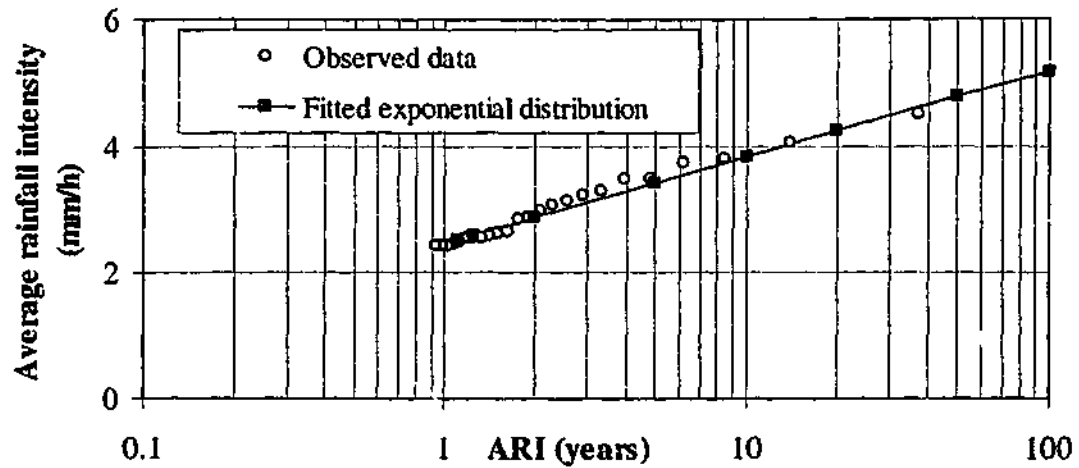


Figure 4-16: Plot of rainfall intensity series of the 8-hour representative duration and the fitted exponential distribution

#### Step 4: Interpolation and extrapolation of the intensity-frequency curves to all durations

To determine the complete IFD curves, the intensity-frequency curves developed for the representative durations are interpolated and extrapolated to all durations. For each of the ARIs used, the steps below are adopted:

- The design rainfall intensity for each of the five representative durations is estimated from the fitted exponential distributions. An example of these estimates for storms of 20-year ARI is given in Table 4-9.

Table 4-9: Estimates of design rainfall intensities for ARI = 20 years

D (h)	I (mm/h)	log(D)	log(I)
2	12.30	0.30	1.09
8	4.23	0.90	0.63
16	3.55	1.20	0.55
32	2.69	1.51	0.43
48	2.47	1.68	0.39

- A second-degree polynomial is fitted to the logarithm of the estimated intensities and the logarithm of the corresponding representative durations (see an illustration in Figure 4-17).

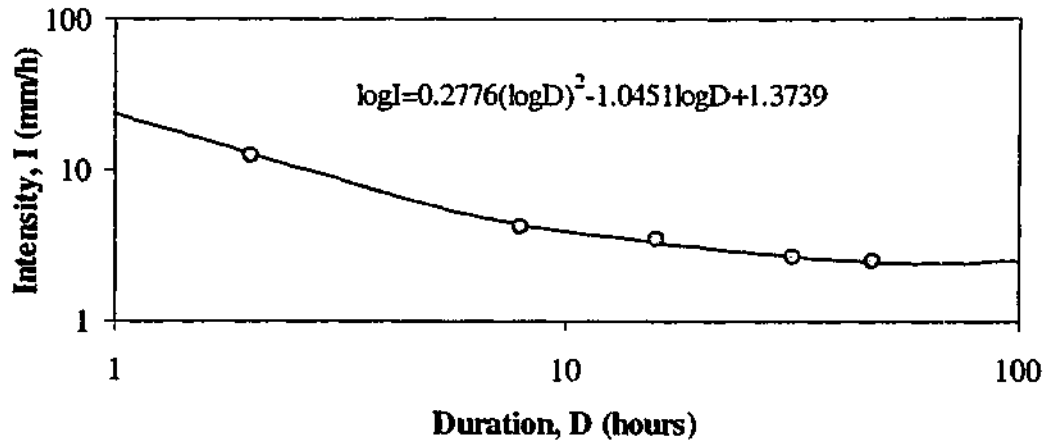


Figure 4-17: Plot of the polynomial curve fitted to the estimated intensities of representative durations (ARI = 20 years)

- The design rainfall intensity for a storm of any duration  $D$  and the specified ARI is finally computed using the coefficients  $b^*$ ,  $c^*$ , and  $e^*$  of this polynomial curve as follows:

$$\log I = b^*(\log D)^2 + c^*(\log D) + e^* \quad (4-6)$$

It is noted that, even though the polynomial intensity-frequency-duration curves were determined from storms with representative durations of 2, 8, 16, 32, and 48 hours, the curves were used to estimate the average rainfall intensity for durations of 1 hour to 120 hours for the study site.

#### 4.5.4 Preliminary results

Using the procedure described above, the design IFD estimates for station 85237 were obtained and are presented in Table 4-10. A plot of these estimates, called the derived IFD curves, is presented in Figure 4-18. It can be seen from the table and figure that the average design rainfall intensity of frequent storms (with ARIs less than 20 years) decreases for increasing event duration. This relationship still holds true for rarer events

(ARIs greater than 20 years) with duration up to 48 hours. However, for rare, long duration storms (ARIs of 20 years or greater, and duration exceeding 48 hours), the average intensity increases although the storm duration increases (see bold values in Table 4-10).

Table 4-10: Derived IFD estimates for station 85237 (rainfall intensity in mm/h)

Duration (D) (hours)	Average recurrence interval (ARI)						
	1 year	2 years	5 years	10 years	20 years	50 years	100 years
1	8.29	11.74	16.40	20.00	23.65	28.52	32.23
2	5.67	7.19	9.16	10.65	12.15	14.12	15.61
6	3.09	3.61	4.30	4.83	5.35	6.06	6.59
12	2.10	2.47	2.96	3.34	3.71	4.20	4.58
24	1.42	1.76	2.21	2.55	2.89	3.33	3.66
36	1.13	1.48	1.94	2.28	2.63	3.09	3.43
48	0.96	1.32	1.79	2.16	2.52	3.00	3.37
72	0.76	1.13	1.65	2.05	2.46	<b>3.01</b>	<b>3.42</b>
120	0.57	0.96	1.54	2.02	<b>2.52</b>	<b>3.21</b>	<b>3.74</b>

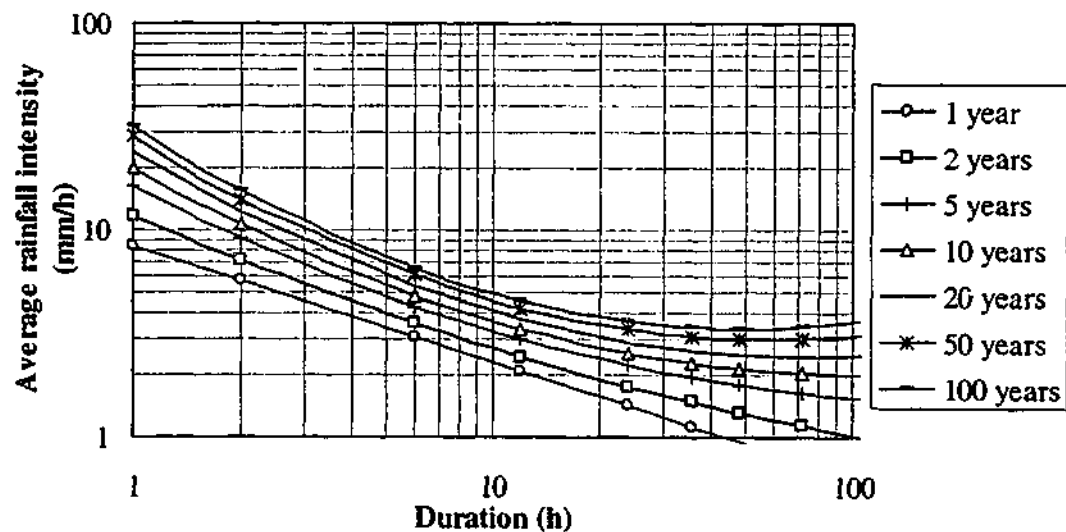


Figure 4-18: Derived IFD curves for station 85237

There are two main factors that may cause the unusual increase in the design rainfall intensity for long duration storms at station 85237. The first factor relates to errors in the data points to which each of the polynomial curves were fitted. As shown in Table 4-9, these data points are the rainfall intensity estimates for storm events of a specified return period corresponding to five representative durations. These intensities were

estimated from the five exponential distributions fitted to the five adjusted rainfall intensity series, which were initially formed by converting the average rainfall intensities of various durations into the intensities of five representative durations. As each of these steps introduces uncertainties to the outcome at the end of the step, the final rainfall intensity estimates are consequently uncertain. The second factor is the common error of extrapolating a regression curve. The second-degree polynomial curve fitted to the rainfall intensity-duration data, as illustrated in Figure 4-17, has a parabolic shape, and therefore, must start going up if it is extrapolated far enough.

#### 4.5.5 Adjustment of the derived IFD curves

To provide better estimates of the design rainfall intensity for rare, long duration storms at station 85237, one possible method is to adjust the tails of the derived IFD curves. This can be done by comparing the derived storm IFD curves with the existing design rainfall IFD curves for storm bursts. For any design site, there are two sets of burst IFD curves available for comparison. The first set of IFD curves is based on rainfall intensity data collected at several sites and analysed using a regional technique, as applied by the Institution of Engineers, Australia (1987). The design data to derive these IFD curves for a specific site are provided by the Institution of Engineers, Australia (1987, Volume 2). The second set is the at-site IFD curves, herein referred to as the IFD-HYDSYS curves, developed by HYDSYS (1994) from data available at the site, using an at-site frequency analysis method consistent with that of the Institution of Engineers, Australia (1987). As the IFD curves derived in the present study were developed using the at-site rainfall data at station 85237, it is relevant to compare them with the IFD-HYDSYS curves.

The IFD-HYDSYS curves are derived for storm bursts, which are periods of intense rain during storm events. Storm bursts of a given duration are obtained from an observed record by progressively passing a 'window' of the specified duration throughout the record, and selecting events that have average intensities greater than some threshold values. The bursts so identified therefore have two characteristics. Firstly, for a specified duration, the bursts selected may overlap, so they are not

independent of each other. Secondly, a burst of a short duration may be a part of a longer duration burst.

In order to compare the derived IFD curves with the IFD-HYDSYS curves, it is important to note that storms defined in this study have sampling properties different from bursts for which the IFD-HYDSYS curves were developed. In this study, any rainfall period is included only once in the storm sample (so all the extracted events are essentially independent), but may have been included several times in the burst sample, because a shorter duration burst may be a part of a longer duration burst, as explained above. Thus the series of storms defined here generally consists of events with average intensities lower than those in the burst series. However, the difference between burst intensities and storm intensities will reduce with increasing duration, because both samples will share common events. As a result, the IFD curves derived for storms defined in this project should always lie below the IFD-HYDSYS curves, but the two curves tend to converge at long storm durations.

An illustration of the comparison of the derived IFD curves and the IFD-HYDSYS curves for station 85237 is illustrated in Figure 4-19. In this figure, the IFD-HYDSYS curve for the ARI of 20 years is plotted together with the derived IFD curve for the same ARI. This figure shows that the derived 20-year IFD curve is only below the corresponding IFD-HYDSYS curve for duration up to 48 hours (approximately). For longer storms, the design average rainfall intensities estimated by the current procedure exceed those of the IFD-HYDSYS curve estimated by HYDSYS. A similar conclusion is drawn for the derived IFD curves of other return periods.

The comparison of the derived IFD curves and the IFD-HYDSYS curves indicates that the IFD-HYDSYS intensity for long duration storms can be used to adjust the tails of the derived IFD curves, as for these storms, the difference between the two sets of curves becomes insignificant. Therefore, for each ARI, two storm events with the duration of 72 hours and 144 hours were used as additional events for fitting the polynomial curves of intensities of varying durations. The average intensities of these storms were assumed to equal the IFD-HYDSYS rainfall intensity estimates for storm bursts of the same duration and ARI.

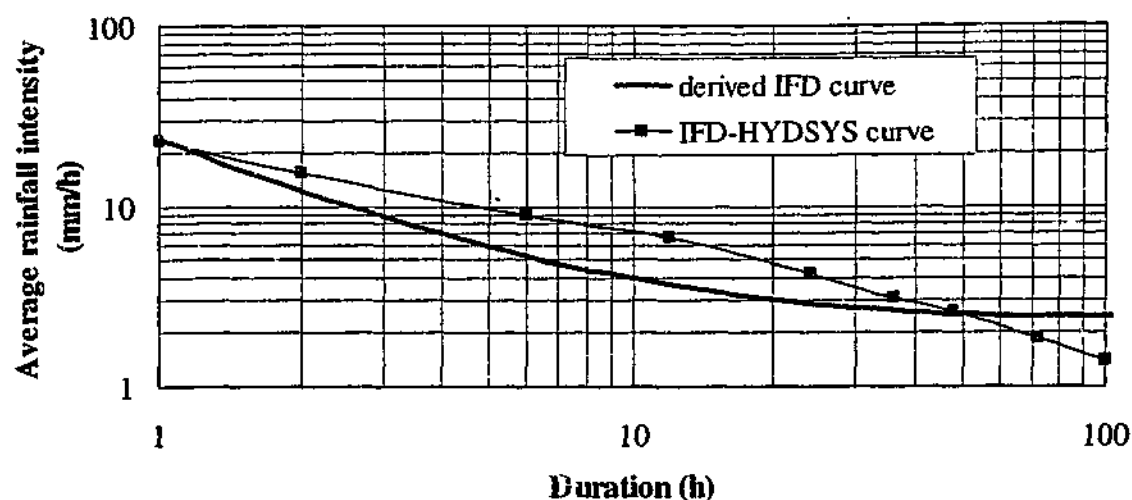


Figure 4-19: Derived IFD curve and the IFD-HYDSYS curve for ARI=20 years (station 85237)

Table 4-11 gives an example of the intensity values (original and additional) for fitting the polynomial curve, and Figure 4-20 illustrates the resulting polynomial curve for design rainfall intensity estimates for storms of 20-year ARI. It is noted from this figure that a linear relationship rather than a polynomial curve may have been sufficient because of the small coefficient of the square term.

Table 4-11: Data used to determine the intensity-duration curve (ARI = 20 years)

D (h)	I (mm/h)	log(D)	log(I)
2	12.30	0.30	1.09
8	4.23	0.90	0.63
16	3.55	1.20	0.55
32	2.69	1.51	0.43
48	2.47	1.68	0.39
72	<b>1.84</b>	1.86	0.27
144	<b>1.01</b>	2.16	0.004

(Bold values are those obtained from IFD-HYDSYS)

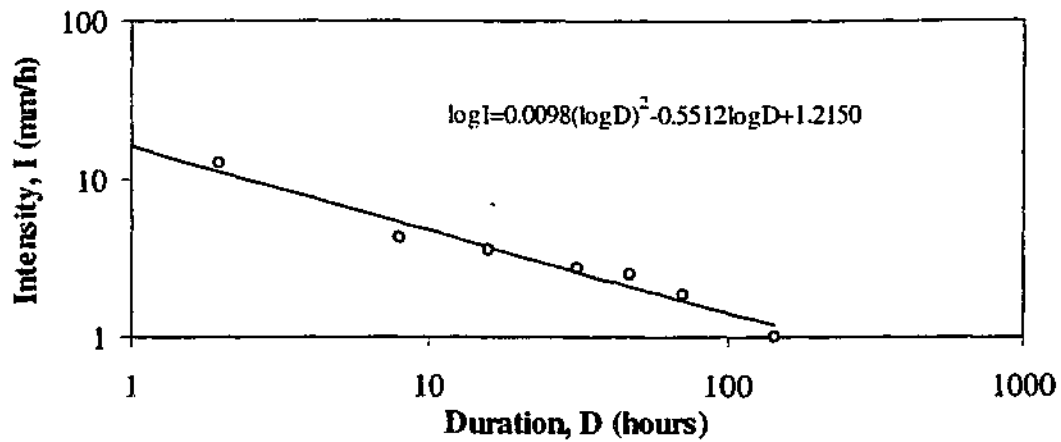


Figure 4-20: Plot of the polynomial rainfall intensity-duration curve (ARI = 20 years)

The derived IFD curves (after adjustment) were then compared with the IFD-HYDSYS curves and the originally derived IFD curves (before adjustment). As an illustration, the three IFD curves for the ARI of 20 years are plotted in Figure 4-21. From this figure, it is clear that, for all durations, after adjustment, the design rainfall intensity at station 85237 decreases as the storm duration increases. In addition, the adjusted IFD curve is always below the IFD-HYDSYS curve for the given ARI, as expected from the difference between the average intensity of storms defined in this study and storm bursts. The same conclusion is reached for the intensity-duration curves of other ARIs used. In general, the adjustments of rainfall intensities of long duration storms are fairly substantial, but justified.

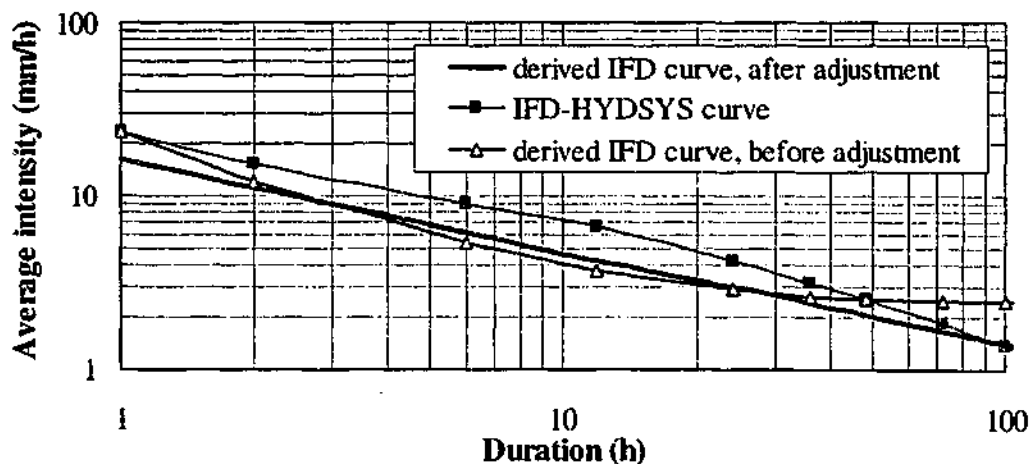


Figure 4-21: Plot of the IFD curves at station 85237 (ARI=20 years)

The final set of the derived IFD estimates for station 85237 is presented in Figure 4-22.

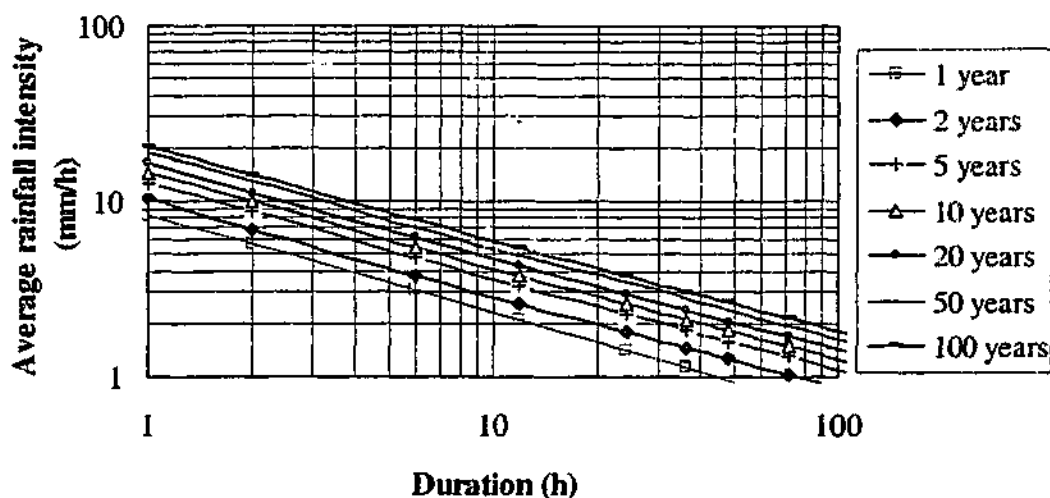


Figure 4-22: The estimated IFD curves at Noojee (pluviometer 85237)

#### 4.5.6 Discussion

The comparison of the derived IFD curves and the IFD-HYDSYS curves indicates that the adopted at-site frequency analysis procedure can give consistent estimates of the design rainfall intensity for events with duration up to 48 hours and ARI up to 100 years for station 85237. However, there are uncertainties in estimates of the average rainfall intensity for long duration, low frequency storms (duration and ARI exceeding 48 hours and 20 years, respectively). This is essentially the result of errors in extrapolating a regression curve, the lack of observed long duration storms, and the use of only five class intervals to represent storm duration, as discussed in Section 4.5.4.

It is obvious that more reliable intensity estimates for long duration and very infrequent storms could be obtained by increasing the corresponding storm sample. This can be achieved by two methods. The first method is to increase the separation time used to define storm events. However, this method also leads to a reduction in the number of short duration events (see Section 4.3.2.1), which in turn affects the reliability of rainfall intensity estimates for these events. In other words, by increasing the separation time used in the storm definition, better estimates of design rainfall intensity for long

duration events may be achieved at the cost of more uncertainties in estimates of short duration events. The second method is to use regional rainfall data for developing the IFD curves. This is considered to be a very effective method, as it not only increases the sample size of long duration storms, but also of short duration events. In addition, the discretisation of storm duration will become more accurate due to the possibility of an increased number of class intervals used. As a result, better rainfall intensity estimates can be obtained for events of any duration and frequency. Whereas the implementation of this method is desirable, it is considered outside the scope of this project.

#### 4.5.7 Summary

In this section, a modified at-site frequency analysis procedure for partial duration series was used to derive the IFD curves at station 85237 for storm events defined in this research. With this procedure, observed rainfall intensities of various durations at the design site were represented by five series having representative durations of 2, 8, 16, 32, and 48 hours. An exponential distribution was then fitted to each series, distributional parameters were estimated, and the goodness-of-fit of the distribution was visually checked. For each representative duration, design rainfall intensities of various ARIs were then estimated from the fitted exponential distributions. For a given ARI, a polynomial curve was next fitted to the design intensities of the five representative durations. The design average rainfall intensities of any duration were finally determined by interpolating and extrapolating the fitted polynomial curve for a given ARI.

It was found that, for storms with duration up to 48 hours and ARIs up to 100 years, the IFD curves derived by the adopted procedure were consistent with the existing IFD curves (for the same site). The latter IFD curves were developed for storm bursts using the method proposed by the Institution of Engineers, Australia (1987). However, there was an unusual relationship between the design rainfall intensity and rainfall duration for longer duration and less frequent events. In particular, for storm events whose ARI exceeding 20 years and duration greater than 48 hours, the design rainfall intensity increased even though the rainfall duration increased. This was attributed to the lack of

observed rainfall data in this range, the extrapolation of the polynomial curves for intensity estimates, and errors in the representation of the observed intensities at the design site by only five series.

In order to provide better estimates of the rainfall intensity for the design site, the upper tails (for long duration storms) of the derived IFD curves were adjusted based on the IFD analysis of storm bursts. It was assumed that the design intensities for storms defined in this study and for storm bursts were equal for durations of 72 hours and 144 hours. These rainfall intensities were used to provide additional data points for the fitting of polynomial equations to the IFD data. The adjusted IFD curves were satisfactory because the relationship between design rainfall intensity and duration was consistent for all durations and ARIs. Nevertheless, it was concluded that more reliable rainfall intensity estimates for storm events of any duration and frequency could be obtained by using regional rainfall data.

## **4.6 STOCHASTIC REPRESENTATION OF TEMPORAL PATTERNS**

### **4.6.1 Background**

Knowledge of the temporal pattern of rainfall (that is, the time distribution of rainfall intensity during storm duration) is important in determining the timing and magnitude of peak flow, especially for urban or small rural catchments where the time of concentration is relatively short and catchment response is less influenced by storage or channel characteristics. In addition, the spatial variability of rainfall influences the generation of runoff, especially for large catchments. However, it seems to be difficult to assign a numerical value to differentiate a small catchment from a large one, as catchment size is not the only index that characterises catchment behaviour. With the lack of artificial storage within the 'medium-sized' catchments under study (less than 500km<sup>2</sup>), the consideration of the temporal pattern as a stochastic factor may be unnecessary but is prudent.

The time distribution of real rainfall events may be influenced by many factors that need

to be reflected in design temporal patterns. These factors may include location, storm duration, storm depth, or season of storm occurrence. As discussed in Section 3.3.3, there are conflicting conclusions about the relationships between rainfall temporal patterns and these factors. For example, whereas design temporal patterns of storm bursts used in Australian design practice are dependent on location, storm duration and frequency (Institution of Engineers, Australia, 1987, Chapter 3), rainfall temporal data at three Spanish stations have shown no correlation with any of the above factors (Garcia-Guzman and Aranda-Oliver, 1993). Thus, before developing a stochastic model of temporal patterns of storm events defined in this study, it is necessary to investigate if the temporal pattern is dependent on season of storm occurrence, storm duration and depth. At this stage, for the relatively small region considered, it is assumed that the 19 selected rainfall sites form a homogeneous region as far as the storm temporal pattern is concerned. It is also noted that the analysis of the dependence of temporal patterns on season is not directly applied in this study, but was conducted for the sake of a broader understanding of the factors that affect the variability of temporal patterns.

To represent the temporal pattern by a statistical model, conditional probability analysis is required if the temporal pattern is dependent on any of the factors above. For example, if temporal patterns vary with storm duration, they then need to be separated into different duration groups. For each duration group, a probability distribution can then be used to characterise the observed temporal patterns in the group. From the adopted model, design temporal patterns can be generated.

This section presents the research undertaken to investigate the dependence of the temporal pattern on season, storm duration and depth, as well as the characterisation of the temporal pattern by a statistical model. The data used for this investigation and the representation of the temporal pattern are also described.

#### **4.6.2 Data**

In order to examine whether the temporal pattern is dependent on any of the above three factors, a large database of observed temporal patterns was required. Initially, this

database consisted of all storm events extracted at the 19 selected pluviometers. However, as these events were recorded at fixed time intervals of one hour, the amount of rain recorded in the first or last hour of a storm usually represents the rainfall that fell in a fraction of an hour. For example, a real rainfall event lasting 5 hours and 25 minutes from 04:50 AM to 10:15 AM would have been recorded as a 7-hour storm from 4:00AM to 11:00AM. Thus, the average hourly rainfall intensity of the first and last hour of any storm is consistently underestimated. As the temporal variation of rainfall events used in this study was represented by the average rainfall intensity in each hourly time step of the storm duration, the underestimation of some of these data values may have affected the analysis outcome. This effect became even more pronounced for short duration events. Thus, to avoid introducing possible errors caused by short duration storms into the results, only the extracted events with duration of at least 4 hours were included in this analysis.

For the 19 sites under investigation, the storm sample selected for this analysis consisted of 3587 storms (with the minimum duration of 4 hours). The average duration of these events was 20 hours, and the average rainfall depth was 35.4mm. As these storms constituted more than 90% of the total number of the observed storms in the test region (N=3975 storms), the selected storm sample was considered to be representative of all rainfall events in this region as far as the time distribution of rainfall is concerned.

### 4.6.3 Representation of temporal patterns

Before explaining how the temporal pattern is defined, it is worth noting that there is a basic difference between the temporal pattern and other rainfall characteristics such as storm duration or depth. Whereas storm duration and depth are 'concentrative' variables, and consequently can be described by one number each, the temporal pattern is a 'distributive' random variable, and therefore needs more than one number in its representation.

In order to describe the temporal pattern by numbers, two alternatives were adopted in this study. The first alternative, suggested by Laurenson (Personal communication, 1998), used 3 statistical characteristics of the dimensionless storm hyetograph. The

second alternative used internal ordinates of the dimensionless storm mass curve. In the literature, the first alternative was used by Yen and Chow (1980), whereas the second by Huff (1967), Garcia-Guzman and Aranda-Oliver (1993), and Robinson and Sivapalan (1997). In this study, the number of mass curve ordinates varies according to the purpose of analysis. For example, the dimensionless storm mass curve was represented by 9, 4, 3 or 2 ordinates in sensitivity analyses for investigating the dependence of temporal patterns on season, storm duration and depth (see Section 4.6.4.2), and by 7 ordinates for representing design temporal patterns (see Section 4.6.5).

To determine the 3 statistical characteristics or mass curve ordinates describing the temporal pattern, the dimensionless storm hyetograph was first computed in order to homogenise observed storm events of heterogeneous durations and total rainfall depths. The dimensionless rainfall hyetograph represents dimensionless rainfall depths computed for equal increments of dimensionless storm time (Figure 4-23). In the present analysis, 10 increments were used to describe the observed dimensionless hyetograph as it was assumed that the overall shape of the pattern is more important than small-scale variations.

#### **Representation by 3 statistical characteristics of the dimensionless hyetograph**

To represent the temporal pattern by 3 statistical characteristics, the mean ( $m_1$ ), standard deviation ( $s$ ), and coefficient of skewness ( $C_s$ ) of the dimensionless hyetograph were used (see Figure 4-23). These characteristics were calculated with reference to the starting time of a rainfall event. The mean is the centre of gravity of the observed dimensionless hyetograph, which represents the dimensionless time from the start of the event to the centroid of the rainfall hyetograph. A large mean value thus indicates that the rain is heavier in the later part of the storm duration, and vice versa. The standard deviation gives an indication of the degree of dispersion of the dimensionless rainfall depth about the mean. The coefficient of skewness specifies the degree of asymmetry of the temporal pattern distribution.

For each observed dimensionless storm hyetograph, these statistical characteristics were computed using the following formulas:

$$m_1 = \sum_{i=1}^n t_i h(t_i)$$

$$s = \left( \sum_{i=1}^n (t_i - m_1)^2 h(t_i) \right)^{1/2} \quad (4-7)$$

$$C_s = \sum_{i=1}^n (t_i - m_1)^3 h(t_i) / s^3$$

where  $h(t_i)$  is the relative rainfall in a time interval ( $\sum_{i=1}^n h(t_i) = 1$ );  $t_i$  is the mid point of a time interval; and  $n$  is the number of time intervals used to define the rainfall hyetograph ( $n=10$  in the present analysis).

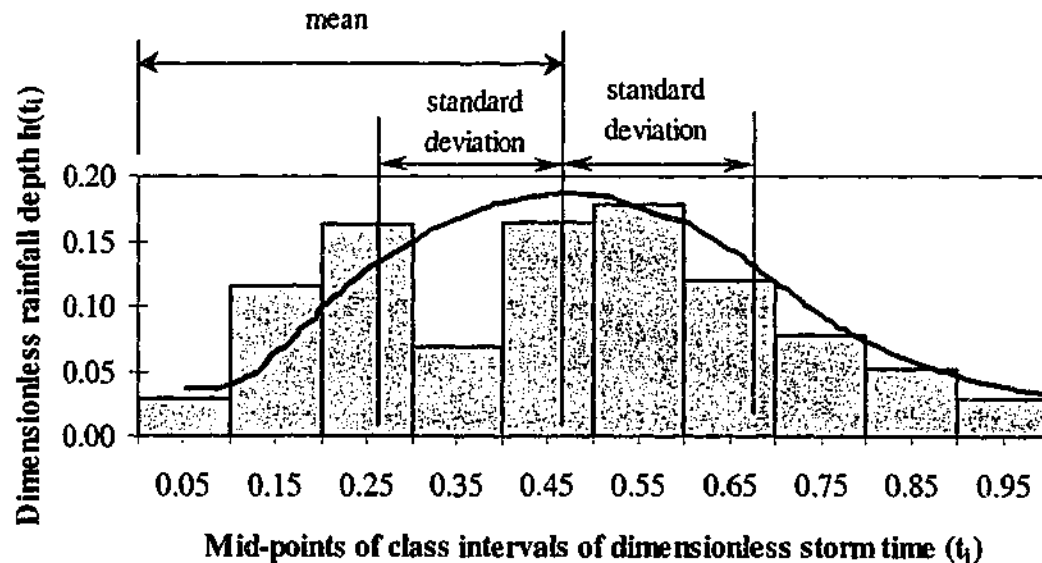


Figure 4-23: Dimensionless rainfall hyetograph and its statistical characteristics

#### Representation by ordinates of the dimensionless mass curve

To describe the temporal pattern by 9 ordinates of the dimensionless storm mass curve, the dimensionless mass curve of the dimensionless storm hyetograph was first determined. The dimensionless mass curve of a storm is a plot of the dimensionless cumulative rainfall depth versus the dimensionless cumulative storm time. At any specified time during the storm duration, the former is the ratio of the accumulated rainfall depth to the total depth, and the latter is the ratio of the time from the start of the storm to the storm duration. The temporal pattern ordinates were then taken as the

*internal ordinates* of the dimensionless mass curve, as the ordinates of the two ends of any mass curve are always 0 (for the low end) and 1 (for the top end). The number of temporal pattern ordinates is thus the number of time increments used to define the corresponding dimensionless rainfall hyetograph minus 1. An example of a temporal pattern defined by 9 ordinates (corresponding to a dimensionless hyetograph defined at 10 equal time intervals) is given in Figure 4-24. Similarly, if a storm hyetograph is defined by 5, 4 or 3 time increments, then 4, 3 or 2 ordinates, respectively, define the storm temporal pattern.

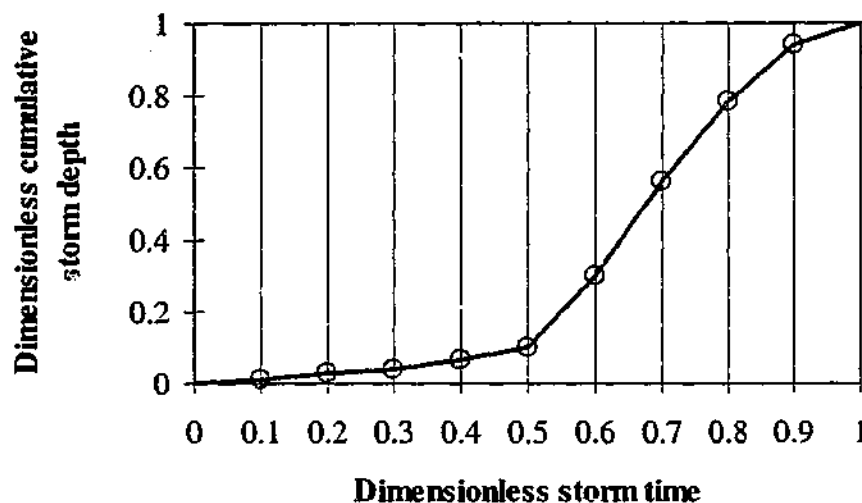


Figure 4-24: 9-ordinate representation of temporal patterns

#### 4.6.4 Dependence of temporal patterns on season, storm duration and depth

Three methods for determining whether the rainfall temporal pattern is dependent on season (or month) of storm occurrence, storm duration or depth have been used in the literature. They are correlation analysis, the chi-square test of independence, and the comparison of Huff curves. Clearly, any one of these methods could be used for the present objective. However, due to the controversial conclusions reached by previous researchers about the relationship between the temporal pattern and the above factors (see Section 3.3.3), it is desirable to use at least two methods to investigate this issue. Therefore, for this present study, correlation analysis and the chi-square test of independence were adopted.

#### 4.6.4.1 Correlation analysis

Correlation analysis measures the degree of linear relationship between two or more random variables. This relationship is characterised by the correlation coefficients computed for each pair of variables. Correlation analysis was applied by Huff (1967) to determine whether "the variance in the time distribution of rainfall" was attributable to the variation in duration and mean rainfall.

The population correlation coefficient ( $\rho_{X,Y}$ ) between two random variables  $X$  and  $Y$  is defined in terms of the covariance of  $X$  and  $Y$  ( $\sigma_{X,Y}$ ) and the standard deviations of  $X$  and  $Y$  ( $\sigma_X, \sigma_Y$ ) as follows:

$$\rho_{X,Y} = \frac{\sigma_{X,Y}}{\sigma_X \sigma_Y} \quad (4-8)$$

Given two samples of size  $n$  with observations  $x_1, x_2, \dots, x_n$ , and  $y_1, y_2, \dots, y_n$ , the sample estimate  $r_{X,Y}$  for  $\rho_{X,Y}$  is similarly given by:

$$r_{X,Y} = \frac{s_{X,Y}}{s_X s_Y} \quad (4-9)$$

in which

$$s_{X,Y} = \frac{1}{n} \sum_{i=1}^n (x_i - \mu_X)(y_i - \mu_Y) \quad (4-10)$$

is the sample covariance,  $s_X$  and  $s_Y$  are the sample estimates of the standard deviation, and  $\mu_X$  and  $\mu_Y$  are the sample means.

The value of  $\rho_{X,Y}$  can range from  $-1$  to  $+1$ . If  $\rho_{X,Y} = \pm 1$ , there is a perfect linear relationship between  $X$  and  $Y$ . If  $\rho_{X,Y} = 0$  or close to it, there is no linear relationship, but other types of dependence may exist between  $X$  and  $Y$ . If  $X$  and  $Y$  are independent random variables, then  $\rho_{X,Y} = 0$ .

Correlation analysis was applied to investigate the relationship between the 3 statistical characteristics describing the temporal pattern and storm duration or depth in the following manner.

- Dimensionless hyetographs of the observed rainfall events were first determined.
- The 3 statistical characteristics of the observed dimensionless hyetographs ( $m_1$ ,  $s$ , and  $C_s$ ) were next computed using Equation (4-7).
- The correlation coefficients between each of these 3 characteristics and storm duration or storm depth were then computed using an EXCEL spreadsheet. Results are tabulated in Table 4-12.
- A visual inspection of the relationship between the temporal pattern characteristics and storm duration or depth was also carried out by plotting each of the computed characteristics against the corresponding storm duration or depth. Two examples of such plots are given in Figure 4-25 and Figure 4-26.

Table 4-12: Correlation coefficients between 3 statistical characteristics of observed dimensionless hyetographs and storm duration or depth

	Mean	Standard deviation	Coefficient of skewness
Duration	0.04	0.23	-0.06
Depth	0.07	0.02	-0.07

In examining the correlation coefficients between the 3 statistical characteristics of temporal patterns and rainfall duration or depth (see Table 4-12), it is clear that for all cases, the maximum absolute value of the correlation coefficient is 0.23, and the minimum absolute value is 0.02. That is, the estimated correlation coefficients are generally well below 1 and very close to 0. The corresponding graphs between each of the 3 temporal pattern characteristics and storm duration or depth indicate no systematic relationship between each pair of variables (see an illustration in Figure 4-25), with the exception of the standard deviation. For this special case, the standard deviation of the temporal pattern seems to increase as storm duration increases (see Figure 4-26). This relationship corresponds to the correlation coefficient of 0.23 between the standard deviation and storm duration. Nevertheless, the coefficient of determination ( $R^2$ ) computed for this case is only 0.05, indicating that only 5% of the variation in the standard deviation of the temporal pattern is explained by the variation in the storm duration. Therefore, using correlation analysis, it can be concluded that the temporal pattern of rainfall, described by 3 statistical characteristics of the dimensionless rainfall hyetograph, is independent of both storm duration and storm depth.

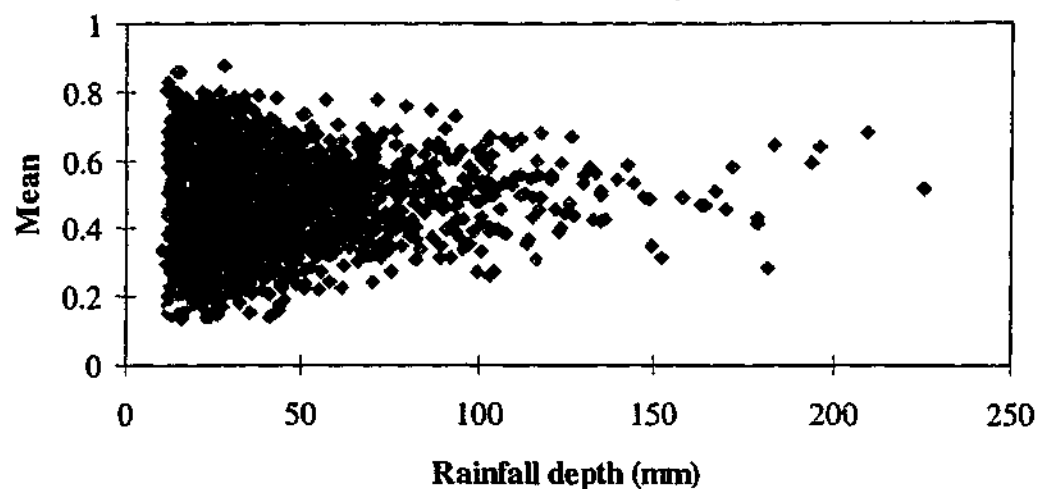


Figure 4-25: Plot of the mean (centre of gravity) of observed dimensionless hyetographs versus rainfall depth

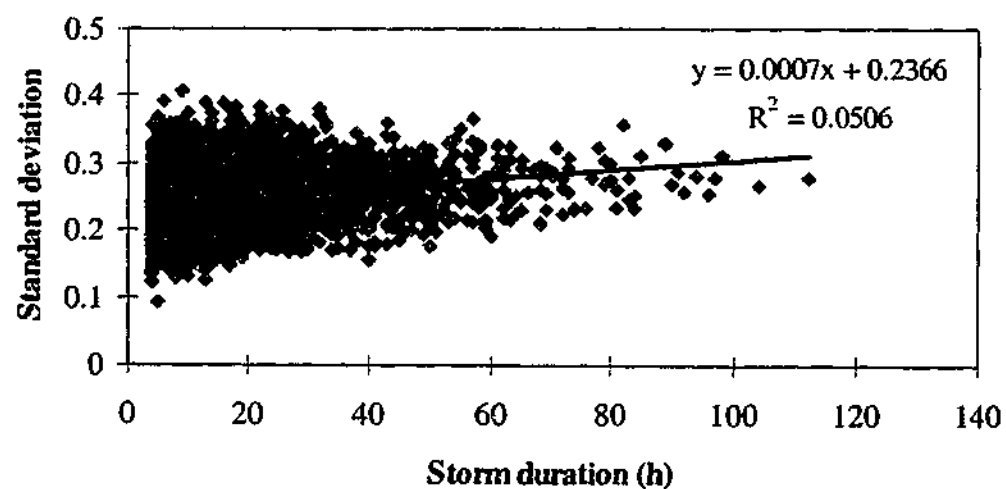


Figure 4-26: Plot of standard deviation (degree of dispersion) of observed dimensionless hyetographs versus rainfall duration

#### 4.6.4.2 The chi-square test of independence

The chi-square test of independence aims to determine whether two variables are associated. For example, it can be used to decide if product price is associated with product quality, or if level of education is associated with income. In hydrology, this test was applied by Garcia-Guzman and Aranda-Oliver (1993) to claim that the

hyetographs of rainfall events observed at three rainfall stations in Spain were independent of storm season, duration and depth. The test, summarised from Daniel (1978), is described in detail in Appendix G.

To apply the chi-square test of independence, it is assumed that a random set of data may be cross-classified according to two criteria, which are the variables of interest in a given situation. The data are then displayed in a contingency table with  $r$  rows and  $c$  columns (see an illustration in Appendix G). To test the null hypothesis that the two criteria are independent, the expected cell frequencies (expected when the assumption of independence of the two variables is true) are computed and compared with the corresponding observed cell frequencies. The null hypothesis may be rejected at the  $\alpha$  level of significance if the computed value of the test statistic  $\chi^2$  exceeds the tabulated chi-square critical value for  $(r-1)(c-1)$  degrees of freedom.

The following section describes the application of the chi-square test of independence to determine if the rainfall temporal pattern is dependent on any of the three factors, namely season of storm occurrence, storm duration and depth. In this particular case, the temporal pattern is represented by 9 ordinates of the dimensionless mass curve (see Figure 4-24). The investigation of the effects on the test results of using different numbers of mass curve ordinates (namely 4, 3 and 2) is also documented.

#### **Dependence on season**

The dependence of the storm temporal pattern on season was examined using the following procedure:

- (a) First of all, the chi-square test was applied to test the null hypothesis (i) that storm temporal patterns are independent of the month of storm occurrence (Test 1).
- (b) To test this hypothesis, observed values of temporal pattern ordinates were arranged in 10 classes. These classes were: (0, 0.1), (0.1, 0.2), (0.2, 0.3), ... , (0.8, 0.9), and (0.9, 1.0). The month of storm occurrence was assigned to 12 levels (months).
- (c) For any observed temporal pattern, the frequency of obtaining a given ordinate within any of the 10 classes above, jointly with the known month of the storm, was counted and placed in the corresponding cell of the observed contingency table.

- (d) The total observed frequency in each cell was then computed by adding the frequencies in the cell for all observed storms.
- (e) The corresponding expected frequency for each cell was computed next.
- (f) Lastly, the chi-square test statistic was computed and compared with the critical value determined for the known degree of freedom of the contingency table. A test statistic smaller than the critical value at a specified level of significance (LOS) indicates that the null hypothesis can not be rejected, that is, temporal pattern ordinates, and therefore temporal patterns, are independent of month. In this case, the variation of temporal patterns with months of the storms can be neglected in the analysis. Otherwise, temporal patterns are dependent on the month in which they occur.

Results of the initial investigation of the dependence of rainfall temporal patterns on months of storm occurrence (Test 1) are summarised in the first row of Table 4-13. It is clear that the chi-square test statistic (203.7) is much greater than the critical value at the 5% LOS (123.2), and therefore, the null hypothesis is rejected. That is, storm temporal patterns are not independent of the month of storm occurrence. Therefore, the variation of rainfall temporal patterns with season of storm occurrence should be accounted for in a stochastic representation of temporal patterns.

Table 4-13: Results of the chi-square test of independence to examine the dependence of storm temporal patterns on season

Test No	Classification into months or seasons (groups of months)	Hypothesis	Degrees of freedom	Critical value at 5% LOS	Test statistic
1	12 months	(i)	99.0	123.2	203.7
2	4 rainfall seasons	(ii)	27	40.1	93.2
3	Summer (Dec. - Mar.)	(iii)	27	40.1	39.4
4	Autumn (April - May)	(iii)	9	16.9	7.0
5	Winter (June - Sep.)	(iii)	27	40.1	28.9
6	Spring (Oct. - Nov.)	(iii)	9	16.9	13.9

The issue now is the degree of dependence of temporal patterns on season (that is, a group of months), and how to form independent sub-samples of temporal patterns within each of which the variation of the temporal pattern with season can be neglected. To do this, a calendar year was tentatively divided into four rainfall seasons as used by

the Bureau of Meteorology for extreme rainfall analysis (Minty et al., 1996). These rainfall seasons are Summer (December to March), Autumn (April to May), Winter (June to September), and Spring (October to November). The procedure described above was next applied to test the two null hypotheses as follows: (ii) between four defined rainfall seasons, temporal patterns are independent of season, and (iii) within each rainfall season, temporal patterns are independent of the month of storm occurrence.

Results of these tests are also tabulated in Table 4-13. It can be seen from this table that the chi-square test statistic computed for the four seasonal groups of temporal patterns (93.2, see Test 2) exceeds the critical value at 5% LOS (40.1). Thus, the null hypothesis (ii) is rejected. By contrast, the test statistic computed for each of the four seasonal groups is less than the corresponding critical value at the 5% LOS (see Tests 3-6 in Table 4-13). As a result, the null hypothesis (iii) can not be rejected. In other words, there is insufficient evidence to conclude that storm temporal patterns in different months within a seasonal group are dependent on the corresponding months of the storms.

In summary, results of the chi-square test of independence showed that observed rainfall temporal patterns, characterised by 9 ordinates of dimensionless mass curves, are not independent of the month in which they occur. Further analyses of the degree of dependence of temporal patterns on season indicated that four distinct seasonal groups of months (rainfall seasons) could be identified. Within these seasons, temporal patterns are independent of the month of storm occurrence.

#### **Dependence on storm duration**

As mentioned in Section 3.3.3, there has been evidence in previous studies that the temporal pattern of short duration storms is different from that of long duration storms (Yen and Chow, 1980; Bonta and Rao, 1989). In Australia, temporal patterns of design storms are also different for different durations (Institution of Engineers, Australia, 1987). For the data set used in the present study, it has also been found that the temporal pattern is dependent on season. Therefore, for each seasonal group, the following two hypotheses were established: (iv) temporal patterns are independent of duration groups, and (v) within each duration group, temporal patterns of storms are

independent of the storm duration. The hypotheses were also tested using the chi-square test of independence.

To apply the chi-square test, the temporal pattern ordinates were still classified in 10 classes as described in step (b) under seasonal dependence. However, for the summer season, the storm duration was divided into three duration groups as follows: (4h – 12h), (13h – 24h), and greater than 24 hours. Similar to step (c), the cell frequency of obtaining a given temporal pattern ordinate within a duration group was determined. Steps (d) through (f) were then undertaken. Subsequently, the tests were applied with only two duration groups of (4h – 12h) and greater than 12 hours for the other seasons.

Table 4-14: Results of the chi-square test of independence to examine the dependence of temporal patterns on storm duration

Rainfall seasons	Classification into duration groups	Hypothesis	Degrees of freedom	Critical value at 5% LOS	Test statistic
Summer	3 groups	(iv)	18	28.9	124.1
	4h - 12h	(v)	72	92.8 (*)	98.0
	13h - 24h	(v)	99	123.2 (**)	138.1
	>24h	(v)	27	40.1	34.6
Autumn	2 groups	(iv)	9	16.9	20.8
	4h - 12h	(v)	72	92.8	55.8
	>12h	(v)	36	51.0	27.7
Winter	2 groups	(iv)	9	16.9	32.8
	4h - 12h	(v)	72	92.8	77.3
	>12h	(v)	36	51.0	44.2
Spring	2 groups	(iv)	9	16.9	45.2
	4h - 12h	(v)	72	92.8	66.8
	>12h	(v)	36	51.0	43.2

Note: (\*) CV at 1% LOS = 102.8  
 (\*\*) CV at 0.5% LOS = 139.0

Results of the examination of the association between the temporal pattern of the observed storms in each of the four seasonal groups and storm duration are summarised in Table 4-14. It is evident from this table that temporal patterns are not independent of the duration groups as hypothesis (iv) is always rejected. As an example, for autumn storms, the test statistic (20.8) is greater than the critical value (16.9). This means that the temporal pattern of autumn storms is dependent on whether the storm duration is in the group of (4h – 12h) or greater than 12h. However, within each of the identified

duration groups, temporal patterns can be considered to be independent of duration because hypothesis (v) is not rejected, as the chi-square statistic is less than the corresponding critical value. An exception is the summer storms in which the storm temporal pattern is dependent on duration in the following three duration groups: (4h – 12h), (13h – 24h), and greater than 24 hours. It is noted that in this case, the storm temporal patterns of the two duration groups, namely (4h – 12h) and (13h – 24h) can be marginally considered to be independent on storm duration at fairly low levels of significance (1% and 0.5%) (see Table 4-14).

#### Dependence on storm depth

In examining whether the temporal pattern of storm events is dependent on storm magnitude, the null hypothesis (vi) was that the temporal pattern of the observed storms in each seasonal and duration group is independent of storm depth. To test this hypothesis, the chi-square test of independence was again used. In applying the test, the observed storm patterns in each specified season and duration group were assigned to the following levels of total depths: (0 – 15mm), (15mm – 20mm), (20mm – 25mm), ..., (55mm – 60mm) and greater than 60mm.

Table 4-15: Results of the chi-square test of independence to investigate the dependence of temporal patterns on season, storm duration, and storm depth

Rainfall seasons	Duration groups	Classification into groups of rainfall depths	Hypothesis	Number of storms	Degrees of freedom	Critical value at 5% LOS	Test statistic
Summer	4h - 12h	all groups	(vi)	686	45	61.7	49.6
	13h - 24h	all groups	(vi)	362	81	103.02	145.4
		2 groups	(vii)	362	9	16.9	46.5
		(0 - 50) mm	(viii)	314	54	72.1	71.9
	> 50 mm	(viii)	48	9	16.9	10.1	
>24h	all groups	(vi)	216	36	51.0	42.5	
Autumn	4h - 12h	all groups	(vi)	232	45	61.7	39.0
	>12h	all groups	(vi)	444	45	61.7	61.6
Winter	4h - 12h	all groups	(vi)	263	45	61.7	25.4
	>12h	all groups	(vi)	659	45	61.7 (*)	67.1
Spring	4h - 12h	all groups	(vi)	384	54	72.1	66.0
	>12h	all groups	(vi)	341	45	61.7	50.2

Note: (\*) CV at 1% LOS = 70.0

Results of the chi-square test are summarised in Table 4-15. From this table, it can be concluded that the temporal pattern is independent of total storm rainfall depth, as the test statistic computed for each rainfall season and duration group is smaller than the

critical value at 5% LOS (but at 1% LOS for winter storms with duration greater than 12 hours). Again, there is an exception for summer storms, in which the chi-square test results show that the temporal patterns of storms in the duration range of (13h – 24h) are dependent on storm depth (see Table 4-15) because the test statistic (145.4) exceeds the corresponding critical value (103.0) at 5% LOS. This means that the variation of temporal patterns with storm depth needs to be considered.

The issue now is how to form sub-groups of temporal patterns so that within each group the dependence of temporal patterns on storm depth can be neglected. To do this, the observed patterns of summer storms in the duration group of 13 to 24 hours were divided into the following two groups of depth: (0 – 50mm) and greater than 50mm. The chi-square test of independence was then applied to test the two null hypotheses as follows: (vii) between the two defined groups of rainfall depth, temporal patterns are independent of rainfall depth groups, and (viii) within each specified group of rainfall depth, temporal patterns are independent of storm depth. Test results are also tabulated in Table 4-15.

It is clear from Table 4-15 that the hypothesis (vii) is rejected because the test statistic of 46.5 exceeds the corresponding critical value of 16.9 at 5% LOS. As a result, the dependence of temporal patterns of summer storms from 13 to 24 hours on storm depth should be taken into consideration. However, there is insufficient evidence to reject the hypothesis (viii) because for each specified group of storm depth, the computed test statistic is less than the corresponding critical value.

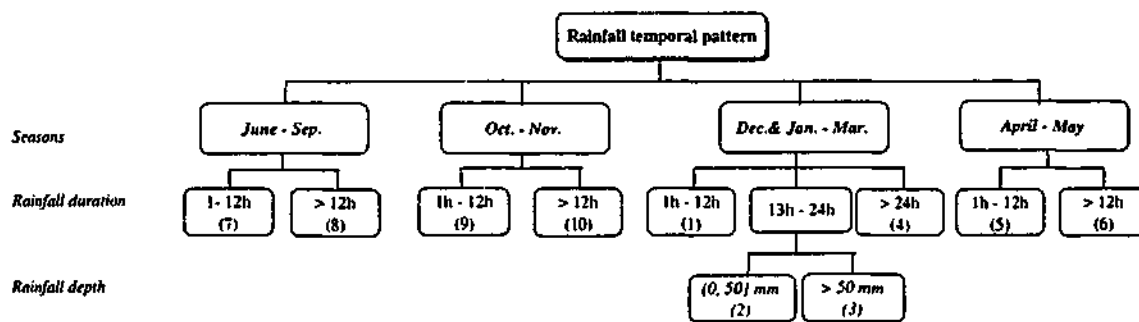
#### **Summary of chi-square test results**

From the investigation of the dependence of the temporal pattern on season, storm duration, and depth, the following conclusions can be made:

- The rainfall temporal pattern, represented by 9 ordinates of the dimensionless mass curve, is dependent on the four seasons of storm events. These rainfall seasons, initially formed using the results of an extreme rainfall analysis undertaken by Minty et al. (1996), are Winter (June to September), Spring (October to November), Summer (December to March) and Autumn (April to May).
- Within each seasonal group, the temporal pattern is also associated with storm duration. In particular, in Spring, Autumn and Winter, the temporal pattern is

dependent on whether the storm duration is less than or equal to 12 hours, or greater than 12 hours. In Summer, storm temporal patterns are associated with three different duration groups, namely, up to 12 hours, from 12 to 24 hours and greater than 24 hours.

- After being so grouped by season and duration, the temporal pattern is independent of rainfall depth, except for summer storms in the mid-range of duration. In this case, the temporal pattern is dependent on whether the rainfall total is greater or less than 50mm.
- In total, there are thus 10 independent groups of temporal pattern, as shown in Figure 4-27. It is worth noting that even though this investigation was undertaken using storm events of 4 hours or greater (see Section 4.6.2), it was assumed that the test results can be applied to storms of any duration from 1 to 120 hours.



Note: The number in brackets represents the temporal pattern group

Figure 4-27: Independent groups of temporal patterns (by the results of the chi-square test of independence)

### Sensitivity analysis

The results of the chi-square test of independence indicated that the storm temporal pattern, represented by 9 ordinates of the dimensionless storm mass curve, was dependent on season, storm duration and depth. By contrast, the correlation analysis showed that the temporal pattern was not correlated with storm duration or depth. The latter conclusion was drawn from an analysis in which the temporal pattern was characterised by 3 statistical characteristics of the dimensionless rainfall hyetograph. As in these two separate analyses the temporal pattern was represented by different numbers of parameters, the contradictory conclusions above could have been the result

of the discrepancy in the number of parameters used to describe the temporal pattern. In order to test this hypothesis, the chi-square test of independence was repeated for the temporal pattern defined by 3 ordinates (that is, the same number of parameters as used in the correlation analysis). Moreover, to gain an insight into the effects of using different numbers of parameters on results of the chi-square test, the test was also undertaken for the temporal pattern defined by 4 and 2 ordinates. An example of a 4-ordinate temporal pattern, already defined in Section 4.6.3, is illustrated in Figure 4-28.

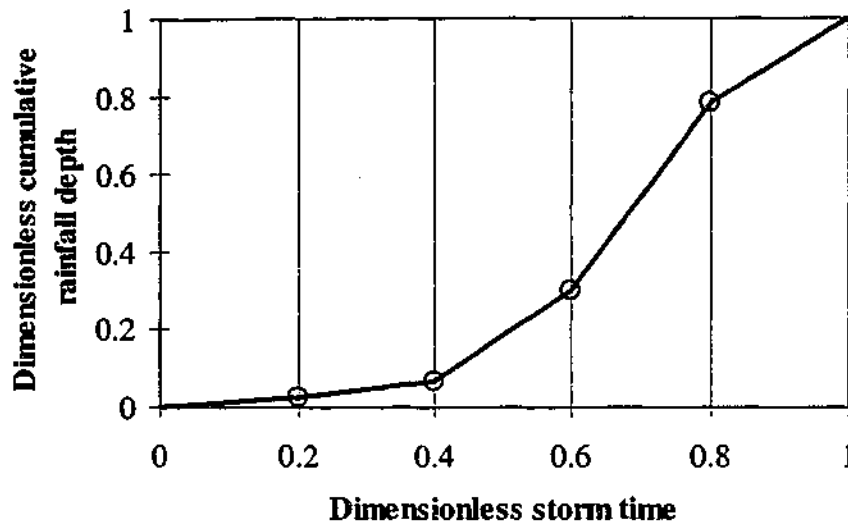


Figure 4-28: 4-ordinate representation of temporal patterns

To investigate the effect on the chi-square test results of the number of ordinates used to characterise mass curves, the procedure described at the beginning of this section was repeated. That is, the test was applied first to test the null hypothesis that temporal patterns, defined by 4, 3 or 2 mass curve ordinates are independent of the month in which they occur. Test results are summarised in Table 4-16. It can be seen from this table that, depending on the number of ordinates used to represent the temporal pattern, different conclusions can be drawn about the association of the pattern with season. When the temporal pattern is defined by 4 ordinates or more, the null hypothesis is rejected at 5% LOS because the computed test statistics exceed the corresponding critical values. Consequently, the variation of the temporal pattern with month of storm occurrence should be taken into account. By contrast, when only 3 ordinates or less are used to characterise the storm temporal pattern, the results of the chi-square test indicate

that there is insufficient evidence to reject the null hypothesis. The entire storm sample of the observed patterns can therefore be regarded as a single group as far as the rainfall temporal pattern is concerned.

Table 4-16: Effects of number of ordinates used to define temporal patterns on results of the chi-square test of independence

Factor under consideration	Number of mass curve ordinates	Degrees of freedom	Critical value at 5% LOS	Test statistic
Season	9	99	123.2	203.7
	4	44	60.5	93.4
	3	33	47.4	44.8
	2	22	33.9	22.5
Duration	2	4	9.5	17.7
	3	6	12.6	51.8

For the simplest cases in which the observed temporal patterns were independent of season (that is, when they were represented by mass curves with 2 or 3 ordinates), the chi-square test was again applied to check if the temporal pattern is associated with storm duration. For this purpose, the storm sample was divided into three duration groups ( $\leq 12$ h, 13h – 24h, and  $> 24$ h). Results are also summarised in Table 4-16. It is evident from this table that, regardless of whether 2 or 3 ordinates are used to represent the temporal pattern, the test statistics computed are always greater than the critical values. This indicates that, in these particular cases, the temporal pattern of storms in all seasons is dependent on storm duration.

By using the same number of parameters to define the storm temporal pattern in two different statistical tests, it is possible to assess the power of the tests to detect any association between the temporal pattern and any of the factors such as season, storm duration and depth. In this particular analysis, the chi-square test seems to be more powerful than the correlation analysis in detecting the dependence of the temporal pattern on duration and depth. However, the power of the chi-square test also reduces with a reducing number of ordinates used in the representation of temporal patterns.

#### 4.6.4.3 Discussion

From the investigation of the dependence of the temporal pattern on season, storm duration or depth using storm events observed at 19 pluviometers used in this study, it was found that different results were obtained depending on the method adopted to represent the temporal pattern and the statistical test used. On the one hand, the use of 3 statistical characteristics to define the rainfall temporal pattern and the correlation analysis to examine this association seem to be blunt measures which led to the conclusion that the time distribution of rainfall intensity was invariant with any of the factors being considered. On the other hand, when the temporal pattern was characterised by the storm mass curve defined at a sufficient number of time steps, the results of the chi-square test of independence indicated that the temporal pattern is dependent not only on season, but also on storm duration and, in one case, on storm depth. In addition, the power of the test used is possibly another factor affecting the analysis outcome, as discussed above.

Of the two contradictory results obtained from the investigation described in this section, the results of the chi-square test of independence for the temporal pattern defined by 9 parameters are judged to be most reliable, and they conform to most findings in previous studies (Huff, 1967; Pilgrim and Cordery, 1975; Yen and Chow, 1980; Institution of Engineers, Australia; 1987; Bonta and Rao, 1989). Results of the chi-square test indicated that the time distribution of rainfall intensity is dependent on the storm season, when four independent seasonal groups were formed based on the seasonal groupings of extreme rainfall (Minty et al., 1996). In each of these seasonal groups, the temporal pattern is generally dependent on two duration groups, the upper limit for the short duration storms being 12 hours. The 12-hour limit may characterise the maximum duration of convective-type storms in this particular study. In the literature, Yen and Chow (1980), and Bonta and Rao (1989) obtained similar results. Their studies showed that storm temporal pattern is significantly affected by the season of the storms, and that the general characteristics of short-duration convective storms differ from those of long-duration cyclonic storms. In Australia, Pilgrim and Cordery (1975) found that the variability of the temporal pattern increases with increasing storm burst duration and decreasing rainfall depth. Similarly, the dependence of the temporal pattern on location and storm duration has been recognised by the use of different

design storm patterns for different climatic zones, storm durations, and levels of severity of the design storm (Institution of Engineers, Australia, 1987).

Results of the analysis carried out in this section so far have indicated significant variation of the temporal pattern with the factors of seasonality, rainfall duration and depth, and with the number of parameters used to describe the temporal pattern. The question now is to what extent this variation is important in flood estimation. This raises two research issues in terms of sensitivity of design flood estimates, namely (i) how many groups of temporal patterns should be used, and (ii) how many parameters are required to adequately characterise the temporal pattern. With regard to (i), temporal patterns could be assigned to up to 10 groups (using the results of the chi-square test of independence) or only one single group (using the results of the correlation analysis). For the present study, however, it was decided to use 10 temporal pattern groups and examine the effect of this on design flood estimates using a sensitivity analysis. With regard to (ii), it is clear that the use of the storm mass curve defined by at least 4 ordinates is preferable to 3 statistical characteristics of the rainfall hyetograph (as 3 parameters are clearly not sufficient to describe the temporal pattern). The minimum number of ordinates required to adequately represent the variability of rainfall intensity during the storm duration and its effects on flood hydrographs are investigated in Chapter 6.

In the section below, the development of a stochastic model to reproduce the observed temporal patterns in the 10 temporal pattern groups is described.

#### **4.6.5 Development of a stochastic model to reproduce observed storm mass curves**

The representation of the observed temporal patterns by a statistical model and the generation of design storm patterns from this model are interrelated as they use the same source formulas in their formulation. Therefore in this section the model selected for generating design storm patterns and the determination of the parameters of this model from the observed temporal patterns are described. The application of the selected model to temporal pattern generation is presented in detail in Chapter 5.

There exist several methods for developing a design temporal pattern for a selected design rainfall depth and duration (Pilgrim and Cordery, 1975; Chow et al., 1988). A review of these is presented in Appendix H. Among these, the multiplicative cascade model presented by Robinson and Sivapalan (1997) has the simplest structure and is the easiest to apply in practice. For these reasons, the model was adopted in this study.

Generally speaking, the multiplicative cascade model can be applied to generate dimensionless rainfall hyetographs with  $2^m$  rectangles (corresponding to dimensionless mass curves defined by  $(2^m-1)$  ordinates), where  $m$  represents the chosen level of disaggregation. For example, when  $m$  equals 5, the design storm depth is disaggregated into a hyetograph with 32 blocks of rainfall, computed at 32 equal time increments of the storm duration. The corresponding storm mass curve is thus represented by 31 ordinates.

The multiplicative cascade model operates on the principle that the disaggregated rainfalls at a disaggregation level should equal the rainfall at the previous level. This principle, illustrated in Figure 4-29, is explained in great detail in the section below.

Let  $w_i$  be some disaggregation parameters ( $0 \leq w_i \leq 1$ ) and  $h(t_1, t_2)$  be the dimensionless rainfall from the dimensionless time  $t_1$  to  $t_2$  of the storm duration ( $0 \leq t_1 < t_2 \leq 1$ ). For example,  $h(0,1)$  is the relative rainfall from the start to the end of a storm. By definition,  $h(0,1)=1$ , which represents the unit dimensionless rainfall hyetograph [see Figure 4-29 (a)].

At the first level of disaggregation ( $m=1$ ), a parameter  $w_1$  is used to break the unit rainfall hyetograph into a hyetograph defined for 2 ( $=2^1$ ) equal intervals of storm duration [see Figure 4-29 (b)]. The disaggregated hyetograph thus has two rectangular blocks whose ordinates are:

$$\begin{aligned} h(0,0.5) &= w_1 \\ h(0.5,1) &= 1 - w_1 \end{aligned} \tag{4-11}$$

Note that the sum of the disaggregated relative rainfalls [ $h(0,0.5)$  and  $h(0.5,1)$ ] is 1.

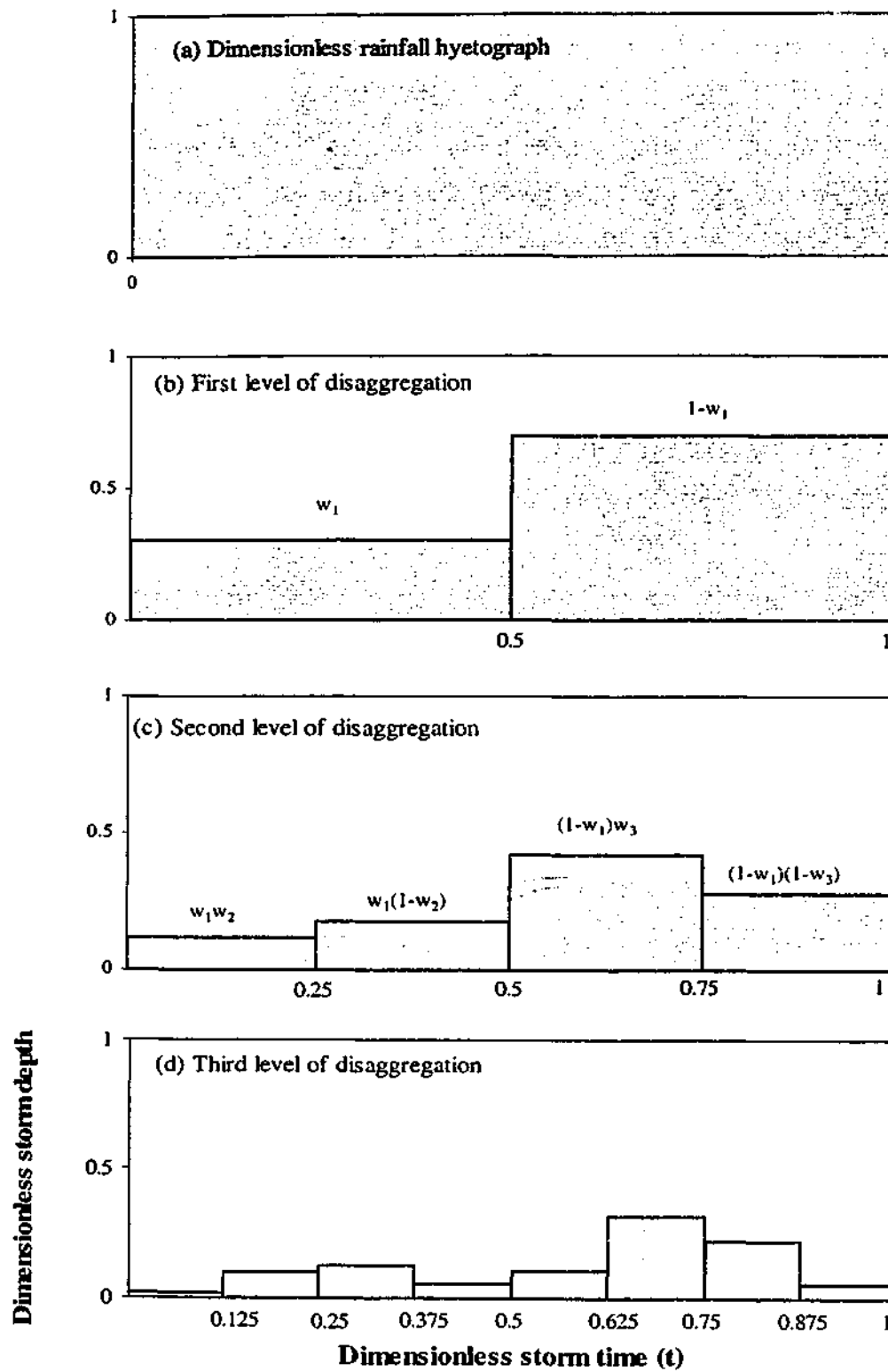


Figure 4-29: Principles of the multiplicative cascade model

At the second level of disaggregation ( $m=2$ ), two additional parameters ( $w_2, w_3$ ) are required, each divides a block of the hyetograph generated in the previous step into two smaller blocks. The dimensionless hyetograph obtained at this step is thus defined for 4 ( $=2^2$ ) equal time increments of the storm duration [see Figure 4-29 (c)]. The ordinates of this hyetograph are determined as follows:

$$\begin{aligned} h(0,0.25) &= w_2 h(0,0.5) = w_2 w_1 \\ h(0.25,0.5) &= (1-w_2) h(0,0.5) = (1-w_2) w_1 \\ h(0.5,0.75) &= w_3 h(0.5,1) = w_3 (1-w_1) \\ h(0.75,1) &= (1-w_3) h(0.5,1) = (1-w_3)(1-w_1) \end{aligned} \quad (4-12)$$

In the above four formulas, it is noted that the sum of the first and second pairs are respectively  $w_1$  and  $(1-w_1)$ , which are the ordinates of the hyetograph obtained at the first disaggregation level.

At the third level of disaggregation ( $m=3$ ), another four parameters ( $w_4, w_5, w_6, w_7$ ) are used to break the hyetograph generated in the previous step into a hyetograph defined for 8 ( $=2^3$ ) equal time increments of the storm duration [see Figure 4-29 (d)]. In particular,  $w_4$  separates the first rectangular block of the hyetograph at the second disaggregation level [that is  $h(0,0.25)$  in Figure 4-29 (c)] into two rectangles [see Figure 4-29 (d)] whose ordinates are:

$$\begin{aligned} h(0,0.125) &= w_4 h(0,0.25) = w_4 w_2 w_1 \\ h(0.125,0.25) &= (1-w_4) h(0,0.25) = (1-w_4) w_2 w_1 \end{aligned} \quad (4-13)$$

As the dimensionless rainfall of the previous level is preserved, the sum of the two disaggregated rectangles is equal to  $h(0,0.25)$ , that is,  $w_1 w_2$ .

Similarly,  $w_5$  is used to break the second rectangle of the second level hyetograph [that is  $h(0.25,0.5)$  in Figure 4-29 (c)] into two rectangular segments as follows:

$$\begin{aligned} h(0.25,0.375) &= w_5 h(0.25,0.5) = w_5 w_1 (1-w_2) \\ h(0.375,0.5) &= (1-w_5) h(0.25,0.5) = (1-w_5)(1-w_2) w_1 \end{aligned} \quad (4-14)$$

The sum of the ordinates of these two rectangles are equal to  $w_1(1-w_2)$ , which is the ordinate of  $h(0.25,0.5)$ .

In a similar manner, the parameters  $w_6$  and  $w_7$  respectively divide the third and fourth rectangular blocks in Figure 4-29 (c) into two smaller rectangles.

The disaggregation procedure above can be continued to higher levels of disaggregation until the desired time scale is reached. In this analysis, the disaggregation process was stopped at the third level-of disaggregation ( $m=3$ ). That is, the multiplicative cascade model was applied to generate rainfall hyetographs with 8 ( $=2^3$ ) rectangular blocks, corresponding to mass curves defined by 7 internal ordinates. While it was considered sufficient for the purpose of this study to represent the storm temporal pattern by 7-ordinate mass curves, it is emphasised that the model can be used to generate rainfall hyetographs at any chosen level of disaggregation. The effect on design flood estimates of representing storm mass curves (and therefore temporal patterns) by a greater number of ordinates is later examined in a sensitivity analysis (see Section 6.5.4).

In order to generate dimensionless rainfall hyetographs that are similar to the observed ones, the disaggregation parameters should be estimated from the observed hyetographs. To do this, the dimensionless mass curves of the observed storms are required. Let  $H(t)$  be the dimensionless cumulative rainfall depths from the beginning of the storm to the dimensionless storm time  $t$  ( $0 \leq t \leq 1$ ) (see Figure 4-30). For example,  $H(0)$  and  $H(1)$  are the relative cumulative storm depths at the start and end of a storm, respectively. By definition:

$$H(0) = 0$$

$$H(1) = 1$$

It is clear that the disaggregation parameters  $w_i$  can be related to  $H(t)$  according to the following relationships established for various disaggregation levels. For example, at the first level of disaggregation:

$$H(0.5) = H(0) + h(0,0.5) = w_1 \quad (4-15)$$

At the second level of disaggregation:

$$\begin{aligned} H(0.25) &= H(0) + h(0,0.25) = w_1 w_2 = w_2 H(0.5) \\ H(0.75) &= H(0.5) + h(0.5,0.75) = w_1 + (1 - w_1)w_3 = H(0.5) + (1 - H(0.5))w_3 \end{aligned} \quad (4-16)$$

At the third level of disaggregation:

$$\begin{aligned}
 H(0.125) &= H(0) + h(0,0.125) = w_1 w_1 w_2 = w_1 H(0.25) \\
 H(0.375) &= H(0.25) + h(0.25,0.375) = H(0.25) + (w_1 - w_1 w_2) w_5 = H(0.25) + (H(0.5) - H(0.25)) w_5 \\
 H(0.625) &= H(0.5) + h(0.5,0.625) = H(0.5) + (H(0.75) - H(0.5)) w_6 \\
 H(0.875) &= H(0.75) + h(0.75,0.875) = H(0.75) + (1 - H(0.75)) w_7
 \end{aligned}
 \tag{4-17}$$

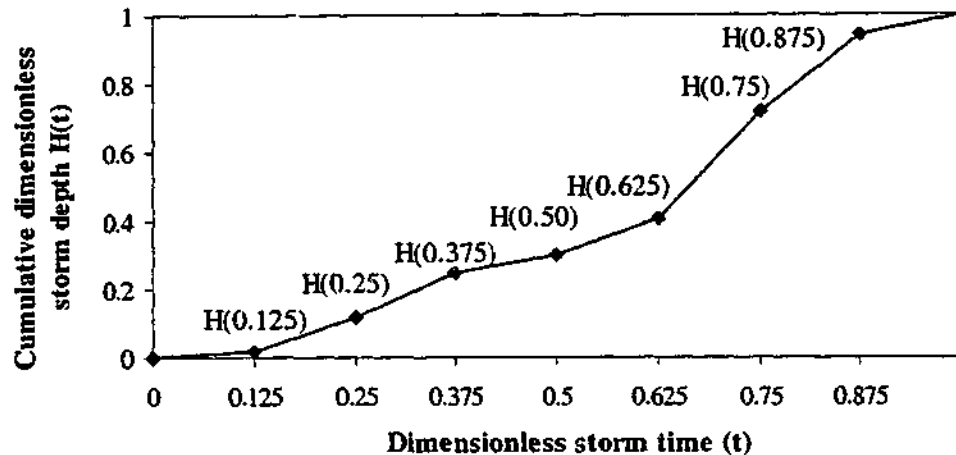


Figure 4-30: Dimensionless mass curve at the third level of disaggregation

In applying the multiplicative cascade model for storm hyetograph generation, the disaggregation parameters can be represented by a probability distribution. The beta distribution, described in Appendix F, was selected for representing these parameters because the parameter estimation of this distribution is very simple. In addition, when being used in the adopted multiplicative cascade model, it can reasonably preserve the characteristics of the observed temporal patterns, as will be shown in Section 5.2.5.2.

The procedure adopted for determining the parameters  $\alpha$  and  $\beta$  of the beta distribution from the observed storm mass curves of each of the 10 temporal pattern groups includes the following steps:

- 7 ordinates of the dimensionless mass curve were computed for each storm.
- For each observed storm  $j$ , the disaggregation parameters  $w_i$  (where  $i$  varies from 1 to 7) were computed from their relationships with the mass curve ordinates using Equations (4-15), (4-16) and (4-17).
- The mean and variance of these  $w_i$  values were then computed, from which the two parameters  $\alpha_j$ ,  $\beta_j$  of the beta distribution representing the disaggregation parameters

of the storm  $j$  were determined using the method of moments (see Appendix F).

- The medians<sup>5</sup> of the computed  $\alpha_j$  and  $\beta_j$  values of all the observed storms in a group were then determined. These median  $\alpha$  and  $\beta$  values, tabulated in Table 4-17, were adopted as the parameters of the beta distribution representing the disaggregation parameters of all the observed storm mass curves in a temporal group.

It is noted that in each temporal pattern group, each of the parameters  $\alpha$  and  $\beta$  varies quite considerably. The typical range of  $\alpha$  is from 0.11 to 24.82, and of  $\beta$  is from 0.27 to 52.4. By representing this great variability of each of the parameters by just the median value, it is clear that the variability of the disaggregation parameters, and therefore of the generated temporal patterns, is significantly reduced.

Table 4-17: Parameters of the beta distribution representing the disaggregation parameters of storm mass curves

Temporal pattern group	Beta distributional parameters	
	$\alpha$	$\beta$
1	2.22	2.06
2	1.52	1.35
3	1.59	1.61
4	2.49	2.44
5	2.86	2.51
6	2.44	2.15
7	3.43	3.12
8	2.77	2.58
9	2.38	2.29
10	2.00	1.93

In examining the parameters of the beta distributions representing the disaggregation parameters of the 10 specified temporal pattern groups, it can be seen that the parameters of the beta distributions of Groups 2 and 3 are relatively similar. This suggests that the same distribution can be used to characterise the disaggregation parameters of these two groups. In other words, the two specified temporal pattern groups might be combined into one single group. As the observed storms in these two

<sup>5</sup> A preliminary analysis indicated that, using the median values of  $\alpha_j$  and  $\beta_j$ , the frequency curves of the observed mass curves and the cumulative frequency curves of the maximum dimensionless intensity were reproduced better than when the mean values were used.

groups have the same duration range (from 13 to 24 hours) but their storm depths are either less than 50mm or greater than 50mm (see Figure 4-27), the combination of these two groups implies that the time variation of rainfall intensity might not be strongly dependent on storm depth. Nevertheless, as there are only 48 observed storm events in the duration group whose storm depths exceed 50mm (see Table 4-15), a larger storm data base would be needed to justify the above postulation.

The adequacy of the beta distributions representing the disaggregation parameters of the observed temporal patterns was tested by comparing the statistical characteristics of the observed patterns and the design temporal patterns generated using these fitted beta distributions. As the generation of design temporal patterns is presented in Chapter 5 (along with the generation of data from other stochastic inputs), the analysis undertaken to check the adequacy of the fitted beta distributions is also presented and discussed in Chapter 5.

#### 4.6.6 Summary

In this section, the investigation of the dependence on season, storm duration and depth of the temporal pattern of the storms recorded at 19 pluviometers used in this study was covered. In this investigation, the rainfall temporal pattern was either represented by 3 statistical characteristics of the dimensionless rainfall hyetograph, or by internal ordinates of the dimensionless storm mass curve. The correlation analysis and the chi-square test of independence were used to examine the dependence of the temporal pattern on the factors of season, storm duration and depth.

Depending on the test used as well as the level of detail of the representation of the rainfall temporal pattern, the dependence of temporal pattern on season, storm duration or depth was or was not detected. On the one hand, the chi-square test of independence appeared to be more powerful than the correlation analysis in detecting this relationship. On the other hand, the chi-square test itself could not detect the dependence of temporal patterns on duration (or depth) when the temporal pattern was described by a small number of ordinates, that is, when not much information of the variation of rainfall intensity during storm duration was given.

Results of the chi-square test indicated that the temporal pattern represented by 9 ordinates was dependent on season, storm duration and depth. For the storm sample used in this study, 4 independent seasonal groups of temporal patterns were formed using seasonal groupings of extreme rainfall in Australia. In each seasonal group, the observed storm patterns were divided into two duration groups, with 12 hours being the upper limit for short duration storms. An exception was the summer storms in which the temporal pattern was dependent on three duration groups, and for one case, on storm depth. As these results conformed to most findings in previous studies, these temporal groupings (10 groups in total) were adopted for further analysis.

The multiplicative cascade model presented by Robinson and Sivapalan (1997) was adopted for generating design temporal patterns. For each of the 10 temporal pattern groups, a beta distribution was also used to represent the disaggregation parameters of the model. The two parameters of the beta distributions were estimated from the analysis of the observed storm patterns.

## **4.7 PROBABILITY DISTRIBUTION OF INITIAL LOSS**

### **4.7.1 Background**

The initial loss – continuing loss model is a runoff production model with two parameters, namely the initial loss and the continuing loss rate. This model is widely used in Australia due to its conceptual simplicity, ease of application, and the ability to reasonably estimate representative values of rainfall losses over a catchment. For these reasons, it was adopted in this research for estimating rainfall excess. As discussed in Section 3.3.1, in the present application, the initial loss is considered to be a random variable and the continuing loss a fixed design value.

Data used for deriving the probability distribution of the initial loss for the La Trobe River catchment at Noojee were the initial losses estimated for various rainfall-runoff events observed at the study catchment. These data were obtained from a parallel study (Rahman et al., 2001). In that study, it was assumed that surface runoff started when a

threshold value of 0.01mm/h was exceeded. The initial loss of a storm event was computed to be the rainfall that occurred before the commencement of surface runoff. The estimated initial losses for different events were also assumed to form a homogeneous sample for frequency analysis.

An at-site frequency analysis procedure was used to analyse the available initial loss data for the study catchment. With this procedure, there are three steps involved, namely the selection of a distributional type, the estimation of distributional parameters, and the checking of the goodness-of-fit of the adopted distribution. Each of these steps involves the choice of a single method among many alternatives, the bases of which are dependent on many factors, such as the feasibility of a particular method, the required accuracy, or ease of application. A brief review of the available methods in each step is presented in Appendix I.

In this section, the correlations of initial loss with rainfall duration and average rainfall intensity are first investigated for the particular catchment. The procedure for developing the probability distribution of the storm initial loss is then described, along with its application to the observed data for the La Trobe catchment. A discussion of results is also presented.

#### **4.7.2 Correlations of initial loss with rainfall duration and average rainfall intensity**

To examine the relationship between the storm initial loss and storm duration or average rainfall intensity, the corresponding correlation coefficients were first computed. The initial loss estimated for each rainfall-runoff event was then plotted against the corresponding storm duration (see Figure 4-31) and average rainfall intensity (see Figure 4-32). It can be seen from Figure 4-31 that storm losses seem to increase as storm durations increase. However, this relationship is very weak, as shown by the low value of the corresponding correlation coefficient (0.29). In addition, the coefficient of determination ( $R^2=0.0854$ ) of the regression line fitted to these sets of initial loss and duration data is close to zero. Similarly, the storm initial losses scatter widely about their corresponding average rainfall intensities, and the estimated correlation coefficient

and  $R^2$  are very close to zero (-0.02 and 0.0007, respectively), as seen in Figure 4-32. Consequently, it is reasonable to assume that the initial loss is independent of storm duration and intensity. The same conclusion has been obtained in a parallel study (Rahman et al., 2001).

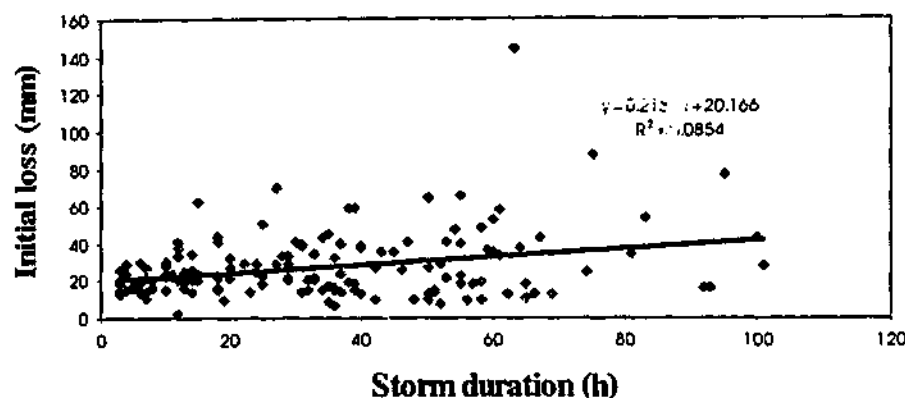


Figure 4-31: Relationship between initial loss and storm duration

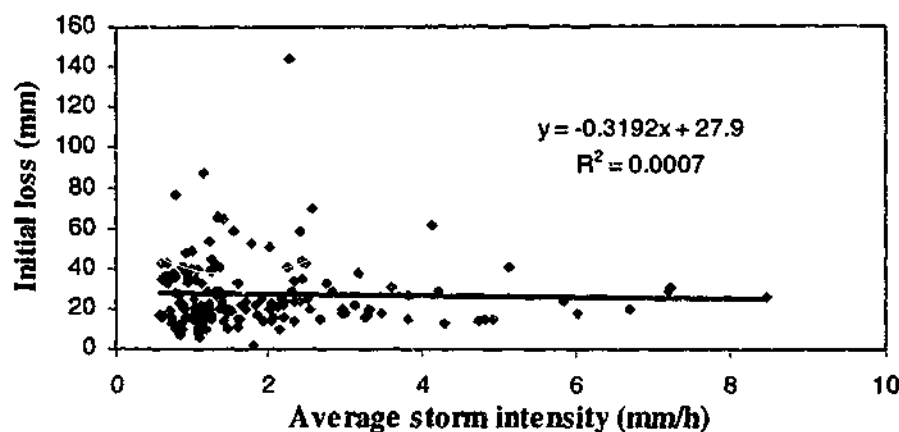


Figure 4-32: Relationship between initial loss and average rainfall intensity

### 4.7.3 Development of the probability distribution of initial loss

#### 4.7.3.1 Selection of a distributional type

In order to determine the parent distribution of a data sample, histograms, moment ratio diagrams, or L-moment ratio diagrams, described briefly in Appendix I, can be used. For this study, the method of histograms was adopted because it is the simplest method

for a preliminary choice. The adequacy of the assumed distribution was later assessed using a goodness-of-fit test.

To determine the histogram of the initial loss for the La Trobe River catchment, the observed frequencies of the initial losses were plotted against the corresponding class intervals. The result is presented in Figure 4-33 where it can be seen that the histogram of the initial loss has a long right tail. The corresponding coefficient of skewness computed for this data sample was 2.7. As theoretical distributions such as gamma, beta, or lognormal are all positively skewed and have the shape similar to this histogram, they could be tentatively selected as the parent distribution for the initial loss for the particular catchment. Nevertheless, the beta distribution was adopted because the parameter estimation and data generation of this distribution are very simple.

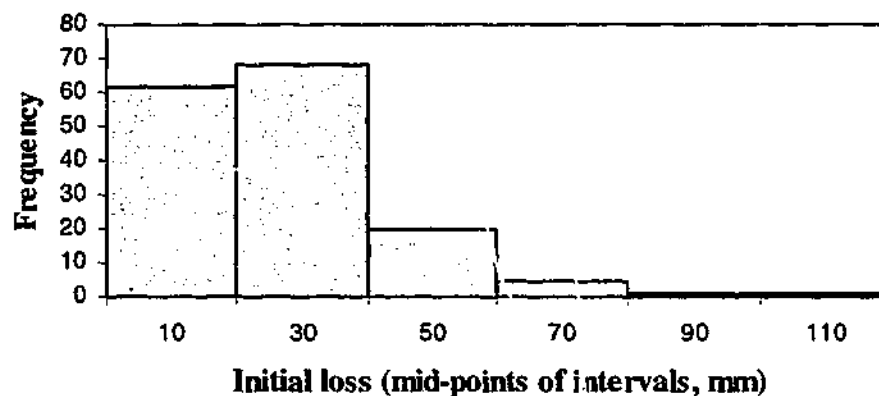


Figure 4-33: Histogram of initial losses for the La Trobe River catchment

#### 4.7.3.2 Estimation of distributional parameters

To estimate the parameters of a distribution, the method of moments, method of L-moments, method of maximum likelihood, or Bayesian methods can be used. An outline of these methods is presented in Appendix I. Of these, the method of L-moments has been popularly used in recent applications because it is less subject to bias in parameter estimates, is able to characterise a wide range of distributions, and is more robust to outliers of data (Hosking, 1990). Nevertheless, for the present study, the method of L-moments is not feasible, because mathematical formulation to compute L-moments of the assumed beta distribution is not readily available. The method of

moments was used instead because it is simple, and more importantly, the product moments of the beta distribution can be readily obtained from statistical texts.

In order to estimate distributional parameters by the method of moments, sample moments are equated to their corresponding distributional moments. For the case of the beta distribution, its two parameters  $\alpha$  and  $\beta$  can be computed from the lower limit ( $a$ ), upper limit ( $b$ ), mean  $[E(Y)]$  and variance  $[\text{Var}(Y)]$  of a data set using Equation (F-7) (see Appendix F).

The two parameters of the beta distribution were computed for the sample of initial losses for the La Trobe River catchment with the following statistics:  $a=1.85\text{mm}$ ,  $b=143.9\text{mm}$ ,  $E(Y)\approx 27.3\text{mm}$ , and  $\text{Var}(Y)=302.7\text{mm}^2$ . The estimated parameters were:  $\alpha\approx 1.6$  and  $\beta=7.2$ . The cumulative probability distributions of the fitted beta distribution and of the observed initial losses are plotted in Figure 4-34.

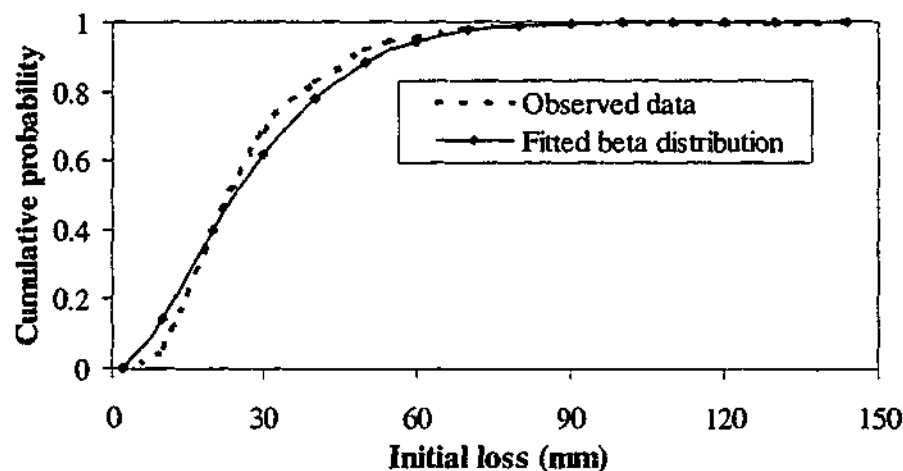


Figure 4-34: Plot of the cumulative distribution function of observed initial losses and the fitted beta distribution

The visual comparison of the cumulative frequency curves of the observed loss data and the fitted beta distribution shown in Figure 4-34 indicates that the two curves match very well for the initial loss of about 60mm or greater. However, for the initial loss below this range, there is quite a difference between the two cumulative frequency curves. Therefore, the adequacy of the fitted beta distribution needs to be further assessed, as described below.

### 4.7.3.3 Checking of the adequacy of the fitted distribution

Common methods for evaluating the goodness-of-fit of a theoretical distribution to a set of data are the Kolmogorov-Smirnov one-sample test, the chi-square goodness-of-fit test, and the probability plot correlation coefficient test (Haan, 1977; Cunnane, 1989; Stedinger et al., 1993). Of these methods, the chi-square goodness-of-fit test is very widely used due to its simplicity and ease of application. For these reasons, this test was selected for assessing how well the adopted beta distribution fits the observed loss data.

In order to apply the chi-square goodness-of-fit test, in general, observed data are first assigned to class intervals. The expected number of observations that falls in each class interval (expected according to the theoretical distribution under test) is then computed by multiplying the expected relative frequency by the number of observations. The test statistic is finally calculated as follows (Haan, 1977):

$$\chi^2 = \sum_{i=1}^{k^*} \frac{(O_i - E_i)^2}{E_i} \quad (4-18)$$

where  $k^*$  is the number of class intervals, and  $O_i$  and  $E_i$  are the observed and expected number of observations in the  $i^{\text{th}}$  class intervals.

The hypothesis that the data are from the specified distribution is rejected at a given level of significance if the computed test statistic exceeds the corresponding critical value of a chi-square distribution with  $k^* - p - 1$  degrees of freedom, where  $p$  is the number of parameters estimated from the data. These critical values can be obtained from Haan (1977, Table E6).

An application of the chi-square goodness-of-fit test for assessing the adequacy of the fitted beta distribution to the observed initial losses for the given catchment is illustrated in Table 4-18. In this application, the observed values of the storm initial loss were divided into five class intervals, as shown in Table 4-18. The number of degrees of freedom of the chi-square distribution used was:  $k^* - p - 1 = 5 - 2 - 1 = 2$ . The critical value at 5% LOS was 5.99. It can be seen in Table 4-18 that the computed test statistic (3.5) is less than the specified critical value. Therefore, for the selected class intervals, the

null hypothesis that the observed initial losses for the La Trobe River catchment are from the specified beta distribution ( $\alpha=1.6$ ,  $\beta=7.2$ ) can not be rejected at 5% LOS.

Table 4-18: Results of the chi-square goodness-of-fit test on initial loss data

Class intervals of storm losses (mm)	Expected relative frequency	Frequency		
		Expected ( $E_i$ )	Observed ( $O_i$ )	$(O_i - E_i)^2/E_i$
0-20	0.401	63.0	62	0.01
20-40	0.379	59.5	68	1.21
40-60	0.163	25.6	20	1.22
60-80	0.048	7.5	5	0.85
80-143.9	0.009	1.4	2	0.24
Test statistic ( $\chi^2$ ) =				3.55

At this point, it is worth noted that results of the chi-square goodness-of-fit test are quite sensitive to the number of class intervals used to summarise the observed data. For example, a subsequent analysis showed that when 6 or 8 intervals were used, the null hypothesis is rejected at 5% LOS (but can not be rejected at lower levels, say 2.5% or 1% LOS). This suggests that the adopted beta distribution is not necessarily the best distribution characterising the storm initial loss for the specified catchment. However, this was discovered late in the study, and no other distribution was investigated.

#### 4.7.4 Summary

The loss model adopted in this research was the initial loss – continuing loss model in which the initial loss was treated as a random variable, and the continuing loss rate as a fixed design value. It was found that the storm initial losses derived for observed rainfall-runoff events for the La Trobe River catchment were independent of storm duration and average rainfall intensity. A two-parameter beta distribution was fitted to these initial losses. Results of the chi-square goodness-of-fit test indicated that the adopted beta distribution provides an acceptable fit to the observed losses for the study catchment.

## 4.8 PARAMETERS OF THE LUMPED RUNOFF ROUTING MODEL

### 4.8.1 Background

Runoff routing models give estimates of a surface runoff hydrograph by routing rainfall excess through a model representing the catchment storage. To obtain the total flood hydrograph, baseflow must be determined separately, and then added to the estimated surface runoff hydrograph.

The runoff routing model adopted in this research, as discussed in Chapter 3, assumes a non-linear relationship between storage and discharge. It has two parameters  $k$  and  $m$ , in which  $k$  is a dimensional coefficient representing storage delay time, and  $m$  is a dimensionless constant representing the non-linearity of catchment response. The adopted model is relatively simple in that it does not take into account the spatial variation of rainfalls and losses over the entire catchment, and assumes only one model storage at the catchment outlet. Due to this simplicity, it was considered necessary to evaluate the performance of this model in design flood estimation by comparing flood estimates obtained from this model with those from a distributed model developed for the catchment. Results of this comparison would give indications of how design floods would have been estimated had a distributed model been used for the catchment.

This section presents the research undertaken to estimate the parameters of the adopted model and evaluate the model performance.

### 4.8.2 Determination of the lumped model parameters

The determination of the parameters of the adopted lumped runoff routing model for the La Trobe River catchment at Noojee, with the catchment area of  $290\text{km}^2$ , consisted of four steps: event selection, baseflow separation, model calibration, and model testing. These steps are described below.

#### 4.8.2.1 Event selection

To select observed rainfall-runoff events for model calibration and testing, two criteria were used. Firstly, there had to be a minimum of five large observed flood events, of which about half were required for model calibration and the remainder for model testing. Secondly, there had to be concurrent rainfall data for the selected floods.

Nine largest flood events were extracted from the flow record of the La Trobe River catchment. The threshold discharge of  $22\text{m}^3/\text{s}$  (corresponding to floods of approximately 5-year ARI) was used for this extraction. Among the extracted floods, only 5 events had concurrent rainfall data. Therefore, these 5 events were selected for calibrating and testing the adopted lumped runoff routing model. Even though it was desirable to obtain more events for model calibration and testing (by reducing the threshold discharge), it was decided to use only the 5 selected rainfall-runoff events, as the use of a smaller threshold discharge would result in even smaller events for analysis. The peak discharge of the selected floods ranged from a minimum of  $24.3\text{m}^3/\text{s}$  to a maximum of  $60\text{m}^3/\text{s}$  (see Table 4-19).

Table 4-19: List of observed floods used for model calibration and testing

Event start date	Peak discharge ( $\text{m}^3/\text{s}$ )	Surface runoff ( $\text{m}^3/\text{s}$ )	Baseflow ( $\text{m}^3/\text{s}$ )	% of baseflow to peak discharge
27/01/1963	24.3	18.6	5.7	23.6
28/05/1969	27.5	15.0	12.5	45.5
5/11/1971	60.0	48.6	11.4	19.0
7/04/1977	25.6	22.2	3.5	13.5
30/06/1980	33.0	31.3	1.7	5.1

#### 4.8.2.2 Baseflow separation

The separation of baseflow from observed (total) streamflow was necessary in determining runoff routing model parameters because only surface runoff is modelled, and thus the calibration and testing procedures relate to surface runoff only.

Many methods are available for baseflow separation (Institution of Engineers, Australia, 1987, Chapter 8). In general, it is necessary to define the start and end of the surface runoff hydrograph and the shape of the baseflow hydrograph. Whereas the start of surface runoff can be easily determined, the determination of the end of surface runoff and the shape of the baseflow hydrograph involves more subjective judgement. In this study, the HYBASE baseflow extraction program (HYDSYS, 1994), based on a recursive digital filter technique, was adopted. In this program, the surface runoff at time step ( $k$ ) is a function of a filter factor, the number of passes, and the total streamflow at time steps ( $k$ ) and ( $k-1$ ). As the filter factor is increased, the baseflow hydrograph becomes flatter, and as the number of passes is increased, the baseflow hydrograph becomes smoother. The choice of the correct combination of these two parameters is also a highly subjective process.

For the La Trobe River catchment, it was necessary to separate baseflow for only one of the five selected flood events (the 1963 flood, see Table 4-19), as the surface runoff hydrographs of the other four events were available from a previous study (Smith, 1998). To do this, the specified flood event was first extracted at hourly time steps from the HYDSYS database. The HYBASE program was then used to estimate baseflow. The surface runoff hydrograph was finally extracted using program HYCSV (HYDSYS, 1994).

Results of the baseflow separation are also presented in Table 4-19 and illustrated in Figure 4-35. In Table 4-19, the estimated surface runoff and the corresponding baseflow under the peak discharge of the five selected floods are listed. In Figure 4-35, the total streamflow hydrograph of the 1963 flood is shown along with the corresponding baseflow hydrograph. It is noted from Table 4-19 that the ratio of baseflow to the peak discharge is relatively high, ranging from 5% to 45% with an average of 21%, for all the events used. Baseflow has been noted to be high for the study catchment by other authors, for example, Smith (1998).

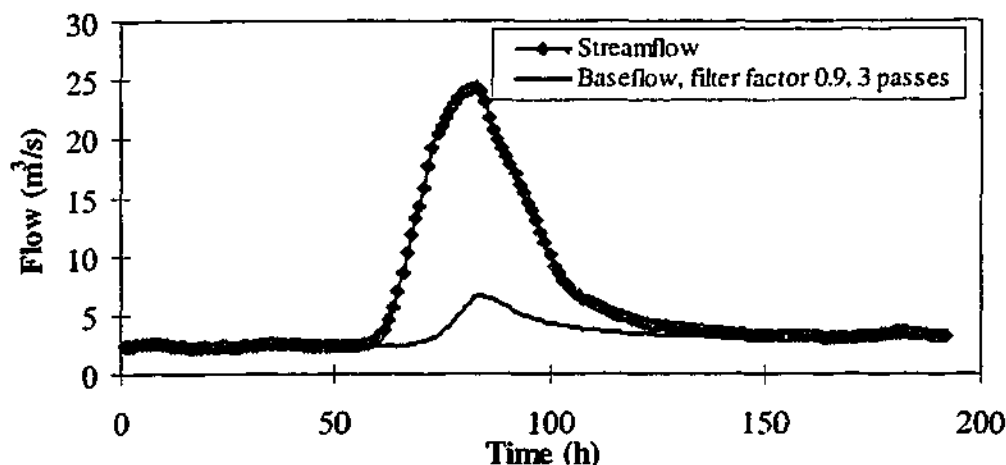


Figure 4-35: Plot of total streamflow and the extracted baseflow (the 1963 flood)

#### 4.8.2.3 Model calibration

The aim of model calibration is to determine the parameters  $k$  and  $m$  of the adopted runoff routing model. For the La Trobe River catchment, the parameter  $m$  was assumed to be 0.8. This value has been recommended in many previous investigations, as documented by the Institution of Engineers, Australia (1987, Chapter 9).

To estimate the routing model parameter  $k$ , a trial and error process was adopted. In this process, the initial loss was varied first so that the rising limb of the estimated surface runoff hydrograph fitted that of the observed hydrograph. The continuing loss rate was then determined to give the correct surface runoff volume. Finally, the parameter  $k$  was varied to match the peak flows of the two hydrographs. For each event, this process was repeated until the observed and estimated hydrographs fitted as closely as possible in terms of flood peak, as this was the flood characteristic of interest. Nevertheless, the time to peak and hydrograph shape were also considered. Three observed rainfall-flood events were used in this calibration (the 1969, 1971, 1980 events). The calibration program was written by Rahman (1999).

Results of the calibration of the runoff routing model for the La Trobe River catchment are presented in Table 4-20. This table shows the values of the storm initial loss, continuing loss rate, and the routing model parameter  $k$  for each of the three events

used, along with the observed and calculated flood peaks and time to peaks. A plot of the observed and estimated surface runoff hydrographs for one calibrated event is presented in Figure 4-36. It is noted here that for all the events used for model calibration, it was very difficult to match the rising limb and the shape of the observed and calculated hydrographs, regardless of changes in the initial loss, continuing loss and the routing model parameter  $k$  used. This situation is clearly illustrated in Figure 4-36.

Table 4-20: Results of model calibration (lumped runoff routing model, La Trobe River catchment) ( $m=0.8$ )

Event	IL (mm)	CL (mm/h)	k	Peak discharge ( $m^3/s$ )			Time to peak (h)		
				observed	calculated	% difference	observed	calculated	% difference
1969	25	3.2	56	15	15.15	1	89	48	-46.1
1971	34	4.3	47	48.6	48.1	-1.0	73	42	-42.5
1980	25	7.9	55	31.3	33.7	7.7	60	46	-23.3

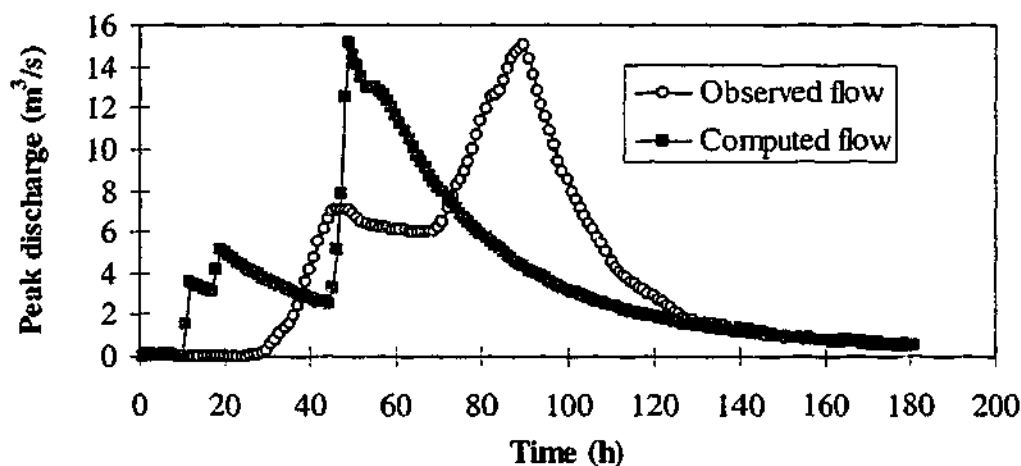


Figure 4-36: Observed and estimated hydrographs (the 1969 flood, model calibration)

Results of model calibration, as shown in Table 4-20 and Figure 4-36, indicate that the adopted lumped runoff routing model satisfactorily reproduces the observed flood peak, but significantly underestimates the time to peak of all the three events used, and does not preserve very well the hydrograph shape. For these events, the difference between the peak discharge of the observed and computed hydrographs is only within the range of 1% and 8%. Nevertheless, there is a discrepancy from 23% up to 46% between the observed and computed time to peak of the hydrographs. It is also noted from Table 4-20 that the continuing loss rate used for the 1980 flood seems to be high (7.9mm/h). However, according to an independent study of data used for loss modelling, the

adopted value of the continuing loss rate for the La Trobe River catchment is reasonable (Hill et al., 1996a).

In order to select a common value of the routing parameter  $k$  for the study catchment, it is noted from Table 4-20 that  $k$  values for the three calibrated events (56, 47, 55) are approximately equal. Therefore, the global parameter  $k$  for the catchment was initially adopted as the average  $k$  value ( $k=53$ ).

#### 4.8.2.4 Model testing

The aim of model testing is to check whether the calibrated runoff routing model with the specified parameters  $k$  and  $m$  ( $k=53$ ,  $m=0.8$ ) can reproduce other observed floods. This was carried out by varying the initial loss and continuing loss rate until the estimated flood hydrographs matched the shape and volume of the observed ones as closely as possible. Two observed rainfall-runoff events that were not used in model calibration (the 1963 and 1977 events) were used in the testing.

Results of the model testing are summarised in Table 4-21. A plot of the observed and estimated flood hydrographs of one test event is also illustrated in Figure 4-37.

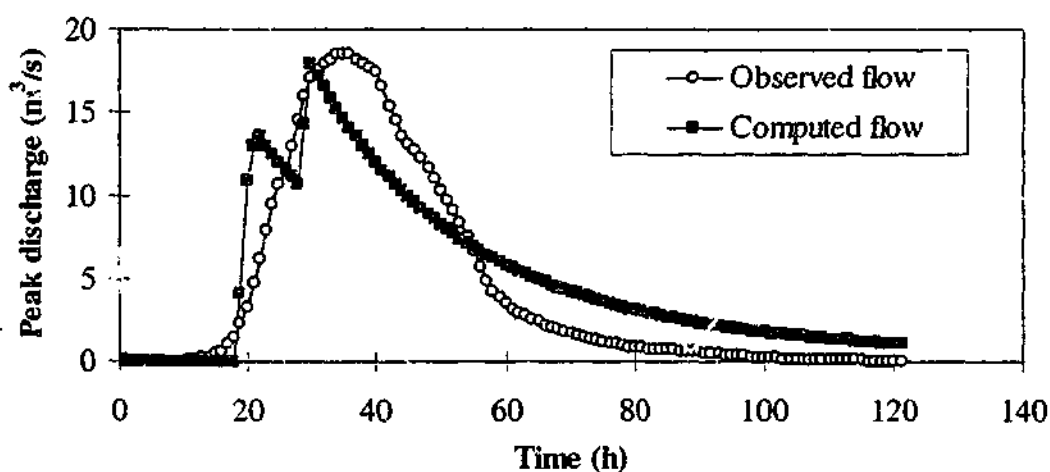


Figure 4-37: Observed and estimated hydrographs (the 1963 flood, model testing)

Table 4-21: Results of model testing ( $k=53$ ,  $m=0.8$ ) - Lumped runoff routing model

Event	IL (mm)	CL (mm/h)	Peak discharge ( $m^3/s$ )			Time to peak (h)		
			observed	calculated	% difference	observed	calculated	% difference
1963	35	9.2	18.6	18	-3.2	34	29	-14.7
1977	0	11	22.2	22.4	0.9	31	23	-25.8

It can be seen in Table 4-21 that the adopted runoff routing model preserves very well the peak discharge. In particular, errors in peak flood estimates are less than 3% for both test events used. On the other hand, the time to peak of the predicted hydrographs is underestimated by at least 15%. In addition, the shape of the observed hydrograph for both test events is not satisfactorily reproduced, as illustrated in Figure 4-37.

As the calibrated model only reproduced well the peak discharge in the test runs, efforts were made to improve its performance by using the two test events for further model calibration. However, results of this analysis indicated that the estimated flood hydrographs were not better predicted both in timing and in shape. Therefore, it was decided to keep the specified values of  $k$  and  $m$  ( $k=53$ ,  $m=0.8$ ) as the parameters of the lumped routing model for the study catchment. Possible reasons for poor model performance and avenues for improvements are discussed below.

#### 4.8.2.5 Discussion

The discrepancy between the observed and calculated surface runoff hydrographs, especially in the time to flood peak and hydrograph shape, in both model calibration and testing could have been caused by many factors. Firstly, the estimation of losses from rainfall and the separation of baseflow in some selected events might have been incorrect. As baseflow was known to be high for the study catchment, the choice of a baseflow separation technique would certainly affect the estimated amount of baseflow, and consequently, the resulting surface runoff and the calibrated routing model parameters, as confirmed in previous studies (Bates and Davies, 1987). In addition, the selection of a combination of the filter factor and number of passes in the adopted baseflow extraction program was highly subjective.

Secondly, the rainfall-runoff data recorded for these events may have been erroneous. As the time to flood peak was underestimated in both model calibration and testing, the data errors might be in the form of a shift in the recorded event time. Nevertheless, after examining all rainfall-runoff events used in this study (see an illustration of a typical event in Figure 4-38), it was evident that the recorded timing of flood of these events was reasonable because the peak flood discharge always occurred after the occurrence of peak rainfall for each individual event.

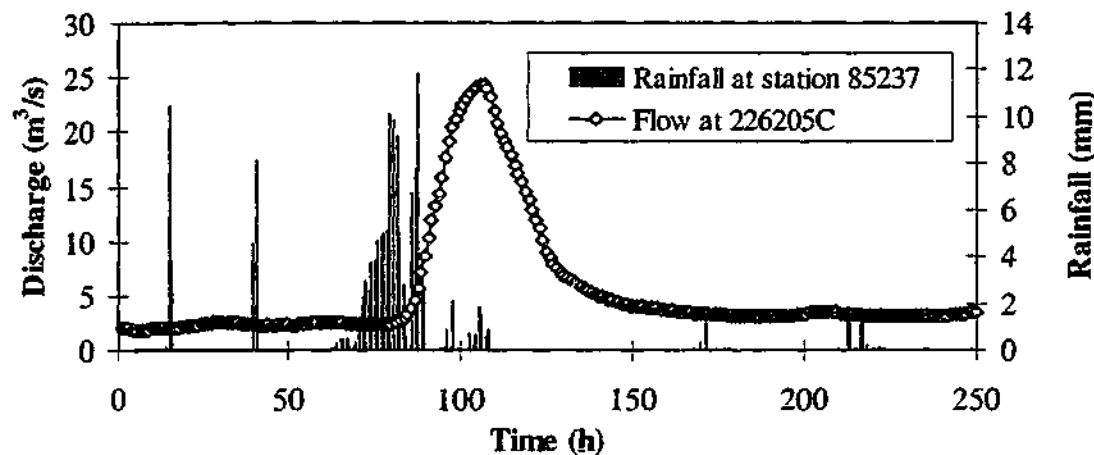


Figure 4-38: Plot of observed flood and the corresponding rainfall event (the 1963 flood)

Thirdly, the estimated rainfall over the catchment may have gross errors. It is obvious that rainfall is highly variable in spatial extent, therefore the use of rainfall data recorded at only one rain gauge might have not been representative of the catchment rainfall and the spatial variation of rainfall over the catchment.

Lastly, the runoff routing model itself may have been inadequate. That is, the non-linearity of the catchment, the hydrologic processes involved in the generation of runoff, or characteristics of the catchment and its drainage network may not have been modelled adequately. In the latter case, for example, the lower reaches of the study catchment might be very flat, resulting in very long delay in the time to flood peak, but the adopted model might have failed to consider this flat slope in the catchment representation. The adopted model could have been improved by using a much larger

value of  $m$  and including some translation, as suggested by the results shown in Figure 4-36 and Figure 4-37. Otherwise, distributed runoff routing models such as RORB (Laurenson and Mein, 1995) could be used to provide more reliable design flood estimates.

To summarise, the calibrated lumped runoff routing model for the La Trobe River catchment satisfactorily reproduced the peak discharge of the observed hydrographs. As this study focussed on the determination of the flood frequency curves of flood peak, the adopted model is considered to be adequate for this purpose. In applying the calibrated model for design flood estimation, it is emphasised that the model is directly applicable only for flood estimates within the range of the flood magnitudes used for model calibration and testing (from about  $20\text{m}^3/\text{s}$  to  $60\text{m}^3/\text{s}$ ). Extrapolation of results beyond this range will involve additional uncertainties.

### 4.8.3 Comparison of lumped and distributed runoff routing models

As mentioned in Section 4.8.1, the comparison of design floods estimated by the adopted lumped runoff routing model with those by a distributed model would give indications of the likely improvements of flood estimates had the more refined model been adopted.

The selection of a distributed model for the La Trobe River catchment was undertaken with the aim to minimise the effort of model calibration. To achieve this objective, it was desirable to use a distributed model readily available for the catchment of interest. In this regard, there are some calibrated catchment RORB and URBS models available from previous studies (Dyer et al., 1994; Baker, 1997; Smith, 1998), but all these models have not yet been independently tested. A preliminary analysis was therefore carried out to select the best model by testing the available models with an observed rainfall-runoff event that was not used in model calibration. Details of this analysis are documented in Appendix J. Analysis results indicated that the equivalent RORB catchment model developed by Baker (1997) reproduced the observed floods relatively well, and therefore was selected for this comparison.

In Baker's model, the study catchment and its drainage system were represented by 11 sub-areas and 15 river reaches (see Figure 4-39). The model parameters were:  $k_c=30$ ,  $m=0.8$ . The theoretical background of the URBS and RORB programs from which Baker's model was developed and modified is also summarised in Appendix J.

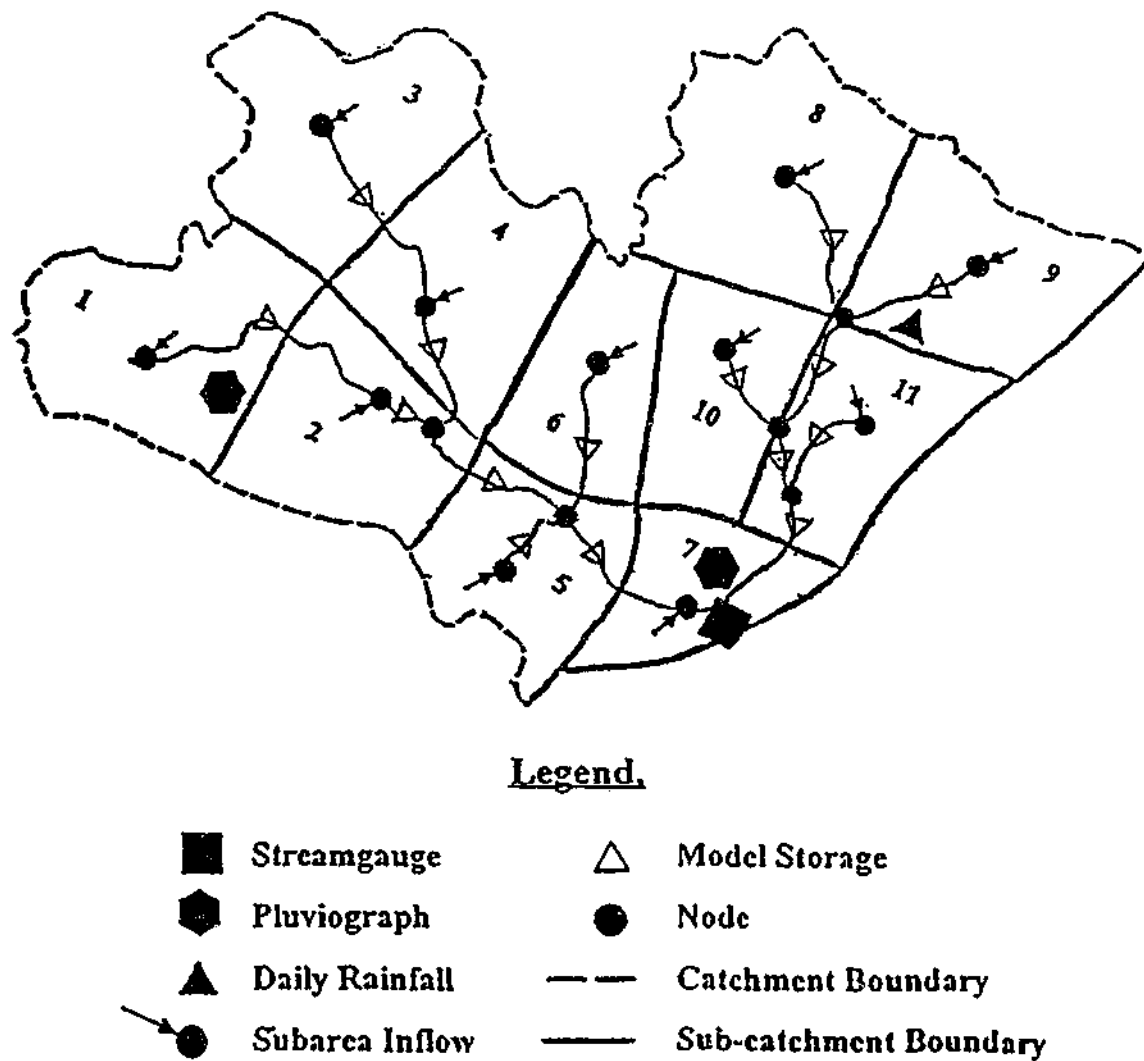


Figure 4-39: Equivalent RORB model for the La Trobe River catchment at Noojee (Baker, 1997)

In order to compare the lumped and distributed models developed for the La Trobe catchment, these models were applied to the five selected rainfall-runoff events (see Table 4-19). In these test runs, the model parameters were fixed and the loss parameters were varied within reasonable limits until the calculated surface runoff hydrographs matched the observed ones in terms of flood volume, hydrograph shape, time to peak

and most importantly, flood peak. Results of this comparison are tabulated in Table 4-22. The percentage differences between hydrograph characteristics determined by the lumped and equivalent RORB models and the observed hydrograph characteristics were also computed and are presented in Table 4-23. A plot of the observed and calculated flood hydrographs for one test event used is also illustrated in Figure 4-40.

Table 4-22: Performance of runoff routing models

Event	Observed hydrograph			Lumped model ( $k = 53, m = 0.8$ )			RORB model ( $kc = 30, m = 0.8$ )		
	Peak discharge ( $m^3/s$ )	Time to peak (h)	Volume ( $10^6 m^3$ )	Peak discharge ( $m^3/s$ )	Time to peak (h)	Volume ( $10^6 m^3$ )	Peak discharge ( $m^3/s$ )	Time to peak (h)	Volume ( $10^6 m^3$ )
1963	18.6	34	2.0	18.0	29	2.2	18.3	40	1.9
1969	15.0	89	2.6	15.9	48	2.4	16.0	59	2.6
1971	48.6	73	5.0	43.3	42	5.0	49.9	49	5.0
1977	22.2	31	2.0	22.4	23	2.5	20.9	29	2.0
1980	31.3	60	4.1	42.0	46	3.7	48.1	53	4.1

Table 4-23: % difference between estimated and observed hydrographs

Event	Lumped model ( $k = 53, m = 0.8$ )			RORB model ( $kc = 30, m = 0.8$ )		
	Peak discharge	Time to peak	Volume	Peak discharge	Time to peak	Volume
1963	-3.2	-14.7	13.3	-1.6	17.6	-1.5
1969	6.0	-46.1	-7.0	6.7	-33.7	0.4
1971	-10.9	-42.5	-1.0	2.7	-32.9	0.2
1977	1.0	-25.8	22.4	-5.8	-6.5	-1.5
1980	34.2	-23.3	-9.5	53.7	-11.7	-1.0

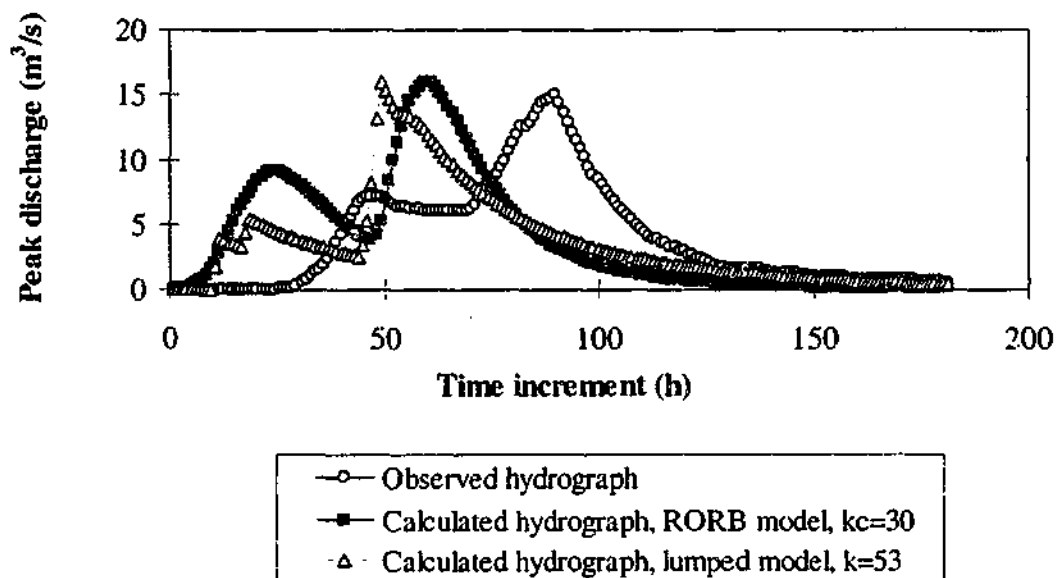


Figure 4-40: Observed and estimated flood hydrographs (the 1969 flood)

In comparing the lumped model with the distributed RORB model calibrated for the La Trobe River catchment at Noojee, it can be seen in Table 4-22 and Table 4-23 that peak discharges of the surface runoff hydrographs calculated by these models are quite similar. For example, compared with the observed peak discharge, errors in the estimated flood peak are generally below 10% for both lumped and distributed models. An exception is the 1980 event for which both models overestimate the observed flood peak by more than 30%.

With regard to other hydrograph characteristics, the lumped model does not preserve the hydrograph shape of the observed events as well as the distributed model, as illustrated in Figure 4-40. Similarly, compared with the observed floods, errors in the time to flood peak estimated by the lumped model are slightly greater than the distributed model. For example, the absolute difference between the estimated and observed timing of flood varies from 14.7% to 46.1% for the lumped model and from 6.5% to 33.7% for the distributed model (see Table 4-23). Thus, both models considerably underestimate the time to flood peak. In addition, as seen in Table 4-22 and Table 4-23, errors in the flood volumes reproduced by the lumped model are greater than those from the distributed model. This is possibly due to errors in estimates of losses from rainfall, especially in the continuing loss rate.

The comparison of the lumped and distributed routing models shows that even though a simple lumped runoff routing model was adopted for this present study, peak flood discharges estimated by this model compared well with those obtained from a distributed model. Therefore, it can be inferred that design floods obtained from the adopted lumped model would be indicative of those estimated by distributed models had the latter been used in Monte Carlo simulation. Both modelled hydrographs do not match well the observed ones in terms of hydrograph shape and time to flood peak, possibly indicating that the available rainfall data is not representative of catchment rainfall, as well as inadequacies of the catchment representation in both models.

#### 4.8.4 Summary

In this study, the runoff routing model adopted for the La Trobe River catchment at

Noojee was a lumped model with a concentrated storage at the catchment outlet. The model does not consider the spatial variation of rainfalls and losses over the catchment. It has two parameters  $k$  and  $m$ , the former represents the storage delay time and the latter characterises the non-linearity of the catchment response to rainfall.

In estimating the parameters of the adopted model,  $m$  was assumed to be 0.8. To evaluate the model parameter  $k$ , five rainfall events observed at one recording rain gauge inside the catchment and the corresponding flood events were used. The calibrated model ( $k=53$ ,  $m=0.8$ ) was found to reproduce the peak discharge of the observed surface runoff hydrographs quite well. On the other hand, the timing of peakflow was significantly underestimated.

Due to the simplicity of the adopted lumped model, design floods estimated by the model were compared with those of a distributed RORB model developed for the same catchment. The objective of this comparison was to assess how flood estimates would have differed had the spatial variability of rainfall and catchment characteristics been considered. Results of the comparison confirmed that the peak flow estimates by both models were quite similar. Therefore, it was concluded that, even though the distributed runoff routing model is clearly superior (both in theory and practice), the adopted lumped model was able to provide adequate estimates of the peak discharge in the range of flood magnitude used for model calibration and testing.

#### 4.9 OTHER FIXED DESIGN INPUTS

In this study, design inputs considered as having fixed design values were the storm continuing loss rate and the design baseflow.

The design continuing loss for the La Trobe River catchment at Noojee was taken to be 4.7mm/h. This value was obtained from a previous study of loss modelling (Hill et al., 1996a).

For the study catchment, the adopted design baseflow was  $0.75\text{m}^3/\text{s}$  (Siriwardena et al., 1997). This is the median pre-storm baseflow derived from monthly median values, which in turn were computed from observed baseflow hydrographs at the catchment outlet. Even though it is desirable to describe baseflow by a hydrograph, for simplicity, the adopted baseflow hydrograph was assumed to be time invariant.

It is noted at this point that baseflows (at the time of the peak discharge) for the five events used for calibrating the adopted runoff routing model for the study catchment ranged from  $1.7$  to  $12.5\text{m}^3/\text{s}$  (see Table 4-19). These values are generally much higher than the adopted design baseflow ( $0.75\text{m}^3/\text{s}$ ), and might be biased towards wet catchment conditions. Therefore, they are considered as not representative of the typical antecedent wetness of the catchment.

#### 4.10 SUMMARY

Results of the analyses documented in this chapter and findings are summarised below.

- Two rural catchments (the La Trobe River catchment at Noojee and the Tarwin River catchment at Dumbalk North) and 19 pluviometers in and around the selected catchments were selected to apply and evaluate the proposed Joint Probability Model for design flood estimation. Observed rainfall and flow data at these sites were checked for homogeneity. Results of the Mann-Kendall test for trend and the CUSUM test for a change in the mean value indicated that the observed rainfall and flow data at the selected sites were homogeneous in time. The La Trobe River catchment was selected for the initial analyses described in this chapter.
- In order to extract storm events from continuous rainfall records, a suitable storm definition was developed in this study. Using the adopted definition, the extracted events had the following characteristics: they are stochastic events, have no significant rain before the start and after the end of the events, and have the potential to produce significant runoff. The extracted events were then checked for consistency, and those that had evidence of errors in data recording or transcription were discarded. In total, there was 3975 observed storms extracted from the 19 selected pluviometers, with an average of seven events per year per station.

- In order to develop the probability distribution of storm duration for the La Trobe River catchment, the Hosking and Wallis method of regional frequency analysis was adopted. Analysis results indicated that homogeneous regions with respect to storm duration could be formed by grouping sites contiguous to the site of interest. A three-parameter Generalised Pareto distribution was used to characterise the storm duration.
- As there was a strong relationship between average rainfall intensity and duration, a conditional probability distribution was used to represent the rainfall intensity. In order to develop the conditional frequency curves of the average rainfall intensity (the IFD curves) for station 85237 within the La Trobe River catchment, a modified version of the at-site frequency analysis procedure developed by Rahman et al. (2001) was adopted. An exponential distribution was fitted to the observed average intensities for each of the five class intervals of storm duration and a polynomial equation was used to generalise the results for all durations. This procedure provided consistent rainfall intensity estimates for short duration and frequent storms, but resulted in some inconsistencies in the intensity estimates for longer duration and rarer events (duration greater than 48 hours and ARI exceeding 20 years). The tails of the derived IFD curves were therefore adjusted using the at-site IFD curves for storm bursts. The adjustments to the initial IFD curves were quite substantial but justified, and preserved the inverse relationship between storm duration and average intensity.
- In order to examine the dependence of rainfall temporal patterns on season, storm duration or depth, correlation analysis and the chi-square test of independence were used. Test results indicated that, depending on the test used and the level of detail of the representation of the temporal pattern, this dependence was or was not detected. According to the results of the chi-square test, the rainfall temporal pattern was dependent not only on season but also on storm duration and depth. Ten independent groups of temporal patterns were defined.
- A multiplicative cascade model was adopted to generate synthetic temporal patterns. For each temporal pattern group, disaggregation parameters of this model were represented by a beta distribution. Parameters of the beta distribution were determined from the observed storm temporal patterns in each group.

- Values of the initial loss of observed rainfall-runoff events for the catchment being studied were obtained from a parallel study. The initial loss was found to be independent of storm duration and average intensity. A beta distribution was then used to characterise the initial loss.
- A lumped runoff routing model was adopted and calibrated for the catchment. The adopted model reproduced well the peak discharge of the observed hydrographs. In comparing the adopted lumped model with a distributed RORB model developed for the same catchment, it was found that design flood peaks estimated by the former compared well with those estimated by the latter and the observed events. Therefore, it was concluded that, even though the lumped model was conceptually simple, it was able to provide adequate approximation of peak flows for the purposes of this study.
- Other inputs to the design flood estimation process that have fixed design values were the continuing loss rate and baseflow. These design values were extracted from results of previous studies.

## Chapter 5

# MODEL APPLICATION

### 5.1 INTRODUCTION

After determining the probability distributions of the important flood producing factors and the representative values of other design inputs, the subsequent step is to estimate design floods using the proposed Joint Probability Model. For this research, Monte Carlo simulation was selected for design flood estimation for three reasons. Firstly, it can take account of the dependence of the random variables involved in the design. Secondly, it has the potential to be easily applied in practice. Finally, a computer program that can be modified to be applied to the data used in this research is readily available.

Broadly speaking, Monte Carlo simulation is a computer experiment used to simulate a physical or mathematical system that is too complicated to be understood properly, and/or appears to be based on random processes. The experiment is performed on a probabilistic model that represents the system and all random variables and other fixed design inputs involved. In the experiment, the probability distributions of the input variables first need to be specified. Different sets of random values of these input variables are then generated from their corresponding probability distributions. Values of the output variable resulting from the joint occurrence of the fixed and variable design inputs are next computed using the adopted simulation model. By repeating the experiment a large enough number of times, a sample of the output can be obtained. Methods of statistical estimation finally can be applied to the output sample in order to provide frequency estimates of the system output. These estimates are also subject to sampling variability due to the statistical nature of Monte Carlo simulation. Thus, one of the fundamental issues of Monte Carlo simulation is how to design the experiment to obtain reliable results.

To increase the accuracy of the system output, two methods can be applied. The first is to repeat the experiment a large enough number of times so that the mean of the output estimates approaches the population mean, according to the law of large numbers (Perlado, 1990). The second is to apply variance reduction techniques (Perlado, 1990; Kottegoda and Rosso, 1997). Broadly speaking, these techniques aim to reduce the standard error or the variance of the simulation outcomes by biasing the probabilistic scheme to the domain of design interest without increasing the sample size. Of these two methods, the generation of a large number of trials is adopted because it is considered to be adequate for the purpose of this study, that is, to estimate design floods with ARIs in the range of 1 to 100 years. In addition, it is simpler and easier for practical applications than using variance reduction techniques.

The application of Monte Carlo simulation to the proposed Joint Probability Model for estimating design floods from design rainfalls involves two stages. The first stage is to generate flood events. This includes the determination of number of random number to be generated, the generation of random values from the probability distributions of the flood causing factors, and the estimation of design floods by passing through the proposed model various combinations of these random numbers and other fixed design inputs. After generating a large sample of synthetic floods, the second stage is to carry out a frequency analysis of these flood events in order to determine the derived flood frequency curve. The objective of this chapter is to report the application of the above two stages to the development of the generated flood frequency curve for the La Trobe River catchment at Noojee.

## **5.2 GENERATION OF RANDOM NUMBERS FROM THE INPUT DISTRIBUTIONS**

### **5.2.1 Background**

A random number is a number selected at random from a population of numbers such that each number in the population has a chance of being selected in accordance with the probability distribution from which the numbers are drawn. Random numbers can

be classified as uniform random numbers and random numbers generated from other distributions. Uniform random numbers, also called uniform random deviates or uniform deviates, are random numbers generated from a uniform distribution, usually on the interval from 0 to 1. Random numbers generated from other distributions are obtained by performing appropriate operations on uniform random numbers.

Many methods are available for generating random numbers. For example, the linear congruential method is most popularly used to generate uniform deviates, and the inverse cumulative distribution function method or the rejection method can be employed to generate random numbers from other continuous distributions (Press et al., 1989). In practice, utility subroutines (also called system-supplied random number generators) are widely used. For example, for FORTRAN language, utility subroutines for selecting the type of generators or for setting and retrieving the seed (the starting value of a sequence of random numbers) are available in the Microsoft International Mathematical Statistical Library (MSIMSL) (Microsoft Corporation, 1995). A collection of subroutines for generating random numbers from common distributions such as uniform, beta, exponential, and normal distributions can also be found in this library. In addition, some subroutines for generating random numbers from a general continuous distribution are also provided.

This section documents the research undertaken to generate random numbers from the statistical distributions of storm duration, rainfall intensity, temporal pattern, and initial loss. It first specifies the number of random numbers to be generated, then describes the application of computer subroutines for generating random data from the above distributions.

### **5.2.2 Number of generated data**

For the present application, the number of random data to be generated depends on many factors such as the degree of accuracy required, the range of flood return periods of interest, the number of random variables involved in simulation, and the degree of correlations among them. When using four random variables (intensity, duration, temporal pattern, and initial loss) in the proposed Joint Probability Model with some

degree of correlations, it was considered adequate to generate 2000 years of data to estimate design floods with return periods of 1 to 100 years. It was also assumed that the generated floods form a partial duration series, therefore the number of random data to be generated (NR) can be determined from the following relationship:

$$NR = \omega_1 \times N_Y \quad (5-1)$$

where  $\omega_1$  is the average number of events per year, and  $N_Y$  is the number of years of data to be generated.

For the La Trobe River catchment, the average number of significant rainfall events per year was 7.6, recorded at pluviometer 85237. Therefore, the data generation scheme was applied to generate 15000 events over the period of 2000 years.

### 5.2.3 Storm duration

In order to generate 15000 random storm durations from the Generalised Pareto distribution representing the storm duration at station 85237, subroutines DRNGCS and DRNGCT of the MSIMSL (Microsoft Corporation, 1995) were used. These subroutines have been developed for generating random numbers from a general continuous distribution using the inverse cumulative distribution function method (Haan, 1977; Press et al., 1989). With this method, a random number can be generated from a probability distribution by equating a randomly generated uniform random number with the cumulative distribution function of the specified probability distribution. More details of this method are documented in appendix K. The cumulative distribution function of the Generalised Pareto distribution is documented by Hosking (1997).

Before using the generated storm durations for design flood estimation, it was necessary to check if the generated data could reproduce the important statistical properties of the observed storm durations. In order to do this, the mean, standard deviation, skewness, and percentiles of the simulated storm durations were computed and then compared with those of the observed storm events. A summary of these statistical properties of the observed and generated storm durations is presented in Table 5-1. It can be seen

from this table that the average duration of the observed storms is reproduced very well in the simulated storms. Other statistical characteristics of the observed storms such as skewness and percentiles of the storm duration are also preserved well in the generated events. However, the standard deviation of the simulated storm duration is slightly greater than that of the historical data. This means that, the duration of the simulated storms is slightly more variable than that of the observed storms. In general, it can be concluded that the generated storm durations for station 85237 preserve very well the statistical properties of the observed storm durations.

Table 5-1: Statistical properties of observed and simulated storm durations

	observed storms	simulated storms
Number of events	167	15000
Mean (h)	23.5	23.6
Standard deviation (h)	18.1	18.9
Skewness	1.1	1.1
25th percentile (h)	9	9
50th percentile (h)	19	19
75th percentile (h)	35	34

#### 5.2.4 Rainfall intensity

In order to determine the average rainfall intensity corresponding to a specified random storm duration and an ARI, the procedure below, developed by Rahman et al. (2001) was adopted.

- An IFD table, showing average rainfall intensities for some selected storm durations and ARIs, was developed for the site of interest (see Table 5-2). The average rainfall intensities shown in this table were computed using the method described in Section 4.5. There are two points to be noted in this table. Firstly, even though the ARI of design floods of interest in this study is from 1 to 100 years, the simulated range of ARIs is much wider (from 0.1 to  $10^6$  years) to allow for various input combinations that might arise during simulation. Secondly, the derived IFD curves for the design site are considered to be reliable in the ARI range from 1 to 100 years (see Section 4.5). Therefore, extrapolation of these curves outside this range is subject to considerable uncertainties.

Table 5-2: IFD table for observed storms at pluviometer 85237 (unit mm/h)

D (h)	ARI (years)												
	0.1	1	1.11	1.25	2	5	10	20	50	100	500	1000	1000000
1	2.21	8.33	8.84	9.42	10.42	12.82	14.60	16.41	18.77	20.66	26.63	28.40	52.26
2	1.82	5.69	5.92	6.17	6.98	8.67	9.95	11.22	12.89	14.17	17.34	18.59	31.93
6	1.49	3.09	3.17	3.26	3.78	4.74	5.47	6.19	7.15	7.86	9.27	9.99	16.33
24	1.22	1.42	1.47	1.53	1.80	2.27	2.62	2.97	3.44	3.79	4.61	4.98	8.49
48	0.38	0.96	1.01	1.07	1.26	1.59	1.83	2.07	2.39	2.65	3.38	3.64	6.64
72	0.21	0.76	0.82	0.88	1.03	1.29	1.48	1.68	1.94	2.15	2.86	3.07	5.89
120	0.16	0.57	0.62	0.69	0.80	1.00	1.14	1.29	1.49	1.66	2.34	2.50	5.20

- A random duration was then generated using the method described in Section 5.2.3.
- A random annual exceedance probability (AEP) to be assigned to the generated storm duration was next generated from a uniform distribution on the interval from 0 to 1. To avoid values of AEP that are too low or too high and are not of direct interest in this study, the following constraint was applied to the generated AEP:  $10^{-6} < AEP < 1 - e^{-\omega_1}$ , where  $\omega_1$  is the average number of storms per year.
- The AEP was then converted into the corresponding ARI for partial duration series by the following relationship (Stedinger et al., 1993):  $ARI = -1 / (\ln(1 - AEP))$ .
- The average rainfall intensity for the specified storm duration and ARI was finally computed by linearly interpolating values of the IFD table on a logarithmic scale. The linear interpolation was considered to be adequate here for two reasons. Firstly, for a given storm duration, a straight line represents the relationship between average rainfall intensity and storm ARI (see Section 4.5.3). Secondly, for a given ARI, a near straight line characterises the relationship of average rainfall intensity and duration. As illustrated in Figure 4-20, this latter relationship is described by a second-degree polynomial function, but due to the very small coefficient of the square term, the polynomial function is closely approximated by straight-line segments on a log-log scale.

## 5.2.5 Temporal patterns

### 5.2.5.1 Generation of design temporal patterns

As mentioned in Section 4.6.5, in this study, the design rainfall temporal pattern is

represented by 7 internal ordinates of the dimensionless storm mass curve. This design pattern represents a dimensionless rainfall hyetograph defined at eight equal time increments of storm duration, each being  $1/8$  of the storm duration. To generate such a design temporal pattern using the multiplicative cascade model (Robinson and Sivapalan, 1997), 7 random numbers are needed.

In order to generate design temporal patterns for each of the 10 temporal pattern groups, the following procedure was adopted. The subroutine RNBET from the MSIMSL was first used to generate 15000 sequences of 7 random numbers from the beta distribution representing the disaggregation parameters for each temporal pattern group. Each sequence of random numbers was then used to construct a dimensionless rainfall hyetograph using the multiplicative cascade model described in Section 4.6.5. An example of a generated dimensionless hyetograph is illustrated in Figure 5-1.

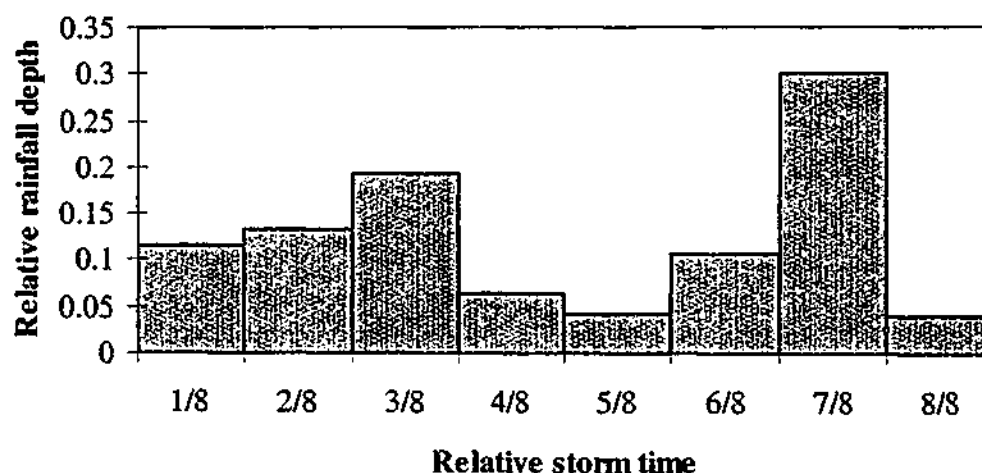


Figure 5-1: An example of a generated temporal pattern

#### 5.2.5.2 Model verification

The generated temporal patterns of rainfall have to be able to reproduce the peak intensity of the observed storm hyetographs. In addition, the correlation between rainfall intensity at one time step and the next, if any, needs to be preserved, as well as the hyetograph statistical characteristics. For these reasons, the adequacy of the model used to generate storm patterns and of the beta distribution characterising the disaggregation parameters of each temporal pattern group was verified by comparing

the observed and generated hyetographs with respect to the distribution of the maximum dimensionless intensity, the lag one auto-correlation<sup>1</sup>, and the frequency characteristics of mass curves.

### Comparison of the maximum dimensionless rainfall intensity

To compare the distribution of the maximum dimensionless intensity, dimensionless rainfall depths at time intervals equal to 1/8 of storm duration, henceforth referred to as dimensionless rainfall intensities, were calculated for each (observed or simulated) storm. For each storm, the maximum dimensionless rainfall intensity ( $i_m$ ) was then determined. This intensity was then assigned to one of the 10 class intervals as follows: (0, 0.1), (0.1, 0.2), ..., (0.9, 1), where (0, 0.1) indicates  $0 < i_m \leq 0.1$ . The above two steps were next repeated for all storms in each temporal pattern group. For each group, the frequency of obtaining the maximum dimensionless storm intensity within each of the 10 specified class intervals was computed. The cumulative relative frequency of the maximum dimensionless intensity was finally determined. Results are tabulated in Table 5-3 and illustrated in Figure 5-2 and Figure 5-3.

Table 5-3: Cumulative relative frequencies of the maximum dimensionless intensity of observed and generated temporal patterns

Temporal pattern group		Class intervals of dimensionless maximum intensity									
		(0, 0.1)	(0.1, 0.2)	(0.2, 0.3)	(0.3, 0.4)	(0.4, 0.5)	(0.5, 0.6)	(0.6, 0.7)	(0.7, 0.8)	(0.8, 0.9)	(0.9, 1.0)
1	Observed	0	0.067	0.523	0.778	0.898	0.952	0.983	0.994	1	1
	Simulated	0	0.025	0.455	0.806	0.949	0.993	0.999	1	1	1
2	Observed	0	0.022	0.427	0.72	0.911	0.965	0.99	1	1	1
	Simulated	0	0.022	0.315	0.675	0.869	0.965	0.987	0.994	1	1
3	Observed	0	0.083	0.354	0.771	0.917	0.958	0.979	1	1	1
	Simulated	0	0.021	0.396	0.646	0.833	0.938	0.979	1	1	1
4	Observed	0	0.074	0.56	0.866	0.972	0.986	0.995	1	1	1
	Simulated	0	0.06	0.579	0.866	0.963	0.995	1	1	1	1
5	Observed	0	0.125	0.578	0.849	0.953	0.983	1	1	1	1
	Simulated	0	0.056	0.556	0.871	0.97	0.996	1	1	1	1
6	Observed	0	0.056	0.565	0.876	0.975	0.993	0.998	1	1	1
	Simulated	0	0.043	0.514	0.858	0.968	0.998	1	1	1	1
7	Observed	0	0.183	0.726	0.894	0.951	0.985	0.996	1	1	1
	Simulated	0	0.068	0.643	0.947	0.996	1	1	1	1	1
8	Observed	0	0.064	0.624	0.921	0.982	0.997	1	1	1	1
	Simulated	0	0.062	0.564	0.879	0.968	0.997	1	1	1	1
9	Observed	0	0.102	0.581	0.826	0.924	0.969	0.987	0.997	1	1
	Simulated	0	0.047	0.526	0.872	0.961	0.99	1	1	1	1
10	Observed	0	0.044	0.463	0.801	0.921	0.971	0.985	0.997	1	1
	Simulated	0	0.029	0.443	0.774	0.956	0.991	1	1	1	1

<sup>1</sup> The lag one auto-correlation, also called lag one serial correlation, is a statistical measure computed for a time series of data to determine if an observation at one time period is correlated with the observation at one time period earlier (or later).

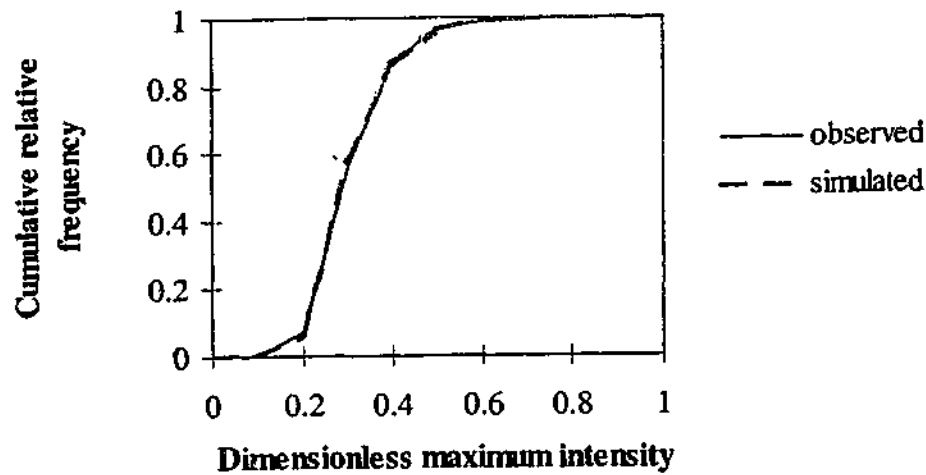


Figure 5-2: Distributions of the maximum dimensionless intensity for observed and generated temporal patterns of Group 4

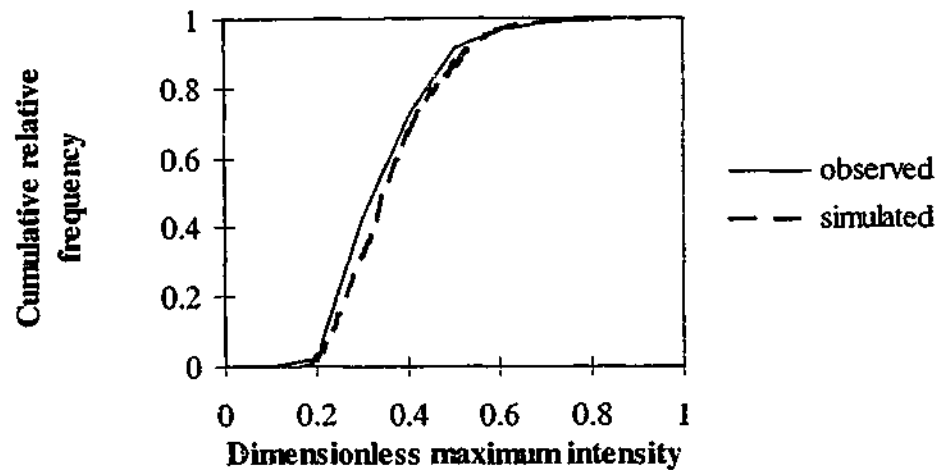


Figure 5-3: Distributions of the maximum dimensionless intensity for observed and generated temporal patterns of Group 2

It can be seen from Table 5-3 that, for temporal patterns of Groups 4, 5, 6, 8 and 10, the cumulative frequency distributions of the maximum rainfall intensity of the observed storm temporal patterns are very similar to those of the generated patterns. This means that the relative frequency of the observed storms having the dimensionless maximum rainfall intensity within a given intensity interval is almost the same as that of the generated data for these temporal pattern groups. For storm patterns of Groups 1 and 9, the observed and simulated intensity distributions are reasonably similar. However, the

observed peak intensity is not very well preserved in the generated storm patterns of Groups 2, 3 and 7, as illustrated in Figure 5-3 for Group 2. In these cases, the frequency of the maximum intensity of the observed storms is either underestimated or overestimated in the generated storms. For example, for Group 7, the relative number of the simulated storms that have the maximum relative intensity in the range of (0.1, 0.2) is much less than that of the observed data. Overall, it can be concluded that the distributions of the maximum rainfall intensity of the observed storms are reasonably well preserved in the simulated storms.

#### Comparison of lag one auto-correlation coefficient

To compare the lag one auto-correlation ( $r_1$ ) of the observed and generated temporal patterns,  $r_1$  was first computed for each storm using the following formula (Haan, 1977, Chapter 11):

$$r_1 = \frac{\sum_{i=1}^{n-1} h_i h_{i+1} - \frac{1}{n-1} \sum_{i=1}^{n-1} h_i \sum_{i=1}^{n-1} h_{i+1}}{\left[ \sum_{i=1}^{n-1} h_i^2 - \frac{1}{n-1} \left( \sum_{i=1}^{n-1} h_i \right)^2 \right]^{1/2} \left[ \sum_{i=1}^{n-1} h_{i+1}^2 - \frac{1}{n-1} \left( \sum_{i=1}^{n-1} h_{i+1} \right)^2 \right]^{1/2}} \quad (5-2)$$

where  $h_i$  is the dimensionless rainfall intensity during the time step  $i$ , and  $n$  is the number of time increments used to define storm hyetographs ( $n=8$  in this case). For each temporal pattern group, the mean and standard deviation of the  $r_1$  values of the observed and generated storms were then calculated and are summarised in Table 5-4. To aid in the comparison process, the limits of the 95% confidence intervals of the estimated mean of  $r_1$  were also computed based on the assumption that the  $r_1$  values for each group were from a normal distribution (see Table 5-5). Due to the large number of storms in each temporal pattern group (see Table 5-5), this assumption was justified.

In assessing values of  $r_1$  for the observed and generated storms, it is clear from Table 5-4 that the mean and standard deviation of  $r_1$  computed for each temporal pattern group are much less than 1, but generally not close to zero. For the observed storms, the highest mean value is 0.392 for temporal patterns of Group 7, and the lowest mean value is 0.12 for Group 4. The standard deviation of the  $r_1$  values is also low, varying from 0.035 to 0.116. However, because of the very large number of the observed storms, the upper and lower limits of the 95% confidence intervals of  $r_1$  (see Table 5-5)

are very close to the computed mean value. Thus for the observed storms, the computed values of the correlation of the dimensionless rainfall intensity at one time step with the intensity at one time step earlier or later are significant. By contrast, the mean and confidence limits of the  $r_1$  values of the generated storms, are much closer to zero (see Table 5-4 and Table 5-5). It can therefore be inferred that the lag one auto-correlation between the dimensionless rainfall at successive time steps is significantly underestimated in the generated storms.

Table 5-4: Mean and standard deviation of lag one auto-correlation coefficients of observed and simulated storm temporal patterns

Temporal pattern group	mean of $r_1$		standard deviation of $r_1$	
	observed	simulated	observed	simulated
1	0.385	0.098	0.099	0.123
2	0.180	0.066	0.116	0.122
3	0.295	0.116	0.113	0.142
4	0.120	0.065	0.128	0.112
5	0.373	0.097	0.102	0.130
6	0.190	0.070	0.127	0.136
7	0.392	0.065	0.099	0.151
8	0.171	0.056	0.113	0.118
9	0.355	0.062	0.109	0.126
10	0.168	0.035	0.120	0.128

Table 5-5: 95% confidence intervals of the lag one auto-correlation coefficient

Group	No. of storms	Observed storms		Generated storms	
		Lower limit	Upper limit	Lower limit	Upper limit
1	686	0.378	0.392	0.089	0.107
2	314	0.167	0.193	0.053	0.079
3	48	0.263	0.327	0.076	0.156
4	216	0.103	0.137	0.050	0.080
5	232	0.360	0.386	0.080	0.114
6	444	0.178	0.202	0.057	0.083
7	263	0.380	0.404	0.047	0.083
8	659	0.162	0.180	0.047	0.065
9	384	0.344	0.366	0.049	0.075
10	341	0.155	0.181	0.021	0.049

The reduced lag one auto-correlation of rainfall intensity at successive time steps of the generated temporal patterns is not surprising because the adopted multiplicative cascade model, as described in Section 4.6.5, does not try to preserve this correlation for the observed storm temporal patterns. However, in reality, there is a tendency of high rainfall values to be followed by high values (rather than randomly distributed), and this would tend to produce larger peaks. Therefore, for design flood estimation, the reduced serial correlation in the generated temporal patterns likely leads to underestimation of design floods.

#### **Comparison of frequency characteristics of mass curves**

To compare the frequency characteristics of mass curves, Huff curves (Huff, 1967) were used. Huff frequency curves, developed from observed storm mass curves, are smooth curves with various levels of severity. For example, the 10% probability curve can be defined as the average mass curve that is equalled or exceeded by 10% of the observed patterns. Being smooth curves, Huff curves reflect the average rainfall distribution with time, and do not exhibit burst characteristics of the observed storms. They provide a quantitative measure of both inter-storm variability and the storm-to-storm variability in a storm sample.

To determine Huff curves of the observed and generated storms for each of the ten temporal pattern groups, the dimensionless cumulative rainfall depths at 8 equal increments of storm duration were first computed for each storm. For all storms in a group, for each time increment, the accumulated dimensionless depths at 9 probability levels from 10% to 90% at equal increments of 10% were then estimated. For each probability level, the computed dimensionless depths at each of the 8 equal time increments were finally plotted on a graph, and a smooth curve was drawn through the plotted points. These smooth curves are termed Huff frequency curves.

The comparison of Huff frequency curves of the observed and generated storms was carried out by plotting the frequency curves at the same probability level on a graph and visually comparing them. Only three probability levels of 10%, 50%, and 90% were used in this comparison because these levels summarise the set of frequency curves and they are generally of interest in practical situations.

Results of the comparison showed that, for any temporal group, Huff frequency curves developed for the generated storms very resembled those of the observed storms. This implies that the variability in the temporal distribution of the observed and generated storms in any group is very similar. A typical example of the observed and simulated Huff frequency curves determined for one temporal pattern group is illustrated in Figure 5-4.

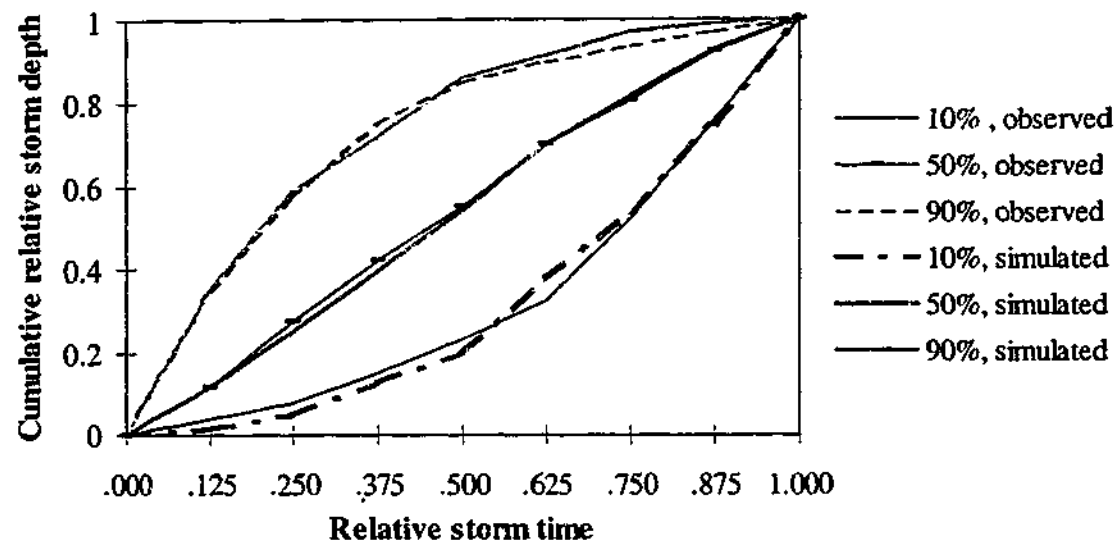


Figure 5-4: Huff frequency curves of the observed and generated temporal patterns of Group 2

In summary, the generated storm temporal patterns reproduced fairly well the distribution of the maximum dimensionless intensity and the frequency characteristics of the observed temporal patterns. However, the lag one auto-correlation between successive storm depths in the observed storms is significantly underestimated in the generated storms.

### 5.2.6 Initial loss

To generate 15000 random values of the initial loss for the La Trobe River catchment at Noojee from the beta distribution characterising the observed storm losses, subroutine RNBET from the MSIMSL was again used. This subroutine is based on the rejection method (Press et al., 1989), the principles of which are described in Appendix K.

To assess the generated initial losses, their statistical properties were computed and compared with those of the observed losses. Results are summarised in Table 5-6. It is evident from this table that the mean and standard deviation of the observed initial losses are relatively well reproduced in the generated loss values. However, the coefficient of skewness of the observed data is significantly underestimated in the generated loss. In addition, there are more low and high loss values in the generated data than in the observed data, as indicated by the estimated 25<sup>th</sup> and 75<sup>th</sup> percentiles. This implies that there is some overestimation and underestimation of the generated storm initial loss values. Therefore, it is difficult to assess how the errors in the estimates of losses translate to errors in design flood estimates. The question of sensitivity of design floods to the representation of the initial loss is further examined in Section 6.5.

Table 5-6: Characteristics of observed and generated initial loss data

	observed storms	simulated storms
Number of events	167	15000
Mean (mm)	27.3	26.9
Standard deviation (mm)	17.4	17.3
Coefficient of skewness	2.7	0.9
25th percentile (mm)	15.8	13.5
50th percentile (mm)	22.2	23.6
75th percentile (mm)	34.4	37.0

### 5.3 ESTIMATION OF FLOOD EVENTS BY MONTE CARLO SIMULATION

After generating the random input values of the storm duration, temporal pattern, initial loss, and determining the corresponding average rainfall intensities, Monte Carlo simulation was applied to generate flood events. As discussed in Section 3.3.3, one important aspect of this simulation process was the consideration of the correlations of the input random variables. How this was allowed for in simulation and the procedure used to simulate flood events are described in the section below.

### 5.3.1 Correlations of flood causing factors

In order to model realistically the flood generation process, the correlations between the flood causing components must be considered. In this research, no relationship was found between the initial loss and storm duration or average rainfall intensity (see Section 4.7.2). However, there was significant statistical evidence of the correlation between rainfall intensity and duration (see Section 4.5.2), and of the variation of the temporal pattern with season of storm occurrence, storm duration, or storm depth (see Section 4.6.4). The above relationships were accounted for in the simulation in the following ways.

With respect to average rainfall intensity, the dependence of rainfall intensity on duration was taken into consideration by the use of IFD curves. That is, average rainfall intensity was conditionally computed for a given storm duration and annual exceedance probability.

To account for the seasonal variation of temporal patterns, it would have been necessary to have other inputs (for example, rainfall intensity, duration, or storm loss) defined on a seasonal basis. However, in the absence of these other seasonal inputs, the following procedure for considering the variation of temporal patterns with season was adopted. It was first assumed that the occurrence of storm events over 12 months follows a uniform distribution. In other words, there is an equal probability of a storm to fall in any month. From this assumption, the occurrence probabilities of the four rainfall seasons defined in this research (as far as the variation of temporal patterns is concerned) were computed and are presented in Table 5-7. In order to assign a storm to a rainfall season, it was further assumed that the first 33% of all the generated storms were summer storms, the next 17% of storms were autumn storms, the next 33% were winter storms, and the last 17% were spring storms (see Table 5-7).

The consideration of the dependence of the storm temporal pattern on duration or depth was straightforward. First, a storm duration was generated. The season of this storm event was next determined using the assumptions described above. The total depth of the storm was then computed. The temporal pattern group of the generated storm was

finally determined from the known information of season of storm occurrence, storm duration, and depth (see Figure 4-27).

Table 5-7: Seasonal probabilities of storm occurrence

	Summer	Autumn	Seasons		Total
			Winter	Spring	
Number of months	4	2	4	2	12
Probability	0.33	0.17	0.33	0.17	1

### 5.3.2 Simulation procedure

In order to compute design floods for the La Trobe River catchment from various combinations of flood causing factors, the procedure below was adopted.

- (a) A storm duration  $D_i$  was randomly generated from the Generalised Pareto distribution (see Section 5.2.3).
- (b) For the generated storm duration  $D_i$ , an  $AEP_i$  was randomly generated from a uniform distribution on the interval from 0 to 1. This  $AEP_i$  was then converted into the  $ARI_i$  for the given storm (see Section 5.2.4).
- (c) The average point rainfall intensity corresponding to the randomly selected duration  $D_i$  and  $ARI_i$  was then computed by interpolating values of the IFD table established for the design site (see Section 5.2.4). To obtain the areal average intensity, the computed point rainfall depth for the specified duration was estimated and then multiplied by the interim areal reduction factor (Siriwardena and Weinmann, 1996) determined for the given catchment area, average recurrence interval, and storm duration.
- (d) The temporal pattern group of the specified storm was next determined by the method described in Section 5.3.1. The design temporal pattern of the storm was then taken randomly from the generated samples of patterns for the particular temporal pattern group (see Section 5.2.5.1).
- (e) A random initial loss value  $IL_i$  was generated from the beta distribution fitted to the observed loss data for the catchment under study (see Section 5.2.6).
- (f) The rainfall excess hyetograph of the specified storm was then estimated by passing the above stochastic design rainfall event characteristics through an initial loss –

continuing loss model with an initial loss of  $IL_1$  and a fixed continuing loss rate ( $CL=4.7\text{mm/h}$ ). This hyetograph was next routed through the calibrated lumped runoff routing model with fixed design parameters ( $m=0.8$ ,  $k=53$ ) to produce a surface runoff hydrograph. A fixed value of the design baseflow ( $0.75\text{m}^3/\text{s}$ ) was then added to the surface runoff hydrograph to obtain the design flood hydrograph. The maximum peak flow of this flood hydrograph was recorded.

The FORTRAN programs to undertake steps (b), (c), (e), and (f) of the above procedure were provided by Rahman (1999).

After repeating the above procedure for 15000 times, a partial duration series with 15000 generated design peak discharges was obtained. A flood frequency analysis was then carried out to determine the frequency distribution of the generated flood series. This analysis is described below.

#### 5.4 DETERMINATION OF DESIGN FLOOD FREQUENCY CURVES

To determine the frequency distribution of the partial duration series of the generated floods, the non-parametric method, outlined in Appendix I, was adopted. In this method, the flood series was first ranked into decreasing order of magnitude. That is, the highest flood was ranked 1, the second highest ranked 2, and so on. The plotting position of the flood ranked  $j$  in the series was then computed using Equation (4-5), where  $N^*$  is the data length in years (in this case,  $N^*=2000$  years). The generated floods in the series were finally plotted on a semi-logarithmic graph paper against their corresponding plotting positions.

The flood frequency curve derived for the La Trobe River catchment is illustrated in Figure 5-5. Due to the very large number of the generated flood events (in the order of thousands), it is evident from Figure 5-5 that design flood peaks for the ARI range of interest (from 1 to 100 years) can be determined directly from this graph without the need for fitting a theoretical probability distribution to the flood series. The estimated design floods for the study catchment, read from Figure 5-5, are tabulated in Table 5-8.

For example, the design peak discharges of 5-year and 100-year ARI for the specified catchment are  $45\text{m}^3/\text{s}$  and  $127\text{m}^3/\text{s}$ , respectively (see Table 5-8). It is noted that, during the simulation process, about 20 flood events with ARIs exceeding 100 years were generated. Nevertheless, as the design floods of interest in this study have ARIs of up to 100 years, those design flood peaks with ARIs exceeding 100 years are not shown in Figure 5-5.

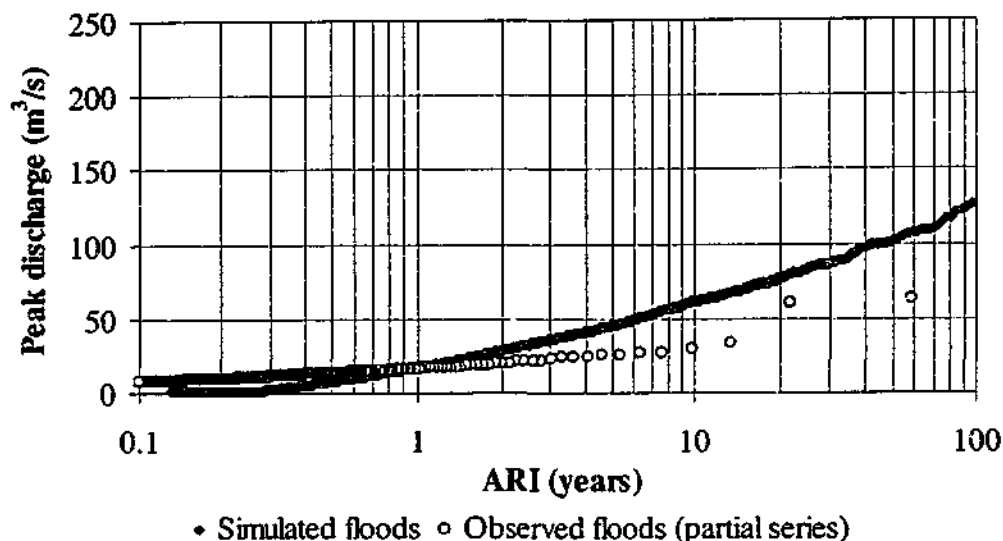


Figure 5-5: The generated flood frequency curve for the La Trobe River catchment

Table 5-8: Design flood estimates for the La Trobe River catchment by Monte Carlo simulation (unit:  $\text{m}^3/\text{s}$ )

	Average recurrence interval (ARI, years)						
	1	2	5	10	20	50	100
Peak discharge	17	29	45	62	76	101	127

As mentioned in the Introduction, design flood estimates by the proposed Joint Probability Model are subject to uncertainty due to sampling variability inherent in Monte Carlo simulation. However, the uncertainty in these estimates may also be induced by the uncertainties in the adopted form and estimated parameters of the probability distributions used to represent design random variables, and by the inadequacy of the runoff routing model adopted to represent the hydrograph formation process, along with errors in its parameter estimation. Whereas the uncertainty of flood

estimates due to sampling variability can be easily assessed by changing the sample size of the generated data, the assessment of the uncertainty due to model or parameter uncertainties obviously is not a trivial task and may require additional sources of data. For these reasons, the former is examined in a sensitivity analysis detailed in the next chapter, and the latter is left for future improvements of the proposed model.

## 5.5 SUMMARY

The application of the proposed Joint Probability Model to the determination of the generated flood frequency curve for the La Trobe River catchment at Noojee was carried out in two stages. The first stage involved the generation of stochastic input data from the relevant distributions, and the generation of flood events using Monte Carlo simulation. The second stage was the frequency analysis of the generated floods.

The stochastic design inputs were the storm duration, average intensity, temporal pattern, and initial loss. Random data for these variables were generated from the corresponding probability distributions using computer subroutines from the Microsoft International Mathematical Statistical Library. The generated data were then checked to ensure that they were able to reproduce statistical properties of the observed data: 15000 random events spanning 2000 years of data were obtained from this step.

The comparison of important statistical characteristics of the observed and generated data for each random input showed different results. Whereas the statistical properties of the observed storm durations were very well preserved in the generated storm durations, there were uncertainties in the estimates of the rainfall intensity outside the ARI range of 1 year to 100 years. In addition, the coefficient of skewness of the observed storm losses was significantly underestimated. With respect to the rainfall temporal pattern, whereas the maximum dimensionless rainfall intensity and the variability of the observed temporal patterns were reasonably well preserved in the generated pattern, the lag one auto-correlation coefficient was underestimated. Errors in these stochastic design inputs have the potential to be transferred to errors in the resulting design flood estimates. This will be further investigated in Section 6.5.

In generating flood events using Monte Carlo simulation, the correlations of design inputs were taken into account. The dependence of rainfall intensity on duration and return period was accounted for by using the conditional probability expressed in the IFD curves. The relationships between a generated storm and season, storm duration, and depth were considered by using temporal patterns from appropriate temporal pattern groups. A partial duration series of 15000 design flood peaks was obtained. The empirical distribution of these generated floods was finally derived using a flood frequency analysis.

## Chapter 6

# MODEL EVALUATION

## 6.1 INTRODUCTION

The evaluation of the proposed Joint Probability Model is a crucial task in determining whether or not it can reduce the bias and uncertainty in design flood estimates. The assessment of bias can be carried out by comparing design floods obtained from the proposed model with the best estimates available for a particular catchment. Likewise, the evaluation of uncertainty can be determined by comparing the estimated floods with those from other methods routinely applied in Australia, using readily available data.

For the catchment under study, the La Trobe River catchment at Noojee, there exist long and concurrent rainfall and streamflow records. Therefore, the two flood estimation methods that would normally be applied are direct flood frequency analysis and the Design Event Approach. Direct flood frequency analysis is the most direct method for design flood estimation for the study catchment because it is based on observed streamflow data. The rainfall-based Design Event Approach is also a suitable design flood estimation method for this site because parameters of its hydrograph model can be calibrated directly from the observed rainfall-runoff events. Therefore, flood estimates obtained from these two methods are used as the basis for the evaluation of the proposed model.

The objective of this chapter is to document the research undertaken to evaluate the design floods estimated by the proposed Joint Probability Model. The chapter starts with the determination of the flood frequency curve for the La Trobe River catchment using direct flood frequency analysis. The estimation of design floods for this site by the Design Event Approach is presented next. The comparison of flood estimates obtained by these techniques with those from the proposed model is then detailed and the validity of the proposed model is discussed. Details of the sensitivity analyses

conducted to determine the effects on design flood estimates of changes in the probabilistic inputs, in other fixed design values and in the sample size of the generated data are next documented. Finally, an additional testing of the method is described in which the proposed Joint Probability Model is applied to another Victorian catchment, the Tarwin River catchment at Dumbalk North, and the results are discussed.

## **6.2 ESTIMATION OF DESIGN FLOODS BY DIRECT FLOOD FREQUENCY ANALYSIS**

As already outlined in Chapter 2, direct flood frequency analysis is a technique that gives estimates of peak flood magnitudes of specified exceedance probabilities by statistical analysis of observed floods at or near the design site. The analysis can be applied to an annual flood series or a partial flood series. The former series consists of the maximum instantaneous peak discharge in each year of record, whereas the latter comprises all independent floods with peak discharges above a selected threshold value. Even though partial flood series is more relevant to practical problems, probability methods have commonly been applied to annual series due to the simplicity of technique and easy interpretation of results (Laurenson, 1987).

In the present study, direct flood frequency analysis was applied to the annual flood series for two reasons. Firstly, the observed annual flood series for the La Trobe River catchment only differs significantly from the partial series for ARIs less than 5 years. Secondly, the procedure for fitting a theoretical probability distribution to an annual series is readily obtainable in the form of a computer spreadsheet (Hill et al., 1996c).

The theoretical basis of the adopted spreadsheet, called the CRCCH Flood Frequency Analysis Spreadsheet (or shortly, the CRCCHFFA Spreadsheet), is briefly described below. The application of this spreadsheet to the observed flow data at the study catchment is then presented in detail, and the design floods obtained are discussed.

### 6.2.1 Theoretical basis

The CRCCHFFA Spreadsheet employs the procedure currently recommended by the Institution of Engineers, Australia (1987) for estimating design floods from observed streamflow data. In this procedure, a log Pearson III (LPIII) distribution is fitted to an annual series of recorded flood peaks by the method of moments, and the confidence limits for the estimated floods are calculated. The procedure includes the following steps:

- Plotting positions of the observed floods are first calculated using Equation (4-5). The observed floods are then plotted against the corresponding plotting positions, preferably on a logarithmic normal probability graph paper.
- Statistics of the annual series, including the mean ( $M$ ), standard deviation ( $S_d$ ), and coefficient of skewness ( $g$ ) of logarithms (to the base 10) of the flood peaks, are next computed.
- Data are then checked for low or high outliers. These are the values at the low or high end of the observed range of floods that depart significantly from the trend of the remaining data. If there are outliers, they should be deleted and the flood statistics  $M$ ,  $S_d$  and  $g$  recomputed using the remaining data.
- Design floods for a range of ARIs are next estimated by the equation:  $\log Q_Y = M + K_Y S_d$ , where  $Q_Y$  is the design flood peak having an ARI of  $Y$ , and  $K_Y$  is the frequency factor for use with the LPIII distribution. Values of  $K_Y$  are tabulated as a function of  $g$  (Institution of Engineers, Australia, 1987, Table 10.2).
- The confidence limits for the estimated floods are then estimated by the following relationship:  $\log(CL_{5,95}(Q_Y)) = \log Q_Y \pm 1.645 \frac{\delta S_d}{\sqrt{N^*}}$ , where  $CL_{5,95}$  are the 5% and 95% confidence limits,  $N^*$  is the record length (in years), and  $\delta$  is a parameter for determining the standard error of the Pearson III distribution (Institution of Engineers, Australia, 1987, Table 10.4). The positive sign applies to the 5% confidence limit, and the negative sign to the 95% limit.
- The fitted distribution is finally plotted on the same graph with the observed data.

### 6.2.2 Application to the La Trobe River catchment at Noojee

The determination of the flood frequency curve for the La Trobe River catchment by direct flood frequency analysis involved three steps. These are the extraction of the annual flood series, the checking of the extracted series for homogeneity and independence, and the application of the CRCCHFFA Spreadsheet to the extracted series.

The annual flood series was extracted from the HYDSYS database using the HYPEAKS program (HYDSYS, 1994). A summary of the extracted peak annual floods from 1961 to 1995 and the corresponding dates of flooding are presented in Table 6-1.

Table 6-1: Annual flood series - La Trobe River catchment at Noojee

Date	Peak annual flow (m <sup>3</sup> /s)	Date	Peak annual flow (m <sup>3</sup> /s)	Date	Peak annual flow (m <sup>3</sup> /s)
03/02/61	13.06	06/02/73	18.09	08/08/85	13.69
29/09/62	16.56	01/05/74	20.43	17/12/86	12.61
29/01/63	24.34	12/08/75	16.88	29/07/87	17.22
17/07/64	15.27	08/08/76	21.44	18/09/88	18.00
25/11/65	12.71	08/04/77	25.63	01/11/89	22.93
29/07/66	10.68	14/06/78	20.91	12/10/90	29.59
01/09/67	7.29	15/10/79	8.22	17/12/91	19.43
27/12/68	15.01	30/06/80	32.99	23/12/92	26.37
01/06/69	27.50	26/05/81	16.55	16/09/93	63.27
28/04/70	16.96	25/01/82	10.98	11/02/94	14.65
08/11/71	59.95	16/10/83	19.27	23/10/95	19.67
30/08/72	9.94	29/07/84	20.96		

As previously discussed, the verification of data used in a statistical analysis is indispensable for a valid frequency analysis to ensure that the data used is a random sample of independent values from a homogeneous population. The verification of the extracted annual flood series for the study catchment for homogeneity was discussed in Section 4.2.3. In order to test if the extracted floods were independent of one another, the dates of the extracted floods in successive years (see Table 6-1) were checked to make sure that they were separated by considerable intervals of time. Results of the

data verification indicated that the extracted floods satisfied the two requirements of homogeneity and independence.

In order to provide an understanding of the flood regime in the study catchment and flow characteristics that were used to estimate future flows for the design site, the statistical properties of the extracted flood series were computed. These were the mean, standard deviation, coefficient of variation, coefficient of skewness, maximum and minimum of the observed floods. Results are presented in Table 6-2. A seasonal distribution of the annual floods is provided in Figure 6-1.

Table 6-2: Statistical properties of the annual flood series - La Trobe River catchment

Flow characteristics	absolute value	log domain ( $\log_{10}$ )
Record length (years)	35	
Mean ( $m^3/s$ )	20.5	1.26
Standard deviation ( $m^3/s$ )	11.9	0.10
Coefficient of variation	0.58	0.08
Skewness	2.49	0.66
Maximum ( $m^3/s$ )	63.3	1.80
Minimum ( $m^3/s$ )	7.3	0.86

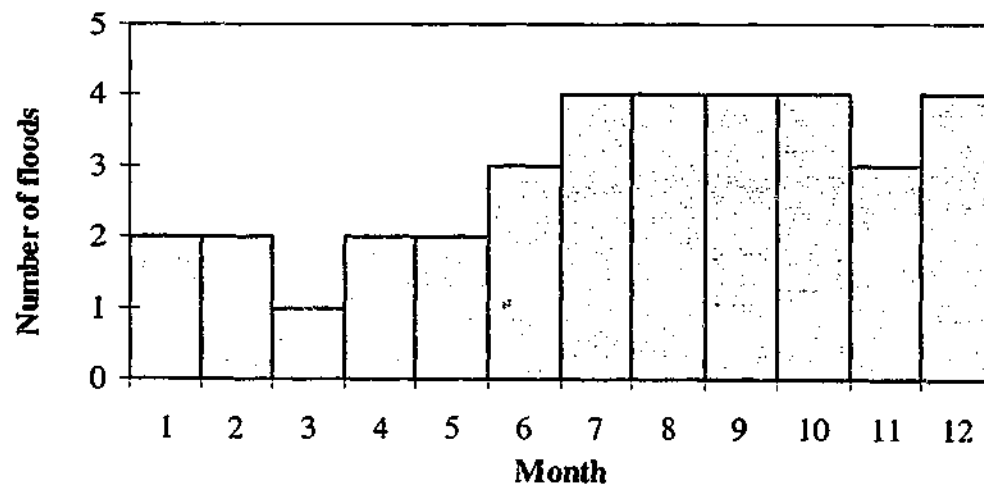


Figure 6-1: Seasonal distribution of annual floods - La Trobe River catchment

To determine the flood frequency curve, the annual flood series was then input to the CRCCHFFA Spreadsheet. Results of this analysis are presented in Table 6-3 and Figure 6-2. In this figure, for comparison, the partial flood series is also plotted using

the procedure described in Section 5.4. The partial flood series, which consists of all flood peaks above a base value of  $14\text{m}^3/\text{s}$ , was provided by Thiess Environmental Services (Dworakovski, Personal communication, 1999).

Table 6-3: Flood estimates by direct flood frequency analysis (LPIII distribution)

ARI (years)	Peakflow ( $\text{m}^3/\text{s}$ )	Confidence limits	
		95%	5%
1	11	9	12
2	17	15	20
5	26	22	31
10	34	27	43
20	42	31	57
50	55	36	84
100	66	39	113

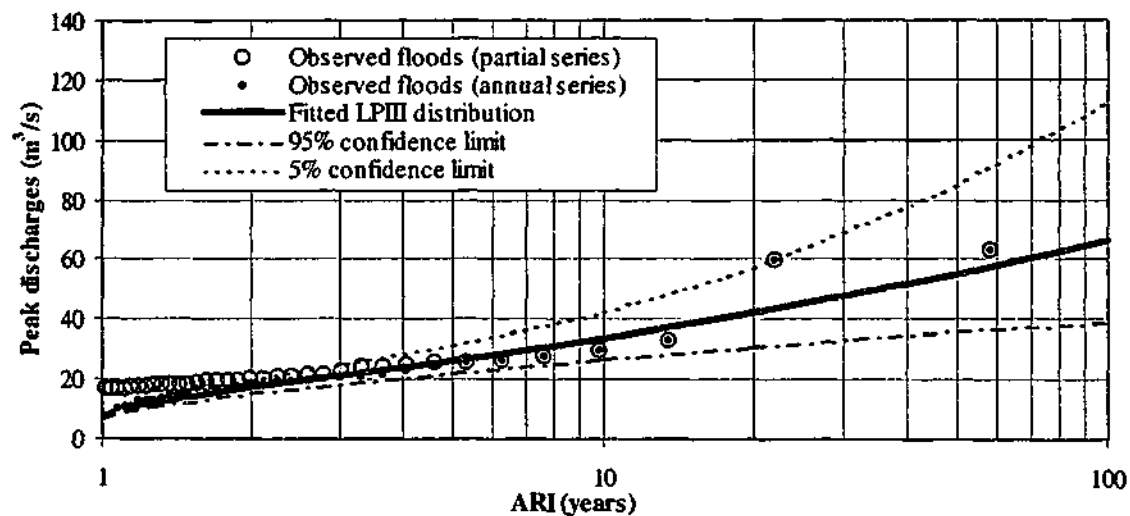


Figure 6-2: Observed peak discharges and the fitted LPIII distribution - La Trobe River catchment at Noojee

### 6.2.3 Discussion

In order to understand the flood regime of the La Trobe River catchment, the timing of floods and the duration of storm events causing major floods are important

considerations. It is evident from Table 6-1 and Figure 6-1 that the recorded annual maximum floods at the given site occur more often from winter to early summer (December) than in the other months of the year. These are the months when the rainfall loss on the catchment is generally low due to the relatively high moisture in the catchment soil. In investigating the concurrent rainfall record at this site, it was found that the duration of the storms (defined in Section 4.3) responsible for these peak floods ranged from a minimum of 26 hours to a maximum of 53 hours with an average of 41 hours. That is, the major floods observed at this catchment were the result of storms with duration of at least one day.

The statistical properties of the observed floods are also useful to provide an overall understanding of the flood flow at the design site. It can be seen from Table 6-2 that the length of flood record at this site is fairly short (35 years). In this record, the observed annual peak discharges vary from a minimum of  $7\text{m}^3/\text{s}$  to a maximum of  $63\text{m}^3/\text{s}$ . The mean and standard deviation of the observed annual peak flows are approximately  $21\text{m}^3/\text{s}$  and  $12\text{m}^3/\text{s}$ , respectively. These statistics indicate that the observed floods are moderately variable. In addition, the coefficient of skewness of the peak flows is positive and quite high (2.5), implying that there are fewer flood peaks above the mean than below the mean, but these high peaks cover a wider range. All these factors would certainly result in difficulties in estimating design floods for the specified site, and in inevitable uncertainty, both in the determination of the true population from which the observed flood data were drawn, and in the resulting flood estimates.

In examining the LPIII distribution fitted to the observed floods, it can be seen from Figure 6-2 that there are no low values of the annual flood series that would have an undue effect on the fitting of the theoretical distribution to the observed flood data. It is also clear that the adopted distribution gives a better fit to the intermediate floods (with return periods up to 15 years) than to the big floods. The flood frequency curve for ARIs greater than 20 years is not very well defined due to the shortness of record and the fact that there were only two big floods on record with return periods exceeding this value. Nevertheless, the computed confidence limits, which represent the probable range of a random sample drawn from the flood population, enclose all the observed flow data except for the second largest flood.

In examining the design floods estimated by the LPIII distribution shown in Table 6-3, it can be seen that the confidence intervals for rare floods are much wider than those of the more frequent floods. For example, the design peak discharge of 100-year ARI is  $66\text{m}^3/\text{s}$ , and the corresponding 90% confidence interval is from  $39\text{m}^3/\text{s}$  to  $113\text{m}^3/\text{s}$ . The ratios of the 95% and 5% flood confidence limits to the 100-year ARI flood estimate are therefore 0.59 and 1.71. By contrast, the 2-year ARI design flood peak is  $17\text{m}^3/\text{s}$  and the corresponding 90% confidence interval is from  $15\text{m}^3/\text{s}$  to  $20\text{m}^3/\text{s}$ . Thus, the ratios of the lower and upper confidence limits to the 2-year ARI design flood are 0.88 and 1.18, respectively. The wide confidence intervals of the rarer floods are the result of both the shortness of record and the variability of the observed floods. Therefore, it may be concluded that there is considerable uncertainty associated with design flood estimates by direct flood frequency analysis for ARIs of 20 years or more, which are of major interest in design.

### 6.3 ESTIMATION OF DESIGN FLOODS BY THE DESIGN EVENT APPROACH

In the Design Event Approach currently applied in Australia, design floods are estimated from *storm bursts*, which are periods of heavy rains during storm events (see Section 4.5.5). In order to estimate design floods by this approach, it is necessary to specify the design rainfall, loss and runoff routing models. However, to provide a fair comparison of the performance of the Joint Probability Model and the Design Event Approach, differences in these design components need to be kept to a minimum. Hence the Design Event Approach employs the same loss model, runoff routing model and the same deterministic inputs as those used in the proposed Joint Probability Model. The parameters of the loss and runoff routing models and other fixed design inputs have been determined and reported in Chapter 4. Nevertheless, the Design Event Approach adopts a different design rainfall model because it uses representative values of rainfall duration and temporal patterns (instead of probability distributions). In addition, the initial loss used also needs to be represented by a fixed design value rather than a probability distribution.

This section describes the estimation of the design rainfall, initial loss, and the resulting flood estimates for the La Trobe River catchment using the Design Event Approach. A discussion of the flood estimates is also provided.

### 6.3.1 Estimation of the design rainfall

The estimation of the design rainfall included the specification of sets of design events for specified ARIs and durations. For each design event, the average rainfall intensity and the corresponding temporal pattern were determined. For design flood estimation by the Design Event Approach, the ARI of the flood output is assumed to equal that of the rainfall input. As the design floods of interest in this study were in the ARI range of 1 to 100 years, the ARIs of the design rainfall input were adopted to be of 1, 2, 5, 10, 20, 50, and 100 years.

To determine the appropriate range of durations of storm bursts to be used in the design, it was necessary to obtain a preliminary estimate of the critical storm duration of the study catchment. This duration can be roughly determined as the time of concentration ( $t_c$ ) of the catchment, which is defined as the travel time from the most remote point on the catchment to the catchment outlet.  $t_c$  can be estimated from the catchment area  $A$  ( $\text{km}^2$ ) by the formula below (Institution of Engineers, Australia, 1987):

$$t_c = 0.76 A^{0.38} \quad (6-1)$$

For the La Trobe River catchment,  $t_c=6.6$  hours. Hence, the burst durations used were 2, 3, 6, 9, 12, 18, and 24 hours.

The average design rainfall intensities for the specified ARIs and rainfall burst durations at the design location were determined using the procedure presented in Chapter 2 (Institution of Engineers, Australia, 1987). In this procedure, a log Pearson III distribution is used to characterise design rainfalls at any location in Australia. For a particular location, this distribution is estimated from the six basic rainfall intensities for a lognormal distribution and one skewness value (to adjust the lognormal to the log Pearson III distribution) determined from the latitude and longitude of the design location. For the La Trobe River catchment, the representative location for estimating

catchment rainfalls was taken as the location of the recording rain gauge at station 85237 (37.88° latitude, 146° longitude). The basic rainfall intensities and skewness value for this location were read from the maps published by the Institution of Engineers, Australia (1987, Volume 2). The skewness of rainfall determined for the design site was 0.35. The estimated average point design rainfall intensities determined for the specified return periods and rainfall durations are presented in Table 6-4. It is important to emphasise at this point that the design rainfall intensities presented in this table represent the average intensities of intense bursts of rain, rather than representing rainfall intensities of the storm events defined in Section 4.3. To obtain the areal average rainfall intensities over the study catchment, the design rainfall intensities shown in Table 6-4 were then multiplied by the interim areal reduction factors (Siriwardena and Weinmann, 1996, Equation 7-17 and Figure C-5) determined for the specified durations, return periods and catchment area (290km<sup>2</sup>).

Table 6-4: IFD estimates at station 85237 (37.88° latitude, 146° longitude) (unit: mm/h)

Duration (hours)	Average recurrence intervals (years)						
	1	2	5	10	20	50	100
2	10.2	13.3	17.3	19.8	23.3	28.1	32.1
3	8.1	10.6	13.6	15.6	18.3	22.1	25.1
6	5.5	7.1	9.1	10.4	12.1	14.5	16.5
9	4.4	5.7	7.2	8.2	9.5	11.4	12.9
12	3.7	4.8	6.1	6.9	8.0	9.6	10.9
18	2.9	3.7	4.7	5.3	6.1	7.3	8.3
24	2.4	3.0	3.8	4.3	5.0	6.0	6.8

In order to determine the temporal patterns of the design events, it is noted that in Australia, design rainfall patterns are developed for eight zones based on climatology and the expected differences in temporal patterns. These design patterns are published by the Institution of Engineers, Australia (1987, Volume 2). For the La Trobe River catchment at Noojee, the temporal patterns of the design rainfall events were selected from the published temporal patterns of Zone 1 for the specified storm durations and ARIs.

### 6.3.2 Estimation of initial loss

Values of the design initial loss for use with the Design Event Approach are published by the Institution of Engineers, Australia (1987, Chapter 6). However, there are three limitations in these design loss values. Firstly, there is a lack of design loss data for a large portion of Australia, especially for Tasmania and areas in the north and west of the Great Dividing Range. Secondly, they were derived from the analysis of large observed flood events that are biased towards wet catchment conditions. Therefore the design initial losses tend to be underestimated and design floods overestimated. Finally, the design initial loss values were derived for complete storms rather than for storm bursts used to determine design temporal patterns and thus tend to be overestimated. For these reasons, these design losses were not used in this analysis.

In the present application, fixed design values of the initial loss of the selected design burst events were determined using a formula developed by Hill et al. (1996a). In this formula, the initial loss ( $IL_b$ ) of a design storm burst is related to the mean catchment storm initial loss ( $IL$ ), the mean annual rainfall ( $MAR$ ), and the event duration ( $D$ ) by the following relationship:

$$IL_b = IL \left( 1 - \frac{1}{1 + 142 \frac{\sqrt{D}}{MAR}} \right) \quad (6-2)$$

where  $IL_b$ ,  $IL$ , and  $MAR$  are in millimetres (mm) and  $D$  in hours.

The design loss estimates for the La Trobe catchment [ $IL=18\text{mm}$  (from Hill et al., 1996a), and  $MAR=1360\text{mm}$ ] are tabulated in Table 6-5. It is clear from this table that the design initial loss of design storm bursts increases with burst duration.

Table 6-5: Design initial loss - La Trobe River catchment

	Rainfall duration (h)						
	2	3	6	9	12	18	24
Initial loss (mm)	2.3	2.8	3.7	4.3	4.8	5.5	6.1

### 6.3.3 Estimation of design floods

In order to estimate design floods for the La Trobe River catchment using the Design Event Approach, the procedure described in Section 2.2.1 was adopted. In this procedure, design floods resulting from storm events of varying durations and return periods were first estimated. For each return period, the critical rainfall duration was next determined using the method described in Section 2.2.1. The design flood for the specified return period was finally taken as the design flood caused by the critical storm duration.

Results of the design flood estimation for the study catchment are summarised in Table 6-6 and illustrated in Figure 6-3. In Table 6-6, flood estimates for various storm durations and ARIs are shown, whereas the design peak discharges and the corresponding critical storm durations for the study catchment are denoted as bold values. In Figure 6-3, the determination of the critical storm duration for an ARI of 20 years is illustrated. It can be seen from this figure that the highest design flood of about  $150\text{m}^3/\text{s}$  is produced by a storm burst event of 12-hour duration. Therefore this duration is adopted as the critical duration for events of 20-year ARI for this catchment.

Table 6-6: Design flood estimates by the Design Event Approach (unit:  $\text{m}^3/\text{s}$ )

Storm duration (hours)	ARI (years)						
	1	2	5	10	20	50	100
2	0.8	2.6	15.4	27.8	47.7	81.3	110.8
3	2.3	7.6	27.1	41.3	67.9	107.9	143.2
6	2.8	14.7	46.2	70.5	106.9	149.2	195.1
9	22.9	46.7	66.9	95.8	138.5	188.0	231.4
<b>12</b>	<b>24.7</b>	<b>52.5</b>	<b>85.3</b>	<b>112.9</b>	<b>152.7</b>	<b>211.7</b>	<b>270.9</b>
18	19.6	41.4	82.2	101.1	149.2	193.4	250.5
24	11.5	37.9	69.6	94.0	121.9	160.5	204.7

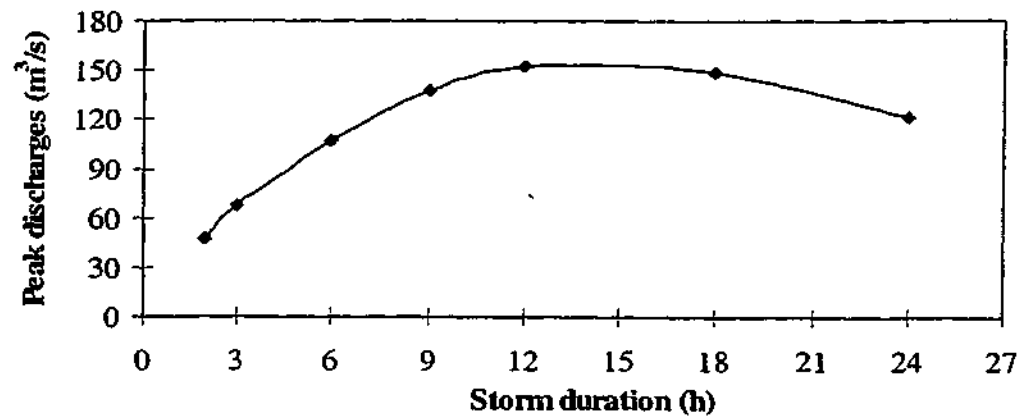


Figure 6-3: Plot of design flood peak against storm burst duration (ARI=20 years)

#### 6.3.4 Discussion

Results of the estimation of design floods for the La Trobe River catchment using the Design Event Approach indicates that for all return periods, the critical rainfall burst duration for this catchment is 12 hours. This critical duration is only a third of the average duration of 41 hours of the observed storm events (determined using the storm definition described in Section 4.3) causing major floods in the study catchment (see Section 6.2.3). One of the reasons that causes the discrepancy in the critical duration is the difference in the definitions of rainfall bursts used in the Design Event Approach and storms defined in this study. That is, a rainfall burst (a period of heavy rainfall) is embedded in a storm, with periods of some rain prior to and after the burst.

In estimating the design flood, it is clear that there are uncertainties in selecting fixed design values of rainfall and loss characteristics, as well as in determining the parameters of the adopted runoff routing model. As a result, the magnitude of the design flood is also uncertain.

#### 6.4 COMPARISON WITH THE JOINT PROBABILITY MODEL

The determination of the best design flood estimates for a catchment provides a basis

against which various flood estimation methods can be compared. For the La Trobe River catchment, these best estimates can be obtained from empirical frequency analysis of the partial flood series for relatively frequent floods, and from direct flood frequency analysis of the annual series for extrapolation to higher ARIs. An ARI of 5 years was adopted as the limit for design flood estimates by these two series, as this is the value below which the observed annual flood series for the La Trobe River catchment differs significantly from the partial series (see Figure 6-2).

It is also noted that design flood estimates by direct flood frequency analysis are only considered to be the best available estimates for a given catchment for a particular range of ARI. The lower limit of this ARI range can be taken as that of the smallest design flood of interest (estimated by frequency analysis of partial flood series). The upper limit of this range ( $ARI_U$ ) can be computed using the following empirical formula (Institution of Engineers, Australia, 1987):

$$ARI_U = FN^{0.5} \exp(0.02N^*) \quad (6-3)$$

where  $N^*$  is the record length in years, and  $F$  is a factor depending on the standard deviation and the coefficient of skewness of the logarithms of the flood values (see Table 12.1, Institution of Engineers, Australia, 1987).

For the La Trobe catchment, the computed value of  $ARI_U$  was estimated to be 15.4 years. This estimate is similar to the conclusion that design floods of up to 20-year ARI obtained by direct flood frequency analysis were the best estimates of floods for the study catchment (see Section 6.2.3). However, with the lack of data for better estimates of more severe design floods, the design flood estimates of 50-year and 100-year ARI by direct flood frequency analysis are still shown for comparison, but given less weight in the performance assessment.

A summary of design floods for the La Trobe River catchment, estimated by flood frequency analysis, the Design Event Approach and the proposed Joint Probability Model is tabulated in Table 6-7. It is noted from this table that design floods of 1-year and 2-year ARI (estimated by flood frequency analysis) are obtained from an empirical analysis of the observed partial flood series using the procedure described in Section 5.4. However, design floods of 5-year ARI or greater obtained from the LPIII

distribution fitted to the annual flood series (see Table 6-3 and Figure 6-2). The bold values indicate the best available design flood estimates for the catchment. In Table 6-7, the ratios of flood estimates obtained from a particular method to the best estimates obtained from flood frequency analysis are also presented. The flood estimates for various ARIs listed for the Joint Probability Model were obtained from Chapter 5. A plot of these estimates against their corresponding return periods is illustrated in Figure 6-4.

Table 6-7: Summary of design flood estimates obtained from different methods

ARI (years)	Flood frequency analysis	Joint Probability Model		Design Event Approach	
	Peak discharges (m <sup>3</sup> /s)	Peak discharges (m <sup>3</sup> /s)	Ratios	Peak discharges (m <sup>3</sup> /s)	Ratios
1	<b>17</b>	17	1.0	25	1.5
2	<b>20</b>	29	1.5	53	2.7
5	<b>26</b>	45	1.7	85	3.3
10	<b>34</b>	62	1.8	113	3.3
20	<b>42</b>	76	1.8	153	3.6
50	<b>55</b>	101	1.8	212	3.8
100	<b>66</b>	127	1.9	271	4.1

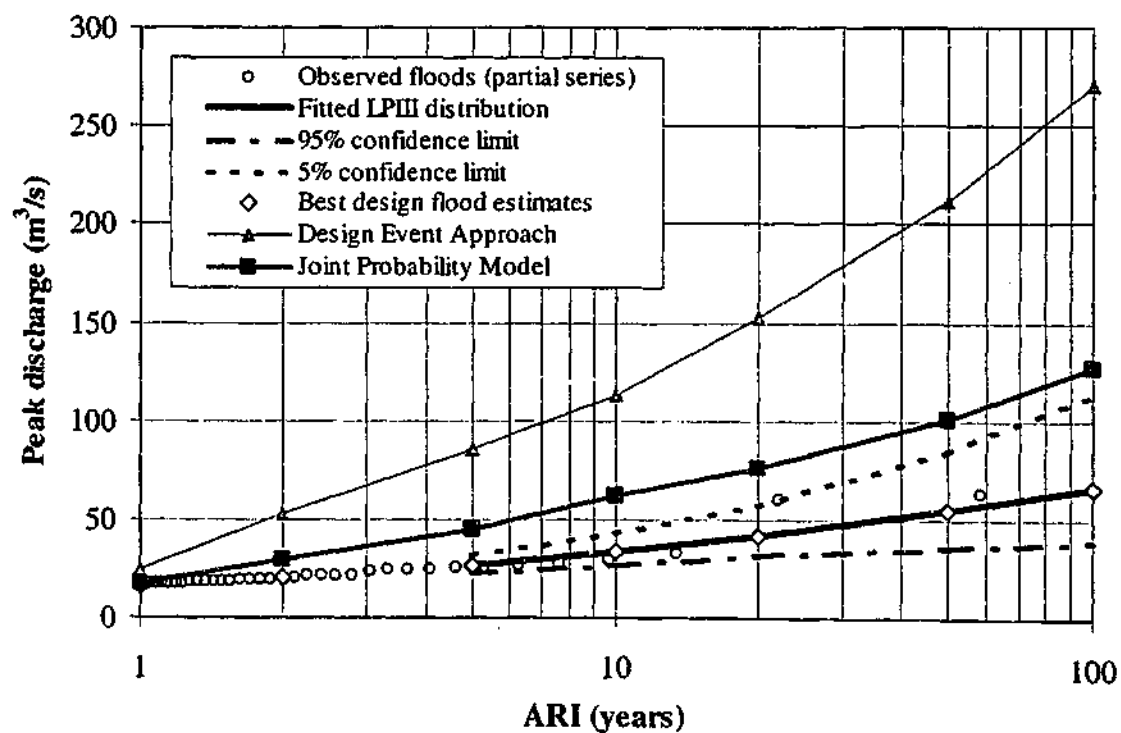


Figure 6-4: Plot of design flood estimates for the La Trobe River catchment

In examining the magnitude of design floods estimated by the three methods, it can be seen from Table 6-7 that, on average, the flood magnitudes estimated by the Design Event Approach are about three times those obtained from flood frequency analysis, except for very frequent floods of 1-year or 2-year ARI. In addition, the ratio of design flood magnitudes predicted by these two methods increases for rarer flood events. By contrast, the flood magnitudes estimated by the proposed Joint Probability Model are at most double those obtained from flood frequency analysis, except for very common floods. The ratios of design floods estimated by the proposed Joint Probability Model to those of flood frequency analysis seem to be stable for all return periods, except for ARIs of 1 or 2 years. It is also evident from Figure 6-4 that design flood estimates by the Joint Probability Model are closer to the upper confidence limits established by direct flood frequency analysis, even though the design floods predicted by these two methods are all outside the 90% confidence intervals. Therefore, it can be concluded that, whereas both the Joint Probability Model and the Design Event Approach overestimate the design flood of a given return period, the proposed new model can give better estimates in terms of flood magnitude for the study catchment.

The reduction in the magnitude of the design floods obtained by the Joint Probability Model compared with the Design Event Approach is the result of the differences in inputs and assumptions used by these two approaches in design. These differences can be found in the definitions of storm events, or in the representation of design inputs and their correlations.

- With respect to the storm definitions used by these methods, as already discussed in Section 4.3 and Section 4.5, storm events used in the proposed Joint Probability Model generally have longer durations than the bursts of rain typically used in the Design Event Approach. In addition, the average rainfall intensity of a storm event is lower than that for a storm burst of the same duration. For example, at station 85237, the average intensity estimate of a storm of 24-hour duration and 10-year ARI is 2.62mm/h (see Table 5-2), whereas the average intensity of a burst of the same duration and ARI is 4.3mm/h (see Table 6-4). The discrepancy in duration and intensity between storm events and storm bursts is clearly due to different sampling. As a storm burst used in the Design Event Approach is defined as the most intense part of a storm event, design floods estimated by the approach are very likely to be higher than those obtained from the Joint Probability Model.

- With regard to the representation of design inputs, whereas the design rainfall depth, duration, temporal pattern, and initial loss are considered as random variables in the proposed Joint Probability Model, only the rainfall depth is regarded as a random variable in the Design Event Approach. All these differences therefore lead to the discrepancy in design flood estimates obtained by the two methods.

Even though the proposed Joint Probability Model can give more accurate estimates of design flood peaks for the La Trobe River catchment, when compared with the best flood estimates obtained by flood frequency analysis, these estimates are still overestimated. This overestimation might be the result of many factors such as the inappropriate assumptions used in the modelling process or errors in the design inputs.

- With regard to the assumptions involved in modelling, it was assumed that the rainfall-runoff response of the study catchment was non-linear and that this non-linearity was represented by a factor of 0.8. Nevertheless, this factor seems to be low for the study catchment, as discussed in Section 4.8. If a larger value of  $m$  with a corresponding lower value of  $k$  had been adopted, for discharges greater than those of the observed floods used in model calibration, the storage would have been greater, and the design discharge would have been less. Furthermore, the study catchment was represented by a lumped model with only one storage. Neglect of distributed storage effects on the catchment could have introduced errors, particularly for floods much smaller or larger than those used in calibrating the lumped model.
- Another implicit assumption involved in application of the proposed Joint Probability Model is the neglect of the seasonal effect of the rainfall and loss. This implies that a summer storm can be randomly combined with a winter loss and vice versa. For such unlikely extreme combinations of design rainfall and loss, design flood peaks can either be overestimated or underestimated.
- Finally, the adopted runoff routing model was calibrated and tested using only five observed rainfall-runoff events. The relatively small number of events used in calibration and testing indicated that they may not be representative of the hydrometeorological conditions at the site. As a result, application of the model for estimating design floods outside the flood range for calibration and testing inevitably is subject to errors and uncertainties.

- In terms of errors in design inputs, it is clear that these errors may occur in both the stochastic inputs (namely, the generated rainfall intensity, duration, temporal pattern, and initial loss), and the deterministic inputs (namely, the continuing loss rate, baseflow, and the runoff routing model parameters). Among these inputs, the generated storm duration is less likely to be a contributing factor to the overestimation of design floods because the statistical properties of the storm duration were reproduced well in the generated storms (see Section 5.2.3). By contrast, there were uncertainties in the design rainfall intensity estimates (especially for events with duration greater than 48 hours and return periods exceeding 20 years) due to the extrapolation and adjustment of the IFD curves, as discussed in Section 4.5. The estimated rainfall for the catchment might also have gross errors, as the use of rainfall data at only one gauge may not adequately represent the catchment average rainfall and the spatial variation of rainfall on the catchment scale. In addition, the adopted multiplicative cascade model clearly underestimates the lag one auto-correlation of the observed temporal patterns (see Section 5.2.5). Likewise, the probability distribution used to characterise the rainfall initial loss for the study catchment does not reproduce very well the coefficient of skewness of the observed losses (see Section 5.2.6). The adopted design baseflow ( $0.75\text{m}^3/\text{s}$ ) also seems to be low compared with the estimated baseflow of the five observed storms used (see Table 4-19). Due to the fact that the generated floods were overestimated, it is also likely that the design rainfall continuing loss and/or the runoff routing parameter  $k$  for the catchment were underestimated. The effects of the uncertainties in these inputs on design flood estimates were therefore investigated, and are presented in the next section.

## 6.5 SENSITIVITY ANALYSES

In order to gain an insight into the performance of the proposed Joint Probability Model, six sensitivity analyses were carried out in this study:

- The first and second analyses aimed to determine how design flood estimates would change if there were changes in estimates of the design rainfall intensity or in the

probability distribution characterising the rainfall initial loss for the La Trobe River catchment.

- The third analysis aimed to determine the effects on design flood estimates of neglecting the dependence of rainfall temporal patterns on season, storm duration and storm depth. Results of this analysis would determine if the subdivision of temporal patterns into ten different groups was practically important.
- The fourth analysis investigated the influence of the resolution used to define rainfall temporal patterns on the resulting floods. Results of this investigation would be necessary in determining the minimum number of parameters to represent adequately the variability of rainfall intensity during storm duration, and its impact on the design floods.
- The fifth analysis aimed to identify the effects on the design flood estimates of the variation in the fixed design inputs, namely the continuing loss rate (CL), the routing model parameter (k), and the design baseflow. Results of these analyses would determine whether these design inputs could have caused the overestimation of the generated flood frequency curve for the study catchment.
- The sixth analysis aimed to examine the effect on flood estimates of changes in the sample size of the design floods generated in the Monte Carlo experiment. Results of this analysis would shed light on the reliability and stability of simulation results.

In the sensitivity analyses outlined above, the base case floods were those determined using the procedure, input distributions and parameter values described in Section 5.3.2, unless otherwise specified. These analyses are described in detail below.

### 6.5.1 Effects of design rainfall intensity

In order to investigate the effects of uncertainties in estimates of the design rainfall intensity at pluviometer 85237 on the resulting floods, the values of the IFD table established for this site were decreased by 20% and 50%<sup>1</sup> whereas other design inputs were kept the same as for the base case. Design floods for these two cases were

---

<sup>1</sup> It would probably have been better to adopt values of 10% and 20% reduction or increase in the design rainfall intensity, as a 50% error in catchment average rainfall is probably too extreme.

computed using the procedure detailed in Section 5.3.2. The frequency curves of the resulting floods were then determined using the method described in Section 5.4. The design flood peaks estimated for various ARIs were finally compared with those of the base case simulation, as tabulated in Table 6-8.

Table 6-8: Design flood estimates ( $m^3/s$ ) from variation of design rainfall intensities

ARI	Base case		20% decrease		50% decrease	
	Peak discharge	Peak discharge	Peak discharge	% difference	Peak discharge	% difference
1	17	7	-60	3	-85	
2	29	12	-58	5	-82	
5	45	21	-54	10	-78	
10	62	28	-55	14	-78	
20	76	36	-53	18	-76	
50	101	47	-54	24	-76	
100	127	59	-53	32	-75	

It is evident from Table 6-8 that changes in estimates of the design rainfall intensity have a very large impact on the resulting flood estimates. For example, a 20% decrease in the average rainfall intensity results in at least a 50% decrease in the corresponding flood peak for any return period when other design inputs were unchanged. For an extreme example in which the average rainfall intensity is reduced by 50%, the resulting peak discharge for the study catchment can be decreased by up to 85%. This result is not surprising as it has been found that the design rainfall depth is one of the most important factors affecting the design flood magnitude (Beran, 1973; Cadavid et al., 1991; Loukas et al., 1996). In general, the percentage of change in flood magnitude is almost stable for all return periods, with a slightly greater reduction of frequent floods.

### 6.5.2 Effects of initial loss

The sensitivity of design flood estimates to variability in the initial loss for the La Trobe River catchment was investigated by using of a constant initial loss of 27.3mm, which is the average of the observed initial losses for the study catchment. Flood events were generated by Monte Carlo simulation using the constant initial loss, whereas other design inputs were kept unchanged. The generated flood frequency curve was then established. The flood peak estimates for various ARIs, summarised in Table 6-9, were

finally compared with the corresponding base case floods (where the initial loss was represented by a beta distribution with the parameters  $\alpha$  of 1.6 and  $\beta$  of 7.2).

Table 6-9: Design flood estimates ( $m^3/s$ ) from different representations of initial loss

ARI (years)	Base case distribution $\alpha = 1.6, \beta = 7.2$	Constant initial loss (27.3mm)	% difference
1	17	11	-33
2	29	19	-34
5	45	31	-32
10	62	41	-34
20	76	51	-32
50	101	70	-31
100	127	82	-36

When using a constant design initial loss for the La Trobe River catchment, it is evident from Table 6-9 that, for all ARIs, the design flood estimates are approximately 30% smaller than those obtained when a statistical distribution was used to characterise the initial loss. In previous studies, it has also been found that small variations in parameter estimates of the loss model could cause significant errors in the derived flood frequency curves (Beran, 1973; Moughamian et al., 1987; McKinnis and Valdes, 1993). Therefore, it can be concluded that design flood peaks are very sensitive to variations in the probability distribution representing the storm initial loss.

### 6.5.3 Effects of temporal pattern groups

As already discussed in Section 4.6.4.3, the temporal patterns of observed storms used in this study can be classified into 10 groups, depending on three factors: season of storm occurrence, storm duration, and storm depth. In estimating design floods using the proposed Joint Probability Model, the dependence of rainfall temporal patterns on season, storm duration, and storm depth was taken into consideration, as described in Section 5.3. This was taken as the base case (see Section 5.3.2). In the following sensitivity analysis, the effect on design flood peaks of neglecting the dependence of temporal patterns on season, storm duration and depth was examined.

To generate design temporal patterns for this analysis, temporal patterns of the observed storms of the 19 pluviometers were first pooled together, regardless of season, storm duration, and storm depth. A beta distribution common to 19 sites was next used to represent the disaggregation parameters of the multiplicative cascade model adopted to generate storm mass curves (see Section 4.6.5). The two parameters ( $\alpha$ ,  $\beta$ ) of this distribution were computed from the observed patterns using the procedure described in Section 4.6.5. Design temporal patterns were finally generated from this common beta distribution using the method detailed in Section 5.2.5.1.

In order to estimate design floods resulting from generated storm events, the procedure detailed in Section 5.3.2 was again adopted. However, in step (d), the design temporal pattern of a synthetic event was taken at random from the sample of the patterns generated from the common beta distribution determined above. Other input components were kept the same as for the base case. The flood frequency curve of the computed flood peaks was finally estimated and compared with the base case curve.

Table 6-10: Design flood estimates ( $m^3/s$ ) from different numbers of temporal pattern groups

ARI	Base case (10 groups)	Dependence neglected (1 group)	
	Peak discharge	Peak discharge	% difference
1	17	18	3
2	29	29	0
5	45	46	3
10	62	62	0
20	76	78	2
50	101	100	-1
100	127	119	-6

Design floods computed when the dependence of temporal patterns on season, storm duration, and depth was considered (base case) and neglected are presented in Table 6-10, along with percentage differences between the estimates for these two cases. It is clear that, when the dependence of temporal patterns on season, storm duration and depth is neglected, design floods may increase or decrease, depending on the ARI of the design flood. Nevertheless, for all ARIs, estimates of the peak discharge differ from the base case floods by at most 6% in absolute values, but more typically by 0 to 3%. In

other words, for the La Trobe River catchment, the consideration of the dependence of the temporal pattern on season, storm duration or depth seems to have only minor effects on design flood estimates. This conclusion is clearly limited to the specific study catchment and needs to be verified by applying the proposed model to a wider range of catchment areas. It should also be borne in mind that, in the present study, design inputs other than the temporal pattern do not vary seasonally.

#### **6.5.4 Effects of number of time increments used to describe temporal patterns**

In this study, a statistical model has been developed for temporal patterns represented by dimensionless hyetographs defined at 8 equal time increments of storm duration. Whereas 8 increments may be adequate to characterise the variability of rainfall intensity during storm duration for short duration storms, they may be inadequate for longer events causing floods in large catchments. Therefore, a sensitivity analysis was attempted to examine the effects on design floods of changes in the number of time increments used to describe the temporal pattern.

The objective above was achieved by doubling the number of intervals used to describe rainfall temporal patterns (observed and generated) from 8 to 16. For simplicity, the base case simulation (for 8 intervals) was chosen as the case in which the dependence of temporal patterns on season, storm duration, and storm depth was not taken into account (see Section 6.5.3). The procedure below was then adopted:

- A beta distribution was first used to represent the disaggregation parameters of the adopted model for generating temporal patterns. Parameters of this beta distribution were computed from the mass curves of the temporal patterns observed at 19 pluviometers using the method outlined in Section 4.6.5.
- Synthetic temporal patterns were next generated from the beta distribution using the procedure described in Section 5.2.5.1.
- Design floods were then computed using these generated temporal patterns whereas other design inputs were kept unchanged.

- The peak flood estimates were finally compared with those of the base case in which the temporal pattern was defined at 8 equal increments of storm duration.

Preliminary results of this sensitivity analysis indicated moderate sensitivity of design floods to the number of time intervals adopted, and that small floods are more sensitive to variations in the number of time increments used to describe temporal patterns than big floods. However, quite substantial work would be required to obtain conclusive results. Whereas these results are desirable, the extra work is considered to be outside the scope of this thesis due to the limited research time.

### 6.5.5 Effects of fixed design inputs

As mentioned at the beginning of Section 6.5, the fixed design inputs to be used in the current sensitivity analysis are the continuing loss rate, the runoff routing parameter  $k$ , and the design baseflow.

#### Continuing loss rate

In order to investigate the effects on flood estimates of changes in values of the continuing loss rate (CL), design floods were computed for loss rate values increased by 20% (corresponding to 5.6mm/h) and 50% (corresponding to 7mm/h) from the base case value (4.7mm/h) used in simulation. Other design inputs were kept the same as for the base case. The resulting flood frequency curves were then estimated and compared with those obtained from the base case. It is noted that the continuing loss rate used in the base case was increased for the sensitivity analysis, because the simulated flood frequency curve was overestimated, suggesting that the base case continuing loss might be low. In addition, a 50% error is quite common due to the high uncertainty in continuing loss values.

Results of this sensitivity analysis are presented in Table 6-11. In this table, design floods estimated for the three values of continuing loss rates are shown, along with the differences relative to the base case floods. It is clear from Table 6-11 that for a 20% increase in the design continuing loss rate, the resulting peak discharges estimated for the La Trobe River catchment decrease from 1% to 8%. Nevertheless, when there is a

50% increase in the continuing loss, the resulting floods reduce only by 6% to 12% in the peak magnitude. As the design loss rate increases, small floods tend to be more affected than large floods, other inputs being kept unchanged. In general, it can be concluded that changes in the design continuing loss rate have moderate effects on the resulting flood estimates, especially at high return periods.

Table 6-11: Design flood estimates ( $m^3/s$ ) from different values of continuing loss rate

ARI	Base case	20% increase		50% increase	
	(CL = 4.7mm/h)	Peak discharge	% difference	Peak discharge	% difference
1	17	16	-5	15	-9
2	29	27	-7	26	-12
5	45	42	-6	41	-10
10	62	57	-8	55	-11
20	76	73	-4	71	-7
50	101	100	-1	95	-6
100	127	124	-3	118	-7

#### Routing parameter k

Similarly, in order to investigate the effects on design flood estimates of changes in the runoff routing model parameter k, the value of k was varied while other fixed design inputs were kept unchanged. In choosing the values of k for the sensitivity analysis, as the design floods were overestimated (see Table 6-7), it was decided to increase k in order to reduce the flood estimates. Hence, two values of k, increased by 20% (corresponding to  $k=64$ ) and 50% ( $k=80$ ) respectively, were used. The estimated floods were then compared with the base case simulation (with  $k=53$ ). At this point, it is worth noting that the adopted variation of k is typical of errors in estimated k-values for gauged and ungauged catchments.

The design flood estimates resulting from three different values of the routing model parameter k are shown in Table 6-12, along with the percentage differences between these flood estimates and the base case floods. It can be seen from this table that, for all ARIs, as k increases, the peak flood magnitude decreases. For example, a 20% increase in the runoff routing model parameter k brings about a decrease from 15% to 20% in the design peak discharge. When k is increased by 50%, the resulting flood peak is reduced by at least 32%. These results indicate that design flood peaks estimated for the La

Trobe River catchment are sensitive to uncertainty in the parameter  $k$  of the runoff routing model.

Table 6-12: Design flood estimates ( $m^3/s$ ) from varying values of the runoff routing model parameter  $k$

ARI	Base case ( $k = 53$ )	20% increase ( $k = 64$ )		50% increase ( $k = 80$ )	
	Peak discharge	Peak discharge	% difference	Peak discharge	% difference
1	17	14	-19	11	-36
2	29	23	-20	18	-37
5	45	38	-16	30	-33
10	62	51	-18	41	-35
20	76	65	-15	52	-32
50	101	86	-15	69	-32
100	127	104	-18	83	-34

### Design baseflow

It has been shown in Section 5.3.2 that in estimating design floods for the La Trobe River catchment, the adopted design baseflow was  $0.75m^3/s$  (base case). However, this value seems to be low compared with the median baseflow of  $5.7m^3/s$  of the observed flood events for the catchment (see Table 4-19). Therefore, the effects on design flood estimates for the study catchment of using the specified median baseflow were examined.

To estimate design floods, it is clear that in this study, a constant value of base flow has been added to all the generated flood peaks. Therefore, design flood estimates corresponding to the new median baseflow were determined by subtracting the old design baseflow of  $0.75m^3/s$  from the base case floods (of all ARIs) and adding the new design baseflow of  $5.7m^3/s$ . The resulting design floods are listed in Table 6-13, along with the base case floods and the percentages of difference between these flood estimates.

It is clear from Table 6-13 that, as the design baseflow increases from  $0.75m^3/s$  to  $5.7m^3/s$ , the corresponding peak discharge increases from  $17m^3/s$  to  $22m^3/s$  for floods of 1-year ARI and from  $127m^3/s$  to  $132m^3/s$  for floods of 100-year ARI. The percentage of change decreases from 29% for the 1-year ARI flood to 4% for the 100-year ARI

flood. Therefore, it can be concluded that uncertainty in the value of the design baseflow mainly affects small floods.

Table 6-13: Design flood estimates ( $m^3/s$ ) from varying values of the design baseflow

ARI (years)	Design baseflow		% difference
	( $0.75m^3/s$ , base case)	( $5.7m^3/s$ )	
1	17	22	29
2	29	34	17
5	45	50	11
10	62	67	8
20	76	81	7
50	101	106	5
100	127	132	4

### 6.5.6 Effects of sample size

As discussed in Section 5.2.2, the sample size of the generated outcomes in a Monte Carlo experiment plays an important role in determining the reliability of these outcomes. In order to examine the effect on design flood peaks of changes in the number of generated data, in this sensitivity analysis a sample of 30000 flood events was generated for the La Trobe River catchment. All other design inputs were kept unchanged (including the seed for random number generation). The estimated peak floods of various return periods were then compared with those of the base case simulation where 15000 data were generated.

A summary of the estimated flood peaks for the sample sizes of 30000 and 15000, along with the percentage difference in these estimates, is given in Table 6-14. It is clear from Table 6-14 that, as the size of the flood sample changes from 15000 to 30000, the estimated peak discharge of very frequent floods of 1 or 2-year ARI remains unchanged. The design flood estimates for return periods of 5 up to 50 years only change at most by 3%. By contrast, the magnitude of floods of 100-year ARI varies quite considerably, by an amount of 12%. It can therefore be concluded that, up to the ARI of 50 years, a stable estimate of the flood frequency curve for the La Trobe River catchment can be derived using a random sample of 15000 data (spanning 2000 years).

Table 6-14: Design flood estimates from varying sample sizes

ARI	Sample size of 15000	Sample size of 30000	
	Peak discharge (m <sup>3</sup> /s)	Peak discharge (m <sup>3</sup> /s)	% difference
1	17	17	0
2	29	29	0
5	45	46	2
10	62	63	2
20	76	78	3
50	101	99	-2
100	127	112	-12

The variation in the estimated peak flood magnitude of 100-year ARI in response to changes in sample size is not surprising. This is attributable to the relatively small number of rare events generated by the Monte Carlo experiment. As design floods of this low probability are the result of extreme combinations of flood causing components (such as very high rainfall of long duration and low losses), to obtain better estimates of these rare floods, a number of methods can be used. The first is to further increase the number of the generated flood events. However, this method may only be adequate for estimating design floods of up to 100-year ARI. The second is to apply more efficient generation methods such as variance reduction techniques. As discussed in Section 5.2.2, these techniques aim to reduce the variance of the simulation results by biasing the sampling scheme in the domain of interest (without changing the sample size). Details of these techniques can be found in Thompson et al. (1997), Perlado (1990), and Kottegoda and Rosso (1997). These techniques are more complicated for routine applications and most relevant to the estimation of floods with ARIs greater than 100 years. They were therefore considered to be beyond the objective of this research.

### 6.5.7 Discussion

Results of the sensitivity analyses described in Section 6.5 indicate that changes in different stochastic and deterministic inputs have different impacts on the derived flood frequency curve for the La Trobe River catchment at Noojee. Whereas the design flood estimates are very sensitive to errors in the estimated design rainfall intensity and initial loss, they are moderately influenced by uncertainties in the selected routing parameter  $k$ , and only slightly affected by the modelling of the dependence of temporal patterns on

season, storm duration, or depth. Uncertainties in the adopted continuing loss rate and design baseflow were found to have more impacts on frequent floods than rare floods. By generating 2000 years of data, it was concluded that the resulting design flood estimates were stable, except for the ARI range beyond 50 years.

From the results of the sensitivity analyses, it can be concluded that the estimation and representation of the design rainfall intensity and loss model parameters are crucial in order to obtain reliable design flood estimates. The same conclusion can be inferred from previous studies (for example, Beran, 1973; Moughamian et al., 1987; Cadavid et al., 1991; Raines and Valdes, 1993; Loukas et al., 1996), as it has been found that small variations in parameter estimates of the rainfall and loss models can cause significant errors in the derived flood frequency curve. By contrast, the modelling of the stochastic nature of the rainfall temporal pattern and the dependence of the temporal pattern on season, storm duration, and depth seem to have minor effects on the design flood peak. In the past literature, Sivapalan et al. (1996) also suggested that peak runoff is not affected by the temporal pattern of rainfall for catchments with response time large compared to storm duration.

The availability of data is another factor that may have considerable impact on the reliability of flood estimates. As discussed in Section 4.5.6, in the current application, the design IFD curves for the La Trobe River catchment were determined from observed rainfall data at only one pluviometer inside the catchment, and therefore were of limited accuracy, particularly for rare storms of long duration. Had additional data from daily rain gauges and supplementary rainfall information in a larger region been used in the derivation of the design IFD curves for the specified site, flood estimates by the proposed Joint Probability Model would have been more reliably determined. Similarly, the statistical distribution representing the initial loss and the routing model parameter  $k$  were also estimated using at-site data. Again, pooling of supplementary information from catchments with similar flood response could have led to better estimates of the loss and runoff routing model parameters, and therefore, of the design floods.

It is clear that the flood frequency curve derived by the proposed Joint Probability Model reflects the variability of key design inputs to the flood generation process

(rainfall intensity, duration, temporal pattern, and initial loss) and their correlations, but not the uncertainty in the selected model representations and parameter estimation. Even though it would be desirable to quantify the effects of this uncertainty on flood estimates by determining the confidence limits of the derived flood frequency curve, as mentioned in Section 5.4, this has been left for future work, due to both the lack of data and the time limits placed on this research.

## 6.6 ADDITIONAL METHOD TESTING

In the analyses described in previous chapters and sections, the proposed Joint Probability Model was applied to estimate design floods for just one catchment, the La Trobe River at Noojee. In order to understand more about the performance of the proposed model, the model was tested on another catchment, the Tarwin River catchment at Dumbalk North (flow gauging station number 227226). As mentioned in Section 4.2.1, this catchment has an area of  $127\text{km}^2$ , and 27 years of flow record (from 1971 to 1997). The pluviometer with the longest record that can be used for rainfall analyses is just outside the catchment boundary and has 22 years of data (station 85106, from 1957 to 1978). The estimation of the derived flood frequency curve for the Tarwin River catchment and the evaluation of the proposed model using observed flow data for this catchment are described below.

### 6.6.1 Estimation of model elements

Before estimating the derived flood frequency curve for the Tarwin River catchment using the proposed Joint Probability Model, as for the case of the La Trobe River catchment, the stochastic and deterministic elements of the model had to be determined. The stochastic elements were the frequency curves of design rainfall intensity, the probability distributions of rainfall duration, temporal pattern, and initial loss. The deterministic elements were the parameters of the lumped runoff routing model, the continuing loss rate, and the design baseflow.

Data used to derive the stochastic elements of the proposed model for the Tarwin River catchment were observed rainfall events extracted from the rainfall record at pluviometer 85106, streamflow data recorded at station 227226, and observed initial losses obtained from a parallel study (Rahman et al., 2001). Similarly, parameters of the lumped runoff routing model for this catchment had already been calibrated and were readily obtainable from the same study. The observed rainfall and streamflow data at those sites have been checked for time homogeneity and the extracted storm events for consistency (see Section 4.2.2).

To determine the probability distribution of storm duration, the IFD curves, and the probability distribution of storm initial loss for the Tarwin River catchment, the methods described in Sections 4.4, 4.5 and 4.7 were adopted. To represent temporal patterns by a statistical model, it is important to note that the temporal pattern was assumed to be independent of location within the relatively small region used in this study. Therefore, the statistical model used to characterise the temporal pattern for the Tarwin River catchment was taken as that developed for the La Trobe River catchment. In this case, the dependence of temporal patterns on season, storm duration, and storm depth was neglected, as it has been shown that this simplification has minor effects on design flood estimates (see Section 6.5.3). A summary of the probability distributions characterising the stochastic inputs, their distributional parameters, and the values of other fixed design inputs is given in Table 6-15.

Table 6-15: Tarwin River catchment at Dumbalk North - Summary of design elements used in the proposed Joint Probability Model

Elements	Type of fitted distribution	Distributional parameters or design values
Rainfall duration	Generalised Pareto distribution	location = 0.577, scale = 1.102, shape = 0.193
Rainfall intensity	Exponential distribution	vary, depending on class intervals of duration
Temporal pattern	Beta distribution	$\alpha = 2.363, \beta = 2.212$
Initial loss	Beta distribution	$\alpha = 1.5, \beta = 1.7$
Baseflow	fixed value	0.18 m <sup>3</sup> /s
Continuing loss rate	fixed value	2.5mm/h
Runoff routing model	fixed value	k = 33, m = 0.8

### 6.6.2 Estimation of the derived flood frequency curve

As discussed in Section 5.2.2, for the purpose of this study, it is considered adequate to generate 2000 years of data. As there was an average of 9.4 significant storm events per year of record for the Tarwin River catchment, the minimum number of data to be generated over 2000 years of simulation was [see Equation (5-1)]:

$$NR = 9.4 \times 2000 = 18800$$

Therefore, the number of generated data for the specified catchment was taken as 20000.

To estimate the design flood frequency curve for the Tarwin River catchment, the procedures detailed in Chapter 5 was adopted. In this procedure, 20000 random sets of data from the input distributions were first generated. Flood events were then generated using Monte Carlo simulation. A frequency analysis was finally carried out to determine the generated flood frequency curve for the catchment.

The derived flood frequency curve for the Tarwin River catchment is illustrated in Figure 6-5. In this figure, it can be seen that the shape of the derived flood frequency curve does not follow closely that of the observed floods. This suggests that some of the non-linearity of the rainfall-runoff process may not be correctly modelled. In addition, design floods of very small ARIs (less than 1 year) are much smaller than the observed floods. One possible explanation for this is that the adopted design baseflow ( $0.18\text{m}^3/\text{s}$ , see Table 6-15) might have been too low. Had a bigger value of the design baseflow been adopted (say,  $5\text{m}^3/\text{s}$ ), design flood estimates would have been increased for all ARIs. However, for big floods of design interest (ARIs of 50 or 100 years), the magnitude of change in the design peak discharge may be insignificant.

Design flood peaks of various return periods for the Tarwin River catchment are summarised in Table 6-16. From this table, it can be seen that, using the proposed model, the design flood peak for the study catchment varies from  $27\text{m}^3/\text{s}$  to  $114\text{m}^3/\text{s}$  for ARIs from 1 year to 100 years.

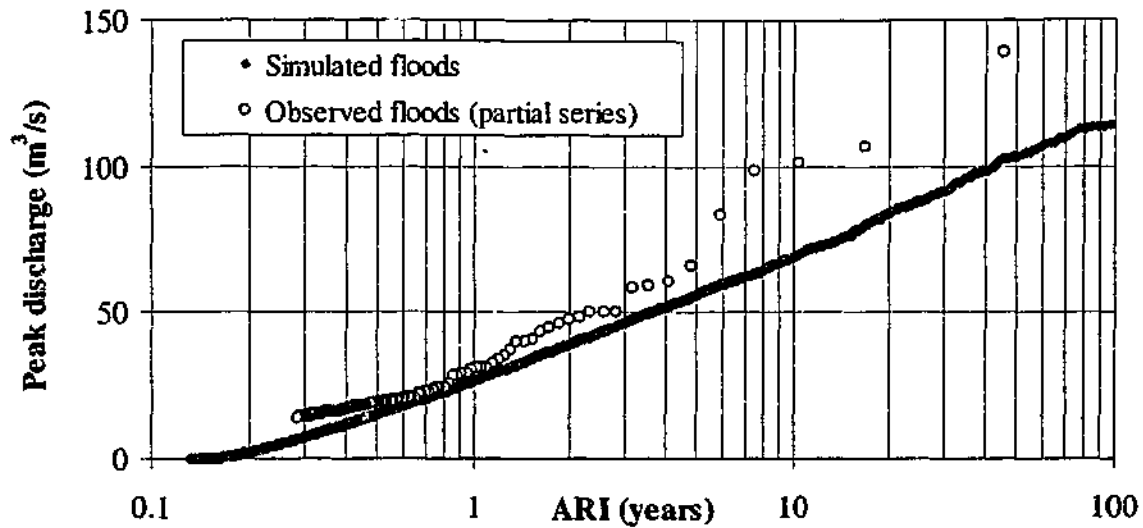


Figure 6-5: Observed floods and the generated flood frequency curve - Tarwin River catchment at Dumbalk North

Table 6-16: Design flood estimates for the Tarwin River catchment by different methods

ARI (years)	Flood frequency analysis	Joint Probability Model		Design Event Approach	
	Peak discharges (m <sup>3</sup> /s)	Peak discharges (m <sup>3</sup> /s)	Ratios	Peak discharges (m <sup>3</sup> /s)	Ratios
1	32	27	0.9	22	0.7
2	47	39	0.8	39	0.8
5	73	56	0.8	58	0.8
10	97	69	0.7	72	0.7
20	120	84	0.7	89	0.7
50	149	103	0.7	114	0.8
100	170	114	0.7	137	0.8

### 6.6.3 Evaluation of the proposed model

To assess the performance of the proposed Joint Probability Model on the Tarwin River catchment, the design floods estimated by this model were compared with the best flood estimates determined by flood frequency analysis and the flood estimates by the Design Event Approach.

To determine the best design flood estimates for the Tarwin catchment, the procedure described in Section 6.2 was first applied to the annual flood series for the site. The outcome of this step was a fitted LPIII distribution and the corresponding 90% confidence intervals (see Figure 6-6). The empirical frequency analysis described in Section 5.4 was next applied to a partial flood series (selected from a threshold discharge of  $30\text{m}^3/\text{s}$ ) in order to provide estimates of more frequent floods. The best design flood estimates for the Tarwin catchment were finally selected as the estimates from partial series analysis for events with return periods less than 5 years, and from the fitted LPIII distribution for return periods of 5 years or greater (see Table 6-16). The return period of 5 years was adopted as the transition between the two flood series as at or above this value the partial flood series does not significantly differ from the annual flood series for the design site.

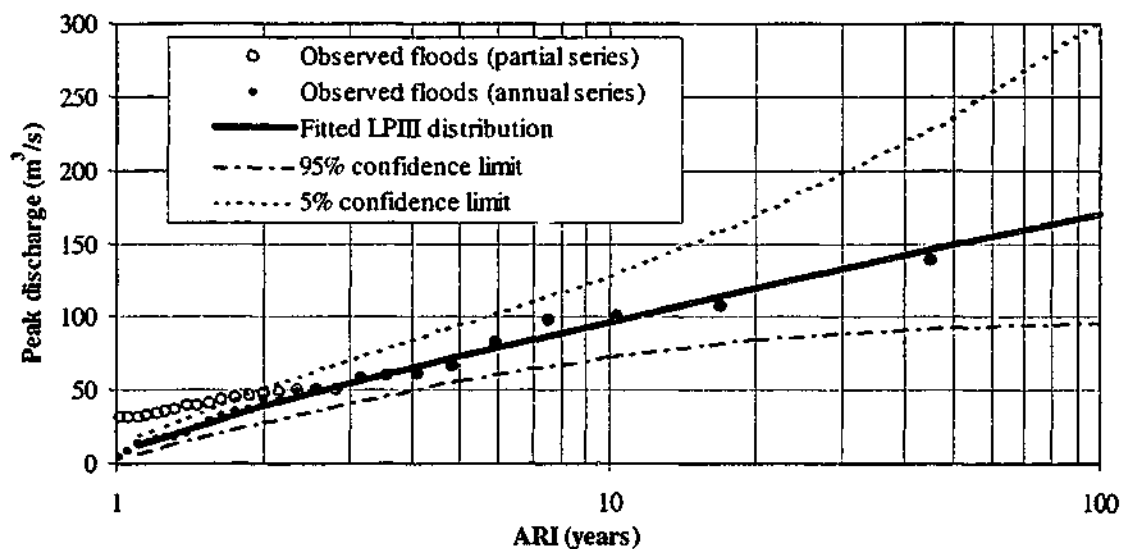


Figure 6-6: Observed floods and the fitted LPIII distribution – Tarwin River catchment

To estimate design floods by the Design Event Approach, the procedure detailed in Section 6.3 was adopted. Results are summarised in Table 6-16 and illustrated in Figure 6-7.

In comparing design floods estimated by the proposed Joint Probability Model with the best estimates determined by flood frequency analysis, it is evident from Table 6-16 that the flood estimates by the proposed model are smaller than those of the flood frequency

analysis for all ARIs. The difference between the flood estimates by these two methods increases from 10% for very frequent floods to 30% for rarer floods. Nevertheless, the flood estimates by the proposed model are all within the 90% confidence intervals determined by direct flood frequency analysis, and very close to the lower 95% limits (see Figure 6-7).

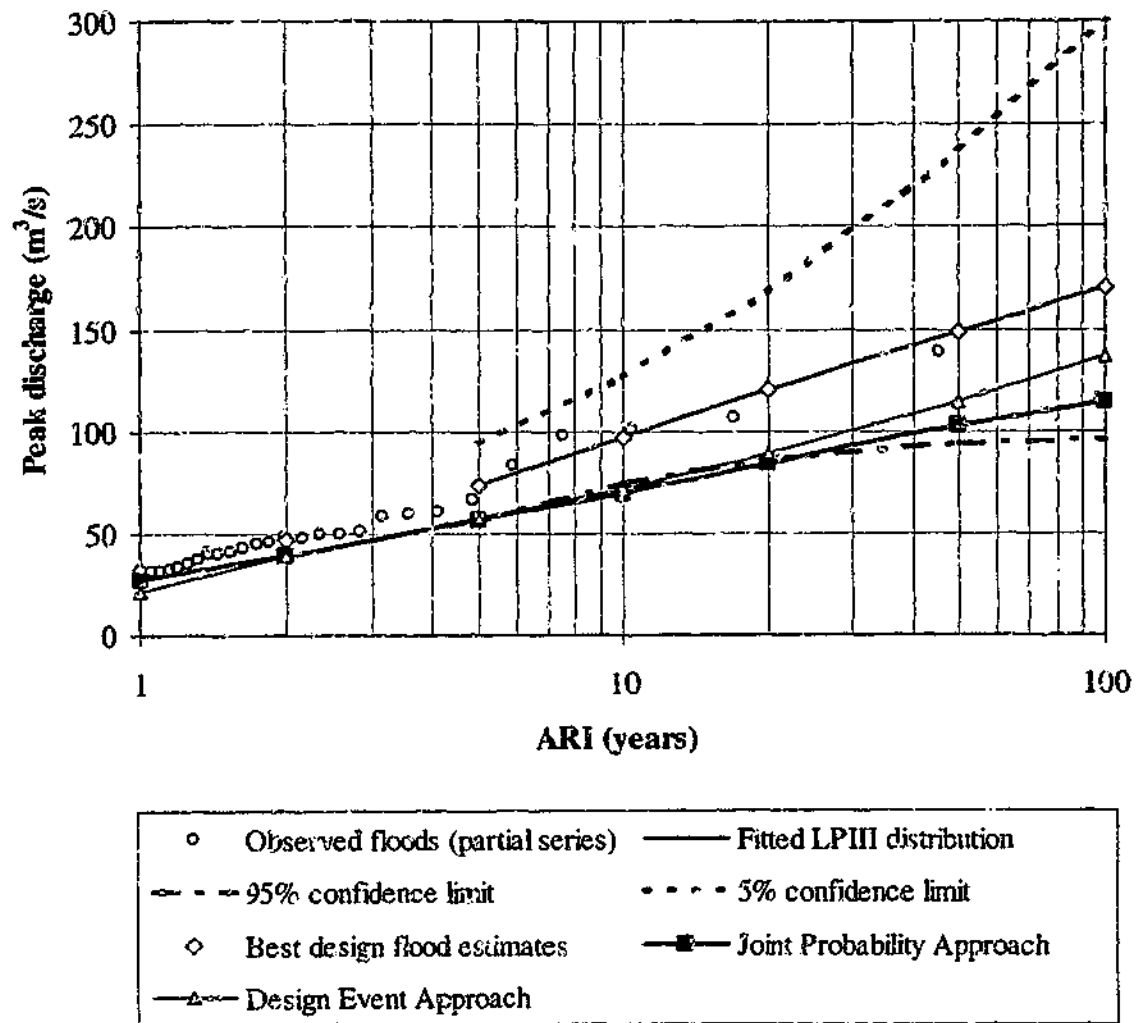


Figure 6-7: Flood frequency curves, Tarwin River catchment

Similarly, estimates of design floods by the Design Event Approach are all less than their corresponding counterparts obtained from flood frequency analysis (see Table 6-16). The difference in flood estimates between these two methods varies from 20% to 30%. However, as clearly indicated in Table 6-16 and Figure 6-7, the flood estimates by the Design Event Approach are always bigger than those obtained by the Joint

Probability Model (except for events of 1-year ARI), and tend to be closer to the estimates by flood frequency analysis.

In general, it can be concluded that, compared with the best flood estimates by flood frequency analysis, both the proposed Joint Probability Model and the Design Event Approach underestimate the design flood peak for the Tarwin River catchment. Nevertheless, the flood peaks estimated by these latter two methods are of similar magnitude, all within the 90% confidence intervals determined by direct flood frequency analysis, and very close to the lower confidence limits.

## 6.7 OVERALL ASSESSMENT OF THE JOINT PROBABILITY MODEL

The applications of the proposed Joint Probability Model to design flood estimation for two Victorian catchments have shown different results. For the La Trobe River catchment, the model overestimates design floods, but the estimated flood peak discharges are not too far from the upper confidence limits established by direct flood frequency analysis. By contrast, for the Tarwin River catchment, the model underestimates the design flood peak, however, these design floods are very close to the lower confidence limits determined by direct flood frequency analysis. Compared with the currently used Design Event Approach, the proposed model performs better for the former catchment, and performs similarly for the latter.

For the two test catchments, the discrepancy of design floods estimated by the proposed model and the best available estimates obtained from flood frequency analysis may have been the result of many factors. As discussed in Section 6.4, these factors include the use of a lumped model for runoff routing, and errors in the assumed degree of non-linearity of catchment response. Uncertainties in determining the design rainfall frequency curves, in estimating the parameters of the stochastic and deterministic models representing the catchment flood response, or in the adopted values of other fixed design inputs, certainly have an impact on the flood estimates. In addition, the average rainfall over the catchment estimated from observed data at only one location

may not be representative of the catchment rainfall and its variability over the study catchment.

An original element of the proposed model was the development of a new storm definition. This has been successfully applied and has shown a number of advantages. Firstly, in the new storm definition, storm events are defined such that the storm duration, rainfall intensity, and temporal pattern can be analysed as random variables. Secondly, the parameters of the storm definition could be changed to suit the particular type of catchment under study. For example, the separation time between successive storms could be increased in order to extract longer storms that are likely to produce runoff for large catchments. Thirdly, the adopted definition produces nearly complete storm events in contrast to storm bursts. Therefore, the modelling of storm losses becomes easier. Finally, in this study, using the proposed storm definition, the storm duration has been characterised by a three-parameter Generalised Pareto distribution. In previous studies (for example, Eagleson, 1972; Wood and Hebson, 1986; Bloeschl and Sivapalan, 1997), the storm duration has been modelled by the exponential distribution, which is a special case of the Generalised Pareto distribution. It is thus clear that this study has described the storm duration in a more general fashion.

However, there are also a few disadvantages in the developed storm definition. As a storm represents a greater portion of the actual rain (rather than just a burst of the rain currently used in design flood estimation in Australia), the temporal pattern becomes more complex, is highly variable, and thus more difficult to model. Consequently, a great deal of effort was spent on correctly modelling this variability. In addition, the difference between the developed storm definition and the currently used storm bursts means that some of the existing design data can not be used directly.

Overall, it can be concluded that the proposed Joint Probability Model is fundamentally sound, theoretically superior to the currently used Design Event Approach, and practically workable. It offers a rigorous method to compute the probability of design floods without the need for the critical storm duration concept. It can model the great variability of real storm event characteristics (storm duration, average intensity, and temporal pattern) and their interactions. Applications of the model to two Victorian catchments showed satisfactory results, even though the performance of the proposed

model could be improved by using a better model for runoff routing and/or better estimates of design inputs and model parameters. Testing of the proposed model on a larger number of catchments is required before a firmer quantitative assessment of the model performance can be made.

## 6.8 SUMMARY

The evaluation of the proposed Joint Probability Model was carried out by comparing design flood estimates for the La Trobe and the Tarwin River catchments obtained from this model with those estimated by flood frequency analysis and the Design Event Approach.

In examining the observed flow data at the La Trobe catchment, it was evident that the floods in the annual series for this site were the results of prolonged storms with the average duration of 41 hours. These peak floods occurred throughout the year but more often in winter and spring when the catchment was relatively wet.

In estimating design floods using direct flood frequency analysis, it was shown that the flood frequency curve for this catchment was not well defined for return periods greater than 20 years, and the corresponding confidence intervals of these flood estimates were also wide. The uncertainty in these design floods was attributed to the shortness of big floods on records. Similarly, there was also uncertainty in design flood estimates obtained by the Design Event Approach, due to many factors such as uncertainties in the choice of fixed design inputs or in estimates of the routing model parameters.

In comparing design flood estimates obtained from the three methods, it was evident that the currently used Design Event Approach significantly overestimated design floods for the La Trobe River catchment. For any given return period, design flood magnitudes were at least three times those estimated by flood frequency analysis. Even though the proposed Joint Probability Model also overestimated design floods for this catchment, the degree of overestimation was reduced to about half. The flood estimates

by the proposed model were not too far from the upper confidence limits determined by direct flood frequency analysis.

In examining the effects of variations or uncertainties in the stochastic and fixed design inputs on the resulting flood estimates, the results of the sensitivity analyses confirmed that the design rainfall intensity plays a key role in design flood estimation. Uncertainties in the adopted design initial loss were found to have considerable impact on estimates of the flood peak discharge. Errors in the routing model parameter  $k$  resulted in moderate changes in the design flood peak. Uncertainties in the design baseflow or the adopted storm continuing loss had more influence on small floods than big floods. These results suggest that in applying the proposed Joint Probability Model to practical situations, in order to obtain better flood estimates, it is crucial to concentrate on the estimation of the design rainfall IFD curves and the parameters of the adopted loss model. More detailed representation of the catchment model for runoff routing is also desirable.

The examination of the sensitivity of the resulting floods to the modelling of the dependence of temporal patterns on season, storm duration, and storm depth showed that, the design flood magnitude estimated for the La Trobe River catchment changed only slightly if this dependence was neglected. Nevertheless, application of the proposed model to a wider range of catchment areas is required to verify this conclusion.

The investigation of the effects of the size of the generated sample of floods on design flood estimates confirmed that for the specified sample size of 15000 (over 2000 years), the generated flood frequency curve in the range of 1-year to 50-year ARI was satisfactorily stable. More reliable flood estimates for ARIs greater than 50 years can be obtained by increasing the generated flood sample or by applying variance reduction techniques.

Results of an additional testing of the proposed model on the Tarwin River catchment indicated that, when compared with the best available flood estimates by flood frequency analysis, the proposed model generally underestimated the design peak discharge. However, the flood estimates by the proposed model were very close to the

lower confidence limits established by direct flood frequency analysis, and of similar magnitude with those determined by the Design Event Approach.

On the basis of the different results for the two test catchments, it was concluded that testing of the proposed model on a larger number of catchments with long flow records is required before a firm conclusion on the quantitative performance of the proposed model can be drawn.

In assessing the proposed model, it has been shown that the storm definition developed for this study has many advantages. These include the ability of modelling the real variations of storm event characteristics, the flexibility of its parameters to be changed to suit a particular catchment, the ease of modelling the catchment wetness conditions, and the ability to describe the storm duration by a general statistical distribution. By contrast, the proposed storm definition also has a few disadvantages. These include the greater complexity of the storm temporal patterns, making it more difficult to model, and the less direct relationship with current design rainfall data.

In summary, the proposed Joint Probability Model is considered to be fundamentally sound and theoretically superior to the currently used Design Event Approach, because it explicitly models the variability of key design inputs and their correlations in the flood generation process. The method is also practically workable. However, design floods estimated by this model are still subject to errors due to uncertainties in model selection or parameter estimation. While it is desirable to quantify the uncertainty in the flood estimates, this has been left for future research due to the lack of data and the limited time frame of this study.

## Chapter 7

# CONCLUSION

This chapter presents a summary of the research reported in this thesis, conclusions drawn from the work, and recommendations for further study.

### 7.1 SUMMARY OF WORK DONE

Throughout this study, the main objective has been the development of a Joint Probability Model for rainfall-based design flood estimation. This objective was achieved by reviewing design flood estimation methods, selecting the most promising approach among various alternatives, developing a conceptual flood estimation model based on the selected approach, and testing the performance of the proposed model on two Victorian catchments.

#### **Review of design flood estimation methods**

The review of rainfall-based design flood estimation methods revealed major weaknesses in the currently used Design Event Approach and the need for an improved method of estimating design floods from design rainfalls. These weaknesses are the underestimation of the variability of real storm events causing floods and associated catchment moisture conditions, the non-scientific basis of the critical storm duration concept and the resulting probability bias in design flood estimates, together with the difficulties in selecting representative values of design inputs to correct the probability bias. These are likely to result in significant uncertainties in flood estimates, which could have considerable economic consequences in the design of hydraulic structures and floodplain management.

Among the rainfall-based design flood estimation methods, Continuous Simulation and the Joint Probability Approach have the potential to overcome the above limitations of the current design procedure. Both methods can account for the great degree of variability of rainfall and loss characteristics, eliminate the need for estimating the critical storm duration, and more rigorously estimate the probabilities of design floods. However, of these two methods, the Joint Probability Approach has greater potential to provide significant improvements in rainfall-based flood estimation in the near future; because, being more closely related to the current Design Event Approach, it is possible to make use of a large body of existing experience and data. This research has focused on the Joint Probability Approach.

The Joint Probability Approach to rainfall-based design flood estimation has two essential elements: deterministic and stochastic elements. The deterministic elements convert a design rainfall event input into a rainfall excess and then into an output of a flood event hydrograph. The stochastic elements include the probability distributions representing the key model inputs, and a derived distribution method for determining the probability distribution of the flood event output.

The review of previous studies of the Joint Probability Approach indicated that even though this approach has been applied to design flood estimation since the 1970s, it has not yet been developed to be a practical design tool, due to many restrictions in the elements used. These are:

- the use of inadequate models of the design rainfall, loss, and catchment response,
- the inadequate consideration of the variability of key flood producing factors,
- simple assumptions about the relationships between stochastic design inputs,
- the use of complicated derived distribution methods, and
- the lack of flexibility to apply the approach to actual catchment conditions.

#### **Development of Joint Probability Model**

Unlike previous models of the Joint Probability Approach, the Joint Probability Model proposed in this study uses an initial loss – continuing loss model and a simple lumped, non-linear runoff routing model that can be easily applied in practice. In addition, it represents key design inputs to the flood generation process (namely, the design rainfall

intensity, duration, temporal pattern and initial loss) by probability distributions, and models the correlations between these design inputs. In order to simulate design floods, it employs Monte Carlo simulation. The distinctive features of the proposed model are the use of a storm definition that can reflect the great variability of real rainfall event characteristics, the consideration of the correlations of design random variables, especially the dependence of rainfall temporal patterns on season, rainfall duration, and depth, and the simplicity for routine applications. At this development stage, the proposed model aims to determine the frequency curve of the peak flood magnitude up to the 100-year ARI by means of a lumped runoff routing model. However, the proposed model is intended for use with a distributed runoff routing model and, in principle, it could be applied to derive the frequency curves of other flood hydrograph characteristics and to more extreme events.

To apply and evaluate the proposed model, two Victorian catchments (the La Trobe River catchment at Noojee and the Tarwin River catchment at Dumbalk North) were selected. The analyses of rainfall inputs used data at 19 pluviometers in and around these catchments. Observed rainfall and flow data at these sites were checked for homogeneity in time. Results of the Mann-Kendall test for trend and the CUSUM test for discontinuity indicated that the data at any particular site were all drawn from the same statistical distribution.

Before developing the probability distributions of rainfall characteristics, a storm definition was developed to extract significant rainfall events from continuous rainfall records. Five parameters were used to define these events, such that they are stochastic events, have the potential to produce significant runoff, and exclude periods of insignificant rain at the start and end of the events. The values of these parameters were determined by exploratory and sensitivity analyses. The extracted events were finally checked for consistency and those with recording errors were eliminated. The adopted storm definition<sup>1</sup> gave an average of seven storms per year per station.

In developing the probability distribution of the storm duration at Noojee, the regional frequency analysis procedure developed by Hosking and Wallis (1997) was adopted.

---

<sup>1</sup> A variant of this storm definition, called 'storm core', has also been investigated in a parallel study (Rahman et al., 2001).

Analysis results showed that homogeneous regions of storm duration could be formed by grouping sites contiguous to the site of interest. A three-parameter Generalised Pareto distribution was used to characterise storm duration. The fitted distribution preserved very well the statistical properties of the observed storm durations.

To determine the frequency curves of the rainfall intensity for the design site, the correlation between average rainfall intensity and storm duration was first investigated. A conditional probability distribution, expressed by the IFD curves, was then used to characterise this relationship. The IFD curves for the design site were determined using at-site frequency analysis of rainfall intensities for selected duration intervals, and a smoothing procedure for other durations. Results indicated that there were uncertainties in average intensity estimates of long duration and low frequency storm events due to the lack of observed data. As a future improvement, it would be desirable to use regional rainfall data to obtain more reliable rainfall intensity estimates.

Before developing a stochastic model for storm temporal patterns, the dependence of the temporal pattern on season, storm duration and depth was examined using correlation analysis and the chi-square test of independence. It was found that, depending on the test used and the level of detail of the characterisation of the rainfall temporal pattern, such dependence might be or might not be detected. When the temporal pattern was represented by a dimensionless mass curve defined by nine ordinates, results of the chi-square test showed that the temporal pattern was dependent on season of storm occurrence, storm duration and even on storm depth (in one case). Based on these results, the observed temporal patterns of the storm events used in this study were divided into ten independent groups.

The multiplicative cascade model presented by Robinson and Sivapalan (1997) was adopted for generating design temporal patterns. For each of the ten temporal pattern groups, disaggregation parameters of this model were generated from a beta distribution whose parameters were determined from the observed dimensionless mass curves in the group. The adopted model satisfactorily reproduced the distribution of the maximum dimensionless rainfall intensity and the frequency characteristics of the observed temporal patterns. However, it underestimated the lag one auto-correlation between successive storm depths of the observed patterns.

Before deriving the probability distribution of storm initial loss, the relationships between the storm initial loss and storm duration and average rainfall intensity were investigated. Analysis results indicated that the initial loss derived for observed events for the La Trobe River catchment was independent of storm duration and average intensity. The probability distribution of the storm initial loss was then derived using an at-site frequency analysis method. A two-parameter beta distribution was again used to represent the initial loss for the catchment.

A trial and error approach was applied to determine the parameters of the lumped runoff routing model for the study catchment. It was shown that the calibrated model reproduced relatively well the peak discharge, but significantly underestimated the time to peak of the observed flood hydrographs. A similar conclusion was drawn when design floods were estimated using a distributed RORB model calibrated for the same catchment. On this basis, it was concluded that, for the purpose of this study, the adopted model was able to give reasonable estimates of the design flood peak.

#### **Model application and evaluation**

In applying the proposed Joint Probability Model for estimating design floods for the test catchments, random rainfall events and loss data were first generated from the frequency distribution of rainfall intensity, the probability distributions of rainfall duration and initial loss, and the stochastic model of temporal patterns. Monte Carlo simulation was then used to simulate flood event hydrographs resulting from various combinations of these design inputs, taking into account the relationships between them. The derived flood frequency curve of peak flows was finally determined using a frequency analysis for partial duration series.

To evaluate the proposed Joint Probability Model, design floods estimated by the model were compared with the estimates obtained from direct flood frequency analysis and the Design Event Approach. For the La Trobe River catchment, it was evident that the proposed model was able to reduce the bias in the results of the Design Event Approach by about 50%. It was also found that the generated flood frequency curve was close to the upper confidence limits for the curve derived from direct flood frequency analysis, while the flood frequency curve determined by the Design Event Approach was far above it. By contrast, for the Tarwin River catchment, the proposed model as well as

the Design Event Approach underestimated the peak flood discharge. However, in this case, the design flood estimates by these two methods were of similar magnitude and very close to the lower confidence limits determined by direct flood frequency analysis.

To examine the effects on design flood estimates of likely errors in the stochastic and fixed design inputs, sensitivity analyses were carried out. It was found that the design rainfall intensity plays a critical role in the estimation of design floods. Uncertainties in estimates of the initial loss and the runoff routing model parameter  $k$  were found to have important effects on the resulting floods. Errors in estimates of the fixed design continuing loss rate or the adopted baseflow had more influence on frequent floods than rare floods. For the present application where the seasonal variations of other design inputs were not considered, the neglect of the variation of the rainfall temporal pattern with season, storm duration and depth was found to have little effect on design flood peaks for the La Trobe River catchment.

In examining the stability of the design floods, results of a sensitivity analysis showed that, for the specified sample size of 15000 events spanning 2000 simulated years, the peak discharge estimates were stable for floods of ARIs less than 100 years. Better estimates of floods with ARIs of 100 years or more could be obtained by increasing the generated flood sample or applying variance reduction techniques.

## 7.2 CONCLUSIONS

From the research conducted in this study, the following main conclusions can be drawn:

- It is desirable to improve the currently used Design Event Approach for estimating design floods from design rainfalls, as the limitations of this approach have led to considerable uncertainty and bias in design flood estimates, which have significant economic impacts on the design of hydraulic structures and floodplain management.
- The proposed Joint Probability Model is theoretically superior to the Design Event Approach and easy to apply in practice. The model adopts the same rainfall-runoff modelling elements as the Design Event Approach, but explicitly takes into account

the variability of the design rainfall depth, duration, temporal pattern, and initial loss, and the relationships between them. Using the proposed model, the probability of design floods can be rigorously determined (within the bounds of uncertainty of design inputs). Furthermore, the non-scientific basis of the critical storm duration concept applied in the Design Event Approach can be avoided. In addition, being closely related to the Design Event Approach, the proposed model can be applied using some of the existing design data and expertise.

- Applications of the proposed model to two gauged Victorian catchments showed different results. Design flood estimates by the model are within the 90% confidence intervals determined by direct flood frequency analysis for one catchment, but outside the intervals for the other. Compared with the Design Event Approach, the model performs better for one catchment but similarly for the other. Further testing of the proposed model on a larger number of catchments is therefore required to obtain firmer conclusions about its performance.
- The flood peak discharge is strongly influenced by estimates of the design rainfall intensity, as expected, and to a lesser extent, by estimates of the storm initial loss and the runoff routing model parameter  $k$ . Therefore, in order to obtain reliable design floods, it is crucial to obtain good estimates of the design rainfall intensity for a catchment. Efforts should also be devoted to the modelling of the design rainfall loss and the parameter estimation of the runoff routing model.
- From the results of the model application and sensitivity analyses, it can be concluded that the proposed Joint Probability Model is practically workable. It can be readily applied to gauged catchments with good pluviograph data and limited streamflow record. For these catchments, it is feasible to derive the statistical distributions of the random design inputs (rainfall intensity, duration, temporal pattern, and initial loss) using observed rainfall and flow data.
- The storm definition developed in this research has proved successful in modelling the great degree of variability of real storm event characteristics. It represents a greater portion of the actual rain than the currently used storm bursts, and therefore makes the modelling of storm loss easier. In addition, its parameters could also be changed in order to represent the typical storms causing floods for a particular catchment.

- Of the issues involved in the modelling of variable design inputs, the model representation of the rainfall temporal pattern required the greatest analysis and development effort. Although temporal patterns were found to depend on season, storm duration, and depth, with limited testing, it was concluded that design flood estimates were relatively insensitive to the modelling of this dependence.
- Even though the proposed Joint Probability Model has only been tested for the design flood peak, the model could be applied to determine the frequency curves of other hydrograph characteristics such as flood volume or time to flood peak. It could also be applied to determine the flood frequency curves for catchments with artificial storage, in which initial reservoir storage content can be considered to be an additional random variable.

### 7.3 RECOMMENDATIONS FOR FUTURE STUDIES

The proposed Joint Probability Model can be further improved in order to become a practical design tool. In this development, the following aspects should be considered.

- **Application of the model to a wider range of catchments:** As the proposed model has been applied to only two catchments, further testing of the model on a larger number of catchments is considered essential. The catchments should be selected such that they represent a wider range of flood hydrology characteristics (size, shape and geographic location). In addition, they should have relatively long and concurrent observed streamflow and pluviograph data, and large floods on record (preferably with ARIs approaching 100 years). Application of the proposed model to such catchments would allow better quantification of the model performance.
- **Incorporation of a distributed runoff routing model:** Clearly, the use of a simple, lumped runoff routing model as adopted in this study is inadequate for design flood estimation, especially for large catchments. This is because the lumped model ignores the spatial variation of rainfall and loss characteristics, and the distributed nature of catchment storage. The use of a distributed runoff routing model would allow the above characteristics to be more realistically modelled and therefore would lead to improved design flood estimates.

- **Derivation of the IFD curves using a regional frequency analysis method:** The at-site frequency analysis procedure used to develop the IFD curves of storm events defined in this study is inadequate, due to the shortness of rainfall record, especially for the estimation of the average intensity for rare events. The use of a regional frequency analysis method clearly could produce better IFD estimates, as the shortness of record at the site of interest can be compensated by pooling data from several sites. In this regard, the procedure developed by Hosking and Wallis (1997) seems to be a promising method.
- **Investigation of an improved model to represent the rainfall initial loss:** The modelling of the storm initial loss could be improved by the investigations of (i) an alternative distribution to represent the initial loss, and (ii) methods for taking into account the dependence of the rainfall loss on season. With respect to (i), in this study, it has been shown that the beta distribution adopted to represent the initial loss for the study catchment is not necessarily the best distribution, and that variations in the model representation of the initial loss have significant effects on design floods. Therefore, it is clear that the examination and adoption of a better statistical distribution for the initial loss would improve the performance of the proposed Joint Probability Model for design flood estimation. With respect to (ii), the variation of the rainfall loss with season is not considered in this research. However, it is obvious that there is a strong correlation between the rainfall loss and season, because infiltration and evaporation losses are higher in summer than in winter. The incorporation of this relationship into the flood generation process would better reflect the real interaction between rainfall and catchment conditions, which should lead to improved design flood estimates. An example of an investigation of the seasonal variation of the initial loss can be found in Hill et al. (1996a).
- **Investigation of a more detailed representation of the temporal pattern:** The stochastic model of the rainfall temporal pattern in this study could be improved in the following two aspects. The first is the incorporation of the auto-correlation into the adopted model. It has been shown in the present study that the multiplicative cascade model adopted to represent the temporal pattern does not reproduce the auto-correlation of rainfall intensity in successive time steps. This may lead to underestimation of design flood estimates, as in reality, high rainfall tends to be followed by high rainfall, and this would tend to produce large peak discharge.

Thus, it is desirable to incorporate the auto-correlation of rainfall intensity into the adopted stochastic model of the rainfall temporal pattern. To achieve this objective, the method recently developed by Seed et al. (1999) or the model proposed by Garcia-Guzman and Aranda-Oliver (1993) could be used. The second is the determination of the minimum number of ordinates necessary to adequately define the temporal pattern of rainfall. In this study, the adopted stochastic model of the temporal pattern has been applied to generate random dimensionless rainfall hyetographs defined at 8 equal increments of storm duration. The adopted number of time increments may be adequate for short duration storms, but possibly inadequate to represent the time distribution of rainfall intensity during the storm duration of longer events, say, greater than 24 hours. In design flood estimation, coarsely defined temporal patterns tend to smooth out the flood peak discharge. Thus it is important to determine the minimum resolution of the temporal pattern in order to correctly model the design flood peak.

- **Stochastic treatment of the spatial variation of rainfall on a catchment scale:** As real rainfall events causing floods vary considerably in time and space, modelling of the spatial variation of rainfall on the catchment scale is considered to be necessary in flood estimation procedures, especially for medium to large catchments. At the time of this study, this was difficult to achieve due to limited number of rain gauges over catchments. Nevertheless, current development in radar-based rainfall estimation is expected to make this objective feasible in the future.
- **Application of the model to ungauged catchments:** In this study, it has been shown that the probability distributions of rainfall duration and temporal pattern can be derived using regional data. Therefore, to apply the model to ungauged catchments, future work is required in order to develop the probability distributions of average rainfall intensity and initial loss using regional data. In this regard, regional design data for storm bursts provided by the Institution of Engineers, Australia (1987) may be used to derive the IFD curves for complete storms. The development of the statistical distribution of the storm initial loss could be carried out using some results of a previous study (Hill et al., 1996a).
- **Uncertainty analysis:** The derived flood frequency curve estimated by the proposed Joint Probability Model reflects the variability of key design inputs (rainfall intensity, duration, temporal pattern, and initial loss), but not the

uncertainties in model selection or parameter estimation. It is therefore desirable to examine the uncertainty of design floods as the result of the uncertainties in design inputs. For example, a Bayesian framework could be used to quantify the uncertainty involved in parameter estimation (Kuczera, 1983a,b), or Monte Carlo simulation could be applied to derive the confidence limits of the flood outputs (Bates and Townley, 1988). It is also worth noting that, so far, the sensitivity analyses conducted in this study have been limited to examining the individual impacts on design flood estimates of input or parameter uncertainty. Further work on combined effects of the uncertainties in these factors is thus needed to get a better understanding of their interactions and compensating effects in design flood estimation.

## REFERENCES

- Ahern, P. A. and Weinmann, P. E. (1982). Considerations for Design Flood Estimation Using Catchment Modelling. Hydrology and Water Resources Symposium, Melbourne, Australia. I. E. Aust. National Conference Publication, 16, 3: 44-48.
- Askew, A. J. (1975). Variations in Estimates of Design Floods. Hydrology Symposium, New South Wales, Australia. I. E. Aust. National Conference Publication, 75/3, 26-30.
- Baker, A. (1997). Application of A Combined AWBM/URBS Catchment Model for Flood Forecasting. Unpublished Masters Thesis, Department of Civil Engineering, Monash University, Australia.
- Bates, B. C. and Davies, P. (1987). Effect of Baseflow Separation Procedures on Surface Runoff Models. Journal of Hydrology, 103: 309-322.
- Bates, B. C. and Townley, L. R. (1988). Nonlinear, Discrete Flood Events Models. 3. Analysis of Prediction Uncertainty. Journal of Hydrology, 99: 91-101.
- Benjamin, J. R. and Cornell, C. A. (1970). Probability, Statistics, and Decision for Civil Engineers. McGraw-Hill.
- Beran, M. A. (1973). Estimation of Design Floods and the Problem of Equating the Probability of Rainfall and Runoff. International Symposium on Design of Water Resources Projects with Inadequate Data, Madrid, Spain. UNESCO, 33-50.
- Beven, K. (1987). Towards the Use of Catchment Geomorphology in Flood Frequency Prediction. Earth Surface Processes and Landforms, 12: 69-82.
- Bloeschl, G. and Sivapalan, M. (1997). Process Controls on Flood Frequency. 2. Runoff Generation, Storm Properties and Return Period. Report ED 1159MS. Centre for Water Research, Department of Environmental Engineering, The University of Western Australia.
- Bonta, J. V. and Rao, A. R. (1988). Factors Affecting the Identification of Independent Storm Events. Journal of Hydrology, 98: 275-293.
- Bonta, J. V. and Rao, A. R. (1989). Regionalisation of Storm Hyetographs. Water Resources Bulletin, 25(1): 211-217.

- Boughton, W. C., Muncaster, S. H., Srikanthan, R., Weinmann, P. E., and Mein, R. G. (1999). Continuous Simulation for Design Flood Estimation – A Workable Approach. Handbook and Proceedings of Water 99 Joint Congress, Brisbane, Australia. I. E. Aust. National Conference Publication, 178-183.
- Boughton, W. C. (2000). Disaggregation of Daily to Hourly Rainfalls for Flood Studies. Working Document 00/2. Cooperative Research Centre for Catchment Hydrology, Monash University, Australia.
- Bras, R. L. (1990). Hydrology - An Introduction to Hydrologic Science. Addison-Wesley Publishing Company.
- Brown, J. A. H. (1982). A Review of Flood Estimation Procedures. Proceedings of the Workshop on Spillway Design, Monash University, Clayton, Australia. Australian Water Resources Council Conference Series, 6: 84-108.
- Cadavid, L., Obeysekera, J. T. B. and Shen, H. W. (1991). Flood Frequency Derivation from Kinematic Wave. Journal of Hydraulic Engineering, ASCE, 117(4): 489-510.
- Carroll, D. G. (1994). Aspects of the URBS Runoff Routing Model. Water Down Under, Adelaide, Australia. I. E. Aust. National Conference Publication, 169-176.
- Chapman, T. G. (1968). Catchment Parameters for a Deterministic Rainfall-Runoff Model. In Land Evaluation. Stewart, G. A., Macmillan, 312-323.
- Chow, V. T., Maidment, D. R. and Mays, L. W. (1988). Applied Hydrology. McGraw-Hill.
- Conover, W. J. (1971). Practical Nonparametric Statistics. John Wiley & Sons.
- Consuegra, D., Meylan, P. and Musy, A. (1993). A Probabilistic Approach to Estimate Design Parameters for Flood Control Projects. Proceedings of the Symposium on Engineering Hydrology, California, USA. ASCE, 455-460.
- Cordery, I. and Pilgrim, D. H. (1983). On the Lack of Dependence of Losses from Flood Runoff on Soil and Cover Characteristics. Hydrology of Humid Tropical Regions with Particular Reference to the Hydrological Effects of Agriculture and Forestry Practice, Hamburg, Germany. IAHS, 187-195.
- Cordery, I., Pilgrim, D. H. and Rowbottom, I. A. (1984). Time Patterns of Rainfall for Estimating Design Floods on a Frequency Basis. Water Science Tech., 16: 155-165.

- Cordova, J. R. and Rodriguez-Iturbe, I. (1983). Geomorphoclimatic Estimation of Extreme Flow Probabilities. Journal of Hydrology, 65: 159-173.
- Cunnane, C. (1988). Methods and Merits of Regional Flood Frequency Analysis. Journal of Hydrology, 100: 269-290.
- Cunnane, C. (1989). Statistical Distributions for Flood Frequency Analysis. Report No. 33. World Meteorological Organisation, Geneva, Switzerland.
- D'Agostino, R. B. and Stephens, M. A. (1986). Goodness-of-Fit Techniques. Marcel Dekker, Inc.
- Daniel, W. W. (1978). Applied Nonparametric Statistics. Houghton Mifflin Company.
- Diaz-Granados, M. A., Valdes, J. B. and Bras, R. L. (1984). A Physically Based Flood Frequency Distribution. Water Resources Research, 20(7): 995-1002.
- Durrans, S. R. (1995). Total Probability Methods for Problems in Flood Frequency Estimation. In Statistical and Bayesian Methods in Hydrological Sciences. Selected papers from the International Conference in Honour of Professor Jacques Bernier, Paris, France. UNESCO Publishing, 299-326.
- Dworakowski, B. (1999). Personal Communication. Thiess Environmental Services Pty. Ltd., Melbourne, Australia.
- Dyer, B. G., Nathan, R. J., McMahon, T. A. and O'Neil, I. C. (1994). Development of Regional Prediction Equations for the RORB Runoff Routing Model. Report No. 94/1. Cooperative Research Centre for Catchment Hydrology, Monash University, Australia.
- Eagleson, P. S. (1972). Dynamics of Flood Frequency. Water Resources Research, 8(4): 878-898.
- Edwards, D. R. and Haan, C. T. (1989). Incorporating Uncertainty into Peak Flow Estimates. Transactions of the American Society of Agricultural Engineers, 32(1): 113-119.
- Fill, H. D. and Stedinger, J. R. (1995). Homogeneity Tests based upon Gumbel Distribution and a Critical Appraisal of Dalrymple's Test. Journal of Hydrology, 166: 81-105.
- Filliben, J. J. (1975). The Probability Plot Correlation Coefficient Test for Normality. Technometrics, 17(1): 111-117.

- Flavell, D. J. and Belstead, B. S. (1986). Losses for Design Flood Estimation in Western Australia. Hydrology and Water Resources Symposium, Brisbane, Australia. I. E. Aust. National Conference Publication, 203-208.
- Fontaine, T. A. and Potter, K. W. (1993). Estimating Exceedance Probabilities of Extreme Floods. Proceedings of the Symposium on Engineering Hydrology, California, USA. ASCE, 635-640.
- Franchini, M., Helmlinger, K. R., Foufoula-Georgiou, E. and Todini, E. (1996). Stochastic Storm Transposition Coupled with Rainfall-Runoff Modelling for Estimation of Exceedance Probabilities of Design Floods. Journal of Hydrology, 175: 511-532.
- Garcia-Guzman, A. and Aranda-Oliver, E. (1993). A Stochastic Model of Dimensionless Hyetograph. Water Resources Research, 29(7): 2363-2370.
- Goyen, A. G. (1983). A Model to Statistically Derive Design Rainfall Losses. Hydrology and Water Resources Symposium, Hobart, Australia. I. E. Aust. National Conference Publication, 220-225.
- Green, W. H. and Ampt, G. A. (1911). Studies on Soil Physics, 1. The Flow of Air and Water through Soils. Journal of Agricultural Science: 4, 11-24.
- Guttman, N. B. (1992). The Use of L-Moments in the Determination of Regional Precipitation Climates. 12th Conference on Probability and Statistics in the Atmospheric Sciences, Toronto, Ont., Canada. American Meteorological Society, 231-241.
- Haan, C. T. (1977). Statistical Methods in Hydrology. The Iowa State University Press.
- Haan, C. T. and Schulze, R. E. (1987). Return Period Flow Prediction with Uncertain Parameters. Transactions of the American Society of Agricultural Engineers, 30(3): 665-669.
- Haan, C. T. and Edwards, D. R. (1988). Joint Probability Estimates of Return Period Flows. Transactions of the ASAE, 31(4):1115-1119.
- Hammersley, I. M. and Handscomb, D. C. (1964). Monte Carlo Methods. John Wiley & Sons.
- Hashino, M. (1986). Stochastic Formulation of Storm Pattern and Rainfall Intensity-Duration Curve for Design Flood. International Symposium on Flood Frequency and Risk Analysis, Barton Rouge, USA. D. Reidel Publishing Company, 303-315.

- Hebson, C. and Wood, E. F. (1982). A Derived Flood Frequency Distribution Using Horton Order Ratios. Water Resources Research, 18(5): 1509-1518.
- Heideman, J. C., Hagen, O., Cooper, C. and Dahl, F. E. (1989). Joint Probability of Extreme Waves and Currents on Norwegian Shelf. Journal of Waterway, Port, Coastal, and Ocean Engineering, 115(4): 534-546.
- Heneker, T. M., Lambert, M. F., and Kuczera, G. (1999). DRIP: A Disaggregated Rectangular Intensity Pulse Model of Point Rainfall. Handbook and Proceedings of Water 99 Joint Congress, Brisbane, Australia. I. E. Aust. National Conference Publication, 539-544.
- Hershenhorn, J. and Woolhiser, D. A. (1987). Disaggregation of Daily Rainfall. Journal of Hydrology, 95: 299-322.
- Hill, P. I. (1994). Catalogue of Hydrological Data for Selected Victorian Catchments. Working Document 94/1. Cooperative Research Centre for Catchment Hydrology, Monash University, Australia.
- Hill, P. I., Maheepala, U. K., Mein, R. G. and Weinmann, P. E. (1996a). Empirical Analysis of Data to Derive Losses for Design Flood Estimation in South-Eastern Australia. Report 96/5. Cooperative Research Centre for Catchment Hydrology, Monash University, Australia.
- Hill, P. I., Mein, R. G. and Weinmann, P. E. (1996b). Testing of Improved Inputs for Design Flood Estimation in South-Eastern Australia. Report 96/6. Cooperative Research Centre for Catchment Hydrology, Monash University, Australia.
- Hill, P. I., Hadgraft, R., Weinmann, P. E., and Goldberg, E. (1996c). Flood Frequency Analysis Spreadsheet. Version 1.5. Cooperative Research Centre for Catchment Hydrology, Monash University, Australia.
- Horton, R. E. (1935). Surface Runoff Phenomena: Part 1, Analysis of the Hydrograph. Horton Hydrological Lab. Pub. 101. Edwards Brothers, Inc., Ann Arbor, MI.
- Hoang, T. M. T. (1997). A Joint Probability Approach to Rainfall-Based Design Flood Estimation. Unpublished PhD Transfer Report. Cooperative Research Centre for Catchment Hydrology, Monash University, Australia.
- Hosking, J. R. M. (1990). L-moments: Analysis and Estimation of Distributions using Linear Combinations of Order Statistics. Journal of Royal Statistics Society, 52(1): 105-124.

- Hosking, J. R. M. (1991). Approximations for Use in Constructing L-moment Ratio Diagrams. Report RC16635. IBM Research Division, T. J. Watson Research Center, Yorktown Heights, N.Y. 10598.
- Hosking, J. R. M. (1997). FORTTRAN Routines for Use with the Method of L-moments – Version 3.02. IBM Research Division, Yorktown Heights, N.Y. 10598.
- Hosking, J. R. M. and Wallis, J. R. (1997). Regional Frequency Analysis. Cambridge University Press.
- Huber, W. C., Cunningham, B. A. and Cavender, K. A. (1986). Continuous SWMM Modelling for Selection of Design Events. Comparison of Urban Drainage Models with Real Catchment Data, Dubrovnik, Yugoslavia. Pergamon Press, 379-390.
- Huff, F. A. (1967). Time Distribution of Rainfall in Heavy Storms. Water Resources Research, 3(4): 1007-1019.
- Hughes, W. C. (1977). Peak Discharge Frequency from Rainfall Information. Proceedings of the ASCE, Journal of the Hydraulics Division. 103(HY1): 39-50.
- HYDSYS (1994). HYDSYS/TS Reference Manual – Release 5.0. HYDSYS Pty. Ltd., ACT, Australia.
- Institution of Engineers, Australia (1987). Australian Rainfall and Runoff – Volumes 1 and 2. Institution of Engineers, Australia, Canberra, ACT, Australia.
- Istok, J. D. and Boersma, L. (1986). Effect of Antecedent Rainfall on Runoff during Low Intensity Rainfall. Journal of Hydrology, 88: 329-342.
- James, W. and Robinson, M. (1986). Continuous Deterministic Urban Runoff Modelling. Comparison of Urban Drainage Models with Real Catchment Data, Dubrovnik, Yugoslavia. Pergamon Press, 347-378.
- Knuth, D. E. (1998). The Art of Computer Programming – Volume 2: Seminumerical Algorithms. Addison-Wesley.
- Kottegoda, N. T. and Rosso, R. (1997). Statistics, Probability, and Reliability for Civil and Environmental Engineers. McGraw-Hill Companies, Inc.
- Kuczera, G. (1983a). Improved Parameter Inference in Catchment Models. 1. Evaluating Parameter Uncertainty. Water Resources Research, 19(5):1151-1162.
- Kuczera, G. (1983b). Improved Parameter Inference in Catchment Models. 2. Combining Different Kinds of Hydrologic Data and Testing Their Compatibility. Water Resources Research, 19(5):1163-1172.

- Kuczera, G. (1994). NLFIT – A Bayesian Nonlinear Regression Program Suite – Version 1.00g. Department of Civil, Surveying, and Environmental Engineering, The University of Newcastle, New South Wales, Australia.
- Lambert, M., Williams, B., Field, W. and Kuczera, G. (1994). Taxonomy of Joint Probability Effects in Coastal Floodplains. Water Down Under '94, Adelaide, Australia. I. E. Aust. National Conference Publication, 3:211-216.
- Laurenson, E. M. (1973). Effects of Dams on Flood Frequency. International Symposium On River Mechanics, Bangkok, Thailand. Asian Institute of Technology, 133-146.
- Laurenson, E. M. (1974). Modelling of Stochastic – Deterministic Hydrologic Systems. Water Resources Research, 10(5): 955-961.
- Laurenson, E. M. (1987). Back to Basics on Flood Frequency Analysis. Civil Engineering Transactions, 47-53.
- Laurenson, E. M. and Pearse, M. A. (1991). Frequency of Extreme Rainfall and Floods. International Hydrology and Water Resources Symposium, Perth, Australia. I. E. Aust. National Conference Publication, 392-399.
- Laurenson, E. M. and Mein, R. G. (1995). RORB Runoff Routing Program User Manual – Version 4. Department of Civil Engineering (in conjunction with MONTECH Pty. Ltd.), Monash University, Clayton, Australia.
- Laurenson, E. M. (1998). Personal Communication. Emeritus Professor, Department of Civil Engineering, Monash University, Clayton, Australia.
- Lin, B. and Vogel, J. L. (1993). A Comparison of L-Moments with Methods of Moments. Proceedings of the Symposium on Engineering Hydrology, California, USA. ASCE, 443-448.
- Linsley, R. K., Kohler, M. A. and Paulhus, J. L. H. (1988). Hydrology for Engineers. McGraw-Hill.
- Loukas, A., Quick, M. C. and Russell, S. O. (1996). A Physically Based Stochastic-Deterministic Procedure for the Estimation of Flood Frequency. Water Resources Management, 10: 415-437.
- Lumb, A. M. and James, L. D. (1976). Runoff Files for Flood Hydrograph Simulation. Proceedings of the ASCE, Journal of the Hydraulics Division, 102(HY10): 1515-1531.

- McCloud, P. (1996). Personal Communication. Lecturer, Department of Mathematics and Statistics, Monash University, Clayton, Australia.
- McCuen, R. H. (1985). Statistical Methods for Engineers. Prentice-Hall, Inc.
- McGilchrist, C. A. and Woodyer, K. D. (1975). Note on a Distribution-free CUSUM Technique. Technometrics, 17(3): 321-325.
- McMahan, T. A. and Mein, R. G. (1986). River and Reservoir Yield. Water Resources Publications.
- Mein, R. G. (1995). Program Roundup – Program D: Flood Hydrology. Catchword (Newsletter No. 35). Cooperative Research Centre for Catchment Hydrology, Monash University, Australia.
- Mein, R. G. and Larson, C. L. (1971). Modelling the Infiltration Component of the Rainfall-Runoff Process. Bulletin 43, Water Resources Research Center, University of Minnesota, Minneapolis, MN.
- Mein, R. G. and O'Loughlin, E. M. (1991). A New Approach for Flood Forecasting. International Hydrology and Water Resources Symposium, Perth, Australia. I. E. Aust. National Conference Publication, 219-224.
- Microsoft Corporation (1995). Microsoft Developer Studio – FORTRAN Power Station 4.0. Microsoft Corporation.
- Minty, L. J., Meighen, J. and Kennedy, M. R. (1996). Development of the Generalised Southeast Australia Method for Estimating Probable Maximum Precipitation. Report No. 4. Bureau of Meteorology, Melbourne, Australia.
- Moughamian, M. S., McLaughlin, D. B. and Bras, R. L. (1987). Estimation of Flood Frequency: An Evaluation of Two Derived Distribution Procedures. Water Resources Research, 23(7): 1309-1319.
- Muzik, I. (1993). Derived Physically Based Distribution of Flood Probabilities. Extreme Hydrological Events: Precipitation, Floods and Droughts, Yokohama, Japan. IAHS, 183-188.
- Nandakumar, N., Mein, R. G. and Siriwardena, L. (1994). Loss Modelling for Flood Estimation – A Review. Report 94/4. Cooperative Research Centre for Catchment Hydrology, Monash University, Australia.
- Natural Environment Research Council (1975). Flood Studies Report. Report No. 1. Natural Environment Research Council, Institute of Hydrology, Wallingford, UK.

- Nguyen, V. T. V. and Rousselle, J. (1981). A Stochastic Model for the Time Distribution of Hourly Rainfall Depth. Water Resources Research, 17(2): 399-409.
- Perlado, J. M. (1990). The Monte Carlo Method. Systems Reliability Assessment. Proceedings of the Ispra Courses on Reliability and Risk Analysis, Madrid, Spain. Kluwer Academic Publishers, 23-43.
- Philip, J. R. (1969). Theory of Infiltration. Advances in Hydroscience, 5: 215-296.
- Pilgrim, D. H. and Cordery, I. (1975). Rainfall Temporal Patterns for Design Floods. Proceedings of the ASCE, Journal of the Hydraulics Division, 101(HY1): 81-95.
- Press, W. H., Flannery, B. P., Teukolsky, S. A. and Vetterling, W. T. (1989). Numerical Recipes – The Art of Scientific Computing (FORTRAN Version). Cambridge University Press.
- Rahman, A., Hoang, T. M. T., Weinmann, P. E. and Laurenson, E. M. (1998). Joint Probability Approaches to Design Flood Estimation: A Review. Report 98/8. Cooperative Research Centre for Catchment Hydrology, Monash University, Australia.
- Rahman, A. (1999). Determination of Derived Flood Frequency Curves by Monte Carlo Simulation: Programs. Unpublished Working Document. Cooperative Research Centre for Catchment Hydrology, Monash University, Australia.
- Rahman, A., Weinmann, P. E., Hoang, T. M. T., Laurenson, E. M. and Nathan, R. J. (2001). Monte Carlo Simulation of Flood Frequency Curves from Rainfall. Technical Report 01/4. Cooperative Research Centre for Catchment Hydrology, Monash University, Australia.
- Raines, T. H. and Valdes, J. B. (1993). Estimation of Flood Frequencies for Ungauged Catchments. Journal of Hydraulic Engineering, 119(10): 1138-1154.
- Rawls, W. J., Ahuja, L. R., Brakensiek, D. L. and Shirmohammadi, A. (1993). Chapter 5: Infiltration and Soil Water Movement. Handbook of Hydrology. McGraw-Hill, Inc.
- Robinson, J. S. and Sivapalan, M. (1997). Temporal Scales and Hydrological Regimes: Implications for Flood Frequency Scaling. Water Resources Research, 33(12): 2981-2999.

- Rodriguez-Iturbe, I., Gonzalez, M. and Bras, R. L. (1982). A Geomorphoclimatic Theory of the Instantaneous Unit Hydrograph. Water Resources Research, 18(4): 877-886.
- Rowney, A. C. (1985). CONTHYMO – A Continuous Simulation Model for Regional Storm Water Management Planning and Analysis. Unpublished PhD Thesis. Department of Civil Engineering, University of Ottawa, Ontario, Canada.
- Rubinstein, R. V. (1981). Simulation and the Monte Carlo Method. John Wiley & Sons.
- Russell, S. O., Kenning, B. F. I. and Sunnell, G. J. (1979). Estimating Design Flows for Urban Drainage. Proceedings of the ASCE. Journal of the Hydraulics Division, 105(HY1): 43-52.
- Salas, J. D. (1993). Analysis and Modelling of Hydrologic Time Series. Handbook of Hydrology. D. R. Maidment, McGraw-Hill.
- Searcy, J. K. and Hardison, C. H. (1960). Double Mass Curves. Manual of Hydrology: Part 1. General Surface-Water Techniques. United States Government Printing Office, Washington, 31-66.
- Seed, A. W., Srikanthan, R., and Menabde, M. (1999). Towards More Realistic Design Storms. Handbook and Proceedings of Water 99 Joint Congress, Brisbane, Australia. I. E. Aust. National Conference Publication, 545-549.
- Shen, H. W., Koch, G. J. and Obeysekera, J. T. B. (1990). Physically Based Flood Features and Frequencies. Journal of Hydraulic Engineering, 116(4): 494-514.
- Siriwardena, L. and Mein, R. G. (1995). Development and Testing of a Variable Proportional Loss Model Based on 'Saturation Curves' (A Study on Eight Victorian Catchments). Working Document 95/2. Cooperative Research Centre for Catchment Hydrology, Monash University, Australia.
- Siriwardena, L. and Weinmann, P. E. (1996). Development and Testing of Methodology to Derive Areal Reduction Factors for Long Duration Rainfall. Working Document 96/4. Cooperative Research Centre for Catchment Hydrology, Monash University, Australia.
- Siriwardena, L., Hill, P. I. and Mein, R. G. (1997). Investigation of a Variable Proportional Loss Model for use in Flood Estimation. Report 97/3. Cooperative Research Centre for Catchment Hydrology, Monash University, Australia.

- Sivapalan, M., Wood, E. F. and Beven, K. J. (1990). On Hydrologic Similarity 3. A Dimensionless Flood Frequency Model Using a Generalized Geomorphologic Unit Hydrograph and Partial Area Runoff Generation. Water Resources Research, 26(1): 43-58.
- Sivapalan, M., Bloeschl, G. and Gutknecht, D. (1996). Process Controls on Flood Frequency 1. Derived Flood Frequency. Report ED 1158MS. Centre for Water Research, Department of Environmental Engineering, The University of Western Australia.
- Smith, D. (1998). Report on Work Completed for Vacation Studentship. Unpublished Report. Cooperative Research Centre for Catchment Hydrology, Monash University, Australia.
- Soil Conservation Service (1972). Section 4: Hydrology. National Engineering Handbook. U. S. Department of Agriculture, Washington D. C.
- Stedinger, J. R., Vogel, R. M. and Foufoula-Georgiou, E. (1993). Chapter 18: Frequency Analysis of Extreme Events. Handbook in Hydrology. D. R. Maidment, McGraw-Hill.
- Terstriep, M. L. and Stall, J. B. (1974). The Illinois Urban Drainage Area Simulator, ILLUDAS. Bulletin 58. Illinois State Water Survey.
- Thompson, K. D., Stedinger, J. R. and Heath, D. C. (1997). Evaluation and Presentation of Dam Failure and Flood Risks. Journal of Water Resources Planning and Management, 216-227.
- US Department of Agriculture (1986). Urban Hydrology for Small Watershed. Technical Release No. 55. Soil Conservation Service, US Department of Agriculture, Washington, DC.
- Viessman, W. J., Lewis, G. L. and Knapp, J. W. (1989). Introduction to Hydrology. Harper Collins Publishers.
- Vogel, R. M. and Fennessey, N. M. (1993). L-Moments Diagrams Should Replace Product Moment Diagrams. Water Resources Research, 29(6): 1745-1752.
- Vogel, R. M. and Wilson, I. (1996). Probability Distribution of Annual Maximum, Mean, and Minimum Streamflows in the United States. Journal of Hydraulic Engineering, ASCE, 69-76.
- Walpole, R. E. and Meyers, R. H. (1993). Probability and Statistics for Engineers and Scientists. Prentice-Hall International, Inc.

- Weinmann, P. E. (1994). On the Origin and Variation of Skewness in Flood Frequency Distributions. Water Down Under '94, Adelaide, Australia. I. E. Aust. National Conference Publication, 265-270.
- WMO (1966). Climatic Change. Technical Note No. 79. World Meteorological Organisation.
- Wood, E. F. (1976). An Analysis of the Effects of Parameter Uncertainty in Deterministic Hydrologic Models. Water Resources Research, 12(5): 925-932.
- Wood, E. F. and Hebson, C. S. (1986). On Hydrologic Similarity I. Derivation of the Dimensionless Flood Frequency Curve. Water Resources Research, 22(11): 1549-1554.
- Wood, J. F. and Alvarez, K. (1982). Review of Pindari Dam Design Inflow Flood Estimate. Proceedings of the Workshop on Spillway Design, Monash University, Clayton, Australia. AWRC Conference Series, 119-140.
- Yen, B. C. and Chow, V. T. (1980). Design Hyetographs for Small Drainage Structures. Proceedings of the ASCE, Journal of the Hydraulics Division, 106(HY6): 1055-1077.

## Appendix A

# JOINT PROBABILITY APPROACH: STATISTICAL BASIS

This appendix introduces some basic statistical concepts relevant to the Joint Probability Approach, along with the theoretical background of the joint probability distribution of random variables. The material presented below is summarised from Benjamin and Cornell (1970), and Walpole and Meyers (1993).

### A.1 SOME IMPORTANT STATISTICAL CONCEPTS

The concepts of probability of intersection, probability of union, and the Theorem of Total Probability are discussed below.

#### A.1.1 Probability of intersection

The intersection of two events  $A$  and  $B_i$ , denoted as  $A \cap B_i$ , is the event that contains all elements common to  $A$  and  $B_i$ . Its joint probability is determined by:

$$\text{prob}(A \cap B_i) = \text{prob}(A|B_i)\text{prob}(B_i) \quad (\text{A-1})$$

where  $\text{prob}(A|B_i)$ , called the conditional probability of event  $A$  given  $B_i$ , is the probability of occurrence of the event  $A$  on the condition that the event  $B_i$  has occurred. Conditional probability is a concept of great practical importance. It provides the capability to re-evaluate the probability of an event using additional information (Walpole and Meyers, 1993).

If the occurrence of event  $B_i$  has no impact on the occurrence of event  $A$ , that is if:

$$\text{prob}(A|B_i) = \text{prob}(A) \quad (\text{A-2})$$

then  $A$  and  $B_i$  are independent events. The concept of statistical independence plays a vital role in all areas of statistical applications. From a practical viewpoint, the analysis of many statistical models may become very complicated if the assumption of independence of certain random variables is not accepted in certain key situations (Benjamin and Cornell, 1970).

For the case of independent events, Equation (A-1) becomes:

$$\text{prob}(A \cap B_i) = \text{prob}(A)\text{prob}(B_i) \quad (\text{A-3})$$

### A.1.2 Probability of union

The union of two events  $A$  and  $B$ , denoted as  $A \cup B$ , is the event that occurs if either  $A$  or  $B$  or both occur. Its probability is computed by:

$$\text{prob}(A \cup B) = \text{prob}(A) + \text{prob}(B) - \text{prob}(A \cap B) \quad (\text{A-4})$$

### A.1.3 Theorem of Total Probability

If  $B_i$  ( $i$  varies from 1 to  $n$ , where  $n$  is a positive integer) represents a set of events which satisfies the following two conditions:

- the events are mutually exclusive, that is,  $\text{prob}(B_1 \cup B_2 \cup \dots \cup B_n) = \text{prob}(B_1) + \text{prob}(B_2) + \dots + \text{prob}(B_n)$ , and
- the events are collectively exhaustive, that is,  $\text{prob}(B_1 \cup B_2 \cup \dots \cup B_n) = 1$ ,

then the probability of another event  $A$  can be determined using the Theorem of Total Probability (Figure A-1) :

$$\text{prob}(A) = \sum_{i=1}^n \text{prob}(A|B_i)\text{prob}(B_i) \quad (\text{A-5})$$

This equation indicates that the probability of event  $A$  is the sum of the joint probabilities of  $A$  and  $B_i$  for all possible  $B_i$  values. Thus, the Theorem of Total

Probability allows the calculation of the unconditional probability of an event from a set of its conditional probabilities. It is considered as one of the workhorses in probability applications (Kuczera, 1994).

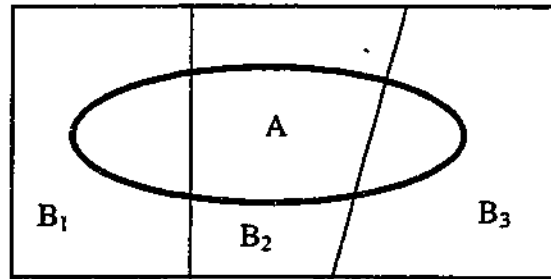


Figure A-1: Venn diagram for the Theorem of Total Probability

The Theorem of Total Probability, expressed in one dimension (B) by Equation (A-5) can also be expanded to two or more dimensions. For example, in three dimensions B, C, D, the theorem can be written for discrete distributions as follows (McCloud, Personal communication, 1996):

$$\text{prob}(A) = \sum_{i=1}^n \sum_{k=1}^m \sum_{x=1}^l \text{prob}(A|B_i, C_k, D_x) \text{prob}(B_i \cap C_k \cap D_x) \quad (\text{A-6})$$

If  $B_i, C_k, D_x$  are independent events, Equation (A-6) becomes:

$$\text{prob}(A) = \sum_{i=1}^n \sum_{k=1}^m \sum_{x=1}^l \text{prob}(A|B_i, C_k, D_x) \text{prob}(B_i) \text{prob}(C_k) \text{prob}(D_x) \quad (\text{A-7})$$

In applying the theorem to the calculation of the probability of design floods, explanations for the terms involved in the above formula are as follows:

- $\text{prob}(A)$  is the unconditional probability of a flood (to be exceeded in any given year),
- $\text{prob}(A|B_i)$  is the conditional probability of a flood given an input  $B_i$  that occurs at the same time as A, not just in the same year,
- $\text{prob}(B_i)$  is the probability of obtaining a value of  $B_i$  for the input B, and
- B, C, D are design random variables, for example, the storm duration, temporal pattern, or loss.

## A.2 JOINT PROBABILITY DISTRIBUTION OF RANDOM VARIABLES

A random variable is a function defined on a sample space. There are two types of random variables: discrete or continuous. A discrete random variable is a random variable that can assume a finite set of values. By contrast, a continuous random variable is a random variable that can assume an infinite set of values.

When two or more random variables are considered simultaneously, their joint behaviour is determined by a joint probability distribution. For discrete random variables, this joint probability distribution is called the joint probability mass function, and for continuous random variables, the joint probability density function. For generality, the section below presents the theoretical background of the joint probability distribution of continuous random variables. The joint probability behaviour of discrete random variables can be studied in standard statistical textbooks.

### A.2.1 Joint probability density function

Consider two random variables  $X$  and  $Y$ . The joint probability that  $X$  lies between  $x_1$  and  $x_2$ , and  $Y$  between  $y_1$  and  $y_2$  is given by:

$$\text{prob}[(x_1 \leq x \leq x_2) \text{ and } (y_1 \leq y \leq y_2)] = \int_{x_1}^{x_2} \int_{y_1}^{y_2} p_{X,Y}(x,y) dy dx \quad (\text{A-8})$$

where  $p_{X,Y}(x,y)$  is the joint probability density function.

The joint cumulative distribution function  $F_{X,Y}(x,y)$ , which represents the joint probability that  $X$  is less than or equal  $x$  and  $Y$  is less than or equal  $y$ , is defined as:

$$F_{X,Y}(x,y) = \text{prob}[X \leq x \text{ and } Y \leq y] = \int_{-\infty}^x \int_{-\infty}^y p_{X,Y}(x,y) dy dx \quad (\text{A-9})$$

The relationship between  $p_{X,Y}(x,y)$  and  $F_{X,Y}(x,y)$  is as follows:

$$p_{X,Y}(x,y) = \frac{\partial^2}{\partial x \partial y} F_{X,Y}(x,y) \quad (\text{A-10})$$

### A.2.2 Marginal distributions

The marginal distributions may be used to describe the behaviour of one of a pair of random variables, regardless of the value of the second random variable. For example, the marginal density function of  $X$ ,  $p_X(x)$ , is obtained by integrating  $p_{X,Y}(x,y)$  over all possible values of  $Y$ .

$$p_X(x) = \int_{-\infty}^{+\infty} p_{X,Y}(x,y) dy \quad (\text{A-11})$$

### A.2.3 Conditional distributions

The distribution of one variable with restrictions or conditions placed on the second variable is called a conditional distribution. For example, the conditional density function of  $X$  when  $Y$  is given is defined by:

$$p_{X|Y}(x | y) = \frac{p_{X,Y}(x,y)}{p_Y(y)} \quad (\text{A-12})$$

### A.2.4 Independence of random variables

Two random variables  $X$  and  $Y$  are independent if the conditional density function equals the marginal density function, that is:

$$p_{X|Y}(x | y) = p_X(x) \quad (\text{A-13})$$

In this case, the joint probability density function of  $X$  and  $Y$  is the product of their marginal density distributions.

$$p_{X,Y}(x,y) = p_X(x)p_Y(y) \quad (\text{A-14})$$

**Appendix B****PREVIOUS STUDIES OF THE JOINT PROBABILITY  
APPROACH TO DESIGN FLOOD ESTIMATION**

This appendix presents a summary of previous studies of the Joint Probability Approach to the estimation of design floods from design rainfalls.

The appendix consists of three tables. Tables B-1, B-2 and B-3 document previous studies that use analytical methods, approximate numerical methods, and Monte Carlo simulation for determining the flood probability distribution, respectively. For each study, the models used to represent the design rainfall, runoff production and runoff routing processes are described. Characteristics of each study, together with the results obtained are also summarised.

Table B-1: Studies based on analytical methods

Authors	Rainfall models	Runoff production models	Runoff routing models	Characteristics of the studies and results
Eagleson (1972)	- rainfall intensity and duration: exponential distributions - uniform temporal patterns	- constant loss rate - partial area concept	kinematic wave theory	- The method was developed for a catchment of V-shape. - Rainfall intensity and duration were assumed to be independent random variables. - The form of the flood frequency curve was influenced by catchment and rainfall parameters. - Flood peaks were overestimated because the kinematic wave equation omitted the attenuation of flows. - A significant improvement of the method could be made by removing the assumption of independence of stochastic inputs.
Wood (1976)	Eagleson's (1972) rainfall model	infiltration rate (represented by different distributions)	kinematic wave theory	- Rainfall intensity, duration, and loss rate were assumed to be independent random variables. - Infiltration rate was characterised by uniform, exponential, or Gamma 1 distribution. - Serious design problems may arise due to parameter uncertainty. For example, the use of a point estimate for the rainfall loss rate underestimated the exceedance probability of a given peak discharge.
Hebson and Wood (1982)	Eagleson's (1972) rainfall model	- constant infiltration capacity - partial area concept	geomorphologic unit hydrograph (GUH)	- The GUH is a linear rainfall-runoff model developed from considerations of physical properties of catchment and drainage networks. - In studying flood frequency behaviour, the GUH appeared to be theoretically more suitable than the kinematic wave method. - Catchment shape plays an important role in flood frequency behaviour.
Diaz-Granados et al. (1984)	Eagleson's (1972) rainfall model	Philip's infiltration equation	geomorphoclimatic unit hydrograph (GcUH)	- The GcUH, developed by Rodriguez-Iturbe et al. (1982), is a modified version of the GUH in that it incorporates climate and catchment geomorphology in rainfall-runoff behaviour. - The flood frequency distribution derived was a function of initial soil moisture. - The model did not perform well in humid regions, possibly because soil moisture may play an important role in estimating rare events.

Wood and Hebson (1986)	- storm intensity: gamma distribution - storm duration: exponential distribution	- Hortonian runoff generation process	dimensionless geomorphologic unit hydrograph	- Random variables (rainfall intensity and duration) were assumed to be independent. - The dimensionless flood frequency curve was derived from dimensionless areal rainfall to improve understanding of hydrologic similarity among basin responses and their influence on flood frequency characteristics.
Moughamian et al. (1987)				- Examined performance of the methods recommended by Hebson and Wood (1982) and Diaz-Granados et al. (1984). - Both methods performed poorly on 3 test basins. - Significant errors in derived flood frequency curves could have resulted from small variations in parameters of the rainfall and loss models. - Eagleson's rainfall model (Eagleson, 1972) did not include any information about the nature of large storms which were responsible for large floods. - The catchment response models used were probably not sufficiently general to describe runoff generation over a wide range of events. - It was recommended that further research should investigate rainfall models that put more emphasis on large storms, and identify qualitative differences in runoff mechanisms influencing floods of different sizes.
Haan and Edwards (1988)	storm intensity: Extreme Value type I distribution	SCS Curve Number method (Soil Conservation Service, 1972)		- Rainfall volume and maximum abstraction from rainfall were assumed to be independent random variables. - For the 7 test catchments and for a given return period, the proposed approach always gave flood volume estimates higher than the current event method. However, the estimates tended to converge for low return periods.
Sivapalan et al. (1990)	- scaled rainfall intensity: gamma distribution - scaled duration: exponential distribution	- infiltration model - partial runoff generation process	generalised GUH	- The generalised GUH is a modified version of the GUH that includes partial area runoff generation by both Hortonian and Dunne mechanisms. - The flood frequency model was theoretically developed but Monte Carlo simulation was used to numerically evaluate the derived dimensionless cumulative distribution function of flood peaks. - Sensitivity analysis showed that the flood frequency curve was strongly influenced by the runoff generation process, the scale of catchments and storms. The flood frequency curve seemed to be the result of mixed runoff production mechanisms, each governing the shape of the curve at a particular range of return periods. - Tests of the method on actual catchments were needed.

Shen et al. (1990)	Eagleson's (1972) rainfall model	Philip's infiltration equation	kinematic wave theory	<ul style="list-style-type: none"> <li>- The flood frequency distribution was analytically derived, but numerical integration was used to practically solve the derived distribution.</li> <li>- For the 4 contrived basins used in the study, it was shown that floods of a given frequency were strongly influenced by soil types and initial soil moisture used in the infiltration model. An accurate estimation of soil properties seemed to be extremely important.</li> <li>- The rainfall-runoff model used in deriving the flood frequency curve was developed for small basins having some specified physical characteristics.</li> </ul>
Cadavid et al. (1991)	Eagleson's (1972) rainfall model	Philip's infiltration equation	kinematic wave theory	<ul style="list-style-type: none"> <li>- The method was derived for catchments conceptualised as two symmetric planes discharging into first order streams.</li> <li>- The derived and observed peak flow distributions deviated appreciably for high events, possibly due to differences in the precipitation process controlling flood formation, and sampling errors in high flood values.</li> <li>- Inaccuracy in the estimation of rainfall parameters, especially the mean intensity, appeared to have a major impact on results.</li> </ul>
Raines and Valdes (1993)	Eagleson's (1972) rainfall model	SCS Curve Number method (Soil Conservation Service, 1972)	geomorphoclimatic unit hydrograph (GcUH)	<ul style="list-style-type: none"> <li>- There was a wide variation in the flood frequency curves derived for 4 test catchments when compared the results obtained from the proposed approach with those obtained from the methods developed by Hebson and Wood (1982), and Diaz-Granados et al. (1984).</li> <li>- The magnitude and slope of the derived flood frequency curve seemed to be strongly influenced by the estimation of rainfall parameters, and the loss model used.</li> </ul>
Sivapalan et al. (1996)	<ul style="list-style-type: none"> <li>- IFD curves (Gumbel distribution)</li> <li>- storm duration (Weibull distribution)</li> </ul>	runoff coefficient	instantaneous unit hydrograph (IUH) based on 3 parallel linear storages	<ul style="list-style-type: none"> <li>- Periods of zero rainfall exceeding two hours were used to separate individual rainfall events.</li> <li>- The joint probability distribution of rainfall intensity and duration was approximated by multiplying the burst IFD curves with the marginal distribution of storm duration.</li> <li>- The study aimed at identifying the processes that control the shape of the flood frequency curve. Results indicated that this shape was influenced by the rainfall temporal pattern and multiple storms, and the non-linear dependence of runoff coefficient on rainfall depth.</li> <li>- It was demonstrated that peak runoff was not affected by rainfall temporal patterns for catchments with response time large compared to storm duration.</li> </ul>

Table B-2: Studies based on approximate numerical methods

Authors	Rainfall models	Runoff production models	Runoff routing models	Characteristics of the studies and results
Laurenson (1974)	Not applicable	Not applicable	Not applicable	<ul style="list-style-type: none"> <li>- Laurenson (1974) proposed a method of modelling systems that contain both stochastic and deterministic components. This is achieved by dividing the system into a sequence of steps, each step transforms an input distribution into an output distribution, which becomes the input to the next step. The probability of the output at each step can be calculated from the Theorem of Total Probability using the input distribution and a transition probability that reflects the deterministic components of the system.</li> <li>- In general, the method offers a wide range of application in hydrology when the stochastic-deterministic nature of the problem needs to be accounted for (Laurenson, 1973; Laurenson, 1974; Ahern and Weinmann, 1982). For example, in extreme flood estimation, the method was applied to compute the frequency of extreme precipitation from the joint distribution of the convergence component of rainfall and dew point (Laurenson and Pearse, 1991).</li> </ul>
Beran (1973)	IFD curves	infiltration loss	unit hydrograph	<ul style="list-style-type: none"> <li>- Rainfall depth, duration, temporal pattern, and catchment wetness index were assumed to be independent random variables.</li> <li>- A storm definition was used to allow any wet spell to contribute a single value to the distributions of depth and duration. However, due to insufficient rainfall record for the development of the statistical distribution of storm depth, existing IFD curves, which were derived from a different storm definition, were used to represent storm depth.</li> <li>- The distribution of storm temporal patterns was described by Huff curves (Huff, 1967).</li> <li>- Given a specific combination of inputs, the probability of the resulting flood was the product of the probabilities of input variables. The flood distribution was then established by summing probabilities in each discharge interval.</li> <li>- The storm losses and rainfall depth are identified as the most important factors affecting the flood magnitude.</li> <li>- The derived flood frequency curve was flatter than the observed one, possibly because of the discrepancy between the storm definitions used.</li> </ul>

Hughes (1977)	IFD curves	SCS Curve Number method (Soil Conservation Service, 1972)		<ul style="list-style-type: none"> <li>- The frequency curves of peak discharge and runoff volume were developed using the Theorem of Total Probability.</li> <li>- Loss rates, characterised by curve numbers, were represented by statistical distributions.</li> <li>- The proposed method produced acceptable results in a test catchment. Nevertheless a complete verification of the procedure was recommended.</li> </ul>
Goyen (1983)	IFD curves	Stochastic Deterministic Loss Model (SDLM) based on the ARBM model	RAFTS model	<ul style="list-style-type: none"> <li>- Rainfall and antecedent soil moisture were assumed to be independent random variables.</li> <li>- The SDLM is a loss model which combines the stochastic nature of rainfall and antecedent moisture index through the deterministic infiltration component of the Australian Representative Basins Model (ARBM) (Chapman, 1968).</li> <li>- The distribution of antecedent moisture index was determined from the water balance described by the ARBM and the Philip infiltration equation.</li> <li>- Laurenson's stochastic-deterministic modelling approach (Laurenson, 1974), which makes use of the Theorem of Total Probability, was employed to determine the probability distribution of flood peaks.</li> <li>- The recommended method gave satisfactory results for an urban catchment.</li> </ul>
Fontaine and Potter (1993)	stochastic rainfall model developed by storm transposition method	SCS Curve Number method (Soil Conservation Service, 1972)	HEC-1, based on the unit hydrograph theory	<ul style="list-style-type: none"> <li>- The discrete probability distribution of antecedent soil moisture was represented by three curve numbers.</li> <li>- The Theorem of Total Probability was used to calculate the exceedance probability of floods from all significant combinations of rainfall and soil moisture conditions.</li> <li>- The method can only be applied to certain types of sites where data about soil moisture, land use, and soil types are sufficient to develop the distribution of antecedent moisture.</li> </ul>
Consuegra et al. (1993)	IFD curves	improved SCS Curve Number method (Rowney, 1985)	unit hydrograph	<ul style="list-style-type: none"> <li>- Rainfall depth and antecedent precipitation index (API) were considered as independent random variables.</li> <li>- The method computed flood return periods from the joint probability of occurrence of rainfall and API.</li> <li>- In applying the method to a watershed, the results obtained compared fairly well with those computed using continuous simulation.</li> </ul>

Table B-3: Studies based on Monte Carlo simulation

Authors	Rainfall models	Runoff production models	Runoff routing models	Characteristics of the studies and results
Beven (1987)	<ul style="list-style-type: none"> <li>- Eagleson's (1972) rainfall model</li> <li>- simulated storm temporal patterns</li> </ul>	TOPMODEL	TOPMODEL	<ul style="list-style-type: none"> <li>- Rainfall intensity and duration were assumed to be independent variables, but the correlation of initial soil moisture deficit and discharge was considered.</li> <li>- The temporal pattern of rainfall was considered as a random variable by adding a random component to the mean rainfall profile for each hour of rain. The random component was assumed to be a first order Markov process with mean, standard deviation, and lag one auto-correlation determined from observed data.</li> <li>- Soil moisture deficit was described by an exponential distribution.</li> <li>- The TOPMODEL is a runoff production and routing model that considers catchment geomorphology and the contributions of surface and sub-surface runoff to flood flows. Model parameters should be determined from soil profile conductivity, soil water storage, or time varying infiltration rate, etc.</li> <li>- The procedure satisfactorily simulated hourly mean flow for a catchment, however, further improvements of the model were suggested.</li> </ul>
Muzik (1993)	rainfall depth described by the Gumbel distribution	modified SCS Curve Number method	unit hydrograph	<ul style="list-style-type: none"> <li>- The modified SCS Curve Number method considers the stochastic nature of initial abstraction (<math>I_a</math>), 5-day antecedent rainfall (P5), and maximum potential soil moisture storage (S).</li> <li>- The dependence of S and P5 was considered.</li> <li>- Monte Carlo simulation was used to generate peak discharge from randomly chosen values of rainfall depth and parameters of the SCS Curve Number model.</li> <li>- Compared with the LPIII plotted for recorded floods at the test catchment, there was a significant difference in the tail of the derived flood frequency curve.</li> </ul>
Bloeschl and Sivapalan (1997)	<ul style="list-style-type: none"> <li>- IFD curves</li> <li>- storm duration (exponential distribution)</li> <li>- uniform storm temporal patterns</li> </ul>		linear reservoir routing method	<ul style="list-style-type: none"> <li>- Rainfall probability was drawn from a uniform distribution.</li> <li>- Monte Carlo simulation was used to calculate peak flows from rainfall depths and randomly selected storm durations.</li> <li>- It was shown that the assumption of equality of rainfall and flood return periods caused significant errors in the estimated flood. For the test catchment, the current event-based method underestimated flood return periods by a factor of at least 2, but this factor may be as large as 10.</li> </ul>

Franchini et al. (1996)	extreme rainfall developed by the stochastic storm transposition method	ARNO model	ARNO model	<ul style="list-style-type: none"> <li>- Temporal patterns and initial soil moisture were assumed to be independent random variables.</li> <li>- ARNO is a 14-parameter rainfall-runoff model representing 2 components: a soil-level water balance and a transfer (routing) component.</li> <li>- Huff curves (Huff, 1967) were used to statistically describe the temporal distribution of storms.</li> <li>- To account for the stochastic nature of moisture conditions, the analysis was repeated for a range of fixed antecedent moisture conditions.</li> <li>- It was demonstrated that, for a given storm depth: (i) the variability of flood peaks was produced from the variability of the temporal distribution of storm depths and initial soil moisture conditions, and (ii) the frequencies of the design storm depth and flood peak were unequal, especially for very wet antecedent moisture conditions.</li> </ul>
Loukas et al. (1996)	<ul style="list-style-type: none"> <li>- rainfall depth: EVI distribution</li> <li>- rainfall duration: 24-hour</li> <li>- rainfall temporal patterns: triangular distribution</li> </ul>	infiltration rate	linear routing model	<ul style="list-style-type: none"> <li>- A triangular distribution was used to statistically model the dimensionless cumulative rainfall depth.</li> <li>- Infiltration loss is a constant for each event and normally distributed from event to event.</li> <li>- Storage factor of fast runoff is normally distributed, and can be computed from catchment geomorphology.</li> <li>- Monte Carlo simulation was used to generate 5000 estimates of runoff hydrograph characteristics (peak hourly, daily discharge, peak flood volume).</li> <li>- Compared with observed data from eight coastal British Columbia basins, the simulated peak hourly and peak daily flows were not significantly different from the observed ones at 5% level, but the simulated flood volume was.</li> <li>- Sensitivity analysis showed that: (i) of the three hydrograph characteristics investigated, hourly peakflow was most sensitive to the variation of rainfall depths and parameter values, and distributional types of storage factor, and (ii) overall, the procedure was not very sensitive to uncertainties in the values and form of model parameters.</li> </ul>

## Appendix C

# LOSS MODELS

### C.1 INTRODUCTION

In rainfall-based design flood estimation, specifying losses from a design rainfall is a recurring issue faced by many hydrologists. With the commonly used Design Event Approach, the design loss is often adopted as a representative value of a recommended range. As the resulting design flood estimate is very sensitive to the adopted value of the rainfall loss, the uncertainty in the correct rainfall loss for use in a design situation constitutes one of the major drawbacks of the Design Event Approach.

To account for the fact that the rainfall loss can take on a range of values depending on the actual condition of the catchment at the time of a rainfall event, the rainfall loss should be represented by a probability distribution. This is one of the aims of the proposed Joint Probability Model for rainfall-based design flood estimation, in which the probabilistic nature of flood causing components is considered. To provide the theoretical background of the development of the probability distribution of the rainfall loss, this appendix introduces elementary loss concepts and models for computing losses from rainfall.

### C.2 ELEMENTARY LOSS CONCEPTS

Before being able to evaluate different models for computing rainfall losses, some important loss concepts need to be clarified. These include (i) loss definitions, and (ii) runoff generation processes. Item (i) plays an important role in loss modelling because the way the rainfall loss is defined determines its estimated value and therefore affects

the resulting design flood. Item (ii) provides a basis for the evaluation and selection of an appropriate loss model for this research.

### C.2.1 Loss definitions

In hydrology, the term "loss" can be roughly defined as the difference between rainfall and runoff. This leads to two possible loss definitions, depending on the type of runoff being referred to. Figure C-1 shows two runoff types together with the components of rainfall and runoff.

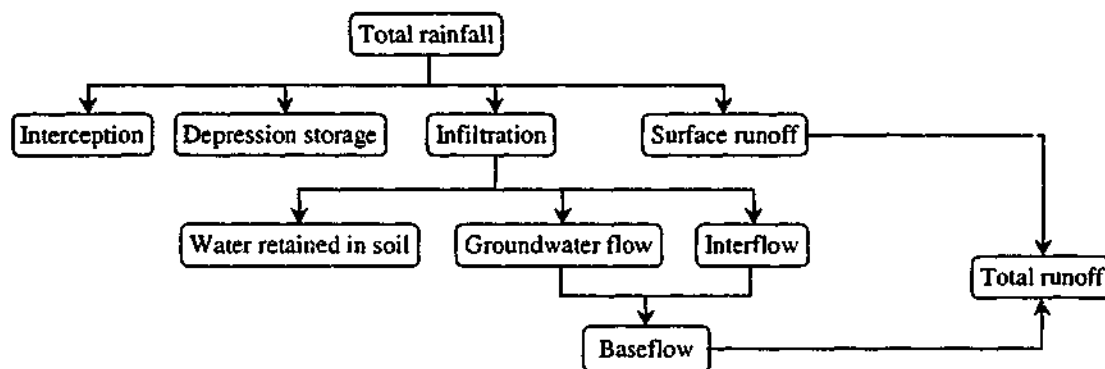


Figure C-1: Components of rainfall and runoff

The first definition relates the loss to the portion of rainfall that does not come out as *total runoff*. The rainfall loss thus comprises the interception loss, depression storage, and only the part of infiltration that replenishes soil moisture deficiencies (see Figure C-1). Baseflow is *not* considered as loss, but added to the surface runoff to produce the total runoff. Depending on the size of the drainage area, the release of baseflow into streamflow may occur within days after the storm event, or more often in months or years (Viessman et al., 1989). This definition of loss is used when long time steps are considered in flood estimation, therefore baseflow has enough time to reach the stream channel. This is relevant to *yield hydrology* where the movement and transfer of water from the atmosphere to the land and back to the atmosphere are usually accounted for on a monthly or annual basis. It is noted that, over a long period of time, the above loss components are eventually the evapo-transpiration transferred from the catchment into the atmosphere (and possibly ground water outflows other than to streams).

The second definition relates the loss to the difference between the rainfall and *surface runoff* (also called direct runoff). From Figure C-1, it can be seen that *baseflow is also a loss component*. This is true for short time intervals such as the duration of a storm, in which case the baseflow has insufficient time to reach the stream channel as it usually has a long response time. This definition of the rainfall loss is applied to *flood hydrology* and adopted in this research. In this case, due to the use of short time periods, evapo-transpiration is neglected during storms.

## **C.2.2 Runoff generation processes**

There are three recognised runoff mechanisms, namely, Hortonian overland flow, saturated overland flow, and interflow. An outline of these mechanisms, summarised from the Institution of Engineers, Australia (1987, Chapter 6) and Viessman et al. (1989), is given below.

### **C.2.2.1 Hortonian overland flow**

The Hortonian runoff mechanism is the classical concept of storm runoff generation. This mechanism assumes that surface runoff occurs on the ground surface when rainfall intensity exceeds infiltration capacity. As infiltration capacity varies from point to point (depending on antecedent rainfall, soil characteristics, or vegetal cover), in theory, Hortonian runoff is not uniform over the catchment. However, in practice, it is often assumed that infiltration capacity, rainfall and, consequently, runoff are spatially uniform.

Hortonian overland flow is likely to occur on impervious surfaces in urban catchments, or in rural catchments with soil layers of low infiltration capacity, as in arid or semi-arid regions (Chow et al., 1988). It is also assumed to be the result of heavy storms because in these cases runoff tends to occur over the entire catchment.

### **C.2.2.2 Saturated overland flow**

The saturated overland flow concept postulates that surface runoff occurs when precipitation falls onto a soil saturated from below, due to the rise of a shallow water table, or the build up of a saturated zone above a soil layer of low hydraulic conductivity. Due to the spatial variability in the soil structure and in the depth to the water table, it is likely that the saturated surface may not cover the entire catchment. This leads to the 'source area' (also called 'partial area') concept in runoff generation, which assumes that the overland flow occurs only on saturated parts of the catchment. These source areas vary during the storm and in different seasons, depending on antecedent conditions and storm rainfall (Linsley et al., 1988).

Saturated overland flow is dominant in a number of cases, for example, in regions with high water tables, at the bottom of slopes or near stream banks where the soil surface is likely to be saturated by underlying water, or in areas with thin soil layers overlying relatively impervious strata.

### **C.2.2.3 Interflow**

Interflow (or through flow) is the part of infiltrated water that moves horizontally in a temporarily saturated zone, often above a nearly impervious soil stratum, to reach a stream channel relatively quickly. It is commonly considered as a component of surface runoff because it rapidly contributes to streamflow during the duration of a storm.

Interflow most often occurs in areas having a shallow and highly permeable surface soil layer lying above an impermeable base.

## **C.3 LOSS MODELS**

Many models are available for estimating the rainfall loss. A description of these models is presented by the Natural Environment Research Council (1975), the

Institution of Engineers, Australia (1987, Chapter 6), and Nandakumar et al. (1994). In general, these loss models can be classified as infiltration models and practical loss models. A brief review of both types of models is presented in the following section.

### **C.3.1 Infiltration models**

Infiltration is generally the most important component of the rainfall loss. It is the process by which water passes through the soil surface into the soil. This process is dependent on many factors such as soil type, soil characteristics, land cover, or rainfall intensity.

There are innumerable models for computing the infiltration loss from rainfall, resulting in various infiltration equations (Viessman et al., 1989; Rawls et al., 1993; Nandakumar et al., 1994). These equations can be classified as theoretical equations and empirical equations. An introduction to these equations is given below.

#### **C.3.1.1 Theoretical equations**

The theoretical infiltration equations are analytically derived to describe the movement of water in porous media. The basis of these equations is Darcy's Law (Rawls et al., 1993) which calculates flow velocity through a saturated porous medium. This equation was then modified in order to reflect the real situation in which water flows in unsaturated soils, and combined with the law of conservation of mass to become the Richard equation. This is a general infiltration equation describing three-dimensional flow in unsaturated soils as a function of time. Finding an analytical solution to this equation is computationally demanding and so far the equation is still considered impractical for routine applications (Nandakumar et al., 1994).

Other well-known physically based infiltration equations include the Philip model (Philip, 1969) and the Green-Ampt model (Green and Ampt, 1911), the latter being modified by Mein and Larson (1971) to calculate the infiltration capacity for different rainfall and surface conditions. The Phillip equation is introduced in more detail here

because it was applied to derive the probability distribution of antecedent soil moisture for estimating design floods (Goyen, 1983). This equation, developed for vertical infiltration into nonlayered homogeneous soils with a constant initial moisture content, takes the following form:

$$q(t) = \frac{1}{2}S_0t^{-1/2} + A^* \quad (C-1)$$

where  $q(t)$  is the infiltration rate at time  $t$ ;  $S_0$  is sorptivity, dependent on initial moisture content and water depth in soil; and  $A^*$  is a constant, assumed to equal the saturated hydraulic conductivity. Both  $S_0$  and  $A^*$  can be estimated using observed data.

### C.3.1.2 Empirical equations

Empirical equations are developed from observations of field experiments to describe and formulate the infiltration process. In these equations, the infiltration rate is generally a function of time, antecedent soil moisture and some soil properties. The earliest empirical infiltration model was proposed by Horton (1935). In this model, infiltration capacity starts with an initial value, decays with time according to an exponential function, and reaches a final constant rate when the soil is saturated. Some other popular infiltration models are the Huggins-Monke model or the Holtan model, an introduction of which is presented by Viessman et al. (1989).

One common feature of these models is that they enable the infiltration loss to be estimated at a point, and that their model parameters should be estimated from observed data. However, as mentioned before, infiltration rates vary from point to point due to many factors such as rainfall intensity, soil characteristics, vegetation cover, and topography. As a result, a number of methods have been proposed to account for the spatial variability of infiltration rates. A review of these methods and their applications in runoff estimation is given by Nandakumar et al. (1994).

In general, the use of infiltration models for computing the rainfall loss from a storm event can be considered as inappropriate for three reasons. Firstly, they neglect the storm losses due to interception and detention storage. These forms of losses follow different laws from infiltration, and may be significant under certain circumstances. For

instance, the interception may be a considerable portion of rainfall in regions with dense vegetation, or the depression loss may be significant for deep storage (Linsley et al., 1988). Secondly, infiltration in itself may not be entirely a loss in that a part of it, the interflow, actually contributes to streamflow. This is true for areas where the interflow runoff mechanism applies. Finally, it may be difficult to determine the coefficients or parameters of some infiltration equations due to the lack of observed data.

### **C.3.2 Practical loss models**

Practical loss models are commonly used in place of infiltration equations because they are conceptually simpler. In essence, these are lumped models because they ignore the spatial variation of the loss during the duration of a rainfall event. Practical loss models can be classified as loss rate models, proportional loss models, initial loss – continuing (or proportional) loss models, and the SCS Curve Number method. A summary of these models is given below.

#### **C.3.2.1 Loss rate models**

The loss rate models can be subdivided into the constant loss rate model and the variable loss rate model.

##### **The constant loss rate model**

The constant loss rate model (also called the  $\phi$  index) is the simplest loss model in which the total loss from rainfall is averaged throughout the rainfall event. The constant loss rate is the rate which equates the volume of rainfall excess (from the rainfall hyetograph) to the surface runoff volume (from the flood hydrograph over the catchment), both of which are measured in the same units. A variation of this model is the  $W$  index, which is the  $\phi$  index minus the average rate of retention by interception and depression storage (Linsley et al., 1988).

The constant loss rate model is suitable for large storms on initially wet catchments, in cases where the Hortonian runoff is dominant, or where the infiltration rate may be assumed constant (Viessman et al., 1989). It is also applicable to storms of long duration, in which cases the time distribution of infiltration may not be very important (Bras, 1990).

The constant loss rate model has many characteristics. It is a simple model with only one parameter. It considers all forms of rainfall losses (including interception, detention storage, and all components of infiltration) regardless of whether it contributes to groundwater flow or interflow, then averages them over the catchment area and throughout the supply period. In addition, it is event dependent, that is, the loss rate derived for one storm is not applicable to another storm.

Traditionally, the event-dependent characteristic of the constant loss rate model is often considered as the main disadvantage of this model. Viessman et al. (1989) argued that unless the constant loss rate is correlated with basin parameters other than runoff, it is of little value. Nevertheless, for cases where the rainfall loss is considered as a random variable, the constant loss rate model may offer the simplest means to derive the probability distribution of the rainfall loss.

#### **The variable loss rate model**

The variable loss rate model, originally introduced by the Natural Environment Research Council (1975), describes the rainfall loss as a curve that decreases as the rain progresses and increases during periods of no rain. The loss rate is thus a random variable inversely related to soil moisture conditions antecedent to and during a storm event. The soil moisture is represented by a catchment wetness index (Natural Environment Research Council, 1975) determined from soil moisture deficit (that is, the amount of water needed to bring the soil to field capacity) and a five day antecedent precipitation index of the accounting period. The latter is the most widely used moisture index that relates the moisture status of the basin directly to rainfall.

The variable loss rate model has many characteristics. For example, it is a complex, multivariate model. It is also a realistic model because it distributes the loss according to the changing moisture condition of the catchment. In addition, the loss rate

computed is dependent on rainfall intensity.

Broadly speaking, the variable loss rate model is more appropriate for flood forecasting than for design flood estimation. This is due to the fact that the variable rate of rainfall loss is estimated from *updated* catchment wetness at the start of each calculation period. This type of information is often available in flood forecasting.

### **C.3.2.2 Proportional loss models**

Like the case of loss rate models, proportional loss models can be subdivided into constant and variable proportional loss models.

#### **Constant proportional loss model**

The constant proportional loss model is equivalent to the runoff coefficient concept because the loss (and therefore runoff) is a fixed proportion of the rainfall rate. In other words, rainfall excess always occurs regardless of the rainfall intensity.

The proportional loss model is best applied to cases where runoff is generated from source areas. An example is urban catchments where the impervious area is often a constant fraction of the total catchment area. In this case, it is assumed that one hundred percent runoff is produced from the impervious areas and none from the pervious areas. Therefore, even when a very light rain occurs, rainfall excess is always generated from the impervious parts of the catchment. This loss model can also be applied to forested rural catchments (Flavell and Belstead, 1986).

#### **The variable proportional loss model**

Adopting the variable source area concept, the variable proportional loss model assumes that as the rain progresses, a greater portion of rainfall contributes to runoff because a greater portion of the catchment becomes saturated.

Many methods have been suggested for computing the variable proportional loss, a summary of which is presented by Siriwardena and Mein (1995). For example, a regional model that relates the variable proportional loss to the antecedent wetness

index, storm rainfall, and catchment characteristics is proposed by the Natural Environment Research Council (1975). In another method, the size and location of catchment source areas, expanded during the storm, are predicted as a function of pre-storm baseflow and rainfall depth (Mein and O'Loughlin, 1991). This approach is then further developed by Siriwardena and Mein (1995), the results of which indicate that the variable proportional loss can be described by a family of curves called the saturation curves. The accuracy in the estimation of these saturation curves is dependent on the estimation of the volumetric runoff coefficient.

Even though the above proportional loss models provide relatively satisfactory results, the main restriction of these models is that they have solely been investigated for flood forecasting purposes.

#### **C.3.2.3 The initial loss – continuing loss model**

The initial loss – continuing loss model (IL-CL) assumes that there is no surface runoff until an initial loss is satisfied. A continuing loss then occurs during the remaining storm duration. The initial loss consists of interception, depression storage and initial infiltration, and the continuing loss can be expressed as a rate or as a proportion of rainfall. The continuing loss rate may be a constant or a variable rate, and so is the proportional continuing loss. In Australia, the initial loss – constant continuing loss rate model is most commonly used due to its simplicity and its ability to approximate the actual loss process (Hill et al., 1996a).

The IL-CL model is appropriate where runoff is generated by the Hortonian process. In this case, it is noted that the continuing loss rate determined for large floods is fairly independent of catchment conditions (Cordery and Pilgrim, 1983; Institution of Engineers, Australia, 1987, Chapter 6).

#### **C.3.2.4 The SCS Curve Number method**

Another popular method for directly computing runoff (and thus relevant for the

estimation of storm losses) is the SCS Curve Number method (Soil Conservation Service, 1972; US Department of Agriculture, 1986). This empirical procedure was originally developed for the estimation of peakflows and runoff volumes for small agricultural catchments, then extended for the estimation of complete hydrographs.

The SCS runoff equation is as follows:

$$Q = \frac{(P - I_a)^2}{(P - I_a) + S^*} \quad (C-2)$$

where: Q is runoff; P is rainfall;  $S^*$  is the maximum retention after runoff begins; and  $I_a$  is initial abstraction, all expressed in units of depth (inches).

For the case  $I_a = 0.2S^*$ , Equation (C-2) becomes:

$$Q = \frac{(P - 0.2S^*)^2}{P + 0.8S^*} \quad (C-3)$$

The SCS Curve Number method essentially adopts an initial loss – variable continuing loss model for the computation of rainfall excess. This is attributed to the fact that it uses the initial water abstraction that is equivalent to the initial loss concept, and the maximum potential water retention which decreases during the rain duration.

As  $I_a$  can be empirically estimated through  $S^*$ , and  $S^*$  is related to soil and conditions of the watershed through a Curve Number, this method allows direct runoff to be directly determined from a specified storm and a series of curves, each curve is represented by a number. The Curve Number is a function of antecedent moisture contents, agricultural land use and treatment, catchment hydrologic conditions and hydrologic soil groups. The last item classifies soils according to their potential to produce runoff (high, medium, or low). The precision of this method is affected by both the choice of the Curve Number and the estimation of antecedent moisture conditions of the catchment.

The SCS Curve Number method is widely used in the United States for agricultural watersheds of up to 2000 acres or 8km<sup>2</sup> (Viessman et al., 1989). In Australia, application of this method to some catchments reveals large errors and substantial bias (Institution of Engineers, Australia, 1987, Chapter 5).

The SCS Curve Number method is recommended for use only when locally derived Curve Number values are available (Institution of Engineers, Australia, 1987, Chapter 5). The method does not consider the storm duration or the rainfall intensity. In addition, the equation used to calculate runoff has no theoretical or empirical justification.

#### **C.4 SUMMARY**

This appendix introduces two different definitions of storm losses and describes the three processes for runoff generation, namely Hortonian overland flow, saturated overland flow, and interflow. It also gives a brief review of infiltration and practical loss models for computing the rainfall loss. Practical loss models appear to be more appropriate for design flood estimation due to their conceptual simplicity and their ability to approximate catchment runoff behaviour.

## Appendix D

# DATA VERIFICATION

### D.1 INTRODUCTION

The reliability of data used in a statistical analysis plays a crucial role in the analysis outcomes. For environmental data such as temperature, rainfall, or flowrate, in order to estimate future values at a given site, it is important that data collected at the site must be a true representation of the quantity being measured and must all be drawn from the same frequency distribution. As this study aims to derive the flood frequency curve from the statistical distributions of rainfall and loss characteristics, it is clear that rainfall and flow data should be inspected before analyses of these data are undertaken.

Broadly speaking, the four requirements of environmental data used in a statistical analysis are homogeneity, stationarity, consistency, and representativeness (McMahon and Mein, 1986). The requirement of homogeneity is that data should be drawn from the same statistical distribution so that they are comparable throughout the period of record. Similarly, a data sample is stationary if its statistical properties do not change with time. Thus, stationarity is essentially homogeneity, expressed in the time domain (Laurenson, Personal communication, 1998). Heterogeneity or non-stationarity is generally caused by shifts in location of gauges, changes in land use or exposure conditions. These may bring about an abrupt change (in the form of a discontinuity, or a jump), or a gradual change (in the form of a trend) which takes place over a period of time in the absolute measurements of a data series. The requirement of consistency is that types and techniques of measurement or the manner of data processing should be consistent. Representativeness of data ensures that samples used in an analysis are representative of the long-term variability of data at a specified location.

For the present study, observed rainfall and flow data were assumed to represent the long-term variability of rainfall or streamflow at any given site, but the verification of

these data for homogeneity and consistency was considered essential. This appendix describes the homogeneity tests used in this study, and applications of these tests to the extracted rainfall and flow data.

## D.2 HOMOGENEITY TESTS

In order to check the homogeneity of rainfall or streamflow at each individual station, a combined procedure using both graphical and statistical methods was employed in this research. The graphical technique, in the form of time-series plots, enabled a quick visual detection of any apparent trend or change in the mean value in the plotted series. Statistical methods with objective measures were then used to verify the conclusions obtained from the time-series plots, as well as to compute the statistical significance of any departure from homogeneity.

The distribution-free CUSUM test (McGilchrist and Woodyer, 1975) and the Mann-Kendall rank correlation test (WMO, 1966) were selected to perform the statistical check because they are simple and can be applied to general cases in which the change point is unknown (for example, when a change in a gauge location is not recorded). In addition, they are not based on any assumption regarding the distribution of the input data set (that is, they are non-parametric or distribution-free tests).

The CUSUM test checks the hypothesis of no change in a distribution against the alternative hypothesis of one single change. Given a number of observations  $X_1, X_2, X_3, \dots, X_i, \dots, X_n$  having the median  $k_m$ , the CUSUM test statistic, called  $\max |V_i|$ , can be computed from:

$$V_i = \sum_{j=1}^i q(X_j - k_m) \quad (D-1)$$

where  $q(x) = 1, x \geq 0$ .

$$q(x) = -1, x < 0.$$

The position of the maximum gives an estimate of the position of the change point where a jump in the mean occurs.

At the 5% level of significance, the upper confidence limit of the test statistic is given by  $1.92\sqrt{n'}$  (for  $n' > 40$ ), where  $n' = n/2$ . For other values of  $n'$ , the confidence limit is given by the product of  $n'$  and the corresponding value given by Conover (1971, Table 16).

The Mann-Kendall rank correlation test checks a time series for a trend without specifying whether the trend is linear or non-linear (Salas, 1993). The null hypothesis that the time series of  $n$  observations  $X_1, X_2, \dots, X_n$  is randomly ordered is tested against the alternative hypothesis that there is a monotone trend in observations.

The Mann-Kendall rank correlation statistic,  $T$ , is computed as follows:

$$T = \left( 4 \sum_{i=1}^{n-1} n_i \right) / [n(n-1)] - 1 \quad (\text{D-2})$$

where  $n_i$  is the number of observations larger than the  $i^{\text{th}}$  observation in the series subsequent to its position.

For  $n > 10$ ,  $T$  is almost normally distributed with the mean of zero and the variance of  $\text{Var}(T)$ , where:

$$\text{Var}(T) = (4n + 10) / [9n(n-1)] \quad (\text{D-3})$$

The 95% confidence limits of  $T$  are  $\pm 1.96\sqrt{\text{Var}(T)}$ .

### D.3 APPLICATION OF HOMOGENEITY TESTS

#### D.3.1 Rainfall data

As the basic data used in rainfall analyses were rainfall events extracted from observed hourly rainfall accumulations, in principle, it would be necessary to check the recorded event rainfall at hourly intervals for homogeneity. Nevertheless, the homogeneity tests were applied to annual series of maximum daily rainfall for two reasons. Firstly, it was considered sufficient to detect heterogeneity on an annual maximum basis, even though partial series of rainfall events was extracted. Secondly, it was assumed that the results

of the homogeneity tests on daily data also apply to hourly data.

The procedure below was adopted to check the homogeneity of rainfall data at each individual recording rain gauge:

- Series of daily rainfalls and the corresponding quality codes were extracted from the rainfall database. The extracted daily series generally had missing data points because rainfall records had gaps and missing data. However, to avoid introducing further uncertainties into the data series, no infilling of gaps or missing data was undertaken.
- The annual series of maximum daily rainfall was then extracted from the daily rainfalls flagged as good continuous records.
- The data series obtained from the above step was plotted against time to visually detect any change in the mean value or trend.
- The Mann-Kendall test for trend and the CUSUM test for discontinuity were then applied to the extracted series to statistically determine if the data series were homogeneous or not. Results are summarised in Table D-1.
- For stations that failed either of the tests, station documents were examined to find out if there was any record of a change in gauge location or in the environment surrounding the gauge.
- If there was evidence of sources of heterogeneity, a decision was made on whether to exclude the whole record or only a part of it from subsequent analyses. In the latter case, the two selected tests were applied to the remaining record to finally verify its homogeneity.

The examination of the time-series plots of the annual series of daily rainfall for each of the 19 rainfall sites used in this study indicated that, there was no identifiable trend or change in the mean of rainfall series for 18 out of 19 sites. An example of these plots is given in Figure D-1, which shows the annual maxima of daily rainfall at station 85237 plotted against time. It can be seen from this plot that the observed annual maxima fluctuate quite randomly. Results of the CUSUM and the Mann-Kendall tests (see Table D-1) also confirm that the assumption of no change in the mean or of no trend in data series can not be rejected at the 5% level of significance (LOS). This is demonstrated by the fact that, at each of the 18 stations (with the exception of station

85103), the test statistic computed for the CUSUM or Mann-Kendall test is less than the corresponding critical value (CV) at 5% LOS (see Table D-1).

Table D-1: Results of homogeneity tests for 19 recording rainfall stations

No.	Station ID	CUSUM test		Mann-Kendall test	
		CV at 5% LOS	Test statistic	CV at 5% LOS	Test statistic
1	85000	7	2	0.393	0.143
2	85026	7	2	0.363	0.000
3	85034	8	5	0.301	0.247
4	85072	11	4	0.219	0.082
5	85103	8	7	<u>0.309*</u>	<u>0.438</u>
6	85106	8	2	0.301	0.004
7	85170	7	3	0.377	0.086
8	85176	8	2	0.301	0.117
9	85236	7	2	0.393	0.209
10	85237	8	5	0.301	0.004
11	85240	10	2	0.244	0.120
12	85256	8	5	0.328	0.111
13	86038	11	8	0.228	0.190
14	86071	14	12	0.127	0.034
15	86142	10	5	0.253	0.113
16	86219	9	2	0.293	0.099
17	86224	9	4	0.268	0.140
18	86234	9	5	0.286	0.116
19	86314	11	3	0.232	0.022

\* CV at 1% LOS = 0.406

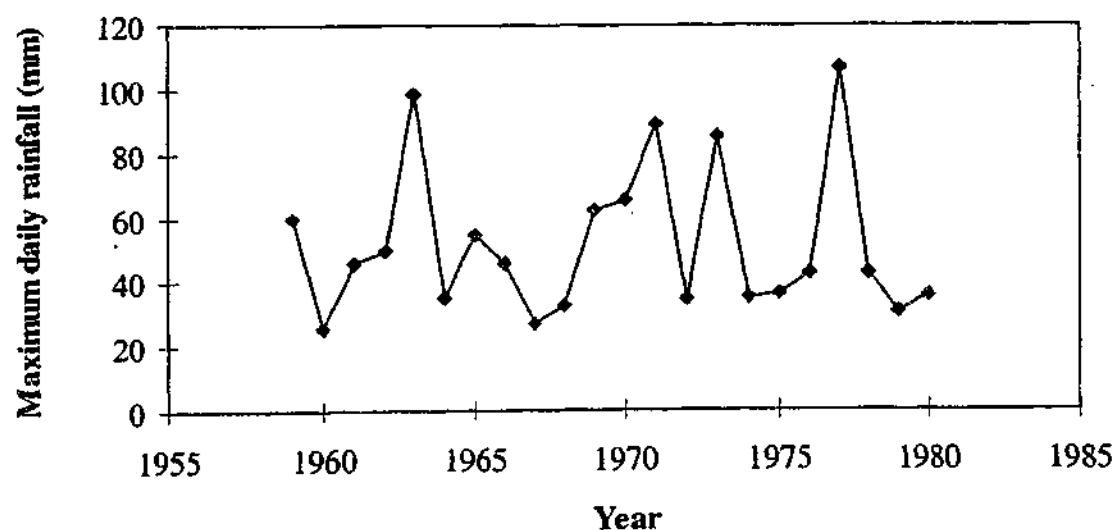


Figure D-1: Time-series plot of annual series of maximum daily rainfall (station 85237)

However, there seems to be problems with the homogeneity of the recorded rainfall data at station 85103. In the time-series plot for this site (see Figure D-2), there seems to be a trend in the daily maxima before 1956. This suggests that there might have been a change in the environment surrounding the gauge at this station. Results of the Mann-Kendall test for rainfall data at this site (see Table D-1) also confirm that the assumption of no trend in the annual series of daily rainfall can not be accepted at 5% LOS because the test statistic (0.438) exceeds the critical value (0.309) at the specified LOS. Nevertheless, an investigation of the station history indicated that there was no record at all of any changes in the type of instrument used for measuring rainfalls, methods of observation, or site conditions at the station before 1964. However, to be conservative, the station data before 1956 were discarded, according to the results of the Mann-Kendall test.

To ensure that the remaining data (that is, annual maxima from 1956 onwards) at site 85103 are homogeneous, the CUSUM and Mann-Kendall tests were again applied to these data. Table D-2 presents the results of these tests. From this table, it is clear that the assumption of no trend or change in the mean of the annual series of maximum daily rainfall from 1956 onwards at station 85103 is not rejected at 5% LOS, because the test statistics are less than the computed critical values. Therefore, this part of the station data was included for subsequent analyses.

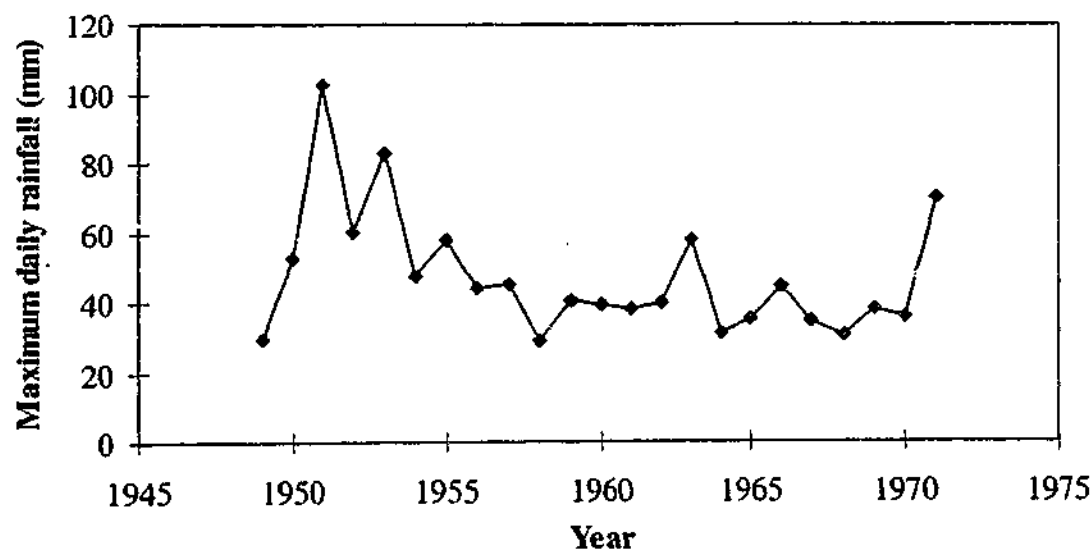


Figure D-2: Time-series plot of annual series of maximum daily rainfall (station 85103)

Table D-2: Results of homogeneity tests (station 85103, data from 1956 onwards)

Station ID	CUSUM test		Mann-Kendall test	
	CV at 5% LOS	Test statistic	CV at 5% LOS	Test statistic
85103	7	4	0.377	0.105

### D.3.2 Streamflow data

To verify the homogeneity of streamflow data for the La Trobe River catchment at Noojee (226205C) and the Tarwin River catchment at Dumbalk North (227226), the CUSUM and Mann-Kendall tests were applied to annual series of instantaneous flows.

The annual series of instantaneous flows can be extracted from the HYDSYS database using the HYPEAKS program in HYDSYS. However, as this program ignores periods of missing data or gaps in the record when outputting peaks (HYDSYS, 1994), it is possible that the extracted flood series may not consist of the true maximum floods that may occur when data are missing. This in turn would cause errors in any subsequent analysis that directly makes use of annual maximum flows. To avoid this, the maximum annual floods for this catchment were obtained from a data-collecting agency (Dworakovski, Personal communication, 1999). In this case, the maximum instantaneous annual flows were extracted from record, together with the number of missing days for each year of record. As there were no missing data in the flow records of the two study catchments, it was concluded that the extracted flood series at each site represented the true maximum annual floods.

The CUSUM and the Mann-Kendall tests were again applied to the extracted annual maximum floods. Test results are summarised in Table D-3, and for illustration, the plot of maximum instantaneous annual flows against time for station 226205C is shown in Figure D-3. From this figure, it can be seen that neither a change in the mean nor a trend in the annual peak discharge at station 226205C is apparent. This is confirmed by the results of the statistical tests in which the test statistics are less than the corresponding critical values at 5% LOS (see Table D-3). Therefore, the assumption that the distribution of annual peak flows for the La Trobe River catchment is homogeneous can not be rejected at the specified level of significance. The same

conclusion is drawn from the examination of flow data for the Tarwin River catchment.

Table D-3: Results of homogeneity tests on observed annual peak flows

Station ID	CUSUM test		Mann-Kendall test	
	CV at 5% LOS	Test statistic	CV at 5% LOS	Test statistic
226205C	11	6	0.232	0.217
227226	6	3	0.268	0.014

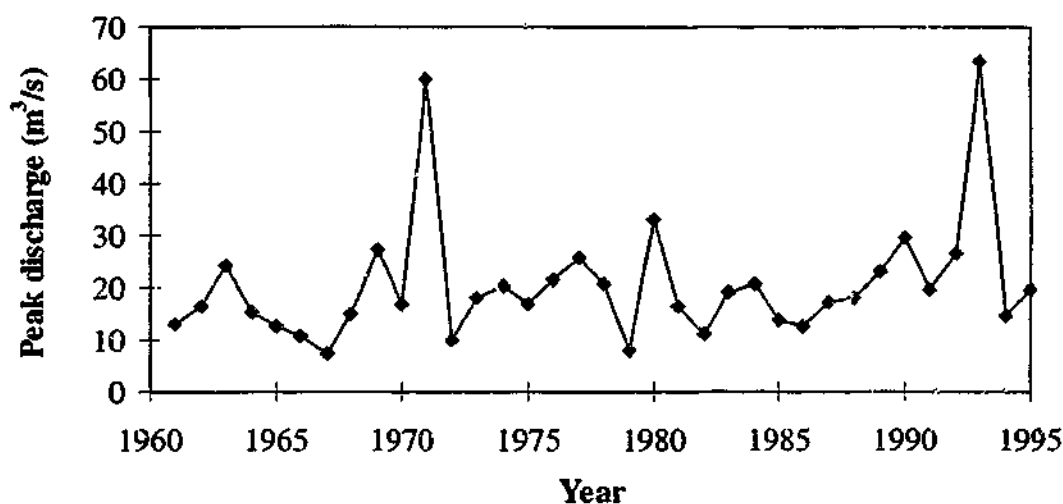


Figure D-3: Time-series plot of annual series of peak discharge (station 226205C)

#### D.4 CONCLUSIONS

In this study, observed rainfall and flow data at the gauging sites used in this study were assumed to be representative of the long-term variability of rainfall or streamflow at the selected sites. Nevertheless, the verification of these data for (time) homogeneity and consistency was considered essential to ensure that these data come from the same probability distribution at any given site. The CUSUM test for discontinuity and the Mann-Kendall test for trend were selected to undertake the homogeneity checks. The tests were applied to annual series of maximum daily rainfall at each of the 19 pluviometers used in this study, and to maximum instantaneous annual flow at the two flow gauging stations. Test results indicated that the observed rainfall and flow data at the selected stations satisfied the requirement of homogeneity.

## Appendix E

## THE HOSKING AND WALLIS REGIONAL FREQUENCY ANALYSIS STATISTICS

This appendix summarises the theoretical background of L-moments, and the development of the Hosking and Wallis statistics for regional frequency analysis. These statistics are the discordancy measure, the heterogeneity measure, and the goodness-of-fit measure. The material described below is mainly summarised from Hosking and Wallis (1997).

### E.1 L-MOMENTS

L-moments, like the conventional product moments, are a way to describe statistical properties of a probability distribution characterising a random variable. L-moments of a statistical distribution are linear functions of probability weighted moments and defined as (Hosking, 1990):

$$\lambda_{r+1} = \sum_{k=0}^r \beta_k (-1)^{r-k} \binom{r}{k} \binom{r+k}{k} \quad (\text{E-1})$$

in which:

$$\begin{aligned} \beta_r &= E\{X[F(X)]^r\} \\ F(X) &= \text{prob}(X \leq x) \end{aligned} \quad (\text{E-2})$$

where  $\beta_r$  are the probability weighted moments, which are expectations of  $X$  times powers of  $F(X)$ , and  $F(X)$  is the cumulative distribution function of  $X$ .

The L-CV (short for coefficient of L-variation, denoted as  $\tau$ ) and the L-moment ratios ( $\tau_r$ ) are defined as follows:

$$\begin{aligned} \tau &= \frac{\lambda_2}{\lambda_1} \\ \tau_r &= \frac{\lambda_r}{\lambda_2} \end{aligned} \quad (\text{for } r \geq 3) \quad (\text{E-3})$$

The above L-moment quantities are useful in summarising *statistical distributions*. For example,  $\lambda_1$  is the mean or the location parameter of the distribution,  $\lambda_2$  is a measure of scale, whereas  $\tau_3$  and  $\tau_4$  are measures of skewness and kurtosis, respectively. The L-CV is analogous to the coefficient of variation used in product moments.

Estimators of distributional L-moments are generally computed from estimators of probability weighted moments of a given data set. Formulas used for these estimates are available in both biased and unbiased forms (Stedinger et al., 1993). (Bias is a statistical term used to denote a tendency of estimates that are consistently higher or lower than the true value). However, for regionalization procedures, unbiased estimates are recommended.

Unbiased estimators ( $b_r$ ) of probability weighted moments of a *sample* can be computed by:

$$b_r = \frac{1}{n} \sum_{j=1}^{n-r} \left[ \frac{\binom{n-j}{r}}{\binom{n-1}{r}} \right] x_{(j)} \quad (\text{E-4})$$

in which  $x_{(n)} \leq \dots \leq x_{(1)}$  represents a sample of  $n$  observations ranked in descending order.

The unbiased sample L-moment estimators ( $l_r$ ) can then be calculated by substituting the unbiased probability weighted moment estimators into the following equation:

$$l_{r+1} = \sum_{k=0}^r b_k (-1)^{r-k} \binom{r}{k} \binom{r+k}{k} \quad (\text{E-5})$$

Similarly, sample estimates of  $\tau$ ,  $\tau_3$ , and  $\tau_4$  are denoted as  $t$ ,  $t_3$  and  $t_4$ , and calculated as follows:

$$t = \frac{l_2}{l_1} \equiv \text{sample L-CV}$$

$$t_3 = \frac{l_3}{l_2} \equiv \text{sample L-skewness} \quad (\text{E-6})$$

$$t_4 = \frac{l_4}{l_2} \equiv \text{sample L-kurtosis}$$

Thus, sample L-moments ( $l_1$ ,  $l_2$ ,  $t$ ,  $t_3$  and  $t_4$ ) are summary statistics of a data *sample*. Like the conventional product moments, sample L-moments can be used to identify the probability distribution from which a sample of data is drawn, or to estimate distributional parameters. They can also be used to construct statistics useful for regional frequency analysis, as described in the next section.

## E.2 THE HOSKING AND WALLIS STATISTICS FOR REGIONAL FREQUENCY ANALYSIS

In order to estimate the dimensionless regional frequency distribution common to all sites in a homogeneous group of sites, the three statistics developed by Hosking and Wallis (1997) can be used. A description of these statistics is given below.

### The discordancy measure ( $D_i$ )

Given a group of sites, the discordancy measure is used to identify discordant sites that seem to have erroneous data. These are the sites whose sample L-moments are markedly different from those of other sites in the group. The discordancy measure at site  $i$ , denoted as  $D_i$ , is defined by:

$$D_i = \frac{1}{3} N (u_i - \bar{u})^T A^{-1} (u_i - \bar{u}) \quad (\text{E-7})$$

in which:

$$u_i = [t^i \quad t_3^i \quad t_4^i]^T$$

$$\bar{u} = N^{-1} \sum_{i=1}^N u_i \quad (\text{E-8})$$

$$A = \sum_{i=1}^N (u_i - \bar{u})(u_i - \bar{u})^T$$

where  $u_i$  is the vector containing the L-CV, L-skewness, and L-kurtosis, respectively, for site  $i$ ;  $\bar{u}$  is the unweighted group average;  $A$  is the matrix of sum of squares and cross-products;  $N$  is the total number of sites in the group; and  $T$  is the superscript denoting transposition of a vector or matrix.

Site  $i$  is declared to be discordant with the whole group if  $D_i$  exceeds a critical value which depends on the number of sites ( $N$ ) in the group. For example, for  $N \geq 15$ , a site can be suggested as discordant if  $D_i \geq 3$ . Critical values for other values of  $N$  are recommended by Hosking and Wallis (1997, Table 3-1).

#### The heterogeneity measure ( $H_i$ )

The heterogeneity measure is used to assess whether a group of sites may reasonably be treated as a homogeneous region<sup>1</sup>. In order to do this, the between-site variations in sample L-moments are compared with the dispersion expected for a homogeneous region that has the same number of sites with the same record lengths as those of the observed data. By repeated simulation of this homogeneous region, the mean and standard deviation of the chosen dispersion measure can be obtained. The comparison between the observed and simulated dispersion is performed using the following statistic:

$$H_i = \frac{(\text{observed dispersion}) - (\text{mean of simulations})}{(\text{standard deviation of simulations})} \quad (\text{E-9})$$

A large positive value of this statistic indicates that the observed L-moments are more dispersed than is consistent with the hypothesis of homogeneity. On the other hand, negative values of  $H_i$  can be obtained. In this case, the dispersion among values of the at-site sample L-CV is less than would be expected. The most likely cause is the cross-correlation between data at different sites. If large negative values of  $H_i$  are obtained (say  $H_i < -2$ ), further examination of the data is then warranted.

<sup>1</sup> A homogeneous region is a group of sites whose frequency distributions are considered to be the same, after appropriate scaling.

Three dispersion measures can be used to assess the homogeneity of a group of sites in different dimensions. The first measure ( $H_1$ ) is based on the sample L-CV, the second ( $H_2$ ) on the weighted average distance from the site to the group weighted mean on the graph of L-CV and L-skewness, and the third ( $H_3$ ) on the weighted average distance from the site to the group weighted mean on the graph of L-kurtosis and L-skewness.

To calculate the heterogeneity measures, assume that the proposed homogenous region has  $N$  sites, with  $n_i$  being the record length of site  $i$ , and sample L-moment ratios  $t^i, t_3^i, t_4^i$ . Let  $t^R, t_3^R, t_4^R$  be the regional average L-CV, L-skewness, and L-kurtosis, weighted proportionally to the sites' record length. For example:

$$t^R = \frac{\sum_{i=1}^N n_i t^i}{\sum_{i=1}^N n_i} \quad (\text{E-10})$$

The heterogeneity measures ( $H_i$ ) defined in Equation (E-9) are thus expressed by:

$$H_i = \frac{V_i - \mu_{V_i}}{\sigma_{V_i}} \quad (i = 1, 2, 3) \quad (\text{E-11})$$

where

$$\begin{aligned} V_1 &= \left\{ \frac{\sum_{i=1}^N n_i (t^i - t^R)^2}{\sum_{i=1}^N n_i} \right\}^{1/2} \\ V_2 &= \frac{\sum_{i=1}^N n_i \left\{ (t^i - t^R)^2 + (t_3^i - t_3^R)^2 \right\}^{1/2}}{\sum_{i=1}^N n_i} \\ V_3 &= \frac{\sum_{i=1}^N n_i \left\{ (t_3^i - t_3^R)^2 + (t_4^i - t_4^R)^2 \right\}^{1/2}}{\sum_{i=1}^N n_i} \end{aligned} \quad (\text{E-12})$$

and  $\mu_{V_i}, \sigma_{V_i}$  are respectively the mean and standard deviation of the dispersion measure  $V_i$ , determined by simulation.

The region is declared to be heterogeneous if the heterogeneity measures are sufficiently large. By simulation, the following values are suggested:

- $H_i < 1$                       acceptably homogeneous
- $1 \leq H_i < 2$                 possibly heterogeneous
- $H_i \geq 2$                       definitely heterogeneous

### The goodness-of-fit measure ( $Z^{\text{DIST}}$ )

Given a homogeneous region of sites, the goodness-of-fit measure can be used to test whether a given distribution gives an acceptable fit to observed data. This measure is developed by comparing how well the fitted distribution matches the regional average L-kurtosis. There are two reasons for choosing the L-kurtosis. Firstly, in an acceptably homogeneous region, L-moment ratios of the sites are well summarised by the regional average. Therefore, the distribution being tested will have the location and scale parameters that can be chosen to match the regional average mean and L-CV. Secondly, the distribution fitted by the method of L-moments has L-skewness equal to the regional average L-skewness. Therefore, the quality of fit is judged by the next higher moment not used in fitting, that is, by the difference between the L-kurtosis of the fitted distribution and the regional average L-kurtosis. To account for possible biases in estimating the L-kurtosis for short record lengths ( $n_i \leq 20$ ), a bias correction for the regional average L-kurtosis is used.

Five general 3-parameter distributions are used in the Hosking and Wallis (1997) procedure to perform the goodness-of-fit test. These are the Generalised Logistic (GLO), the Generalised Extreme Value (GEV), the Generalised Pareto (GP), the Lognormal (LN), and the Pearson type III (PIII). For a particular candidate distribution, the goodness-of-fit measure is defined as:

$$Z^{\text{DIST}} = \frac{(\tau_4^{\text{DIST}} - t_4^R + B_4)}{\sigma_4} \quad (\text{E-13})$$

in which  $\tau_4^{\text{DIST}}$  is the L-kurtosis of the fitted distribution, where DIST can be any of the above five candidates;  $B_4$  is the bias of  $t_4^R$ ; and  $\sigma_4$  is the standard deviation of  $t_4^R$ , obtained by repeated simulation of a homogeneous region whose sites have the same record lengths as those of observed data.

A distribution gives an adequate fit to the observed data if  $Z^{\text{DIST}}$  is sufficiently close to zero. Under the assumptions that the at-site L-kurtosis estimators have independent identical normal distributions, and that there is no cross or serial correlation in the data, the candidate distribution gives an adequate fit if  $|Z^{\text{DIST}}| \leq 1.64$ .

## Appendix F

## STATISTICAL DISTRIBUTIONS

This appendix presents details of two statistical distributions, the Generalised Pareto distribution and the beta distribution, used in this study. The former was used to represent the duration of storm events, whereas the latter characterised the rainfall temporal pattern and initial loss. The material documented below is summarised from Hosking and Wallis (1997), and Benjamin and Cornell (1970).

## F.1 THE GENERALISED PARETO DISTRIBUTION

The Generalised Pareto distribution is a distribution with three parameters:  $\xi$  (location),  $\alpha$  (scale),  $\kappa$  (shape).

The probability density function  $p(x)$  of this distribution is given as follows (Hosking and Wallis, 1997):

$$p(x) = \alpha^{-1} e^{-(1-\kappa)y}$$

$$y = \begin{cases} -\kappa^{-1} \log\{1 - \kappa(x - \xi)/\alpha\}, & \kappa \neq 0 \\ (x - \xi)/\alpha, & \kappa = 0 \end{cases} \quad (\text{F-1})$$

The cumulative distribution function  $F(x)$  is defined by:

$$F(x) = 1 - e^{-y} \quad (\text{F-2})$$

and the range of  $x$  is given by:

$$\begin{aligned} \xi \leq x \leq \xi + \alpha/\kappa & \quad \text{if } \kappa > 0 \\ \xi \leq x < \infty & \quad \text{if } \kappa \leq 0 \end{aligned} \quad (\text{F-3})$$

There are some cases, depending on the shape parameter  $\kappa$ , in which the Generalised Pareto distribution becomes a special distribution. These cases include:

- $\kappa = 0$ : exponential distribution
- $\kappa = 1$ : uniform distribution on the interval  $\xi \leq x \leq \xi + \alpha$

## F.2 THE BETA DISTRIBUTION

The beta probability distribution is a very flexible distribution as it can assume a wide variety of shapes by varying its parameters. It is generally defined over the interval from 0 to 1, but can also be transformed to any interval from a to b. The probability density functions of the beta distribution are described below, along with the method for estimating distributional parameters. The special shapes that the distribution can represent are also documented.

### F.2.1 Beta distribution on the interval (0,1)

On the interval from 0 to 1, the beta distribution is a two-parameter distribution with the probability density function defined as follows:

$$p_X(x) = \frac{\Gamma(\alpha + \beta)}{\Gamma(\alpha)\Gamma(\beta)} x^{\alpha-1} (1-x)^{\beta-1} \quad (\text{F-4})$$

where  $0 \leq x \leq 1$ ;  $\alpha > 0$ ,  $\beta > 0$ ;  $\Gamma(\cdot)$  is the gamma function; and  $\alpha$  and  $\beta$  are the two parameters of the distribution.

The mean and variance of the beta distribution, denoted as  $E(X)$  and  $\text{Var}(X)$ , respectively, are computed by:

$$E(X) = \frac{\alpha}{\alpha + \beta} \quad (\text{F-5})$$

$$\text{Var}(X) = \frac{\alpha\beta}{(\alpha + \beta)^2 (\alpha + \beta + 1)}$$

Parameters of the beta distribution can be estimated by the method of moments by equating the mean and variance of a data sample to those of the population.

### F.2.2 Beta distribution on the interval (a,b)

On the interval from a to b, the beta distribution function takes the following form:

$$p_Y(y) = \frac{\Gamma(\alpha + \beta)}{\Gamma(\alpha)\Gamma(\beta)(b-a)^{\alpha+\beta-1}} (y-a)^{\alpha-1} (b-y)^{\beta-1} \quad (\text{F-6})$$

where  $a \leq y \leq b$ .

The mean and variance of this distribution are:

$$\begin{aligned} E(Y) &= a + \frac{\alpha}{\alpha + \beta} (b - a) \\ \text{Var}(Y) &= (b - a)^2 \frac{\alpha\beta}{(\alpha + \beta)^2(\alpha + \beta + 1)} \end{aligned} \quad (\text{F-7})$$

Like the case of the beta distribution on the interval from 0 to 1, parameters of the beta distribution on the interval from a to b can be easily computed by the method of moments.

There is a linear relationship between the beta density function and the beta cumulative distribution function defined on the interval from 0 to 1 [ $p_X(x)$  and  $F_X(x)$ , respectively] and their counterparts defined on the interval from a to b [ $p_Y(y)$  and  $F_Y(y)$ ]. These relationships are defined below:

$$\begin{aligned} F_Y(y) &= F_X\left(\frac{y-a}{b-a}\right) \\ p_Y(y) &= \frac{1}{b-a} p_X\left(\frac{y-a}{b-a}\right) \end{aligned} \quad (\text{F-8})$$

### F.2.3 Distributional shapes

The beta distribution can assume a wide variety of shapes (see Figure F-1), depending on its parameter values. It has some special cases, some of which are listed below:

- Rectangular distribution:  $r=1, t=2$
- Triangular distribution:  $t=3$ , and  $r=1$  or  $2$
- Symmetrical distribution about  $x=0.5$  if  $r=0.5t$

In the above cases,  $r=\alpha$  and  $t=\alpha+\beta$ , where  $\alpha$  and  $\beta$  are the two parameters of the beta distribution.

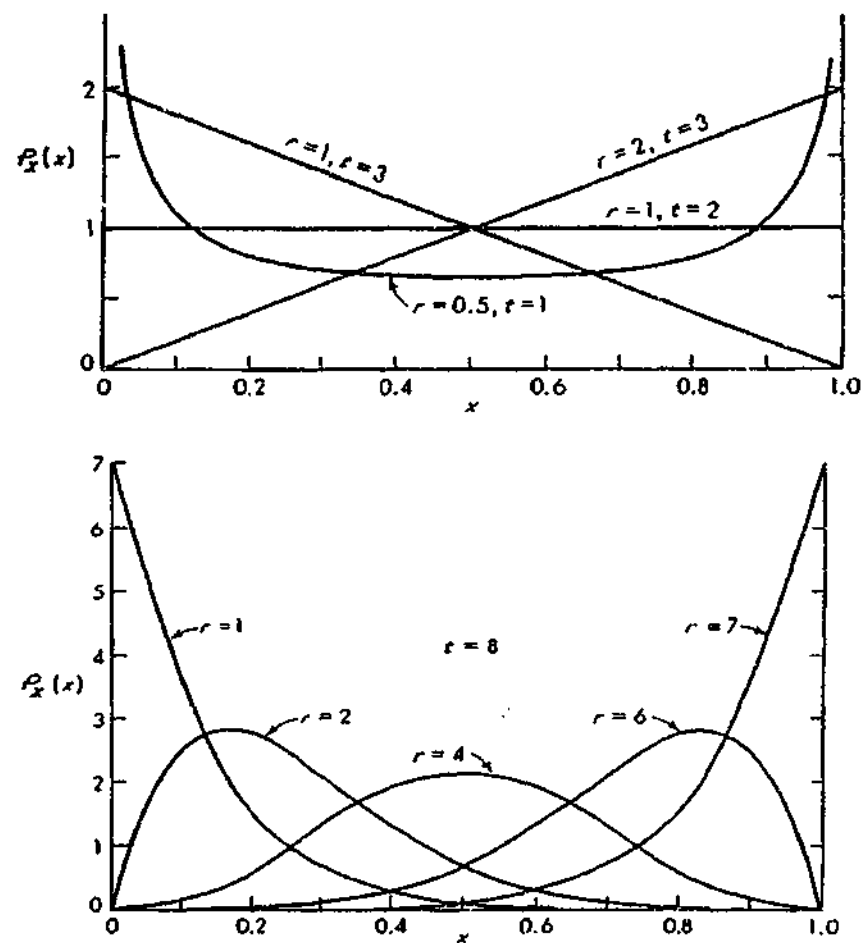


Figure F-1: Shapes of the beta distribution (Benjamin and Cornell, 1970)

## Appendix G

## THE CHI-SQUARE TEST OF INDEPENDENCE

This appendix presents the theoretical background of the chi-square test of independence. The test is used to determine whether two variables are associated. The material described below is summarised from Daniel (1978).

It is assumed that an observed set of data forms a random sample of size  $n$ , and that these data may be cross classified according to two criteria, so that each observation belongs to one and only one level of each criterion. The criteria are the variables of interest in a given situation. The data may be displayed in a contingency table as shown in Table G-1.

Table G-1: Contingency table for the chi-square test of independence

<i>First criterion of classification</i> Level	<i>Second criterion of classification</i> Level					Total	
	1	2	...	j	...		c
1	$n_{11}$	$n_{12}$		$n_{1j}$		$n_{1c}$	$n_{1.}$
2	$n_{21}$	$n_{22}$		$n_{2j}$		$n_{2c}$	$n_{2.}$
.							
.							
i	$n_{i1}$	$n_{i2}$		$n_{ij}$		$n_{ic}$	$n_{i.}$
.							
.							
r	$n_{r1}$	$n_{r2}$		$n_{rj}$		$n_{rc}$	$n_{r.}$
Total	$n_{.1}$	$n_{.2}$		$n_{.j}$		$n_{.c}$	$n$

where  $n_{ij}$  is the observed frequency of cell  $ij$ ;  $r$  is the number of rows;  $c$  is the number of columns; and  $n$  is the total number of observations.

To test the null hypothesis that the two criteria of classification are independent, the cell frequencies expected when the assumption of independence of the two variables is true are computed and compared with the corresponding observed cell frequencies.

The test statistic (called the Pearson chi-squared statistic) is computed in the following manner. If the two criteria of classification are independent, then the probability of the joint occurrence of two levels of each observation is equal to the product of their individual probabilities. In other words, the probability of counting an observation in cell  $ij$  is equal to the probability of counting it in the  $i^{\text{th}}$  row times the probability of counting it in the  $j^{\text{th}}$  column. To obtain  $N_{ij}$ , the expected frequency of cell  $ij$ , the probability of counting the observation in cell  $ij$  is multiplied by the total sample size. Thus:

$$N_{ij} = n \left( \frac{n_i}{n} \right) \left( \frac{n_j}{n} \right) \quad (\text{G-1})$$

which gives:

$$N_{ij} = \frac{n_i n_j}{n} \quad (\text{G-2})$$

Thus, the expected frequency of cell  $ij$  is the product of row total ( $n_i$ ) and column total ( $n_j$ ) divided by the total sample size ( $n$ ).

The test statistic is then computed as follows:

$$\chi^2 = \sum_{i=1}^r \sum_{j=1}^c \left[ \frac{(n_{ij} - N_{ij})^2}{N_{ij}} \right] \quad (\text{G-3})$$

This test statistic is approximately distributed as a chi-squared distribution when the null hypothesis is true.

The null hypothesis that the two criteria of classification are independent may be rejected at the  $\alpha$  level of significance if the computed value of the test statistic  $\chi^2$  exceeds the tabulated chi-square critical value for  $(r-1)(c-1)$  degrees of freedom. These critical values at various levels of significance are available for contingency tables with up to 100 degrees of freedom.

It is noted that  $\chi^2$  is approximately distributed as a chi-squared distribution if the expected cell frequencies ( $N_{ij}$ ) are large. In general, the minimum cell frequency of 5 is recommended. However, the minimum  $N_{ij}$  of 1 is acceptable for contingency tables with more than one degree of freedom, and only 20% or fewer of the cells with expected cell frequency less than 5. It is also noted that rows and columns of contingency tables may be interchanged without affecting the results.

## Appendix H

# METHODS FOR DEVELOPING DESIGN TEMPORAL PATTERNS

### H.1 INTRODUCTION

Methods for developing a design temporal pattern for a design rainfall depth and duration can be divided into four groups. They are methods based on IFD curves, methods based on analyses of observed hyetographs, rainfall disaggregation models, and sampling from historical patterns. In this appendix, all these methods are critically assessed in order to select a method suitable for this study.

### H.2 METHODS BASED ON IFD CURVES

In order to develop a design rainfall temporal pattern for a design rainfall depth and duration, some methods based on design IFD curves of rainfall have been proposed. The commonly used methods in this category include the alternating block method and the instantaneous intensity method (Chow et al., 1988).

With the alternating block method, the storm duration  $D$  is divided into  $n$  equal time increments of  $T$  (that is  $D=nT$ ). The average rainfall intensity for each of the durations  $T, 2T, 3T, \dots, nT$  is then determined from the IFD curves at the site location, and the corresponding rainfall depth computed. The incremental rainfall depth to be added for each unit of time  $T$  is then taken as the difference between successive rainfall depths. Next, these incremental rainfall depths are reordered such that the maximum depth occurs at the centre of the storm duration. The design storm hyetograph is finally determined by rearranging the remaining depths in descending order alternately to the left and right of the central maximum depth. In Australia, this method has been slightly modified by Boughton (2000) in order to disaggregate daily totals into hourly rainfalls.

With the instantaneous intensity method, the principle is similar to that employed in the alternating block method. That is, the rainfall depth for a time interval around the storm peak is equal to the depth given by the IFD curves. The only difference is that the rainfall intensity is considered to vary continuously throughout the storm.

Even though methods for developing design temporal patterns from the IFD curves are simple, they can not be adopted in this research for two reasons. Firstly, the patterns derived are unrealistic because they represent a series of unrelated values of rainfall intensities from a variety of storms, rather than a sequence of intensities in a particular storm. Secondly, they fail to characterise the variability of temporal patterns of real rainfall events. That is, for a given storm duration and depth, each of these methods can produce a single design temporal pattern, as opposed to multiple patterns that happen in the real life.

### **H.3 METHODS BASED ON ANALYSES OF OBSERVED HYETOGRAPHS**

Temporal patterns of design rainfall can also be derived from analyses of observed rainfall hyetographs. Some of the well-known methods in this category include the average variability method (Pilgrim and Cordery, 1975), the triangular hyetograph method (Yen and Chow, 1980), and Huff's method (Huff, 1967).

The average variability method is the basis on which design temporal patterns currently used in Australia are derived. With this method, the design pattern for a given storm duration is determined from the observed heaviest bursts of the same duration in the following manner. First of all, each of the bursts is divided into the same number of periods. The periods in each burst are then ranked according to the amount of rain in each period; rank 1 denoting the period of most intense rain. For all bursts, an average rank is determined for each period. The period with lowest average rank is then taken as the heaviest rainfall period of the design pattern, whereas the period with largest average rank denotes the period of slightest rain of the design pattern. In order to determine the percentage of rain in each period of the design pattern, for each storm burst, the percentages of rainfall per period are arranged in descending order of

magnitude. For all observed storm bursts, the average percentage of the heaviest periods is computed and then assigned to the heaviest period of the design pattern. The average rainfall percentage of other less intense rainfall periods of the design pattern is similarly determined. Thus, the design temporal patterns derived in the above manner represent the average variability of intense bursts of rain.

The triangular hyetograph method aims to derive design rainfall hyetographs of a triangular shape. This method is very simple because once the design rainfall depth and duration are known, the base length and the height of the triangular hyetograph can be determined. In order to determine the location of the peak intensity, a storm advancement coefficient  $r_a$ , defined as the ratio of the time before the peak to the total storm duration, is used. For example, a value of  $r_a$  of 0.5 corresponds to a storm with the peak intensity occurring in the middle of the storm, whereas  $r_a$  less than 0.5 is used for early-peaked storms, and  $r_a$  greater than 0.5 for late-peaked storms. A suitable value of  $r_a$  is determined as the mean of the observed values of  $r_a$  computed for a series of storms of various durations, weighted according to the duration of each storm event.

In Huff's method, the time distribution patterns of heavy storms were developed for four quartile groups, depending on whether the heaviest rainfall occurred in the first, second, third or fourth quarter of the storm duration. Other factors such as storm duration, storm types, or mean rainfall were found to have small effects on the time distribution patterns. In each quartile group, dimensionless mass curves of nine probability levels, ranging from 10% to 90% with 10% increments, were developed (see Figure H-1). For example, the 90% curve can be defined as the distribution that is equalled or exceeded by 10% or less of the storms. These empirical probabilistic mass curves, called Huff curves, are smooth because they reflect average rainfall distribution with time and do not exhibit the burst characteristics of observed storms. The first quartile 50% mass curve has been used in a storm drainage simulation model by Terstriep and Stall (1974).

Regardless of their conceptual simplicity, both the average variability method and the triangular hyetograph method can not be used directly in the present research due to at least one or more of the following reasons:

- They do not represent the variability of observed temporal patterns;

- Simple hyetograph shapes (for example, triangles) are inadequate to represent the actual variation of rainfall intensity in typical rainfall events; and
- They were developed such that when being used with average values of other design inputs, the resulting design flood is assumed to have the same probability as that of the design rainfall.

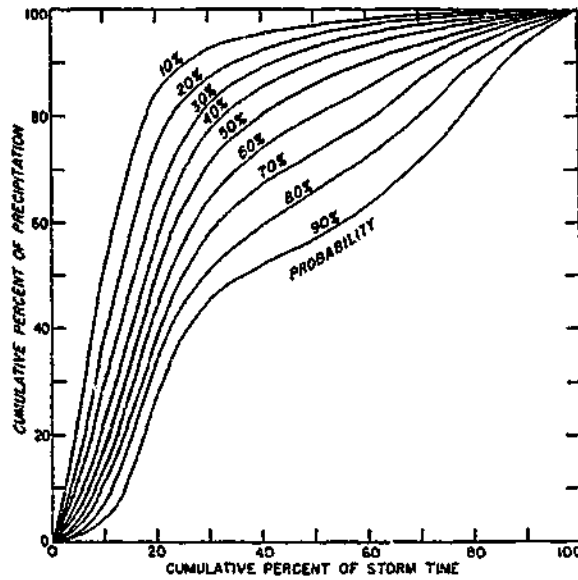


Figure H-1: Time distributions of first quartile storms (Huff, 1967)

For the comparison of observed and modelled patterns, Huff's method seems to be partially relevant to this study because it can describe characteristics of rainfall temporal patterns in probabilistic terms. In applying this method, it may be necessary to examine the effects of storm types, storm duration, or seasonal variation on the time distribution of rainfall. Results of this investigation would be useful in dividing observed storms into groups before constructing Huff curves for each individual group.

#### H.4 RAINFALL DISAGGREGATION MODELS

There exist many disaggregation schemes for simulating the temporal distribution of rainfall within storm events. These include methods proposed by Nguyen and Rousselle (1981), Hashino (1986), Hershenthorn and Woolhiser (1987), Garcia-Guzman and Aranda-Oliver (1993), Robinson and Sivapalan (1997), and Heneker et al. (1999).

Among these, the model proposed by Garcia-Guzman and Aranda-Oliver (1993), and the multiplicative cascade model by Robinson and Sivapalan (1997) are conceptually simple and appear to be simple enough for practical applications. The models are therefore described in detail below.

The objective of the model proposed by Garcia-Guzman and Aranda-Oliver (1993) was to disaggregate the total depth of a rainfall event of a specified duration into hourly rainfall depths. In this model, the temporal pattern was characterised by the dimensionless storm mass curve defined at hourly time steps. The ordinates of the dimensionless mass curve were assumed to be ordered samples from a beta distribution. Parameters of the beta distribution were estimated from observed storm data. Given a rainfall event of a specified duration, the hyetograph of the design event was determined by generating random numbers from the fitted beta distribution. These ordered random numbers (in ascending order of magnitude) represented the ordinates of the mass curve of the design storm pattern.

When applying this model to the observed rainfall data at three stations in Southern Spain, it was shown that the model reasonably preserved the lag one auto-correlation between rainfall depths at successive time steps, the maximum dimensionless hourly precipitation, and Huff frequency curves of the historical rainfall temporal patterns. This model was applied by Loukas et al. (1996) to determine stochastic design temporal patterns for design rainfall.

In the multiplicative cascade model (Robinson and Sivapalan, 1997), the dimensionless storm mass curve was used to describe the temporal pattern of rainfall, and Huff frequency curves (Huff, 1967) were used to summarise the characteristics of observed temporal patterns. The model parameters were represented by a beta distribution whose distributional parameters were determined by trial and error such that the Huff frequency curves of the generated storm patterns matched the observed Huff frequency curves. The model employed a multiplicative cascade structure to determine mass curve ordinates as a function of random numbers drawn from the fitted beta distribution. In essence, the multiplicative cascade structure aims to generate rainfall hyetographs with  $2^m$  rectangles, where  $m$  is the level of disaggregation, chosen to obtain the desired time step of temporal patterns at the end of the disaggregation process.

## H.5 SAMPLING FROM HISTORICAL PATTERNS

To generate a design temporal pattern for a given design storm depth and storm duration, a very simple method is to sample from historical temporal patterns. This requires pluviograph data of good record lengths so that a large sample of all observed temporal patterns for the specified duration could be determined. The design temporal pattern for the defined event can then be randomly taken from the sample of dimensionless temporal patterns for the corresponding duration. This method has been applied by Rahman et al. (2001) in a parallel project to determine the flood frequency curve resulting from events defined as storm cores.

## H.6 METHOD SELECTION

For the purpose of this study, the method selected for generating design temporal patterns should be able to produce multiple patterns to reflect the great variability of temporal patterns of real storm events. The modelled patterns should also preserve the characteristics of observed patterns. In addition, the adopted method should be simple enough to apply in practice.

Of the four groups of methods for developing design temporal patterns discussed above, it is clear that none of methods based on IFD relationships or on analyses of observed hyetographs can be used in this research. This is mainly because they are incapable of representing the variability of temporal patterns of real rainfall events.

Of the remaining groups of methods, Huff's method has the advantage of being able to characterise the temporal pattern in probabilistic terms. However, this method was not selected for this project because Huff curves are only a statistical summary of data, not actual patterns of individual storms. Furthermore, the ordinates of these curves are developed without taking into account the correlation of rainfall intensity in successive time periods.

The sampling of historical patterns is also a promising method because it is simple and

it can model the variation of temporal patterns from event to event. However, one possible problem of this method is that it can only characterise patterns that are actually observed, but not the patterns that could have equally likely occurred.

As far as rainfall disaggregation models are concerned, the models introduced by Garcia-Guzman and Aranda-Oliver (1993) and Robinson and Sivapalan (1997) are the simplest in terms of model structure. Nevertheless, the multiplicative cascade model proposed by Robinson and Sivapalan (1997) was adopted in this research because it is mathematically much simpler than the other. Moreover, it is the easiest for implementing in design applications and when tested with observed data, it produced good results.

## **H.7 CONCLUSIONS**

In this appendix, four groups of methods for developing design temporal patterns of rainfall were briefly reviewed. The multiplicative model proposed by Robinson and Sivapalan (1997) was adopted in this research.

## Appendix I

# AT-SITE FREQUENCY ANALYSIS METHODS

## I.1 INTRODUCTION

The primary objective of methods for at-site frequency analysis is to determine the probability (or recurrence interval) of an event of a given magnitude using data at a specified site. There are several at-site frequency analysis methods, as described by Haan (1977, Chapter 7) and Stedinger et al. (1993). In general, these methods can be divided into two groups, namely non-parametric and parametric methods. In the former, the probability distribution representing a set of data is determined without a priori assumption regarding the underlying distribution of the data values. By contrast, in the latter, it is necessary to assume the parent distribution of the data set at the outset of the analysis. The objective of this appendix is to present a brief review of the most commonly used techniques available in these two groups.

## I.2 NON-PARAMETRIC METHODS

In order to determine the frequency distribution of an observed data set using non-parametric methods, three steps are undertaken. Firstly, a plotting position for each observed data is computed. The plotting position can be defined as a distribution-free estimator of a cumulative distribution function (Hosking, 1990). Secondly, the observed data and their corresponding plotting positions are plotted on a graph. Finally, a curve that best fits the plotted points is drawn subjectively or by means of mathematical or statistical smoothing functions. This curve represents an empirical distribution of the data. From the fitted curve, quantiles at specified probability levels can be estimated.

The non-parametric methods are easy to apply, and probably most appropriate for very long series of data (in the order of hundreds to thousands) in which quantile estimates of the parameter of interest can be read directly from the graph without the need for fitting a curve through the plotted data points. However, for more general cases, they are not widely used for frequency analysis due to their arbitrary and subjective nature (Haan, 1977). In addition, the extrapolation of probabilities outside the range of observations can not be reliably determined. Finally, regionalisation of the frequency curve is difficult to achieve.

### **1.3 PARAMETRIC METHODS**

To develop the probability distribution of a random variable using parametric methods, the following three steps can be undertaken: selection of a distributional type, estimation of distributional parameters, and checking of the adequacy of the fitted distribution. Each of these steps involves the choice of one single method among a variety of alternatives. A brief introduction to the most commonly used methods in each step is presented below and their characteristics are discussed.

#### **1.3.1 Selection of a distributional type**

To tentatively determine the parent distribution of an observed set of data, histograms, moment ratio diagrams, or L-moment ratio diagrams of the observed data can be used. Histograms are plots that show the frequencies of occurrence versus class intervals of the observed data. The histogram shape gives an indication of the probability distribution that underlies the data.

Moment ratio diagrams and L-moment ratio diagrams are constructed on the basis that any probability distribution has specific values (or ranges of values) for its coefficient of variation ( $C_v$ ), coefficient of skewness ( $C_s$ ), and coefficient of kurtosis ( $C_k$ ). Therefore, sample estimates of these quantities can be used to preliminarily specify the distribution

underlying the sample (McCuen, 1985). Moment ratio diagrams include plots of  $C_v$  versus  $C_s$  (for identifying two-parameter distributions), and  $C_k$  versus  $C_s$  (for identifying three-parameter distributions). On these graphs, the moment ratios of different theoretical statistical distributions are plotted, along with those of the observed data. The distribution most suitable to describe the data is taken as the theoretical distribution closest to the plotted points on the graphs. The same principle is applied to construct the L-moment ratio diagrams, but L-moment ratios (L-CV, L-skewness, and L-kurtosis) are used instead of the conventional product moments ratios ( $C_v$ ,  $C_s$ ,  $C_k$ ).

L-moment ratio diagrams are considered as a diagnostic tool superior to histograms and moment ratio diagrams in identifying a parent distribution from which a sample is drawn (Cunnane, 1989; Vogel and Fennessey, 1993). There are two main reasons for this. Firstly, they are based on unbiased sample estimates of L-moment ratios. By contrast, estimates of conventional product moment ratios (in particular,  $C_s$ ) are highly biased, especially for small samples. And secondly, they are more reliable than histograms because the shape of a histogram generally depends on sample size and the class intervals used, especially for small samples (McCuen, 1985).

### 1.3.2 Estimation of distributional parameters

Parameters of a distribution can be estimated using non-Bayesian or Bayesian methods (Stedinger et al., 1993). In the former, distributional parameters are considered as fixed design values, whereas in the latter, as random variables. Characteristics of these methods are summarised in Table I-1.

Table I-1: Parameter estimation methods

Groups	Methods	Principles	Characteristics
Non-Bayesian methods	Method of moments	Distributional parameters are estimated by equating sample product moments to theoretical moments.	<ul style="list-style-type: none"> <li>- This method is conceptually simple and easy to apply.</li> <li>- Parameter estimates are generally biased, therefore bias correction factors often need to be used (Cunnane, 1989).</li> <li>- Estimates of parameters of three-parameter distributions may not be feasible for small samples because the coefficient of skewness may not be reliably estimated (Cunnane, 1989).</li> <li>- For highly skewed distributions, the accuracy of parameter estimates is severely affected if there are data errors (Haan, 1977).</li> <li>- Estimates of the coefficients of skewness and kurtosis are not always easily interpreted in terms of distributional shape (Hosking, 1990; Guttman, 1992).</li> </ul>
Non-Bayesian methods	Methods of L-moments and probability weighted moments (PWM)	Distributional parameters are estimated by equating sample L-moments (or PWM) to theoretical moments.	<ul style="list-style-type: none"> <li>- These methods enable more secure inferences about the parent distributions of small samples, and are able to characterise a wide range of distributions (Hosking, 1990).</li> <li>- They are more robust to outliers of data, and less subject to bias in estimation.</li> <li>- Sometimes they can be more accurate than the method of maximum likelihood (Hosking, 1990).</li> <li>- L-moments have been developed for only standard distributions such as the uniform, exponential, Gumbel, normal, Generalized Pareto, Generalized Extreme Value, Generalized Logistic, Lognormal, Pearson type III, and Kappa distributions (Hosking and Wallis, 1997).</li> </ul>

Table I-1: Parameter estimation methods (continued)

Group	Methods	Principles	Characteristics
Non-Bayesian methods	Method of maximum likelihood	Distributional parameters are the values that maximise the probability of obtaining a sample.	<ul style="list-style-type: none"> <li>- This method is generally preferred to the method of moments (Haan, 1977) because parameter estimates are most efficient (Cunnane, 1989), and asymptotically unbiased for very large samples (Haan, 1977).</li> <li>- It is mathematically complex and therefore difficult to obtain parameter estimates for some distributions (Lin and Vogel, 1993).</li> <li>- It sometimes performs poorly when there is a significant deviation of observations from the fitted distribution (Stedinger et al., 1993).</li> </ul>
Bayesian methods (Stedinger et al., 1993)		Posterior distributions of parameters are determined by combining prior (regional) information with a sample likelihood function via Bayes' Theorem	<ul style="list-style-type: none"> <li>- These methods allow parameter uncertainties to be modelled explicitly.</li> <li>- They provide a theoretically consistent framework for the integration of at-site observations with regional and other hydrologic information.</li> <li>- They are generally used in regional analysis.</li> </ul>

### **1.3.3 Checking of the adequacy of the fitted distribution**

After estimating parameters and quantiles of a distribution, the suitability of the adopted distribution should be checked to ensure that the distribution could reproduce the features of the data that are important to a particular application. In order to do this, graphical or analytical methods can be employed.

#### **1.3.3.1 Graphical methods**

Graphical methods allow a visual inspection of the adequacy of a distribution fitted to a data set. To do this, a plotting position for each observation is first computed. The observed data are then plotted on a graph along with their corresponding plotting positions. The adopted theoretical distribution is finally plotted on the same graph. The adopted distribution is considered to be acceptable if, over the probability range of interest, it fits closely to the observed data.

Even though simple and easy to apply, the obvious disadvantage of using graphical methods for checking the adequacy of a fitted distribution is that it is difficult to decide if deviations of the observations from the fitted distribution are statistically significant or purely due to sampling variability.

#### **1.3.3.2 Analytical methods**

The analytical methods aim to test the null hypothesis that a given data set comes from an assumed distribution. A vast number of techniques are available to achieve this goal, as presented by D'Agostino and Stephens (1986) and Cunnane (1989). Among these, the Kolmogorov-Smirnov one-sample test, the chi-square goodness-of-fit test, and the probability plot correlation coefficient test are popularly applied in hydrology. These tests are briefly reviewed below.

In the Kolmogorov-Smirnov one-sample test, the theoretical cumulative distribution function underlying a data set is assumed to be completely specified. That is, no parameter of the distribution is estimated from the observed data. Under this assumption, for each observed data point, the deviation from the data to the theoretical cumulative curve is determined. The test statistic is then taken as the maximum of the computed deviations. The Kolmogorov-Smirnov test thus provides bounds within which every observed data point should lie if the sample is actually from the assumed distribution. To test the hypothesis that the given data comes from the assumed distribution, the test statistic is compared with the critical value for a given level of significance. The Kolmogorov-Smirnov one-sample test can also be applied to cases in which distributional parameters are estimated from observed data. Nevertheless, for these cases, critical values of the test are smaller than those given in the case that the distributional parameters are completely specified (Haan, 1977).

The chi-square goodness-of-fit test is one of the most commonly used tests for checking the fit of a data sample to a hypothesised population distribution. This test is applicable to discrete data, or to continuous data expressed in a discrete form by using class intervals on a continuous scale. The test statistic is constructed from the actual and expected number of observations in the class intervals. Critical values for the test statistic are dependent on the number of parameters of the adopted theoretical distribution.

The Kolmogorov-Smirnov one-sample test and the chi-square goodness-of-fit test are simple and easy to apply. However, it is argued that neither of these tests is very powerful because of the high probability of accepting the null hypothesis when it is actually false (Haan, 1977). In addition, these two tests also lack power in determining the best-fit distribution among a group of alternatives (Cunnane, 1989).

The probability plot correlation coefficient test was originally introduced by Filliben (1975) for testing if a probability distribution with unspecified location and scale parameters is a normal distribution. However, it can be readily extended to test non-normal distributional hypotheses. The test statistic uses the correlation between ordered observations and the corresponding fitted quantiles determined by the plotting position

of each observation. A near unity value of the test statistic indicates that the observed data could have come from the fitted distribution.

The probability plot correlation coefficient test is considered as a powerful goodness-of-fit test (Stedinger et al., 1993). It can also be used to select the best-fit distribution from a set of candidate distributions (Cunnane, 1989). Nevertheless, critical values for the test statistic are only available for certain distributions such as the normal, Lognormal, uniform, Generalised Extreme Values and Pearson type III distributions. This prevents application of the test to other distributions such as the beta or Generalised Pareto distribution that are used in this study.

#### **1.4 SUMMARY**

In this appendix, methods for determining the parent statistical distribution of a data set using at-site frequency analysis procedures are described and discussed. In general, parametric methods are preferable to non-parametric methods. With parametric methods, there are three steps involved, namely selection of a distributional type, estimation of distributional parameters, and checking of the adequacy of the fitted distribution. Many methods are available to carry out each of these steps. Among these, L-moment diagrams, method of moments, method of L-moments, and the chi-square goodness-of-fit test are popularly used in routine applications due to their simplicity and ease of application without sacrificing much accuracy.

## Appendix J

# SELECTION OF A DISTRIBUTED RUNOFF ROUTING MODEL FOR THE LA TROBE CATCHMENT

### J.1 INTRODUCTION

This appendix documents the research undertaken to select a distributed runoff routing model for the La Trobe River catchment at Noojee (catchment area of 290km<sup>2</sup>). The selection is restricted to those RORB and URBS runoff routing models that had already been developed and calibrated for the catchment by others.

In this appendix, an introduction to the catchment's distributed runoff routing models available from previous studies is first presented. The theoretical background of two runoff routing programs for developing these models is then summarised, together with a detailed description of the two corresponding catchment models. Finally, the selection of the best available model is reported.

### J.2 AVAILABLE DISTRIBUTED RUNOFF ROUTING MODELS

Available distributed runoff routing models for the La Trobe River catchment can be divided into two groups: RORB and URBS models. RORB catchment models had been developed by Dyer et al. (1994) and Smith (1998), whereas an URBS catchment model had been developed by Baker (1997). Of these models, as reported by Baker (1997), the model parameters estimated by Baker compared favourably with those developed by Dyer et al. (1994). Therefore, in order to select the best distributed model, only the catchment models and the corresponding parameters determined by Baker (1997) and Smith (1998) were tested and are reported in the following section.

## J.2.1 RORB model

### J.2.1.1 Theoretical background

RORB (Laurenson and Mein, 1995) is a spatially distributed, non-linear runoff and streamflow routing program for calculating flood hydrographs from rainfall and other channel inputs. The program can also be used for retarding basin design and flood routing in channels.

To simulate a given catchment and its stream system, the catchment is divided into sub-areas bounded by catchment divides and ridge lines. The stream network is also subdivided into reaches, each of which is associated with a model storage.

To model streamflow on the catchment, RORB performs a sequence of operations described by numeric control codes specified in the catchment data file. The routing process starts with the deduction of losses from rainfall for each sub-area. The rainfall excess at the catchment upstream end is then routed to the first stream confluence where the rainfall excess hydrograph is stored. The rainfall excess hydrograph from another sub-area contributing to another branch of the confluence, if any, is then added to the stored hydrograph. This step is repeated until the modelling of all areas contributing to other branches of the confluence is completed. The combined hydrograph is then routed downstream in a similar fashion until it reaches the catchment outlet.

To compute stream discharge, the following non-linear storage-discharge relation is assumed:

$$S = 3600kQ^m \quad (J-1)$$

where  $S$  is the storage ( $m^3$ );  $Q$  is the outflow discharge ( $m^3/s$ );  $m$  is a dimensionless exponent which reflects the catchment's non-linearity; and  $k=k_c k_r$  is a dimensional coefficient, which is a function of the relative delay time computed for the reach storage under consideration ( $k_r$ ) and an empirical coefficient applicable to the entire catchment and its stream network ( $k_c$ ).

The two main parameters of RORB are  $k_c$  and  $m$ . They are evaluated by a trial and error procedure (by means of fit and test runs) using concurrent observed rainfall and

flood data for a particular catchment. Once determined, these parameters are fixed for the given catchment and can be used to estimate floods resulting from hypothetical design conditions (design runs).

### J.2.1.2 Smith's RORB model for the La Trobe River catchment

In Smith's RORB model, the La Trobe River catchment at Noojee was represented by 19 sub-areas and 28 channel reaches (see Figure J-1 and Table J-1). Four observed rainfall-runoff events were used to calibrate the model parameters  $k_c$  and  $m$ . Data files of the rainfall events and the corresponding surface runoff, together with the RORB catchment file, are available in electronic form (Smith, 1998).

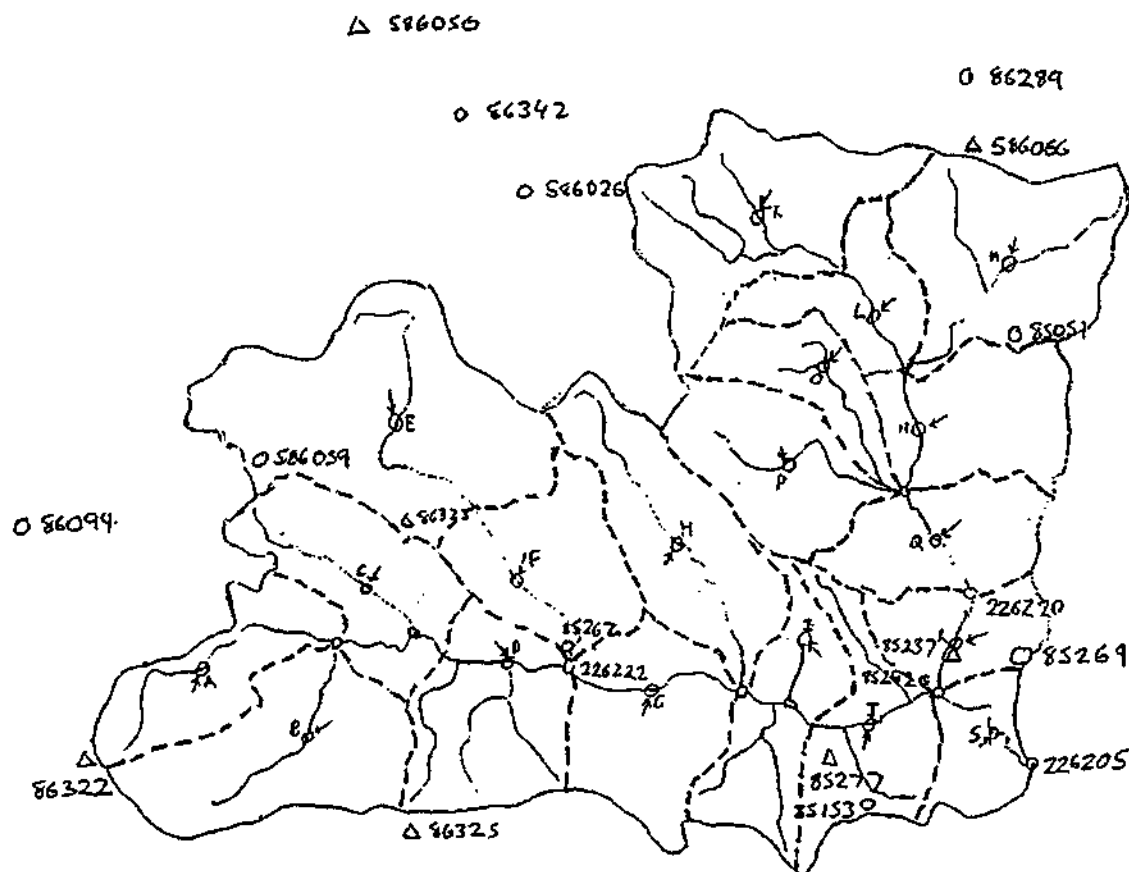


Figure J-1: Smith's RORB model for the La Trobe River catchment at Noojee (Smith, 1998)

A summary of some statistical characteristics of the observed surface runoff used for model calibration and the calibrated parameters of the catchment model ( $m=0.8$ ,  $k_c=43.3$ ) is also presented in Table J-1. Generally speaking, the calculated hydrographs preserved well the flood peak and flood volume of the observed hydrographs, but the time to peak was not satisfactorily reproduced.

Table J-1: Summary of distributed models of the La Trobe River catchment at Noojee ( $m=0.8$ )

Study	Catchment formulation		No. of fitted events	Range of calibrated flows ( $m^3/s$ )			Average $k_c$
	No. of sub-areas	No. of reaches		Minimum	Maximum	Average	
Baker (1997)	11	15	7	7.3	59.9	26.8	26.05
Smith (1998)	19	28	4	25.6	59.9	36.45	43.3

## J.2.2 URBS model

### J.2.2.1 Theoretical background

URBS (Carroll, 1994) is a modified and extended version of RORB in which key words are used in place of the numeric codes used in RORB for describing the model sequence of operations. The representation of catchment and channel network in URBS is identical to that used in RORB. The two main parameters of URBS are  $\alpha$  and  $m$ . There is a relationship between the parameter  $\alpha$  of URBS and the parameter  $k_c$  of RORB as follows:

$$\alpha = \frac{k_c}{d_{av}} \quad (J-2)$$

where  $d_{av}$  is the average flow distance (in km) in the channel network of sub-area inflows.

The above relationship indicates that URBS and RORB are interchangeable in operation. That is, a given RORB catchment model with the parameters  $k_c$  and  $m$  can be converted into an equivalent URBS model with the parameters  $\alpha$  and  $m$ . In other words, a RORB model developed for a given catchment can be easily modified to be run using URBS and vice versa.

### J.2.2.2 Baker's URBS model for the La Trobe River catchment

In Baker's URBS model, the La Trobe River catchment was characterised by 11 sub-areas and 15 river reaches. Seven observed rainfall-runoff events were used for model calibration. The average value of  $\alpha$  obtained from calibration was 1.8, and  $d_{av}$  was 14.47. Therefore using Equation (J-2), the average  $k_c$  for the equivalent RORB model for the same catchment was computed to be 26.05. The catchment model was available in hard copy, whereas none of the rainfall-runoff events used in model fitting was available.

Details of the URBS model for the La Trobe River catchment and the average  $k_c$  value for its equivalent RORB model are summarised in Table J-1. Overall, for the events used in fitting runs, this model predicted flood hydrographs with sufficient accuracy in terms of the flood peak magnitude and the time to flood peak.

## J.3 SELECTION OF A DISTRIBUTED RUNOFF ROUTING MODEL

In order to select the best distributed runoff routing model for the study catchment, the two available models were tested using an independent event which was not used in the fitting runs. The event selected for testing was the flood event from 2100 hours on 27/1/1963 to 0000 hours on 30/01/1963, with a peak flow of  $24.3\text{m}^3/\text{s}$ , produced by 120.9mm of rain in 52 hours.

The following procedure was adopted:

- The URBS model for the La Trobe catchment was modified to be able to run with RORB.
- Rainfall depths at the daily and recording gauges within and near the study catchment for the period concurrent with the selected flood event were then extracted from the HYDSYS database (HYDSYS, 1994). The rainfall depths obtained were next recorded on the catchment map at their corresponding gauge location. Lines of equal rainfall depths (isohyets) were then drawn. Rainfalls on sub-catchment areas were approximately computed by interpolating between these isohyetal lines.

- For each of the two catchment models, the RORB program was run with the selected rainfall-runoff event and the fixed model parameters ( $k_c$  and  $m$ ) shown in Table J-1. In each run, the initial loss and continuing loss rate were varied until the observed and estimated flood hydrographs matched.

A summary of the values of the initial loss, continuing loss and the fixed  $k_c$  used to compute the flood hydrograph is presented in Table J-2. In this table, the flood peak discharge and the corresponding time to peak of the observed and calculated hydrographs are also given. An example of the flood hydrographs estimated by Smith's and Baker's models and the corresponding observed flood is illustrated in Figure J-2.

Table J-2: Comparison of URBS and RORB models (test run, the 1963 flood,  $m=0.8$ )

Catchment model	IL (mm)	CL (mm/h)	$k_c$	Peak discharge ( $m^3/s$ )			Time to peak (h)		
				Observed	Calculated	% difference	Observed	Calculated	% difference
Smith (1998)	30	11.19	43.30	18.6	15.3	-17.6	34	51	50.0
Baker (1997)	30	11.17	26.05	18.6	21.3	14.5	34	38	11.8

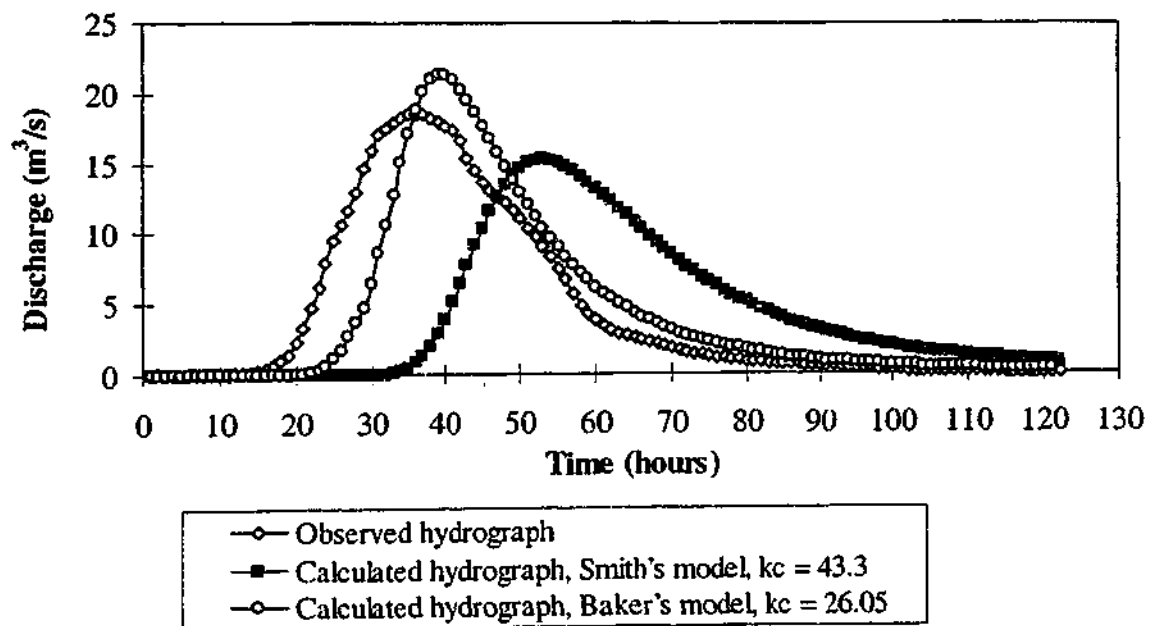


Figure J-2: Flood hydrographs estimated by Smith's and Baker's models (testing run,  $m=0.8$ , the 1963 flood)

In comparing the performance of the available distributed models for the La Trobe catchment, it can be seen from Table J-2 and Figure J-2 that Baker's model (with  $k_c=26.05$ ,  $m=0.8$ ) gives better estimates of both the flood peak and time to peak than Smith's model. Therefore this model was adopted as the best distributed runoff routing model for the specified catchment.

To improve the estimate of  $k_c$  for the selected model, the test event was also used for fitting. As the estimated flood peak is greater than the observed one (see Table J-2),  $k_c$  needs to increase so that the computed flood peak decreases. As a final test, Baker's model with  $k_c=30$ ,  $m=0.8$  was used to test all the five flood events, of which four data files were documented by Smith (1998), and the other one was compiled in this study. Results of this final test are shown in Table J-3 and illustrated in Figure J-3.

Table J-3: Baker's model - Summary of model testing ( $k_c=30$ ,  $m=0.8$ )

Event	IL (mm)	CL (mm/h)	Peak discharge ( $m^3/s$ )			Time to peak (h)			Volume ( $10^6 m^3$ )	
			observed	calculated	% difference	observed	calculated	% difference	observed	calculated
1963	30	11.2	18.6	18.3	-1.6	34	40	17.6	1.96	1.93
1969	0	4.8	15.0	16.0	6.7	89	59	-33.7	2.58	2.59
1971	8	4.6	48.6	49.9	2.7	73	49	-32.9	5.02	5.03
1977	23	10.2	22.2	20.9	-5.8	31	29	-6.5	2.01	1.98
1980	0	6.1	31.3	48.1	53.7	60	53	-11.7	4.11	4.07

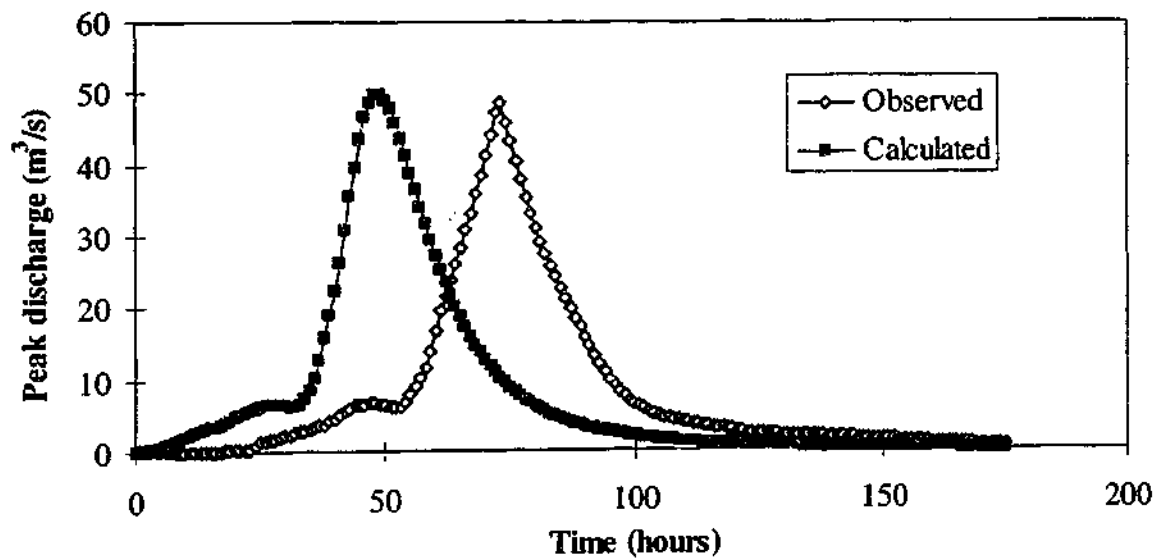


Figure J-3: Observed and calculated hydrographs (Baker's model,  $k_c=30$ ,  $m=0.8$ , the 1971 flood)

In examining the performance of Baker's model of the La Trobe catchment, it is evident in Table J-3 that this model preserves well the observed flood peak and the flood volume for four of the five flood events used. Differences between the peak discharge or flood volume of the computed and observed flood hydrographs are less than 7%, except for the 1980 flood. Nevertheless, the time to peak of the observed hydrographs is not reproduced well in the estimated hydrographs. The difference in the lag time between the observed and computed hydrographs is also different from event to event.

#### **J.4 SUMMARY**

There are three distributed runoff routing models available for the La Trobe River catchment at Noojee. Parameters of these models had been calibrated but not yet tested. In order to select the best distributed model available, two of these models were tested with an observed rainfall-runoff event not used in model calibration. Results indicated that Baker's model (Baker, 1997) produced better estimates of the peak flood discharge and the time to flood peak than Smith's model (Smith, 1998). Therefore, Baker's model with  $k_c$  of 30 and  $m$  of 0.8 was adopted as the best available distributed runoff routing model for the study catchment.

## Appendix K

### DATA GENERATION

This appendix provides the theoretical bases of the computer subroutines used in this research for random number generation. It first describes the linear congruential method for the generation of random numbers from a uniform distribution, which forms the basis of the data generation from any other distributions. The inverse cumulative distribution method and the rejection method for generating random numbers from other continuous distributions are then documented. More details of these methods can be found in Haan (1977), Press et al. (1989), and Knuth (1998).

#### K.1 THE LINEAR CONGRUENTIAL METHOD

In the linear congruential method, a sequence of NR uniformly distributed random numbers  $X_1, X_2, \dots, X_{NR}$  ( $NR \geq 0$ ) can be obtained by setting:

$$X_{NR} = (a_0 X_{NR-1} + c_0) \text{ mod } m_0 \quad (\text{K-1})$$

where mod  $m_0$  is the modulus of  $m_0$  ( $0 < m_0$ ),  $a_0$  is the multiplier ( $0 \leq a_0 < m_0$ ),  $c_0$  is the increment ( $0 \leq c_0 < m_0$ ),  $X_0$  is the starting value (also called the seed, where  $0 \leq X_0 < m_0$ ), and NR is the length of the sequence.

The integer parameter values of  $m_0$ ,  $a_0$ ,  $c_0$ , and  $X_0$  are usually selected such that the length of the generated sequence is long and the speed of generation is fast. For the special cases in which  $c_0=0$  and  $c_0 \neq 0$ , the linear congruential method is termed the multiplicative congruential method and the mixed congruential method, respectively.

## K.2 THE INVERSE CUMULATIVE DISTRIBUTION METHOD

In the inverse cumulative distribution function method, it is assumed that  $p_Y(y)$  is the probability density function of the probability distribution of interest. It is also assumed that  $F_Y(y)$ , the cumulative distribution function of  $p_Y(y)$ , exists and that it is a monotonically increasing function on the  $(0, 1)$  interval. Under these assumptions, in order to generate a random value  $y$  from  $p_Y(y)$ , a uniform random number  $x$  is chosen between 0 and 1. The selected random number is then related to the cumulative distribution function by the relationship:  $F_Y(y) = x$  (see Figure K-1). Finally, the required random value  $y$  is obtained by solving the above equation for  $y$ .

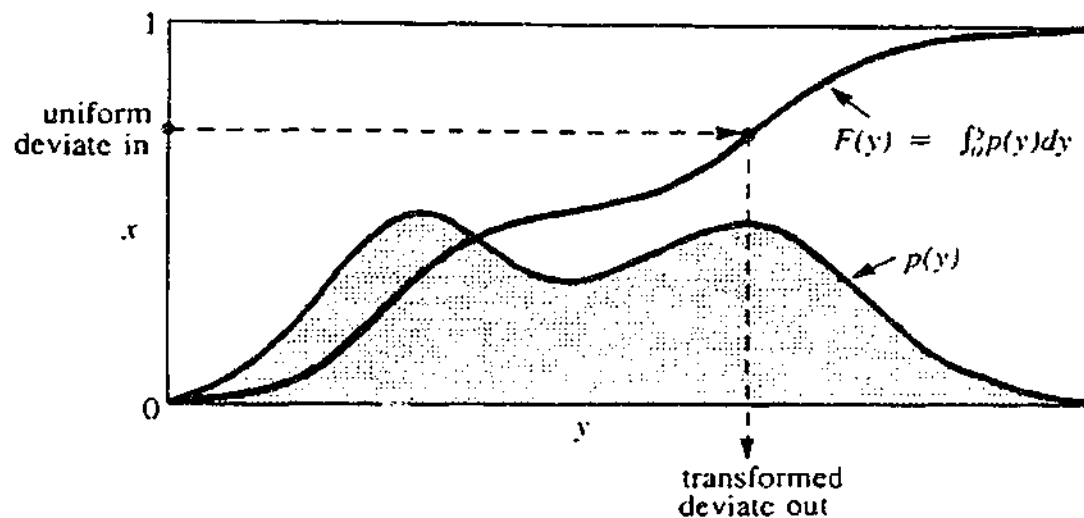


Figure K-1: The inverse cumulative distribution function method (Press et al., 1989)

## K.3 THE REJECTION METHOD

The rejection method is used when the cumulative distribution function of the variable of interest  $X$  does not exist, thus the inverse cumulative distribution function method can not be applied.

In the rejection method, the distribution function  $p(x)$  from which random numbers are to be generated is plotted on a graph so that the area under this curve is one unit.

Another function  $f(x)$ , called the comparison function, is then chosen such that its cumulative distribution function exists, and when plotted on the same graph it is everywhere above  $p(x)$ . In order to generate a random value from  $p(x)$ , the inverse cumulative distribution function method is first used to generate a random deviate  $x_0$  from the distribution  $f(x)$ . To decide whether to accept or reject  $x_0$ , a second uniform deviate is then generated. If this second value is less than the ratio  $p(x_0)/f(x_0)$ , that is the random point  $[x_0, f(x_0)]$  lies within the area under the original probability distribution  $p(x)$ ,  $x_0$  is accepted (see Figure K-2) Otherwise,  $x_0$  is rejected, a new random deviate of  $f(x)$  is then generated and the procedure above is repeated.

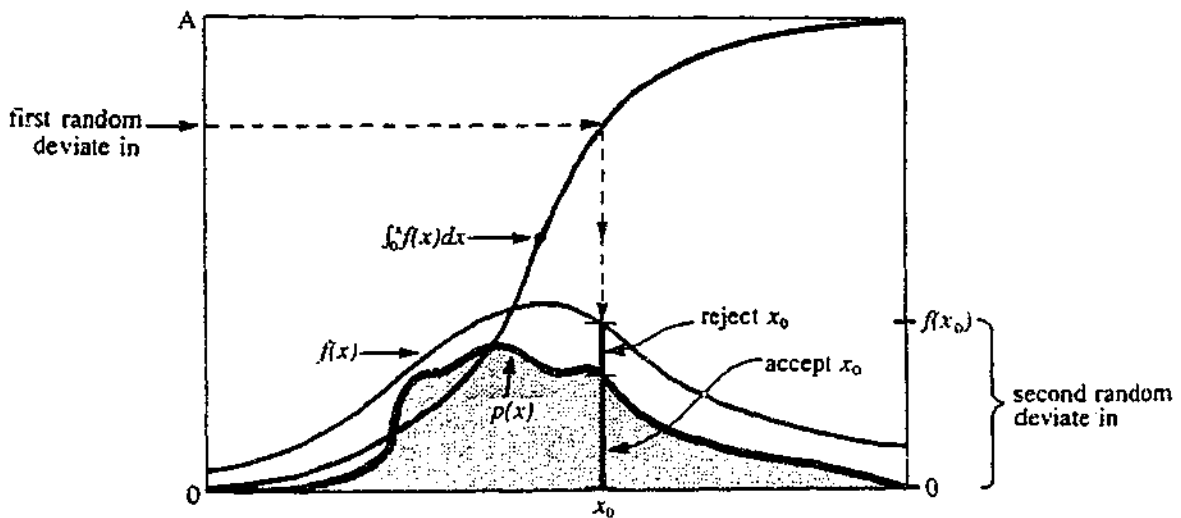


Figure K-2: The rejection method (Press et al., 1989)

## Appendix L

## CONFERENCE PAPERS

This appendix contains the conference papers that were written based on the research conducted in this study.

- Paper 1: Weinmann, P.E., Rahman, A., Hoang, T.M.T., Laurenson, E.M., Nathan, R.J. (2000). Monte Carlo Simulation of Flood Frequency Curves from Rainfall – The Way Ahead. Proceedings of the 3<sup>rd</sup> International Hydrology and Water Resources Symposium, Perth, Australia. I. E. Aust. National Conference Publication, 564-569.
- Paper 2: Hoang, T.M.T., Rahman, A., Weinmann, P.E., Laurenson, E.M., Nathan, R.J. (1999). Joint Probability Description of Design Rainfalls. Handbook and Proceedings of Water 99 Joint Congress, Brisbane, Australia. I. E. Aust. National Conference Publication, 379-384.
- Paper 3: Weinmann, P.E., Laurenson, E.M., Rahman, A., Hoang, T.M.T. (1999). Improved Design Flood Estimation through Joint Probability. Proceedings of the 2<sup>nd</sup> Inter-Regional Conference on Environment-Water, Lausanne, Switzerland. Presses Polytechniques et Universitaires Romandes. Paper 2.2 on CD-ROM.
- Paper 4: Weinmann, P.E., Rahman, A., Hoang, T.M.T., Laurenson, E.M., Nathan, R.J. (1998). A New Modelling Framework for Design Flood Estimation. International Symposium on Storm Water Management and International Conference on Hydraulics in Civil Engineering, Adelaide, Australia. I. E. Aust. National Conference Publication, 393-398.

# Monte Carlo Simulation of Flood Frequency Curves from Rainfall – The Way Ahead

P E Weinmann<sup>1,2</sup>, A Rahman<sup>2,3</sup>, TMT Hoang<sup>2,4</sup>, E M Laurensen<sup>1</sup> and R J Nathan<sup>5</sup>

<sup>1</sup> Department of Civil Engineering, Monash University, Clayton, Victoria; <sup>2</sup> Cooperative Research Centre for Catchment Hydrology; <sup>3</sup> Queensland University of Technology, Brisbane; <sup>4</sup> Bureau of Meteorology, Melbourne; <sup>5</sup> Sinclair Knight Merz, Melbourne

**Abstract :** This paper summarises the results of a 3-year research project by the CRC for Catchment Hydrology (CRCCH). It identifies significant shortcomings in the current Design Event Approach to rainfall-based design flood estimation, and argues that substantial improvements in the accuracy and reliability of flood estimates can be obtained from a more rigorous treatment of probability aspects in the generation of design floods. Application of the proposed Monte Carlo Simulation approach to three test catchments in Victoria has produced promising results, and has demonstrated the feasibility and in-principle advantages of the approach. The paper discusses how far the CRCCH work has advanced towards resolving the main research issues, and outlines desirable future development work to allow the new method to be routinely applied as a design tool.

## 1 INTRODUCTION

Where reliable flood data are available for the site and conditions of interest, flood frequency analysis is generally the most direct and most accurate method for estimating design floods for average recurrence intervals (ARIs) less than 100 years. However, for most Australian catchments, reliable streamflow records are either unavailable, of insufficient length or quality to allow reliable flood frequency analysis, or do not relate to the current or future catchment conditions of interest. In all these situations, a significant degree of *extrapolation* beyond the range of available flood observations is involved, and flood data thus has to be substituted or supplemented by rainfall and catchment data, and by knowledge of flood generation processes. The knowledge gained from well-gauged catchments is embodied into hydrological models (eg. loss models, runoff routing models), and can then be applied to other catchments.

Because of the widespread use of rainfall-based design flood estimation methods as a basis for designing structures and other development exposed to flood risks, any shortcomings in the currently applied methods may have significant economic implications; continued improvements in methodology and design data are thus desirable.

This paper identifies inherent shortcomings of the Design Event Approach to rainfall-based design flood estimation, discusses results of research into a proposed method that promises significant improvements, and indicates the direction of desirable future development of the method to allow its application in design practice.

## 2 THE CURRENT APPROACH AND ITS LIMITATIONS

### 2.1 Conceptual basis of the Design Event Approach

The current Design Event Approach represents a combination of conceptual hydrologic modelling and 'black-box' modelling approaches. The input to the modelling process consists of *probabilistic design rainfall events* of pre-selected duration, formed by combining design values of rainfall intensity with corresponding temporal and areal patterns of rainfall. Conceptual hydrologic models are then used to transform a selected design rainfall input event firstly into a runoff event (by use of a loss model), and then into a *design flood hydrograph output* (by use of a runoff routing model). This design flood may include a baseflow component (i.e. delayed contributions from previous rainfall events). The 'black-box' aspect is introduced when models calibrated to *actual observed events* are applied for modelling of *probabilistic events*, with design inputs or parameters adjusted arbitrarily to produce the desired output probability characteristics.

Figure 1 shows a schematic representation of the Design Event Approach. The approach embodies the important assumption that, for each rainfall duration, there is a unique (typical) combination of all the model inputs and model parameters that transforms the design rainfall of given average recurrence interval (ARI) into a flood hydrograph output of the same ARI.

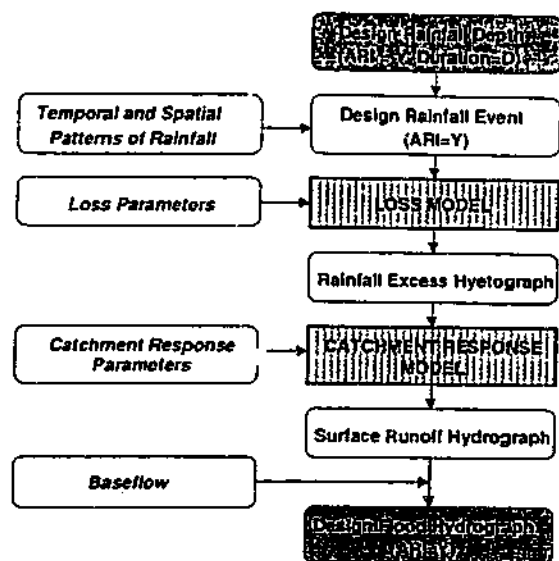


Figure 1 Schematic representation of the Design Event Approach:

The approach also assumes that, for a given catchment and selected ARI, there is *critical rainfall duration* that produces the design flood. However, the critical rainfall duration for a catchment is not known a priori, but depends on the interplay of catchment characteristics, as reflected in the loss and runoff routing models, (eg. catchment size and shape, runoff production and drainage network characteristics), and rainfall characteristics (average rainfall intensity, temporal and areal variability). A number of trial rainfall durations thus need to be applied; the one producing the highest flood peak (or volume) for the specific case is then adopted as the critical duration. Figure 2 illustrates the process of deriving design floods based on the critical rainfall duration concept.

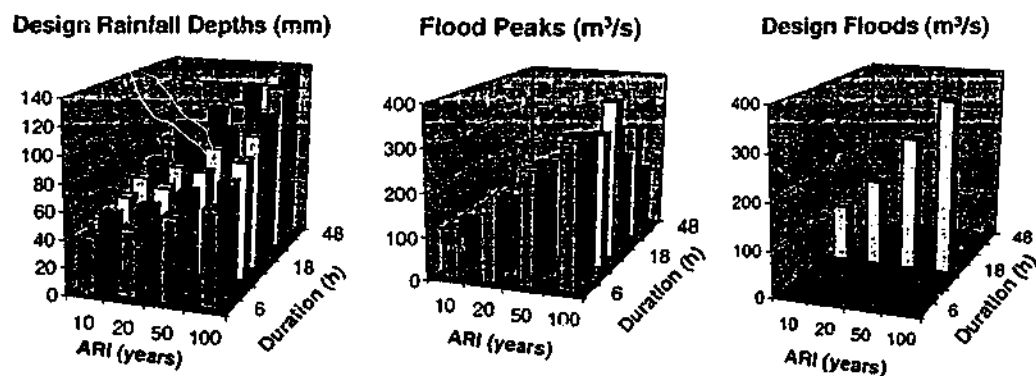


Figure 2 The critical rainfall duration approach to design flood estimation

## 2.2 Theoretical limitations and practical problems of the Design Event Approach

It is well known that actual floods of a given peak magnitude could be the result of quite different rainfall events, combined with a range of other flood producing factors. Relatively moderate storms occurring on saturated catchments have produced major historic floods, while very heavy storms falling on dry catchments may have only resulted in moderate flooding. The task of defining a *typical combination of flood producing factors* for application in the Design Event Approach is made particularly difficult by the fact that flood response to rainfall is generally non-linear and can be highly non-linear. This means that average conditions of rainfall or loss are unlikely to produce average flood conditions. While the stated intent of the Design Event Approach of "probability-neutral" transformation of design rainfalls into design floods is quite clear and plausible, its practical implementation is fraught with difficulties and pitfalls for the unsuspecting designer.

The problems inherent in the 'critical rainfall duration' concept are best illustrated by reference to observed flood series. The events forming an observed series of annual floods correspond to different rainfall durations

and thus define a *marginal distribution of flood magnitude* (regardless of rainfall duration). The arbitrary selection of the 'critical rainfall duration' as the basis for estimating the design flood is equivalent to an assumption that "the marginal distribution of flood magnitude is equal to the conditional distribution of flooding for the critical rainfall duration". There is no reason why this assumption should be true in the general case.

The effect of the critical duration assumption is a systematic bias in flood frequency estimates, resulting in a tendency to over-estimate the magnitude of design floods (Blöschl et al, 1997). In practice, this systematic error has to be compensated by arbitrary corrections, such as increased losses or greater storage delays in runoff routing models. These corrections tend to obscure any relationships that may exist between design parameters and information derived directly from flood observations, thus making the task of deriving reliable design parameters for ungauged catchments more difficult.

Recent developments in design flood estimation have generally concentrated on specific components of the overall design flood estimation process, e.g. rainfall areal reduction factors, losses or runoff routing parameters. Improvements in the estimation of these *individual factors* have been achieved by using a broader database, sounder methods of analysis and/or better explanatory variables. However, due to the complex interactions of the different factors and the clouding effects of corrections applied in the calibration to flood frequency results, it has not been possible to realise the full benefits of these developments (Hill et al. 1996.).

As an example, Hill et al. (1996) found that, while there is theoretical justification for the use of the more consistent set of 'filtered' temporal patterns of design rainfall, their use in conjunction with other improved design inputs tends to underestimate design floods. The 'correction factor' built into the 'unfiltered' patterns generally leads to better design flood estimates, but the internal inconsistencies contained in these patterns can produce inconsistent flood estimates for different rainfall durations. This requires the designer to make difficult and highly subjective decisions in the selection of a critical rainfall duration.

### 3 THE WAY AHEAD: HOLISTIC SIMULATION OF DESIGN FLOODS FROM RAINFALL

The main problem with the Design Event Approach is that it does not adequately allow for the large variability of the flood producing factors, and the interactions between them. The simplistic treatment of important probability aspects in the flood formation process severely limits the scope for further improvements in design flood estimates. Such improvements require a more realistic representation of how the key factors work together to produce floods. CRCCH Project FL1 (Holistic approach to rainfall-based design flood estimation) has investigated two different approaches for deriving design floods: the Continuous Simulation Approach and the Joint Probability Approach. Both attempt to simulate more realistically how floods are formed from rainfall inputs, but they do so in quite a different fashion.

In the *Continuous Simulation Approach*, a long continuous time series of streamflow (and floods) is derived from observed or synthetically generated time series of rainfall and evaporation, using appropriate runoff generation and hydrograph formation models (Boughton et al., 1999). From this simulated streamflow time series, the flood events of interest can be extracted and analysed by conventional frequency analysis. The Continuous Simulation Approach is conceptually the most desirable one, as it can simulate most closely the way an actual flood series is produced. However, at the moment its application is limited to gauged catchments.

In the *Joint Probability Approach*, the frequency distribution of a selected flood characteristic is derived by combining the probability distributions of key input variables (Rahman et al., 2000). Rather than producing a time series of floods, the flood events are only generated in the probability domain; the simulated flood series contains no information on the timing or sequencing of events. The joint probability approach can be regarded as a further development of the currently used design event approach, but treats probability aspects more rigorously.

Since the pioneering work of Eagleson (1972), many derived flood distribution methods based on joint probability principles have been developed and tested in research projects. Some of these methods are reviewed in Rahman et al. (1998). Their limited application in practice can be attributed to the fact that many of the methods are constrained in their generality by employing simplistic runoff production and transfer functions. There is also a lack of specific design data to allow the application of these methods to ungauged catchments. The Monte Carlo simulation method described below is intended to overcome many of these limitations.

## 4 THE ELEMENTS OF THE PROPOSED MONTE CARLO SIMULATION APPROACH

### 4.1 General

The proposed approach employs a Monte Carlo simulation technique to generate say 10,000 flood events at the point(s) of interest, from which a very long series of peak flows or flood volumes can be extracted. Conventional flood frequency analysis is then applied to this partial flood series to produce a frequency curve of design floods. In developing the new method, emphasis was placed on improved representation of those elements in the flood generation process that have a dominant influence on the derived flood frequency distribution. The loss and runoff routing models used in the Design Event Approach are generally adequate and can thus be applied in their present form, but important probabilistic elements in the flood estimation process need to be represented more realistically. This involves the simulation of stochastic runoff events from the probability distributions of their main characteristics.

### 4.2 Simulation of stochastic runoff events

Precipitation, in the form of rainfall, is the main flood-producing factor in most situations in Australia. The process of simulating flood events thus starts with generating *stochastic rainfall events*. Two types of rainfall events have been defined as part of this project:

- (i) a *complete storm* comprises those parts of the rainfall time series that can be regarded as forming a single event as far as the flood response of the catchment is concerned, and
- (ii) a *storm core* represents that part of a complete storm with the highest relative rainfall intensity.

Historic rainfall records from pluviograph stations in and around a catchment are analysed to identify the partial series of significant rainfall events and their stochastic properties. Rainfall events are only selected for the analysis if they have the potential to produce a flood, with the average rainfall intensity over the duration of the event being used as an indicator of event magnitude. Typically, an average of 3 to 7 events per year are selected.

The rainfall characteristics of interest for simulation are (i) the rainfall event duration ( $D$ ), (ii) the average rainfall intensity ( $I$ ), (iii) the temporal pattern ( $TP$ ) and (iv) the areal pattern ( $AP$ ) during the event. The variation of the first three of these variables is represented by their probability distributions, while the areal rainfall pattern is assumed to be constant (generally uniform). Information on the correlations between the rainfall variables is also required, to ensure that the generated stochastic rainfall events preserve the characteristics of real observed rainfall events. Rainfall intensity is so strongly dependent on duration that it needs to be represented by a conditional distribution of intensity for a given duration. A more detailed discussion of the stochastic representation of rainfall events is given in Hoang et al. (1999).

The next step in the simulation is the transformation of the rainfall events into *stochastic runoff events*, by application of a loss model. In accordance with current practice for the Design Event Approach, a conceptual loss model, the initial loss-continuing loss model, is applied. The initial loss parameter ( $IL$ ), which can vary widely between different flood events, is represented by a probability distribution, while the continuing loss parameter ( $CL$ ) is generally less variable for a given catchment and thus represented by a fixed value.

The statistical models used to represent the stochastic variation of the selected three rainfall characteristics and one loss parameter are summarised in Table 1, together with the data used to estimate their parameters. Further details are given in Rahman et al. (2000) for storm cores, and Hoang (2000) for complete storms, respectively.

Table 1 Derivation of probability distributions of key variables in Monte Carlo simulation model

CHARACTERISTIC	TYPE OF STATISTICAL MODEL	PARAMETERS FROM
Rainfall Duration ( $D$ )	Exponential Distribution (Storm Cores) Gen. Pareto Distrib. (Complete Storms)	Regional Rainfall Data
Rainfall Intensity ( $I$ )	Exponential Distribution (Conditional on Rainfall Duration)	Catchment Rainfall Data
Rainfall Temporal Pattern ( $TP$ )	Sampling from Observed Storms, or Multiplicative Cascade Model	Regional Rainfall Data
Initial Loss ( $IL$ )	Beta Distribution	Catchment Rainfall and Streamflow Data

### 4.3 Modelling of hydrograph formation – runoff routing

The Monte Carlo simulation framework developed in the CRCCH project is intended for application with any of the non-linear, semi-distributed runoff routing models (e.g. RORB, Laurenson and Mein, 1997) currently used with the Design Event Approach. A simpler conceptual runoff routing model (with a single non-linear storage concentrated at the catchment outlet) was used in the initial applications of the proposed Monte Carlo simulation approach described below. For these medium size catchments (less than 500 km<sup>2</sup>), the simpler model provides an adequate indication of the catchment's runoff routing response, but a semi-distributed runoff routing model could be expected to produce more accurate results. It would also be more flexible in reproducing special catchment features, such as natural or artificial storage basins, or the effects of changes to the drainage system.

## 5 INITIAL RESEARCH OUTCOMES

The proposed Monte Carlo simulation methodology has so far been applied to four catchments in Victoria, Australia, ranging in size from 78 to 290 km<sup>2</sup>. Here the *storm core* simulation results for the Boggy Creek catchment (catchment area 108 km<sup>2</sup>, mean annual rainfall 1020mm) are presented. The simulation procedure was applied to a partial series of 10,000 storm/runoff events, with an average of 5 events per year, equivalent to an annual series of 2000 years. Figure 3 shows the comparison of the simulated flood frequency curve with the observed one. Some design flood estimates obtained from the Design Event Approach are also shown.

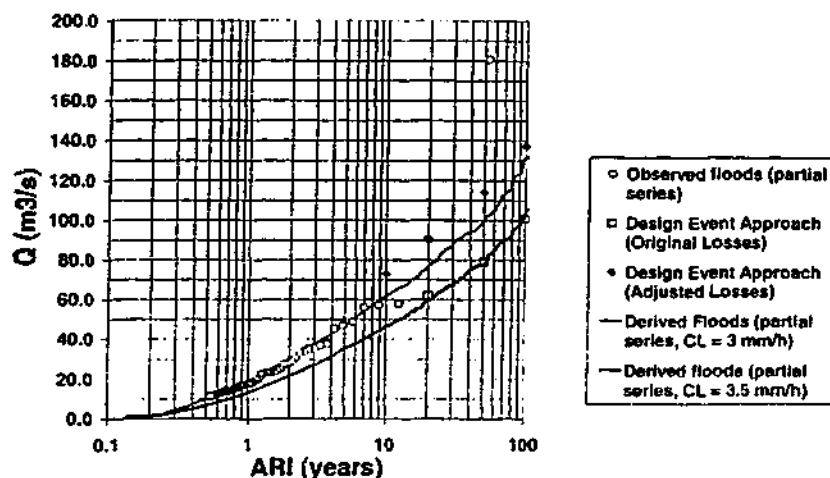


Figure 3 Comparison of derived and observed flood frequency curves for Boggy Creek catchment

The evaluation of the results is made difficult by the fact that the true flood frequency curves are not known. The magnitude of the 1993 flood in the Boggy Creek catchment (180 m<sup>3</sup>/s) had only been estimated, and the available flood record is relatively short (32 years). This introduces considerable uncertainty into the 'observed' flood frequency curve. Two sets of results are shown for the Design Event Approach, both obtained with the same RORB model of Boggy Creek catchment. The first set used the initial and continuing loss parameters from model calibrations, the second is based on an adjusted continuing loss rate, so as to match the 'observed' flood frequency curve for an ARI of 20 years. The flood frequency curve from Monte Carlo simulation with independently derived design inputs, shown by the heavier line, underestimates the observed flood frequency curve. However, the second line shows that a much better overall match between simulated and observed flood frequency curves can be obtained by a small adjustment of the continuing loss rate from 3.5 to 3 mm/h.

Results for the other catchments indicated similar performance of the Monte Carlo simulation approach, with deviations from the 'observed' flood frequency curves being generally less than 25% in the range of floods that could be confidently estimated from flood frequency analysis. Sensitivity analyses indicated that the simulated flood frequency curves are very sensitive to correct representation of the conditional distribution of rainfall intensity, and moderately sensitive to the representation of temporal patterns and initial loss.

Overall, the results of the initial applications show that the principles employed in the Monte Carlo simulation approach are sound, and that the approach is workable in practice. The application in gauged catchments is straightforward and, by eliminating the concept of 'critical duration', avoids arbitrary smoothing of inconsistent results. The simulation of 10,000 stochastic runoff and flood events takes less than half an hour on a standard personal computer.

## 6 TURNING THE RESEARCH RESULTS INTO PRACTICAL TOOLS

While the results of the initial applications of the proposed method for deriving flood frequency curves by Monte Carlo simulation are promising, there is a need for more extensive testing of the method on a broader range of catchments. A significant amount of development work is still needed to turn the method into a user-friendly tool that can be widely applied in design practice. The method offers the prospect of using much of the currently available regionalised design rainfall and loss data, and should thus also be applicable to ungauged catchments. Further research and development should address the following high priority objectives:

- to incorporate into the method one of the currently used semi-distributed runoff routing models, to allow more detailed representation of catchment features and modelling of spatially varying catchment rainfall;
- to combine the at-site rainfall frequency estimates for storm cores with regional design rainfall estimates;
- to better represent significant seasonal effects by replacing annual rainfall and loss characteristics by values derived from a seasonal analysis;
- to improve the regional estimation methods for continuing loss and runoff routing parameters.

Some of these research and development initiatives would also benefit the Design Event Approach but, for the reasons stated earlier, the benefits of any future flood estimation research can only be fully realised, if some of the fundamental deficiencies in the current approaches are addressed first. The proposed Monte Carlo simulation approach promises to overcome these limitations.

## 7 CONCLUSIONS

This paper has highlighted some of the theoretical and practical limitations of the currently used Design Event Approach to rainfall-based design flood estimation. It has argued that substantial improvements in design flood estimates are only possible if the variability and interaction of flood producing factors are better allowed for. Both the Continuous Simulation Approach and the proposed Monte Carlo Simulation Approach described in this paper can overcome these limitations, and have the potential to be routinely applied in the future. The Monte Carlo simulation approach has the advantage that it can utilise some of the models and design data used with the Design Event approach; this will allow it to be more readily applied to flood estimation in ungauged catchments. The results of the initial applications of the proposed Monte Carlo Simulation approach are very promising. Further testing, and development of the approach into a practical design tool, are therefore highly desirable.

## 8 REFERENCES

- Blöschl, G. and Sivapalan, M. (1997). Process Controls on Flood Frequency: 2. Runoff Generation, Storm Properties and Return Period. Centre for Water Research, Uni. of W.A., Rep. ED 1158 MS, (Subm. to Water Resources Research.)
- Boughton, W. C., Muncaster, S. H., Srikanthan, K., Weinmann, P. E. and Mein, R. G. (1999). Continuous simulation for design flood estimation – a workable approach. Proceedings WATER99 Joint Congress, Brisbane vol.1, pp. 178-183, I.E.Aust., Canberra.
- Eagleson, P.S. (1972). Dynamics of flood frequency. Water Resources Research, Vol. 8, NO. 4, pp 878-898.
- Hill, P. I., Mein, R. G. and Weinmann, P. E. (1996). Testing of improved inputs for design flood estimation in south-eastern Australia, Report 96/6, CRC for Catchment Hydrology, Monash University, Melbourne, 76 pp.
- Hoang, T.M.T., Rahman, A., Weinmann, P.E., Laurenson, E.M. and Nathan, R.J. (1999). Joint probability description of design rainfalls. WATER99 – Joint Congress, Brisbane. I.E.Aust., Canberra, Vol. 1, pp 379-384.
- Hoang, T.M.T. (2000). A joint probability approach to rainfall-based flood estimation. PhD Thesis, Monash University, (in preparation).
- Laurenson, E.M. and Mein, R.G. (1997). RORB – Version 4, Runoff routing program, User manual. Dept. of Civil Engineering, Monash University.
- Rahman, A., Hoang, T.M.T., Weinmann, P.E. and Laurenson, E.M. (1998). Joint Probability Approaches to Design Flood Estimation: A Review. CRC for Catchment Hydrology, Report No. 98/8, Monash University.
- Rahman, A., Weinmann, P.E., Hoang, T.M.T., Laurenson, E.M. and Nathan, R.J. (2000). Flood frequency curves derived by Monte Carlo simulation. CRC Research Report, (in preparation).

## ACKNOWLEDGMENTS

The authors wish to thank the Parties of the CRC for Catchment Hydrology for data and funding support, and Professor Russell Mein and other members of the Project Reference Panel for helpful suggestions and review throughout the project.

## Joint Probability Description of Design Rainfalls

T.M.T. Hoang<sup>1</sup>, A. Rahman<sup>1</sup>, P.E. Weinmann<sup>1</sup>, E.M. Laurenson<sup>1</sup>, R.J. Nathan<sup>2</sup>

<sup>1</sup>Cooperative Research Centre for Catchment Hydrology, Monash University

<sup>2</sup>Sinclair Knight Merz, Victoria

### SUMMARY

In the currently applied rainfall-based flood estimation methods, design storms for pre-defined durations are represented by probabilistic design rainfall intensities and fixed temporal patterns. This does not adequately reflect the great degree of variability of real storm events and, in catchments with strongly non-linear runoff response, may lead to significantly biased flood estimates. The paper proposes a new definition for storm events of random duration. It demonstrates that a joint probability description of design rainfall using these new storm events is quite feasible, and explores their potential for practical design flood estimation applications.

### 1. INTRODUCTION

All rainfall-based design flood estimation methods start from the premise that a probabilistic design rainfall input can be transformed into a flood frequency output. Available methods range from the simple Rational Method to complex rainfall-runoff simulation models. The degree of simplification adopted by a specific method determines the error and bias introduced into the derived flood frequency distribution compared to the 'true' distribution. The operational aim of any practical design flood estimation method is to minimise errors and bias by adequately representing all aspects of the catchment hydrologic system that significantly influence its flood outputs.

One factor thought to have a significant influence on derived flood frequency distributions is the large variability of hydrologic variables from event to event. The non-linear nature of the catchment response to rainfall inputs means that a simple representation of highly variable inputs or parameter values by their mean or median values, as in the commonly applied *design event approach*, is likely to introduce bias into the derived flood distribution [1], [2]. The *Joint Probability Approach* to design flood estimation, being investigated as part of the CRC for Catchment Hydrology's Project FL1, aims to overcome this problem by an appropriate probabilistic representation of the key flood-producing or flood-modifying variables.

In this paper we concentrate on the storm rainfall characteristics that are influential in defining the flood frequency distribution. The principal characteristics of a rainfall event considered here are its duration, average intensity and the within-event temporal pattern. Random variability of rainfall over a catchment is allowed for through an areal reduction factor, while spatial trends in rainfall, although important in some catchments, have not been allowed for at this stage. Pre-storm rainfall is important in determining initial loss associated with a storm event. However, as our analysis of Victorian data has shown little correlation between storm event rainfall and pre-storm rainfall, the distribution of initial loss will be derived independently of the storm rainfall analysis.

The research described in this paper builds on previous research applications of the Joint Probability Approach, in particular by Blöschl and Sivapalan [3] using data from catchments in Austria; our work is specifically oriented towards exploring the potential of the approach for practical application in Australia. At this stage the analysis has been restricted to rainfall data from a limited region in Victoria [2].

### 2. DATA COLLATION AND CHECKING

The derivation of the joint probability distribution of rainfall duration, intensity, and temporal pattern requires continuously recorded rainfall data from a representative set of pluviograph stations. For this study, hourly rainfall records from 19 pluviometers in South-eastern Victoria, have been used. The stations are spread over a region of approximately 30,000 km<sup>2</sup>, extending from Melbourne in the west to Sale in the east. Record lengths range from a minimum of 14 years to a maximum of 123 years (Melbourne pluviograph), with an average of 23 years.

The hourly rainfalls obtained from the above gauges were checked for homogeneity with respect to time. As stated by many authors, e.g. [4], [5], and [6], this is an important check before any hydrologic frequency analysis is undertaken, to avoid biased results due to possible errors in data collection, changes in station environments, and observers. The CUSUM test [7] (for a change in the mean) and the Mann-Kendall rank correlation test [4] (for trend in data series) were applied to test for homogeneity of the annual maxima of daily rainfall totals. Of the 19 pluviometers used, only one station failed the Mann-Kendall trend test. After checking the station documentation and a plot of the data series at the station against time, only 5 years of record had to be discarded.

### 3. STORM EVENT DEFINITION

In the joint probability description of design rainfalls, the key rainfall characteristics (duration, intensity, and temporal pattern) are treated as random variables. Before determining the joint distribution of these three characteristics, a storm definition is required to separate the time series of hourly rainfall observations into individual rainfall events. A storm of interest for flood estimation is one that has the *potential to produce a flood*. In this study, two types of storm events were defined: complete storms and storm cores.

A *complete storm* for the purposes of this approach is defined in three steps (Figure 1):

- Step 1: A 'gross' storm is a period of rain starting and ending with a 'non-dry hour' (ie hourly rainfall greater than C1 mm), preceded and followed by at least h 'dry hours'.
- Step 2: Any period of insignificant rainfall at the beginning or end of a gross storm (referred to as 'dry period') is then cut off from the gross storm to produce the 'net' storm of duration D. (A period is 'dry' if all hourly rainfalls in the period are  $\leq C2$  mm, and the average rainfall intensity during the period is  $\leq C1$  mm/h).
- Step 3: The net storm is then assessed in regard to its severity and only kept as a 'significant' storm if it has the potential to produce a flood. This assessment is performed by firstly comparing the average rainfall intensity of the net storm ( $RFI_D$ ) with a threshold intensity for that storm duration:  $RFI_D \geq F1 \times (I_d^2)$ . A second criterion is then applied to allow for the possibility of a storm-internal period of heavy rainfall (duration d and average intensity  $RFI_d$ ) producing a flood:  $RFI_d \geq F2 \times (I_d^2)$ , where  $I_d$  and  $I_d$  are respectively the estimated 2-year ARI intensities for the durations D and d.

In this analysis, we have adopted  $h = 6$  hours,  $F1=0.4$ ,  $F2=0.5$ ,  $C1=0.255$  mm/h and  $C2=1.2$  mm. This produced an average of 7 storms per year of rainfall record.

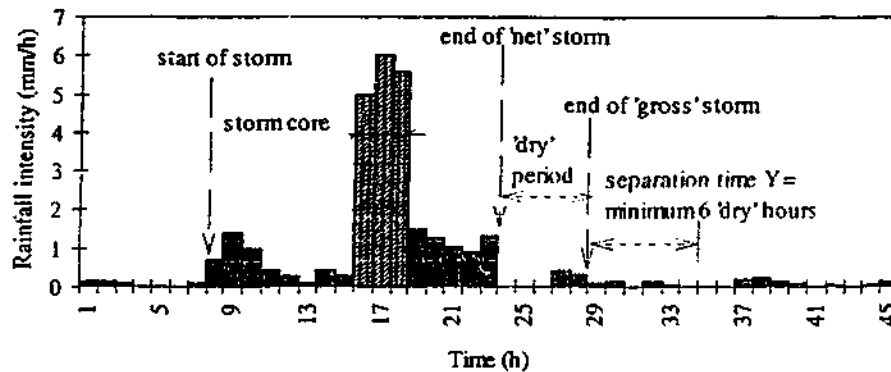


Figure 1: Storm definition

For each complete storm, a *storm core* can be identified, which is defined as "the most intense rainfall burst within a complete storm". It is found by calculating the average intensities of all possible storm bursts, and the ratio with the threshold intensity  $I_d$  for the relevant duration d, then selecting the burst of that duration which produces the highest ratio. In the example storm shown in Figure 1, the storm core has a duration of 3 hours.

It is clear that the flood production potential of a rainfall event depends not only on the storm characteristics but also on catchment factors that determine the flood regime, such as the time of concentration [8]. A particular set of storm definition parameters is thus only relevant to catchments within a limited regime range.

### 4. DISTRIBUTION OF RAINFALL DURATION

With storms selected using the above event definition, storm duration is a random variable with an unknown probability distribution. Regional frequency analysis by the method of Hosking and Wallis [6] was applied to identify the distribution of duration of the complete storm and storm core events in the selected rainfall data set.

The procedure is as follows:

- Define a homogeneous region of sites with similar rainfall characteristics. Criteria used for forming regions may include gauge elevation, site physiography, or geographical contiguity with the site of interest, etc.
- Compute the discordancy measure D for each site in the region. Discordant sites have markedly different at-site sample L-moments from those in the group; therefore their data merit a close examination.

- Compute the heterogeneity measures  $H$ ,  $H(2)$ , and  $H(3)$  to assess if the proposed region is acceptably homogeneous. If these measures exceed a critical value for homogeneity, the region should be redefined.
- For an acceptably homogeneous region, compute the goodness-of-fit measure  $Z$  to select a distribution that yields an acceptable fit to the data points for each site. The selected distribution should have  $|Z| \leq 1.64$ .

Preliminary results for *complete storms* indicate that the whole study area is not homogeneous with respect to storm duration, but smaller regions can be formed by grouping sites contiguous to the site of interest. The 3-parameter generalised Pareto (GP) distribution has been found to be the most appropriate to describe the duration of complete storms in the test region.

For *storm cores*, the whole study area forms a homogeneous region, and the 1-parameter exponential distribution was found to be the appropriate distribution. Figure 2 shows the distribution of storm duration (for storm cores and complete storms) for Station 86071 (Melbourne).

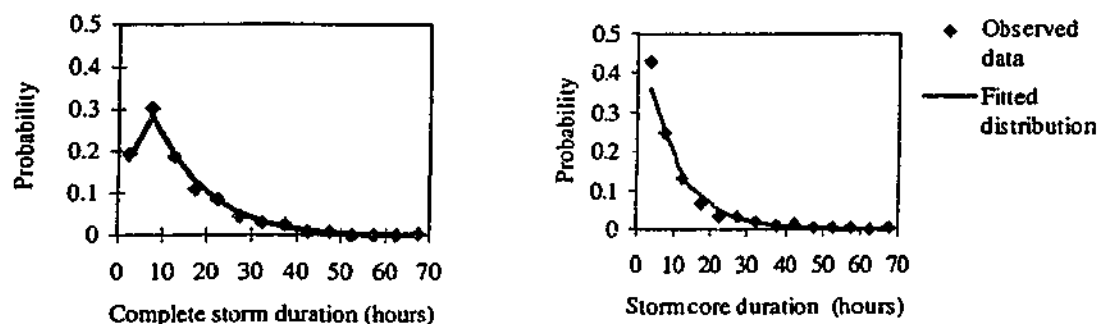


Figure 2: Distribution of storm duration at Melbourne

##### 5. CONDITIONAL DISTRIBUTION OF RAINFALL INTENSITY

The strong relationship between rainfall duration and average rainfall intensity means that the distribution of intensity ( $I$ ) for both complete storms and storm cores needs to be conditioned on duration. The procedure adopted to develop intensity-frequency-duration (IFD) curves for complete storms or storm cores is as follows:

- The range of storm event durations  $D$  is divided into a number of class intervals (with a mid point for each class): e.g. 1h, 2-3h, 4-12h, 13-36h, 37h and greater.
- For the data in each class interval (except the 1h class), a linear regression line is fitted between  $\log(D)$  and  $\log(I)$ . The slope of the fitted regression line is used to adjust the intensities for all durations to the mid point.
- For each class, an exponential distribution is fitted to the adjusted data series  $I_i$  ( $i = 1, \dots, M$ ), where  $M$  is the number of data points in a class. Quantiles are obtained from  $I(T) = I_0 + \beta \ln(\lambda T)$  where  $I_0$  is the smallest value in the series;  $\beta = \sum I_i/M - I_0$ ;  $\lambda = M/N$ ;  $N$  is the number of years of data; and  $T$  is the ARI. Adopting this procedure, design rainfall intensity values  $I(T)$  are computed for ARI = 2, 5, 10, 20, 50 and 100 years.
- The computed  $I(T)$  values for each duration range are used to fit a second degree polynomial between  $\log(D)$  and  $\log(I)$  for a selected ARI. This is the basis of the storm core or complete storm IFD curves in Figure 3.

A key issue is whether the IFD curves for the random duration storm events used in our study,  $IFD_{\text{com.storm}}$  and  $IFD_{\text{storm core}}$ , are similar to the currently used design rainfall IFD curves. The derived IFD curves for a station can be compared with two other IFD curves: (a) regional design values for fixed duration storm bursts from ARR87 ([9], Chapter 2 and Vol 2), referred to as  $IFD_{\text{ARR}}$ ; and (b) values from at-site analysis of storm bursts using procedures consistent with ARR87 ( $IFD_{\text{burst}}$ ). The type (b) curves are more directly comparable with the at-site IFD curves developed here.

The ARR87 bursts and the storm cores used here have different sampling properties: an observed intense rainfall spell is included only once in the storm core database, but it may have been included several times in the burst rainfall database, as a shorter duration burst may form part of a longer duration burst. Thus the burst series will consist of higher values relative to storm cores, and hence  $IFD_{\text{storm core}}$  will be located below  $IFD_{\text{ARR}}$ . Similarly with  $IFD_{\text{comp.storm}}$ . However, the difference will reduce with increasing duration; at higher durations both the

samples will share many common events. The empirical results for the 19 stations analysed are generally consistent with the above sampling properties of bursts, complete storms and storm cores (see Figure 3).

Examination of the results of our IFD analysis for different stations shows a fairly regular relationship between  $IFD_{storm\ core}$  and  $IFD_{burst}$ . The ratio of these two IFD curves, the *IFD adjustment factor*, depends on D and ARI, as shown in Figure 4. The IFD adjustment factor could be used to estimate storm core IFD values from ARR87 IFD values for a given duration and ARI, but further work is required to generalise the relationship of the adjustment factor with duration and ARI. For complete storms, the relationship between  $IFD_{comp.storm}$  and  $IFD_{burst}$  appears to be less consistent, offering little scope for derivation of design IFD adjustment factors.

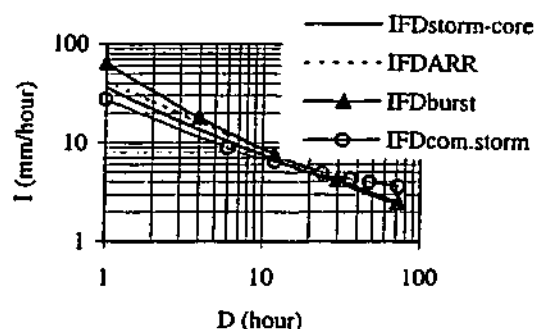


Figure 3: Comparison of IFD curves for Melbourne

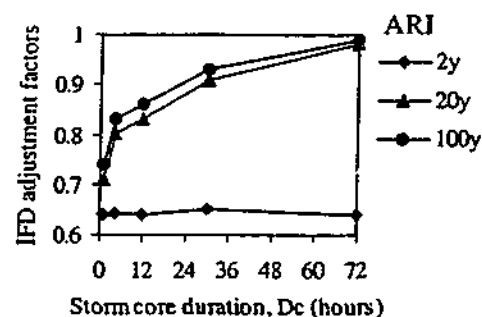


Figure 4: Typical IFD adjustment factors

#### 6. PROBABILISTIC RAINFALL TEMPORAL PATTERNS

The probabilistic description of rainfall temporal patterns is made complex by their multi-variate nature: current design temporal patterns (Vol 2, ARR87 [9]) are defined by up to 24 parameters. We characterise the time distribution of rainfall during a storm using *storm mass curves*, graphs of dimensionless cumulative rainfall depth versus dimensionless storm time, with 8 to 10 equal time increments.

Temporal patterns may vary not only with location, but also with season, storm duration and storm severity. The analysis of rainfall data for the probabilistic description of temporal patterns thus has to start by checking of observed temporal patterns for differences with respect to season of storm occurrence, storm duration, and storm depth. This was performed by using contingency tables and the chi-square test for homogeneity, described in [10]. Garcia-Guzman and Aranda-Oliver [11] also applied the test for the same purpose. It was assumed that, for the relatively small region considered, the storm patterns did not depend on location within the region.

To apply the test, a contingency table was established for a hypothesised grouping (e.g. into seasons), the chi-square statistic computed and then compared with the value of the statistic that would be obtained from a homogeneous population (e.g. no distinct seasonality). The tests were performed for different groupings of storm events in relation to season, storm duration and severity. For each factor, the events were first grouped into small units (e.g. single months) and, if the data was shown to be homogeneous within those groups, larger groups (e.g. several months) were formed and tested. The results of this analysis for *complete storms* in Figure 5 indicate that, when temporal patterns are characterised by mass curves using 10 equal time intervals, the time distributions of rainfall are heterogeneous with regard to season of storm occurrence, storm duration, and (in one case) total storm depth. The practical significance of these results for flood estimation is yet to be confirmed by simulation studies.

For *storm cores*, the time distributions of rainfall are not dependent on season and total storm depth but on storm durations, yielding two groups: (a) up to 12 hours duration, and (b) greater than 12 hours duration.

For design flood applications, the observed mass curves in each group now need to be represented by a model, to allow *generation of synthetic mass curves*. In its simplest form, the model would consist of randomly drawing a dimensionless pattern from the sample of observed mass curves in the relevant group. The adopted model employs a multiplicative structure [8] to disaggregate rainfall from a given depth and duration. It first finds the relative rainfall depth at the mid-point of rainfall duration, then at the mid-points of the two intervals created, and so on. The model was used to generate temporal patterns of 8 blocks.

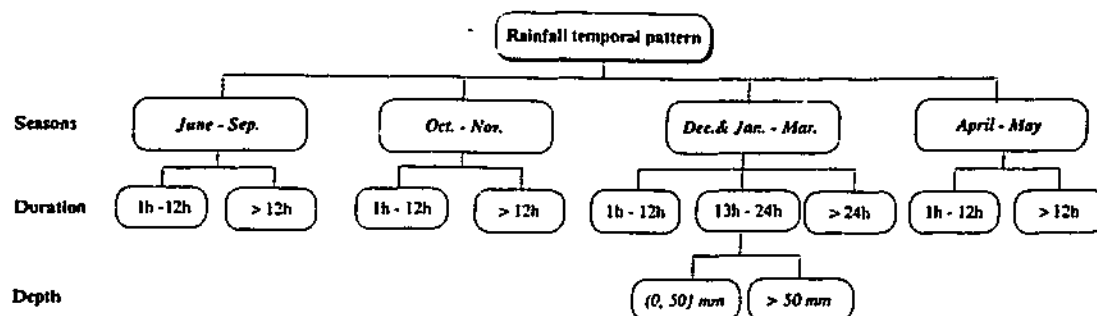


Figure 5: Factors affecting temporal patterns (complete storms)

For each temporal pattern group, the steps in the generation process are as follows:

- Fit a beta distribution to all observed mass curves in the group. The parameters of this distribution are selected as the medians of the parameters of the individual beta curves in the group.
- Generate synthetic storm hyetographs from the beta distribution.

The performance of the generation model has been assessed by comparing the following characteristics of the observed and generated sets of patterns:

- the cumulative frequency curve of maximum dimensionless intensity, a measure of peakiness (Figure 6),
- the lag one auto-correlation coefficients, a measure of persistence in temporal patterns, and
- the Huff frequency curves [12], a measure of temporal pattern variability (Figure 7).

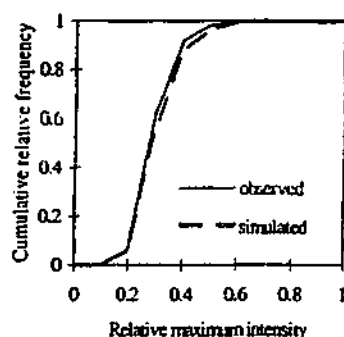


Figure 6: Comparison of cumulative relative frequency of maximum intensity (June-September, >12h, complete storms)

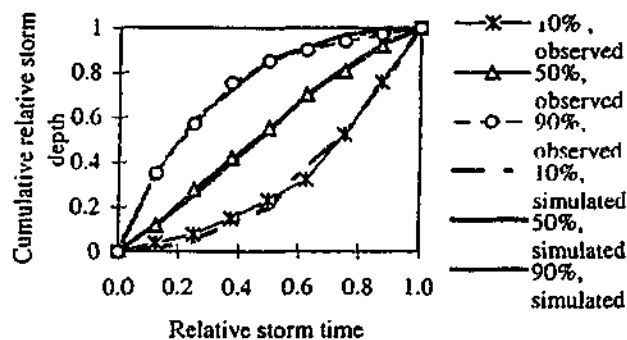


Figure 7: Comparison of Huff frequency curves (December-March, 13h-24h, up to 50mm)

The results from the application to the data set from 19 stations indicate that the model preserves the characteristics of observed *complete storms* relatively well. The accurate representation of the less complex *storm core* temporal patterns poses less of a challenge.

## 7. JOINT DISTRIBUTION OF DESIGN RAINFALL

Together, the marginal distribution of storm duration, the conditional distribution of rainfall intensity and the generation model for temporal patterns define the joint distribution of rainfall events to be used for design. In practical application, a set of complete storm or storm core design events would be generated by first generating a random duration, then a rainfall intensity for this duration and finally a temporal pattern for the corresponding duration and intensity group (at this stage neglecting the seasonality of temporal patterns) [2].

## 8. DISCUSSION

The preliminary project results presented in this paper demonstrate that it is feasible to describe design rainfall characteristics for a site (or a small region) in a joint probability framework that better accounts for the variability between rainfall events and the interaction between different rainfall characteristics. Work is currently under way

to combine these new design rainfall characteristics for complete storms and storm cores with probability distributed initial loss values, and to apply them to selected test catchments to determine their derived flood frequency distributions. The method employs a Monte Carlo simulation framework, initially with a lumped, non-linear runoff routing model for sensitivity studies, but eventually with a semi-distributed runoff routing model to allow a comparison with results from the current design event approach and from flood frequency analysis.

If these test applications confirm the potential of the Joint Probability Approach to produce less biased estimates of design floods, further work will be necessary to allow the wider application of the approach to practical design flood estimation problems. In particular, *regional methods* to estimate rainfall event duration, average intensity and temporal pattern will be required. For storm duration, this will involve further research on the regional variation of the distribution parameters and the climate characteristics responsible for it. For the design rainfall intensities associated with storm cores, it is proposed to make use of the established link with the rainfall IFD data for storm bursts provided in ARR87. The sensitivity studies will determine to what extent the variability of temporal patterns with season, duration and depth influences the derived flood frequency distribution.

Intuitively, it appears preferable to define complete storms rather than storm cores for use in design flood estimation, particularly as initial losses are more readily determined for complete storm events. However, our analyses have shown that complete storms are characterised by more complex and more variable distributions of rainfall duration and temporal pattern compared to storm cores. It is also more difficult to relate the rainfall intensities of complete storms to the design IFD data available in ARR87. Further work is required to fully assess the relative merits of these two approaches for practical application.

## 9. CONCLUSION

The research work on joint probability representation of design rainfall characteristics described in this paper has led to the following conclusions:

- It is quite feasible to derive a joint probability distribution of storm rainfall duration, average intensity and temporal pattern, either for complete storms or for storm cores (the most intense portion of a complete storm), but storm cores appear to offer greater potential for practical application with current design data.
- The treatment of rainfall event duration as a random variable leads to lower design rainfall intensities for a given duration than indicated by the IFD information in ARR87; for storm cores there appears to be a more useful systematic relationship between the rainfall intensities derived by the two approaches.
- Further work is required to test the performance of the overall Joint Probability Approach to design flood estimation and to develop regional methods for estimating the required distribution parameters.

## 10. ACKNOWLEDGMENT

The authors gratefully acknowledge the members of the FL1.1 Project Reference Panel for their valuable suggestions and review of the work, and the Bureau of Meteorology for providing additional rainfall data.

## 11. REFERENCES

1. Rahman, A., T.M.T. Hoang, P.E. Weinmann and E.M. Laurenson. *Joint Probability Approaches to Design Flood Estimation: A Review*. CRC for Catchment Hydrology, Report No. 98/8, 70p, 1998.
2. Weinmann, P.E., A. Rahman, T.M.T. Hoang, E.M. Laurenson and R.J. Nathan. A New Modelling Framework for Design Flood Estimation. 'HydraStorm '98', Adelaide, Australia, 1998, pp 393-398.
3. Blöschl, G. and M. Sivapalan. Process Controls on Flood Frequency: 2. Runoff Generation, Storm Properties and Return Period. Centre for Water Research, Uni. of W.A., Rep. ED 1158 MS, (Subm. to Water Res. Res.)
4. WMO, *Technical Note No. 79: Climatic Change*. World Meteorological Organisation, 1996.
5. Stedinger, J.R., R.M. Vogel, and E. Foufoula-Georgiou. *Frequency Analysis of Extreme Events*, in *Handbook in Hydrology*, D.R. Maidment, Editor. 1993, McGraw-Hill. p. 18.48.
6. Hosking, J.R.M. and J.R. Wallis, *Regional Frequency Analysis*. 1997: Cambridge University Press.
7. McGilchrist, C.A. and K.D. Woodyer, Note on a Distribution-free CUSUM Test. *Technometrics*, 1975. 17(3): p. 321-325.
8. Robinson, J.S. and M. Sivapalan, Temporal Scales and Hydrological Regimes: Implications for Flood Frequency Scaling. *Water Res. Res.*, 1997. 33(12): p. 2981-2999.
9. ARR87. *Australian Rainfall and Runoff - A Guide to Flood Estimation*. Inst. of Engrs, Australia, 1987.
10. Daniel, W.W., *Applied Nonparametric Statistics*. 1978: Houghton Mifflin Company.
11. Garcia-Guzman, A. and E. Aranda-Oliver, A Stochastic Model of Dimensionless Hyetograph. *Water Res. Res.*, 1993. 29(7): p. 2363-2370.
12. Huff, F.A., Time Distribution of Rainfall in Heavy Storms. *Water Res. Res.*, 1967. 3(4): p. 1007-1019.



2<sup>nd</sup> Inter-Regional Conference on Environment-Water 99

## IMPROVED DESIGN FLOOD ESTIMATION THROUGH JOINT PROBABILITY

P. E. Weinmann, E. M. Laurenson, A. Rahman, T. M. T. Hoang  
CRC for Catchment Hydrology, Dept. of Civil Engineering, Monash University, Australia

*This paper places rainfall-based flood hydrograph estimation into the broader context of the design flood estimation process. It shows up weaknesses in the current methods of dealing with stochastic elements in design flood estimation and proposes a joint probability approach to overcome these weaknesses. The initial application of the approach to a small number of rural catchments in Victoria, Australia showed promise for further development into a practical flood design tool.*

### 1 INTRODUCTION

Flood design generally requires the estimation of a flood frequency curve; i.e. a relationship between the magnitude of a selected flood characteristic (e.g. peak flow rate or maximum flood level at a site) and its probability of exceedance. This flood frequency curve can be based either directly on the analysis of observed flood data, or on simulating floods from more basic hydrologic catchment inputs, like rainfall. Ideally, the simulation methods would try to represent in a realistic fashion all the factors involved in producing a flood and modifying it on its passage through the catchment. However, practical simulation methods involve a substantial degree of simplification, relating to the nature of the basic inputs, the physical realism of the deterministic models involved, and the treatment of the probabilistic aspects of the flood simulation process.

This paper first discusses important distinctions between different flood estimation approaches, in particular the role of deterministic models and stochastic elements in the flood estimation process. It then explores the potential of a more holistic flood estimation approach, based on concepts of joint probability analysis.

### 2 OVERVIEW OF DESIGN FLOOD ESTIMATION PROCESS

In an ideal situation, flood design would be based directly on statistical analysis of a very long, homogeneous time series of reliable flood observations at the site of interest. Such analysis would require only limited knowledge and understanding of the causative factors of floods, as all the important factors would be adequately represented in the flood data.

However, in most practical design situations, the adopted flood estimation methods have to deal with the following limitations in the available flood observations:

- they are only available for a limited time period;
- they do not relate directly to the specific site, flood characteristic or flood magnitude of interest;
- they are only of limited accuracy and reliability;
- they do not form a homogeneous time series, as they reflect changes in climate, catchment or site characteristics.

These practical constraints on available flood information limit the scope of direct frequency analysis of flood observations. A degree of extrapolation in time, space, flood magnitude and generality of results is typically required. This means that the design flood estimation process has to start at an earlier stage, using different design inputs, and transforming them into the required flood design outputs by means of models, as indicated in Figure 1. The hydrologist or flood designer then requires a range of supplementary data for the hydrometeorological, hydrological and hydraulic stages of the estimation process, plus the empirical or process-based knowledge incorporated into the models of the transformation processes. Compared to direct frequency analysis of flood characteristics, the design flood simulation process represents a more mature form of the science of flood estimation: the knowledge of *what* has happened must be supplemented by knowledge of *how* it happened [1].

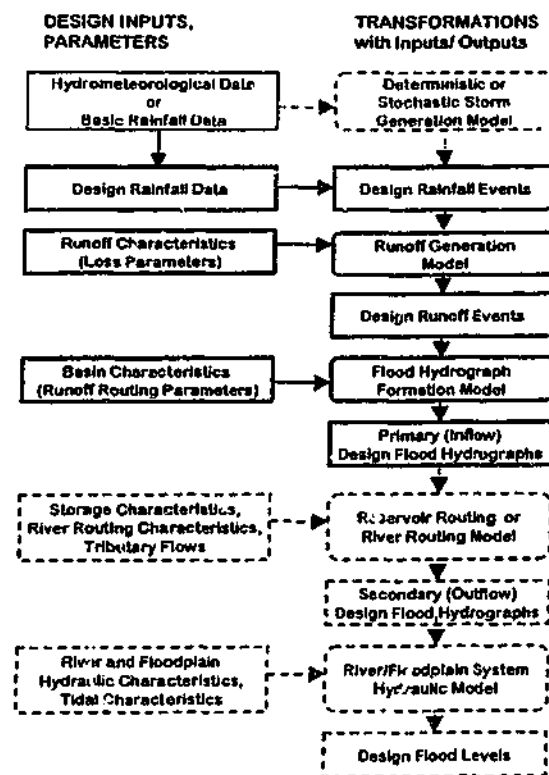


Fig. 1 Diagrammatic representation of different stages in design flood estimation process (shaded boxes represent models)

The schematic diagram in Figure 1 shows the main stages of the overall process; some of them consist of several processes and sub-models with sets of inputs/parameters. Together, these sub-models form a complex modelling framework that should reflect the physical and stochastic nature of the flood formation and flood modification process.

While the basic hydrometeorological data consists of continuous time series, the flood designer's direct interest is on probability distributions of defined events, e.g. annual, maximum peak flows. In the most complete modelling framework, the *continuous modelling approach* (the continuous time series of hydrometeorological and secondary inputs) are used to simulate a complete time series of streamflow (or flood levels) at the point of interest [2]. From this simulated output time series, the required event characteristics can be extracted and subjected to frequency analysis. The advantage of this approach is that, when using historic time series data, most of the important dependencies between inputs are implicitly allowed for. However, when extended input data series are to be derived by data generation techniques, these dependencies need to be explicitly built into the data generation models.

In the more commonly applied *design event approach*, the primary input time series (rainfall) is subjected to frequency analysis to derive a probability-based design input. This is combined with representative values of other inputs/parameters to construct design events of given average recurrence interval (ARI) which are then transformed by the estimation models into output events of the same ARI. The assumption of 'probability-neutral' transformations involved in this approach and its potential effect on derived flood frequency distributions is further discussed below.

In the remainder of this paper, an improved stochastic framework for event-based flood estimation is outlined. The specific focus is on the transformation of design rainfall inputs to the primary design flood hydrograph output (highlighted parts of Figure 1) using joint probability principles. The authors' application of joint probability concepts to other parts of the flood estimation process is described in [3], [4], [5] and [6].

### 3 DETERMINISTIC AND STOCHASTIC MODELLING ELEMENTS

The design flood estimation approaches outlined above contain both stochastic and deterministic elements. The stochastic elements are the unexplained (random) factors that give rise to the probability distributions of variables, and the unexplained relationships between variables that are measured by statistical correlation. On the other hand, the deterministic modelling elements express those relationships between variables that are direct enough and sufficiently understood to be represented by simple parametric models. This stochastic-deterministic modelling framework has been formulated and explored by Laurenson [3] and Klemes [1].

It is worth noting that the term 'deterministic' is used here not to indicate a unique causal relationship between inputs and outputs, but rather a pragmatic conceptual link that approximates the true (but generally unknown) dependence of outputs on inputs with sufficient accuracy for the practical purposes of flood estimation. The deterministic links are closely related to the concept of statistical correlation between variables (or statistical dependence). In the conventional sense, a deterministic relationship between two variables implies a correlation coefficient that has an absolute value of one. However, the random factors involved in the transformation of

inputs to outputs (expressed as probability distributions of model parameter values) mean that the relationship between *individual* inputs and outputs is not fully deterministic, but there exists a one-to-one relationship between their probability distributions.

In past flood estimation practice, the degree of sophistication of a flood estimation method has been judged principally on the basis of its deterministic modelling elements, depending mainly on whether their basis was purely empirical or physical/conceptual. Over-simplistic assumptions in the deterministic modelling components place clear limitations on the degree of allowable extrapolation of modelling results in the time, space and probability domains. Similarly, the representation of stochastic modelling elements can range from complex to simplistic, with important effects on the flood estimation results. The stochastic elements thus deserve equal attention in the development of reliable and efficient flood estimation methods.

Probability distributions of *flood estimation inputs* are generally multi-variate and multi-parametric in nature (e.g. rainfall should be characterised by distributions of its average intensity and its variability in time and space). However, for the sake of convenience, their dimensionality is often reduced (by making simplistic assumptions regarding some of the dimensions), and one- or two-parameter distributions are assumed for the remaining dimension(s). Similarly, despite their well-known random variability, *model parameters* are frequently assumed to be invariant, i.e. their probability distribution is represented only by a measure of central tendency, the mean or the median of observed values.

The adequate representation of *dependencies (correlations)* between different inputs and model parameters is another important stochastic modelling element. In many practical design flood estimation methods such dependencies are neglected, and the computationally simpler case of independence is assumed (e.g. initial loss had been assumed to be independent of rainfall burst duration [7]). Significant dependencies between variables used in the flood estimation process can be allowed for either through deterministic relationships between the variables (e.g. rainfall intensity-frequency-duration relationships) or by approximate methods to preserve the statistical correlations between variables.

#### 4 THE DESIGN EVENT APPROACH AND ITS LIMITATIONS

The design event approach applied in Australia for rainfall-based flood hydrograph estimation [7] is similar to the approach applied in other parts of the world. It involves the definition of the design inputs and parameters indicated in the first column of Table 1, and their application with appropriate deterministic models of the runoff generation and hydrograph formation phases. The basic premise of the approach is that, by using appropriate representative values of the secondary inputs and model parameters, the primary input of design rainfall for a given average recurrence interval (ARI) will be transformed into a flood output of corresponding ARI.

Although conceptual in nature, the deterministic models applied with this approach, and their parameter estimation methods, have a direct physical or empirical basis. Unfortunately, the solid basis of the deterministic models is not matched by appropriate treatment of the probability aspects of flood estimation [8]. The only stochastic input considered is the average rainfall intensity for a given rainfall burst duration; all model parameters are represented by single representative values, usually selected as the mean of the values obtained from model calibration runs or, in un-

gauged catchments, from regional estimation equations. Apart from the dependence of average rainfall intensity on burst duration, the dependence of rainfall temporal patterns on rainfall duration and intensity is also allowed for, as is the dependence of the rainfall areal reduction factor on rainfall duration and catchment area (see Table 1).

This simplistic treatment of the stochastic aspects of flood estimation, assuming an ARI-neutral transformation of rainfall input to flood output, has been shown to lead to potentially significant bias in derived flood frequency curves [9]. Furthermore, the concept of deriving a critical rainfall duration for a given ARI (as the one that results in the largest flood outputs) has no sound statistical basis.

DESIGN ELEMENT	MODELLING CHARACTERISTIC	ADOPTED REPRESENTATION	DEPENDENCIES MODELLED
Time Basis	Season	Non-seasonal (Annual)	
Rainfall Event Input	Event Type (ET)	<b>Stochastic Events</b> (Complete Storms or Storm 'Cores')	
	Duration (D)	<b>Stochastic</b>	<b>ET</b>
	Average Intensity (I)	<b>Stochastic</b>	<b>ET, D</b>
	Areal Reduction Factor	Deterministic	D, Area
	Temporal Pattern	<b>Stochastic</b>	<b>ET, D, I</b>
	Spatial Pattern	Uniform	
Loss Parameters	Initial Loss (IL)	<b>Stochastic</b>	<b>ET, D</b>
	Continuing Loss (CL)	Mean (from calibration)	
Runoff Routing Parameters	Non-linearity Param. (m)	Fixed Value	
	Attenuation Param. (K)	Mean (from calibration)	<b>m</b>
Baseflow Input	Baseflow at Peak	Mean (of observations)	

Table 1 Summary of stochastic elements in adopted joint probability modelling approach (Bold text indicates modifications to current Design Event Approach)

## 5 MODELLING COMPONENTS OF IMPROVED APPROACH

A reliable and efficient design flood estimation approach should concentrate on those elements in the estimation process that have a dominant influence on the output flood frequency distribution(s). These include critical deterministic and stochastic modelling elements, as well as their interactions. One important aspect that needs to be considered in this context is the strongly non-linear response of most hydrologic-hydraulic systems to system inputs - it can have a significant influence on the derived flood frequency distributions.

The proposed improved approach to design flood estimation can be termed stochastic design event simulation. It employs Monte Carlo simulation techniques to derive the empirical distributions of selected flood output characteristics from distributions of key inputs and parameters [10]. The simulation uses the same deterministic modelling elements as the design event approach, but joint probability concepts are introduced to represent more correctly the most important stochastic elements in the flood estimation process. These include:

- definition and use of stochastic design events,
- representation of most important design rainfall input characteristics and loss parameters by probability distributions,
- modelling of all important dependencies between inputs and parameters.

Table 1 summarises the adopted representation and highlights the differences with the currently applied design event approach. Two different definitions of stochastic rainfall-runoff events have been developed and trialed in the research by the Cooperative Research Centre for Catchment Hydrology (CRCCH). A *complete storm* event includes all the significant rainfall within a rainfall event that has the potential to produce flood runoff, while a *storm core* represents only the most intense part of a complete storm, i.e. the part whose average intensity has the highest ARI [11]. With both types of events, rainfall duration is treated as a random variable.

The input/parameter probability distributions are based on the analysis of observed storms and resulting hydrographs. For gauged catchments, this can be based directly on rainfall/streamflow data, but for ungauged catchments the distributions have to be determined from regional estimation methods. In the example applications used to test the approach, the rainfall inputs were described by probability distributions of rainfall duration, average intensity and temporal pattern, with an additional distribution for a loss parameter. Table 2 summarises the types of data and the statistical distributions/models used in the stochastic description of these inputs/parameters. Due to the multi-parametric nature of temporal patterns, their variability was represented either empirically, by re-sampling of observed patterns, or by data generation techniques, using a multiplicative cascade model [12].

CHARACTERISTIC	BASIC DATA	TYPE OF STATISTICAL MODEL
Rainfall Duration (D)	Regional Rainfall	Exponential Dist. (Storm cores) Gen. Pareto Dist. (Comp. storms)
Rainfall Intensity (I)	Catchment Rainfall	Exponential Distribution (with adjusted upper tail)
Rainfall Temporal Pattern (TP)	Regional Rainfall	Sampling from observed storms Or Multiplicative Cascade Model
Initial Loss (IL)	Catchment Rainfall/Streamflow	Beta Distribution

Table 2 Derivation of probability distributions of key inputs/parameters

In the example applications of the joint probability approach described below, a single non-linear storage was used to transform the runoff input into a flood hydrograph output at the catchment outlet ( $K$  and  $m$  are respectively the coefficient and the exponent in the power function relating storage to discharge). Compared to the commonly used, semi-distributed runoff routing models such as RORB [13], this involves some loss of modelling accuracy and flexibility [12].

## 6 RESULTS AND DISCUSSION

The prototype version of the joint probability methodology has so far been applied to four catchments in Victoria, Australia, ranging in size from 78 to 290 km<sup>2</sup>. The application in the Avoca River, Boggy Creek and Tarwin River catchments was based on storm core events [10], while complete storms were used in the La Trobe

River catchment [12]. The Monte Carlo simulation procedure was applied to a partial series of 10 000 storm/runoff events, with an average of 5 events per year.

Figure 2 shows the empirical distribution of flood peaks for the Boggy Creek catchment produced by the joint probability simulation procedure summarised in Tables 1 and 2, and compares it with the observed flood series. It should be noted that the individual design inputs/parameters have been derived independently, with only a small adjustment to the fixed continuing loss parameter to produce a better overall match between simulated and observed distributions. It is particularly noteworthy that the simulation method was able to correctly reproduce the non-linearities in the flood production process over a large range of flood magnitudes.

There is considerable scope for improvement of the procedure by more detailed representation of the following modelling elements:

- use of semi-distributed or distributed runoff routing model,
- seasonal rather than annual analysis of rainfall and loss characteristics,
- stochastic treatment of spatial variations of catchment rainfall,
- stochastic treatment of continuing loss parameter.

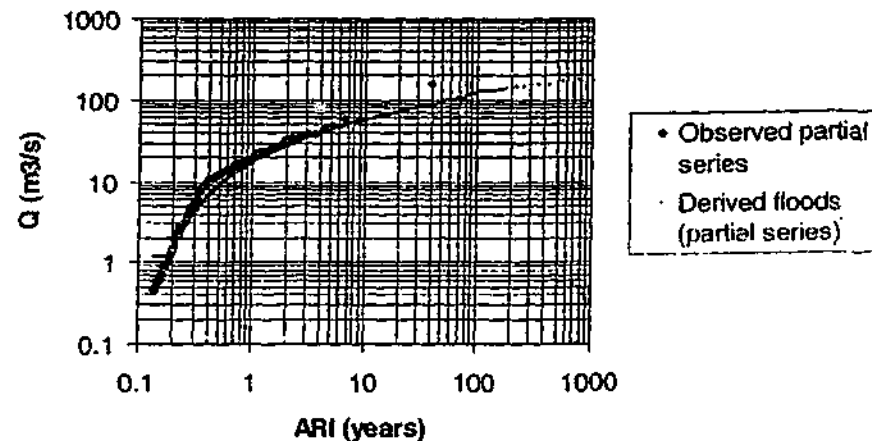


Fig. 2 Comparison of simulated flood frequency curve with observed partial flood series (Boggy Creek catchment, storm core events)

The practical scope for the last three of these improvements will depend on the availability of appropriate data bases for an adequate definition of the seasonal distributions of rainfall and loss characteristics. In particular, the relatively sparse distribution of rain gauges over catchments makes it difficult to define spatial patterns of rainfall, but current developments in radar-based rainfall estimation are expected to improve this situation.

For application to ungauged catchments, the distributions of rainfall and loss characteristics will have to be derived from regional estimation techniques. As indicated in Table 2, our work has shown that the distributions of rainfall duration and temporal pattern can be derived from regional data. It has also been shown [10,12] that a strong link exists between the locally derived conditional distributions of rainfall intensity for storm cores and complete storms, and the regional design information

for rainfall intensity-frequency-duration provided in Australian Rainfall and Runoff [7]. With regard to the regional estimation of loss parameter distributions, previous work at the CRC for Catchment Hydrology [14] has shown some promise, provided the dependencies of losses on season, rainfall event type and duration are allowed for.

In a further improvement, the stochastic description of inputs and parameters could be refined to reflect not only the natural variability but also the uncertainty due to various error sources.

## **7 CONCLUSION**

This paper has placed rainfall-based flood hydrograph estimation into the broader context of the design flood estimation process. It has shown up weaknesses in the current methods of dealing with stochastic elements in design flood estimation and proposed a joint probability approach to overcome these weaknesses. In the initial application of the approach, the rainfall duration, rainfall intensity and temporal pattern, as well as a loss model parameter, were represented by probability distributions and then transformed into an empirical flood distribution, by means of Monte Carlo simulation.

Testing on a limited number of catchments has proved the feasibility of the approach and showed promise for further development into a practical flood design tool. One strength of the approach is that it can use proven deterministic modelling components (loss and runoff routing models) and combine them with improved representations of stochastic elements. Compared to the continuous modelling approach, it has the advantage of being able to draw on available regional design information for application to ungauged catchments. Further testing on a broader range of catchments and identification of critical modelling components is desirable.

## **8 ACKNOWLEDGEMENTS**

The authors gratefully acknowledge the contributions of other project team members of CRCCH Project FL1 to the ideas outlined in this paper, in particular Dr Rory Nathan and Prof. Russell Mein.

## 9 REFERENCES

- [1] Klemes, V. Physically based stochastic hydrologic analysis. *Advances in Hydroscience*, Vol. 11 (Ed. V.T. Chow), Academic Press, N.Y. 1978; 285- 356.
- [2] Bradley, A.A., Cooper, P.J., Potter, K.W. and Price, T. Floodplain mapping using continuous hydrologic and hydraulic simulation models. *Journal of Hydrologic Engineering*, ASCE, 1(2), 1996, 63-68.
- [3] Laurenson, E.M. Modelling of stochastic-deterministic hydrologic systems. *Water Resources Research*, Vol. 10 No. 5, 1974, 955-961.
- [4] Pearce, M.A. and Laurenson, E.M. Real probabilities for real floods. *ANCOLD 1997 Conference on Dams*, Australian Committee on Large Dams.
- [5] Laurenson, E.M. Effect of dams on flood frequency. *Proc. Intern. Symp. on River Mechanics*, Vol. 2. Intern. Assoc. for Hydraulic Res., 1973, 133-146.
- [6] Weinmann, P.E. and Nathan, R.J. *Joint probability analysis in spillway adequacy studies (including seasonal effects)* Report prepared for the NSW Department of Land and Water Conservation, 1997.
- [7] I.E.Aust. *Australian Rainfall and Runoff – A guide to flood estimation*. Institution of Engineers, Australia, Canberra, 1987.
- [8] Rahman, A., T.M.T. Hoang, P.E. Weinmann and E.M. Laurenson. *Joint Probability Approaches to Design Flood Estimation: A Review*. CRC for Catchment Hydrology, Report No. 98/8, Monash University, 1998.
- [9] Blöschl, G. and Sivapalan, M. Process Controls on Flood Frequency: 2. Runoff Generation, Storm Properties and Return Period. Centre for Water Research, Uni. of W.A., Rep. ED 1158 MS, (Subm. to Water Resources Research, 1997)
- [10] Rahman, A., Weinmann, P.E., Hoang, T.M.T., Laurenson, E.M. and Nathan, R.J. *Flood frequency curves derived by Monte Carlo simulation*. CRC Research Report, 1999 (in preparation).
- [11] Hoang, T.M.T., Rahman, A., Weinmann, P.E., Laurenson, E.M. and Nathan, R.J. Joint probability description of design rainfalls. *Water 99 – Joint Congress, Brisbane, Australia*. Institution of Engineers, Australia, 1999. (In press)
- [12] Hoang, T.M.T. *A joint probability approach to rainfall-based flood estimation*. PhD Thesis, Monash University, 1999 (in preparation).
- [13] Laurenson, E.M. and Mein, R.G. *RORB – Version 4, Runoff routing program, User manual*. Dept. of Civil Engineering, Monash University, 1997.
- [14] Hill, P.J., Maheepala, U.K., Mein, R.G. and Weinmann, P.E. Empirical analysis of data to derive losses for design flood estimation in south-eastern Australia. CRC for Catchment Hydrology Report No. 96/5, Monash University, 1996.

## A New Modelling Framework for Design Flood Estimation

P E Weinmann<sup>1</sup>, A Rahman<sup>1</sup>, T Hoang<sup>1</sup>, E M Laurensen<sup>1</sup>, R J Nathan<sup>2</sup>

<sup>1</sup>CRC for Catchment Hydrology, Department of Civil Engineering, Monash University, Australia

<sup>2</sup>Sinclair Knight Merz, Victoria

**Summary:** The widely used Design Event Approach to rainfall-based design flood estimation is based on the assumption that the Average Recurrence Interval of the main design rainfall input (average intensity for given rainfall duration) is preserved in the transformation to the design flood output. Recent research has drawn attention to the limitations of this approach. The proposed new modelling framework uses existing loss models and runoff routing models as the deterministic elements in the simulation of a derived flood frequency curve. However, it makes explicit allowance for the probability-distributed nature of the key variables and for the dependencies between them. The key variables described in the paper are the duration, average intensity and temporal pattern of complete storms or intense rainfall bursts, and the initial loss parameter.

### 1 INTRODUCTION

Flood design and floodplain management decisions require estimates of flood peaks and corresponding flood levels. If adequate streamflow data is available at or near the site of interest, the flood estimates can be derived directly from flood frequency analysis, but in catchments with limited streamflow data or in catchments subject to major land use changes, design floods are generally estimated based on design rainfalls. Depending on the purpose of the flood estimate, simple design rainfall-based methods are applied, such as the Rational Method for urban drainage design, or more detailed modelling approaches are adopted, as in the case of flood design of major structures.

With all methods of rainfall-based design flood estimation, a key issue to be resolved is how the *design rainfall input* for a given Average Recurrence Interval (ARI) can be transformed into a *design flood output* of corresponding ARI. For the simple case of the 'Probabilistic Rational Method' [Australian Rainfall and Runoff (ARR)87, Chapter 5, (1)] this problem has been directly addressed by using calibration data from gauged catchments to ensure that the derived design runoff coefficient for the gauged site correctly transforms the design rainfall frequency curve into the 'observed' flood frequency curve at the catchment outlet. However, the simplifying assumptions made when transferring the design runoff coefficients from gauged to ungauged catchments place severe constraints on the applicability and accuracy of the method.

For the unitgraph or runoff routing modelling approaches, such calibration is much more difficult to achieve, as several interacting inputs and parameters are involved. The current practice aims to define hypothetical 'design events' of model inputs and model parameters that can be considered representative in a probability sense, that is they should transform the design rainfall input of given ARI into a flood output of the same ARI. The problem of finding the critical rainfall duration for a specific design situation is addressed by a trial-and-error approach, adopting the rainfall duration that

produces the largest flood outputs for a given input ARI. With this design practice, the equivalence of input and output ARI is not intrinsically assured but, unless checked against regional or at-site flood information, remains an assumption that is satisfied only for a limited set of conditions (2). The question to what extent the current approach introduces bias into flood estimates has only been partly resolved (3).

The purpose of this paper is to outline research directed at finding an alternative, more holistic, modelling framework for rainfall-based design flood information.

### 2 DESIGN EVENT APPROACH - LIMITATIONS

The rainfall-based flood estimation techniques used currently are based on the Design Event Approach in that design rainfall intensity for specified duration and ARI is used in combination with "typical values" of other relevant model inputs and parameters to obtain design flood estimates, as indicated in Figure 1.

The key assumption involved in the Design Event Approach is that the representative design values of the inputs/parameters at the above steps can be defined in such a way that they are "ARI neutral" i.e. they result in a flood output that has the same ARI as the rainfall input. However, there are no definite guidelines on how to select the appropriate values of the inputs/parameters in the above steps except for the rainfall depth, which is described by a probability distribution. A designer is commonly in the situation to select a representative input/parameter value (e.g. median value from a sample of inputs or fitted parameter values) from a wide range. For example, in the case of eastern Queensland, the recommended range of initial loss is 0 to 140 mm [ARR87, Chapter 6, (1)]. Due to the non-linearity of the transformation process involved, it is generally not possible to know a priori how a representative value for an input should be selected to preserve the AEP. The arbitrary treatment of various inputs/parameters in the Design Event Approach can lead to inconsistencies and significant bias in flood estimates for a

given ARI. This is likely to result in systematic under- or over-design of engineering structures, both with important economic consequences.

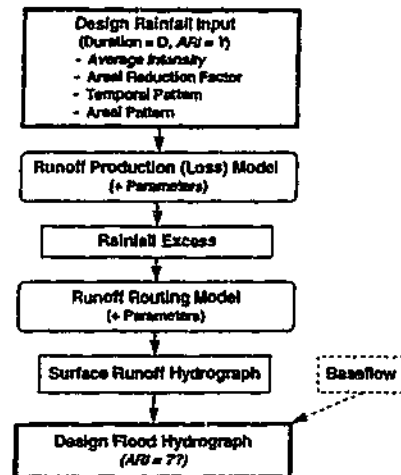


Fig 1 Design Event Approach to rainfall-based design flood estimation

### 3 OPTIONS FOR IMPROVEMENTS

To overcome the limitations associated with the Design Event Approach, a number of methods have been proposed: (a) an 'Improved' Design Event Approach; (b) a Joint Probability Approach; and (c) Continuous Simulation.

In the 'Improved' Design Event Approach, the same flood estimation procedure (Figure 1) is used but with better (more representative) estimates of design parameters and inputs. This approach could provide improvement to some extent, but will still be subject to the basic limitation of the current Design Event Approach: the probability of the resulting flood is assumed to be equal to that of the causative rainfall event.

The Joint Probability Approach recognises that any design flood characteristics (e.g. peakflow) could result from a variety of combinations of flood producing factors, rather than from a single combination, as in the Design Event Approach. For example, the same peak flood could result from a moderate storm on a saturated basin or a large storm on a dry basin. Thus, a Joint Probability Approach, where the output probability distribution reflects the influence of all the probability distributed inputs and parameters and accounts for their correlation structure, will provide a more realistic representation of the flood generation process.

Another promising alternative to the Design Event Approach is Continuous Simulation using deterministic catchment models or rainfall-runoff process models. This approach is being evaluated in a parallel research project by the CRC for Catchment Hydrology (4). Although the approach appears to hold considerable potential in the long term, as it tries to model the processes involved in flood generation more directly, it will have to overcome some major difficulties (e.g.

adequate modelling of soil moisture redistribution during normal and flood periods) before it can provide a practical design tool for routine flood estimation.

The greater immediate promise of the Joint Probability Approach stems from the fact that it can readily utilise the (deterministic) models and much of the design data used with the current Design Event Approach. The approach therefore has the potential to lead to significant improvements in flood estimation with relatively modest efforts in the near future. It is the approach that forms the basis of the modelling framework outlined in this paper.

### 4 JOINT PROBABILITY APPROACH - OVERVIEW

The aim of the Joint Probability Approach is the determination of a *derived distribution* of a selected flood characteristic. This design flood estimation procedure can be thought of as a combination of deterministic and stochastic hydrologic modelling elements (5). The stochastic elements are reflected in the adopted distributions of the input variables and parameters, as well as in the assumed correlation structure. These are generally determined not only from the data at the site but from a broader information base for the region. The transformation of catchment inputs into outputs is deterministic in nature, and is achieved by means of a rainfall-runoff model.

The Derived Distribution Approach was pioneered by Eagleson (6) who used an analytical method to derive the probability distribution of peak streamflow from an idealised V-shaped flow plane. His approach assumed that storm duration and intensity are independent random variables with a joint exponential probability density function. He adopted a partial area runoff generation model and a runoff routing model based on Kinematic Wave Equations. A similar analytical approach has been adopted in some later applications (e.g. 7) for idealised conditions, but it has limited applicability to real catchment situations.

A number of researchers (e.g. 5, 8, 9) have used an approximate method in that the continuous distributions of hydrologic variables have been discretized by dividing the possible range of a random variable into class intervals. The Theorem of Total Probability is then applied to derive the joint probability distribution of the output in a discrete form. An example of this approach is the 'Transposition Probability Matrix Method' developed by Laurenson (5). The method partitions a design problem into a sequence of basic probability transformation steps, each step transforming an input distribution into an output distribution by means of a deterministic relation between the input and output of a step. The output distribution from the previous step then becomes the input to the next step. The approach has been adopted in several practical cases (e.g. 2, 10).

Some investigators (e.g. 3, 11, 12) adopted a Monte Carlo Simulation Approach to determine a *derived flood distribution*. This involves random sampling from continuous distributions of input variables and parameters, and use of a rainfall-runoff model to obtain the flood hydrograph. The

procedure is repeated  $N$  times ( $N$  in the order of thousands), and the  $N$  different values of the output variable are then used to determine the derived distribution.

We found that most of the previous applications employing the Joint Probability Approach were confined to theoretical studies; mathematical complexity, difficulties in parameter estimation and limited flexibility constrain the application of these techniques in practical situations (13). From the consideration of practical applicability and ability to account for dependence between the input variables, Monte Carlo simulation and the application of the Total Probability Theorem to discretized distributions appear to be the most promising methods to determine derived flood frequency distributions. Among these, Monte Carlo simulation offers greater flexibility.

## 5 KEY ELEMENTS OF PROPOSED MODELLING FRAMEWORK

The proposed modelling framework is based on three principal elements:

- (i) a (deterministic) hydrologic modelling framework to simulate the flood formation process;
- (ii) the key model variables (inputs and parameters) with their probability distributions; and
- (iii) a stochastic modelling framework to synthesise the derived flood distribution from the model input/parameter distributions.

These elements are discussed below:

### 5.1 Hydrologic Modelling Framework

The proposed hydrologic model of the flood formation process involves the same components as the models most commonly used with the current Design Event Approach (see Figure 1): a runoff production function (or loss model), and a runoff transfer function (or runoff routing model).

#### Runoff Production Function - Loss Model

A runoff production model (or loss model) is needed to partition the gross rainfall input into effective runoff (or rainfall excess) and loss. Most of the previous derived distribution studies (e.g. 6, 9) have used an empirical equation (such as Horton's equation) or a more physically based equation (such as Phillip and Green Ampt equations) to estimate the rainfall excess.

In design practice, use of simplified lumped conceptual loss models is preferred over the mathematical equations because of their simplicity and ability to approximate catchment runoff behaviour (14). This is particularly true for design loss which is probabilistic in nature and for which complicated theoretical models may not be required. On this basis, the *initial loss-continuing loss model* appears to offer the greatest potential for the present joint probability study.

#### Transfer Function - Runoff Routing Model

A catchment response model is needed to convert the rainfall excess hydrograph produced by the loss model into a surface runoff hydrograph. The models commonly used in previous joint probability studies include: Kinematic Wave Model (e.g.

6), Geomorphologic Unit Hydrograph Model (e.g. 7), Unit Hydrograph Method (e.g. 8, 11), and Clark's Model (9).

In Australian flood design practice, it is common to use a semi-distributed and non-linear type of catchment response model, referred to as *runoff routing model*. This type of model appears preferable to the models mentioned above because, being distributed in nature, it can account for the areal variation of rainfall and losses, and consider catchment non-linearity. Examples of models in this group include RORB (15) and URBS (16), a further development of the concepts embodied in RORB. There is a considerable body of experience available on appropriate parameter values for RORB and similar models for different types of catchments in Australia. Based on its ready adaptability for the purposes of this project, the URBS model has been adopted.

### 5.2 Variables to be Treated in Probabilistic Fashion

The major factors affecting runoff production are: rainfall duration, rainfall intensity, temporal pattern of rainfall, areal pattern of rainfall and storm losses. Factors affecting hydrograph formation are the catchment response characteristics embodied in the runoff routing model (model type, structure, and parameters) and design baseflow. Ideally, all the variables should be treated as random variables, but consideration of a smaller number of variables without sacrificing much accuracy is preferable, to reduce the data requirements and allow easier application in practice. The selection of variables to be considered as random variables is described below.

#### Rainfall variables:

*Rainfall depth*, as the direct input to rainfall-runoff process, is undoubtedly the most important variable, and its probability distribution is already being considered in the Design Event Approach. Rainfall events that have the potential to produce floods vary considerably in their duration, and the inclusion of *rainfall duration* as a random variable in this study is thus considered essential. In order to analyse the probability distribution of rainfall duration, a rainfall event needs to be defined in such a way that both the rainfall duration and the average rainfall intensity for that duration become random variables [unlike the burst definition in ARR87 (1) where rainfall bursts have predetermined durations].

*Rainfall temporal pattern* varies significantly between storms and has been found to have a significant effect on the shape and peak magnitude of a flood hydrograph (3). Differences of up to 50% in flood peaks may result from different assumed temporal patterns (17). From the findings of these studies, it is clear that temporal pattern is an important variable, and needs to be considered as a random variable.

For design flood estimates, the effects of random variability of rainfall over a catchment are considered through the use of *areal reduction factors* (ARFs). These modify the design point rainfall intensities to average catchment rainfall intensities. The single-valued ARFs in the current edition of ARR87 (1) or the more recent values produced for Victoria by

the CRC for Catchment Hydrology (18) are considered adequate for this study.

An areal rainfall pattern needs to be considered where there are systematic trends in catchment rainfall, such as strong orographic effects or "rain shadow" areas. For the present study, the modelling of the rainfall areal pattern as a random variable is considered less important because: (i) for most catchments, consideration of rainfall areal pattern as a random variable will have a lesser effect on the results than is the case for rainfall duration, intensity and temporal pattern; and (ii) due to limited rainfall data availability on a catchment scale, it would be difficult to derive its probability distribution.

#### Loss Variables:

In the previous joint probability studies, loss has been found to be the most influential variable (e.g. 8, 19). The strong influence of loss values on design flood estimates is based on the fact that loss conditions can vary widely, and a given rainfall occurring on a dry watershed produces a significantly smaller flood than the same rainfall occurring on a wet watershed. In many cases, loss is the most important factor and hence will be treated as a random variable here.

#### Catchment Response Parameters and Baseflow:

It is expected that the incorporation of the probabilistic nature of the rainfall and loss characteristics will result in significant reduction of bias and uncertainties in design flood estimates associated with the current Design Event Approach. Consideration of runoff routing and baseflow variables as random variables would then be of secondary importance (13); thus the effects on design flood estimates of randomness of these variables may be examined as a refinement to the present method at a later stage.

To summarise, we will consider rainfall duration, rainfall intensity, rainfall temporal pattern and losses as primary random variables in the new modelling framework.

### 5.3 Stochastic Modelling Framework

The basic idea underlying the proposed new modelling framework is that the distribution of the flood outputs can be directly determined by simulating the possible combinations of hydrologic model inputs and parameter values. For each run of the combined loss and runoff routing model, a specific value for each input and model parameter will be drawn from its respective distribution. Any significant correlation between the variables can be allowed for by using conditional probability distributions. For example, the strong correlation between rainfall duration and intensity can be allowed for by first drawing a value of duration and then a value of intensity from the conditional distribution for that duration interval.

The two stochastic modelling frameworks to be investigated in the project are the deterministic simulation approach and the stochastic or Monte Carlo simulation approach. In the first approach, employed with Laurenson's Transposition Probability Matrix Method (5), the probability distributions of model inputs and parameters are used in a discrete form, and the probability distribution of the output from a modelling

step is determined by enumerating all possible combinations and calculating their cumulative probabilities. The procedure is then repeated for the next modelling step, using the output distribution from the previous step as the input distribution for the next step.

In the Monte Carlo Simulation approach, all inputs and parameters required for a model run are selected randomly from their probability distributions (but allowing for significant correlations through the use of conditional distributions). The results of the run (i.e. the flood characteristics of interest) are then stored and the Monte Carlo simulation process is repeated a sufficiently large number of times to fully reflect the range of variation of input and parameter values in the generated output. The computational efficiency of the simulation process can be enhanced by judicious sampling from the probability distributions (12). The output values of a selected flood characteristic (e.g. peak inflow to a dam) can then be subjected to a frequency analysis to determine the flood quantiles of interest.

The proposed modelling framework provides the ability to concurrently determine flood characteristics at many points of interest in a system. As an example, it will be possible to determine frequency curves for both inflows and outflows from a reservoir or a retarding basin. In the case of outflows from a storage with significant variation at initial storage content, the probability distribution of initial storage content will be required as an additional model input. Again, important correlations would need to be considered through conditional probability distributions.

In principle, it would be possible to extend the modelling framework by coupling a hydrologic model with other components that have probabilistic inputs or parameters, e.g. a hydraulic model or a flood damage model (12).

## 6 DISTRIBUTIONS OF KEY VARIABLES

### 6.1 Rainfall Duration and Average Rainfall Intensity

The initial research has concentrated on the identification of the probability distributions of rainfall intensity and duration. In the proposed modelling framework, a rainfall event needs to be defined in such a way that both rainfall duration (D) and average intensity (I) become random variables. Several previous applications (e.g. 6, 8) treated storm duration and intensity in simplified fashion as independent random variables; this is likely to result in a steeper derived flood frequency curve (3). A statistical description of rainfall similar to Bloschl and Sivapalan (3) seems to be appropriate and has been adopted here. It uses the marginal distribution of duration together with the conditional distribution of rainfall intensity given a duration. The conditional distribution of rainfall intensity is equivalent to the commonly used intensity-frequency-duration (IFD) curve, widely used in design practice. This approach captures the correlation existing between rainfall intensity and duration.

### Complete storms:

At the beginning, we need a meaningful storm definition. We define a storm rainfall event as starting at the onset of rain, being separated from the next event by at least  $Y$  hours of zero rainfall, and having a minimum average intensity above a given threshold. As the average rainfall intensity reduces with duration, the threshold intensity needs to be defined as a function of duration, expressed as a proportion of the design rainfall intensity for a selected frequency. Thus the adopted threshold intensity for duration  $D$  is:  $I_0(D) = b \times I_D$ , where  $b$  is a reduction factor and  $I_D$  is the design rainfall intensity of 2 years ARI and duration  $D$ , as provided in ARR87 (1). A smaller value of  $b$  would result in a greater number of events with lower average intensity; an appropriate value of  $b$  needs to be determined by trial-and-error. A rainfall event with an average intensity less than the threshold value but containing a shorter period of intense rainfall embedded within the storm is also of interest. For this type of event, a new threshold value  $bb \times I_d$  is used, where  $d$  is the duration of the intense part.

The rainfall events selected by the above procedure are called *complete storms* henceforth. With this definition (for  $Y = 6$  hours,  $b = 0.5$ ,  $bb = 0.6$ ), rainfall events have been identified for a number of pluviograph stations in Victoria. The resulting distribution of rainfall duration has the shape of a truncated Gamma distribution, as shown in Figure 2. A conditional distribution of average rainfall intensity  $I_D$  for *complete storms* of duration  $D$  can also be derived.

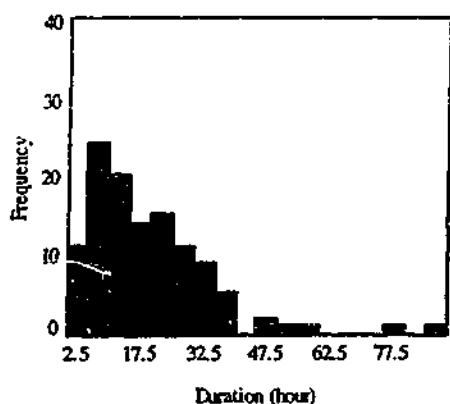


Fig 2 Distribution of rainfall duration (complete storms)

### Storm-cores:

The available IFD information in ARR87 is not based on complete storms but on *periods of intense rainfall within complete storms*, called bursts. If this existing information is to be used with the proposed new approach, it is more useful to undertake the design rainfall analysis in terms of storm bursts. However, as the duration of the bursts in the ARR87 analysis was predetermined rather than random, it is necessary to consider a new storm burst definition that will produce randomly distributed storm burst durations. These newly defined storm bursts will be referred to as *storm-cores* henceforth.

For each *complete storm*, there will be one *storm-core*; it is the burst of that duration which is associated with the greatest relative average intensity compared to the threshold. With this storm-core definition, the distribution of storm-core duration for a number of pluviograph stations of Victoria has been obtained; it has the shape of an exponential distribution, as shown in Figure 3.

The key issue is whether the conditional distribution of rainfall intensity for bursts following this new definition will be similar to the ARR87 IFD curves. The IFD curves derived in this project, based on *storm-cores*, are clearly lower than the ARR87 values. Further testing on a broader data set is in progress to confirm the nature of the relationship between the two types of IFD curves.

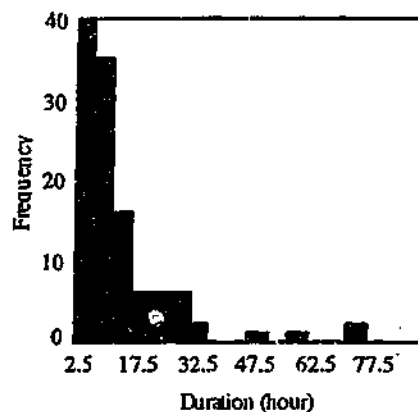


Fig 3 Distribution of rainfall duration (storm-cores)

### 6.2 Rainfall Temporal Pattern

The methods available to represent the variability of temporal patterns in observed storms range from a database of actual storm (or runoff) patterns (9), over empirical distributions of storm profiles (20), to theoretical distributions and synthetic storm patterns (21). A trade-off has to be made between simplicity of approach and flexibility of application, particularly when the approach is to be applied to ungauged catchments.

Temporal patterns are strongly correlated with rainfall duration, and weaker correlations with rainfall intensity and season also appear to be present. If proven, they will be modelled through *conditional* distributions of storm patterns.

### 6.3 Initial Loss Parameter

For a specific catchment, initial loss values associated with different storms vary more significantly than continuing losses. The focus in this project is therefore on deriving a probability distribution of initial loss from observed storm rainfall and streamflow data. We proposed to base these distributions mainly on the results of the empirical analysis of data for South-Eastern Australia by Hill et al. (14).

The work of Hill et al. (14) has shown strong correlations between initial loss and rainfall duration, and how initial loss reduces with decreasing rainfall burst duration. We propose to address the still unresolved issue of a possible correlation between initial loss and rainfall intensity in a parallel project, using results from continuous rainfall-runoff modelling.

## 7 CONCLUSION

Previous research and practical experience have demonstrated the theoretical and practical limitations of the currently applied Design Event Approach to rainfall-based design flood estimation. One alternative approach investigated in the CRC for Catchment Hydrology's Research Project FL1 is based on the application of joint probability principles to the key variables involved in the flood generation process.

Initial project work, including an extensive literature review (13), has led to the following conclusions:

- The loss models and runoff routing models currently used in Australia form a suitable basis for the deterministic hydrologic modelling framework.
- The key model inputs and parameters to be represented by probability distributions are the duration, average intensity and temporal pattern of complete storms or intense rainfall bursts, and the initial loss parameter (and, if storage outflows are of interest, the initial storage content).
- Further analysis and testing is required to determine the extent to which currently available Australian flood design data can be used to define the required probability distributions of these variables.
- Monte Carlo simulation provides a suitable stochastic modelling framework to synthesise the derived flood characteristics distributions from the model input/parameter distributions.

Work is continuing to address the outstanding research issues and to test the modelling framework in a range of practical design flood estimation situations.

## ACKNOWLEDGMENTS

The authors would like to thank the members of the Project Reference Panel, specially Dr Bryson Bates, Prof Russell Mein and Dr Sri Srikanthan, for their inputs to the development of this modelling framework.

## REFERENCES

1. Institution of Engineers Australia (1987): Australian Rainfall and Runoff: A Guide to Flood Estimation. I.E.Aust., Canberra.
2. Ahern, P.A. and Weinmann, P.E. (1982): Considerations for Design Flood Estimation Using Catchment Modelling. Hydrol. and Water Resour. Symp., Melbourne, pp. 44-48.
3. Blöschl, G. and Sivapalan, M. (1996): Process Controls on Flood Frequency. 2. Runoff Generation, Storm Properties and Return Period. Water Resour. Res. (submitted).
4. Muncaster, S.H., Weinmann, P.E. and Mein, R.G. (1997): An Application of Continuous Hydrologic Modelling to Design Flood Estimation. 24<sup>th</sup> Hydrol. and Water Resour. Symp., Auckland, pp. 77-82.
5. Laurenson, E.M. (1974): Modelling of Stochastic-Deterministic Hydrologic Systems. Water Resour. Res. 10, 5, 955-961.
6. Eagleson, P.S. (1972): Dynamics of Flood Frequency. Water Resour. Res., 8, 4, 878-898.
7. Diaz-Granados, M.A., Valdes, J.B. and Bras, R.L. (1984): A Physically Based Flood Frequency Distribution. Water Resour. Res., 20, 7, 995-1002.
8. Beran, M.A. (1973): Estimation of Design Floods and the Problem of Equating the Probability of Rainfall and Runoff. Symp. on the Design of Water Resour. Projects with Inadequate Data, Madrid, Spain, pp. 33-50.
9. Russell, S.O., Kenning, B.F.I. and Sunnell, G.J. (1979): Estimating Design Flows for Urban Drainage. J. Hydraul. Div., ASCE, 105, 43-52.
10. Laurenson, E.M. and Pearse, M.A. (1991): Frequency of Extreme Rainfall and Floods. Intl. Hydrol. & Wat. Resour. Symp., Perth, pp. 392-399.
11. Muzik, I. (1993): Derived, Physically Based Distribution of Flood Probabilities. Extreme Hydrological Events: Precipitation, Floods and Droughts (Proc. Yokohama Symp., July 1993, IAHS Publ. No. 213, pp. 183-188.
12. Thompson, D.K., Stedinger, J.R. and Heath, D.C. (1997): Evaluation and Presentation of Dam Failure and Flood Risks. J. Water Res. Planning and Mgmt. 123, 4, 216-227.
13. Rahman, A., Hoang, T., Weinmann, P.E., and Laurenson, E.M. (1997): Joint Probability Approaches to Design Flood Estimation: A Review. Unpublished Research Report. CRC for Catchment Hydrology, Dept. of Civil Eng., Monash University, pp. 78.
14. Hill, P.I., Mein, R.G., Weinmann, P.E. (1996): Testing of Improved Inputs for Design Flood Estimation in South-Eastern Australia. CRC for Catchment Hydrology Report 96/6, Dept. of Civil Eng., Monash University.
15. Laurenson, E.M. and Mein, R.G. (1997): RORB Version 4 Runoff Routing Program User Manual, Dept. of Civil Eng., Monash University, pp. 186.
16. Carroll, D.G. (1994): The BCC Catchment Management Runoff Routing Model Manual, Version 3.3, Brisbane City Council, Brisbane.
17. Cordery, I., Pilgrim, D.H. and Rowbottom, I.A. (1984): Time Patterns of Rainfall for Estimating Design Floods on a Frequency Basis. Water Science Tech., 16, 155-165.
18. Siriwardena, L. and Weinmann, P.E. (1996): Derivation of Areal Reduction Factors for Design Rainfalls in Victoria. CRC for Catchment Hydrology Report 96/4, Dept. of Civil Eng., Monash University, pp. 60.
19. Haan, C.T. and Schulze, R.E. (1987): Return Period Flow Prediction with Uncertain Parameters. Transactions of the ASCE, 30(3): May-June, 665-669.
20. Huff, F.A. (1967): Time Distribution of Rainfall in Heavy Storms. Water Resour. Res. 3, 4, 1007-1019.
21. Hashino, M. (1986): Stochastic Formulation of Storm Pattern and Rainfall Intensity-Duration Curve for Design Flood. Intl. Symp. on Flood Frequency and Risk Analysis, Barton Rouge, U.S.A., V. P. Singh (ed.), D. Reidel Publishing Company, pp. 303-315.